Micropollutant degradation, product formation and mass transfer in ozonation water treatment

(Alternative Format Thesis)

Zoumpouli, Garyfalia

Award date:
2021

Awarding institution:
University of Bath

Micropollutant degradation, product formation and mass transfer in ozonation water treatment

Garyfalia Zoumpouli

A thesis submitted for the degree of Doctor of Philosophy

University of Bath

Department of Chemical Engineering

March 2021

Declaration of authorship

I am the author of this thesis, and the work described therein was carried out by myself personally, with any collaborative work stated and acknowledged within the corresponding text. The raw experimental data that were analysed and discussed in Chapter 2 were produced by Fernanda Siqueira Souza and Bruce Petrie. The original idea for the experimental design used in Chapter 3 was developed by Oliver Happel and Marco Scheurer, and their experimental results have been included in this chapter along with those produced by the author of this thesis. Parts of the work presented in Chapter 4 were done in collaboration with Jakob Kämmler. Parts of the work presented in Chapter 5 were done in collaboration with Zhuoyue Zhang.

Candidate's signature

Acknowledgments

I would like to thank my supervisor Dr Jannis Wenk for his help and support throughout the PhD and for sharing his expertise and ideas with me. My PhD years have been both enjoyable and productive, and this is largely thanks to him. I am also grateful to my co-supervisors, Prof Barbara Kasprzyk-Hordern and Prof John Chew, for their valuable advice and contributions to the research.

A special thanks goes to the Centre for Sustainable Chemical Technologies, the EPSRC and the University of Bath for providing funding and many opportunities that enhanced my PhD, especially attending conferences and doing an internship abroad. I also greatly appreciate the technical and administrative assistance provided by the Department of Chemical Engineering, and the facilities and technical support provided by the Material and Chemical Characterisation Facility (MC^2).

I would like to thank all the collaborators that contributed to the research presented in this thesis: Dr Oliver Happel and Dr Marco Scheurer at the Water Technology Center in Karlsruhe, Germany; Jakob Kämmler and Prof Mathias Ernst at the Hamburg University of Technology in Hamburg, Germany; Dr Fernanda Siqueira Souza at the La Salle University in Rio Grande do Sul, Brazil; Robert Baker, Dr Caitlin Taylor and Dr Kathryn Proctor at the University of Bath. Big thanks to Dr Carsten Prasse and his research group at Johns Hopkins University in Baltimore, USA for hosting me in their lab, showing me around Baltimore and helping me have such a great internship experience. Also thank you to the Chemical Engineering undergraduate researchers that I supervised, for their work inside and outside the lab.

A huge thanks goes to CSCT Cohort ’16, the Wenk group, Office 2.05/3.01 and the rest of the people I met during these four and a half years at the University of Bath, for their much appreciated advice, moral support and fun weekends in Bath and elsewhere.

Last but not least, thank you to my parents Voula and Tasos, and my siblings Effie and Ippokratis, for their love and support all these years, and to my dearest friends Mara, Theano, Haris and Ria for always being there for me even though we were thousands of kilometres apart.

Abstract

Ozone is a strong oxidant used in water and wastewater treatment for disinfection, removal of taste, colour and odour and abatement of trace organic contaminants (TrOCs). TrOCs, such as pharmaceuticals, have been attracting growing attention in the last decades due to their widespread presence in the environment and their ecotoxicological effects. The ozone-induced oxidation of water constituents generates a very large number of known and unknown by-products, including bromate formed from bromide and structurally diverse transformation products of TrOCs. The mass transfer of ozone is important for both process efficiency and reaction pathways and is conventionally achieved via bubble-based systems. In order to address the major issues surrounding ozonation treatment, this PhD thesis investigated the abatement of TrOCs, the formation of ozonation products and the bubble-less transfer of ozone.

A multi-compound ozonation study was performed by utilising liquid chromatography-mass spectrometry to provide a large dataset on the ozone reactivity of environmentally relevant TrOCs. The ozonation of 90 compounds with diverse chemical structures was studied in pure buffered water, tap water and wastewater effluent at three specific ozone doses and three pH levels. A review of the literature revealed that little information is known on the ozonation kinetics of illicit drugs and their metabolites. The experiments showed that most illicit drugs, such as cocainics, amphetamines and ecstasy-group compounds, are ozone-resistant.

In addition to the reactivity of the parent compounds, investigating the biodegradation of ozonation products of TrOCs is important to assess the efficiency of advanced treatment schemes involving ozonation and a subsequent biofiltration step. A Continuous Ozonation merged with Biofiltration (COMBI) laboratory system was developed to perform investigations that were previously only feasible at large-scale or pilot-scale plants. After an equilibration time of three weeks, biodegradable ozonation products, for example the main product of carbamazepine, were removed in the sand filtration columns. In contrast, other compounds, such as trifluoroacetic acid formed from fluoxetine, passed through the columns at unchanged concentrations.

The abatement of TrOCs using ozone requires the design of efficient ozonation processes. The use of membrane contactors for the bubble-less transfer of ozone into

water and wastewater is a promising alternative to conventional bubble-based methods. Polymeric membranes made of polydimethylsiloxane (PDMS) and polytetrafluoroethylene (PTFE) were tested in a single tube membrane contactor and in a multi-tube hollow fibre module. High removals of TrOCs at their inherent concentrations in wastewater effluent were achieved using membrane ozonation. However, the analysis of bromate formation in bromide-containing groundwater indicated that the non-uniform distribution of ozone inside a membrane contactor can lead to elevated bromate concentrations that exceed the regulatory limit of 10 $\mu g\ L^{-1}$.

Finally, a case study for the ozonation of a specific group of substances was conducted. The study focused on the ozonation kinetics and transformation products of substituted furans. Despite being a widespread moiety in natural and synthetic chemicals, the aqueous ozonation of furan rings was previously poorly understood. The analysis of transformation products targeted α,β-unsaturated dicarbonyl compounds, which are well known toxicophores. The formation of 2-butene-1,4-dial and other α,β-unsaturated dicarbonyls was demonstrated in aqueous ozonation for the first time. Despite the low yield of these substances, which reached maximum values of 7%, their high toxicity raises concern about their presence in treated water.

Overall, this thesis achieved a better understanding of the ozone reactivity and transformation products of TrOCs, including compound classes such as illicit drugs and substituted furans that had not been studied comprehensively with ozone before. In addition, the developed experimental setups can facilitate future research on ozonation-biofiltration treatment and on bubble-less transfer of ozone. The results of this thesis have led to three publications in peer-reviewed journals, while two further manuscripts are currently being prepared.

Dissemination

Journal articles

Zoumpouli GA, Baker R, Taylor CM, Chippendale MJ, Smithers C, Ho SSX, Mattia D, Chew YMJ, Wenk J. A Single Tube Contactor for Testing Membrane Ozonation. Water. 2018;10(10):1416.

Zoumpouli GA, Scheurer M, Brauch H-J, Kasprzyk-Hordern B, Wenk J, Happel O. COMBI, continuous ozonation merged with biofiltration to study oxidative and microbial transformation of trace organic contaminants. Environmental Science: Water Research & Technology. 2019;5(3):552-63.

Zoumpouli GA, Siqueira Souza F, Petrie B, Féris LA, Kasprzyk-Hordern B, Wenk J. Simultaneous ozonation of 90 organic micropollutants including illicit drugs and their metabolites in different water matrices. Environmental Science: Water Research & Technology. 2020;6(9):2465-78.

Zoumpouli GA, Zhang Z, Wenk J, Prasse C. Aqueous Ozonation of Furans: Kinetics and Transformation Mechanisms Leading to the Formation of α,β-Unsaturated Dicarbonyl Compounds. Manuscript submitted.

Kämmler J, Zoumpouli GA, Chew YMJ, Wenk J, Ernst M. Natural organic matter (NOM) colour removal and bromate formation by membrane ozonation of groundwater. Manuscript in preparation.

Conference presentations

Zoumpouli GA, Happel O, Kasprzyk-Hordern B, Wenk J. Understanding the fate of trace organic contaminants in natural engineered water treatment combined with pre-ozonation. 2018. Oral presentation at the Fifth International Conference on Small and Decentralized Water and Wastewater Treatment Plants (SWAT 5), Thessaloniki, Greece.

Zoumpouli GA, Ho SS, Chew YM, Wenk J. Bubble-less ozonation with non-porous membranes: Experiments and CFD modelling. 2019. Oral presentation at the 9th International Water Association Membrane Technology Conference & Exhibition for Water and Wastewater Treatment and Reuse (IWA-MTC 2019), Toulouse, France.

Table of contents

List of Tables

List of Figures

Abbreviations

ACE	acesulfame
AOP	advanced oxidation process
BaQD	1-(2-benzoic acid)-(1H,3H)-quinazoline-2,4-one
BaQM	1-(2-benzoic acid)-4-hydro-(1H,3H)-quinazoline-2-one
BDA	2-butene-1,4-dial
BHF	3,4-bis(hydroxymethyl)furan
BQD	1-(2-benzaldehyde)-(1H,3H)-quinazoline-2,4-one
BQM	1-(2-benzaldehyde)-4-hydro-(1H,3H)-quinazoline-2-one
CBZ	carbamazepine
CFD	Computational Fluid Dynamics
CID	collision induced dissociation
COMBI	Continuous Ozonation merged with Biofiltration
DBP	disinfection by-product
DF	diclofenac
DF-IQ	diclofenac-2,5-iminoquinone
DI	deionised
DMF	2,5-dimethylfuran
DMS	dimethylsulfamide
DOM	dissolved organic matter
EEM	excitation-emission matrix
ESI	electrospray ionization
EU	European Union
FA	2-furoic acid
FDCA	furan-2,5-dicarboxylic acid
FFA	furfuryl alcohol

FLX	fluoxetine
FPA	3-(2-furyl)propanoic acid
FRS	furosemide
GC	gas chromatography
HRMS	high resolution mass spectrometry
HRT	hydraulic residence time
IC	ion chromatography
ICP	inductively coupled plasma
ID	inner diameter
KET	ketoprofen
LC-MS	liquid chromatography-mass spectrometry
MBBR	moving bed biofilm reactor
MFA	2-methyl-3-furoic acid
MQL	method quantification limit
MRM	multiple reaction monitoring
NAC	*N*-α-acetyl-cysteine
NAL	*N*-α-acetyl-lysine
NDMA	*N*-nitrosodimethylamine
NFT	nitrofurantoin
NOM	natural organic matter
O-6-MAM	6-monoacetylmorphine
OH-DF	5-hydroxydiclofenac
OMP	organic micropollutant
***p*CBA**	*para*-chlorobenzoic acid
PDMS	polydimethylsiloxane
PTFE	polytetrafluoroethylene
PVDF	polyvinylidene fluoride
QSAR	quantitative structure–activity relationship
RAN	ranitidine
RDA	reactivity-directed analysis
RU	Raman units
SI	Supplementary Information

SPE	solid phase extraction
SUVA	specific UV absorbance
TF	total fluorescence
TFA	trifluoroacetic acid
TN	total nitrogen
TOC	total organic carbon
TOF	time of flight
TP	transformation product
TRA	tramadol
TrOC	trace organic contaminant
UHPLC	ultra high performance liquid chromatography
UV-Vis	ultraviolet-visible
WHO	World Health Organization
WT	wall thickness
WW	wastewater

Chapter 1: Introduction and general literature review

Ozone is an oxidant and disinfectant widely used in water and wastewater treatment. Ozonation is one of the most promising technologies for the abatement of trace organic contaminants, such as pharmaceuticals. This PhD thesis investigates the implications of ozonation products and ozone mass transfer for the treatment of water and wastewater. The Introduction gives an overview on water and wastewater treatment, followed by the background of ozone science and engineering and of trace organic contaminants in the water cycle. The aim of the Introduction is to set the research conducted as part of this thesis into context, and to present the objectives that the research pursued. A specific introduction and literature review on each research topic is included in the corresponding chapter (Chapters 2 to 5).

1.1 Water treatment

Water treatment is the processing of water to achieve a water quality that meets the standards set by the end users through their regulatory agencies (1). The production of water that is safe to drink and aesthetically pleasing is often achieved through a treatment train at a water treatment plant (or waterworks), where a number of processes remove different water constituents, including particles, natural organic matter, anthropogenic chemicals, bacteria and viruses (2).

An overview of commonly used water treatment processes is presented in Table 1.1.1. A conventional treatment train for surface water consists of coagulation, flocculation, sedimentation, granular media filtration and disinfection (3). In addition to conventional treatment, the application of advanced treatment may be necessary for various reasons such as corrosion control or removal of pesticides. Advanced treatment processes include softening, ion-exchange, adsorption, membrane filtration and chemical oxidation (2).

Disinfection refers to the inactivation of microorganisms in water, so that they are no longer able to cause disease to the consumers. The five main disinfectants used for

drinking water production are free chlorine, combined chlorine (chloramines), chlorine dioxide, ozone and ultraviolet (UV) light (4). Chemical oxidation processes are used for the oxidation of reduced inorganic species (e.g. iron and manganese), synthetic organic compounds (e.g. pesticides and industrial chemicals) and compounds imparting taste and odour to the water. Many oxidants also have disinfecting properties. The most common chemical oxidants used in water treatment are chlorine, ozone, chlorine dioxide and permanganate (5). In addition to those, advanced oxidation processes (AOPs) are based on the generation of reactive radical species, predominantly hydroxyl (OH) radicals. While some AOPs are well-established (e.g. UV/hydrogen peroxide and ozone-based AOPs), numerous others are still in the development stage (6, 7).

Table 1.1.1. Overview of processes used in water and wastewater treatment. Adapted from (2, 8).

	Water treatment	**Wastewater treatment**
Pre-treatment and primary treatment	Screening Storage Equalization Neutralization Aeration Chemical pre-treatment Coagulation Flocculation Sedimentation	Screening Sedimentation Flotation Oil separation Equalization Neutralization
Secondary treatment	Rapid sand filtration Slow sand filtration Disinfection	Activated sludge Aerated lagoons Trickling filters Anaerobic treatment
Tertiary or advanced treatment	Activated carbon Ion exchange Chemical oxidation Membrane processes	Activated carbon Ion exchange Reverse osmosis Nutrient removal processes Chemical oxidation/disinfection

The dissolved organic matter (DOM) present in water sources has important implications for water quality and treatment. DOM in natural waters consists mainly of natural organic matter (e.g. humic substances) and is a complex mixture of aromatic and aliphatic hydrocarbons with various functional groups attached (9). In the 1970s it was discovered that the reaction of natural organic matter with chlorine can lead to the formation of disinfection by-products (DBPs) that are a hazard to human health and should, thus, be regulated (10). Since then, more than 700 by-products of different

disinfectants have been identified, but only a fraction of them has been rigorously studied and characterised (11, 12).

New challenges for water treatment are constantly arising. The decreasing availability of high-quality water sources as a result of population growth, urbanisation and climate change is driving the utilisation of alternative water resources (e.g. treated wastewater) and the implementation of advanced water treatment schemes. Moreover, 'contaminants of emerging concern' are naturally-occurring or manmade chemicals or materials which have been recently discovered or are suspected to be present in various environmental compartments, and which may affect living organisms (13). These include, among many others, pharmacologically active compounds, nanomaterials and microplastics (14). Contaminants of emerging concern are usually not regulated but can affect future legislation and water treatment practice (see also Sections 1.5 and 1.6).

1.2 Wastewater treatment

Wastewater is defined as used water from any combination of domestic, industrial, commercial or agricultural activities, surface runoff/stormwater, and any other sewer inflow or infiltration (15). In many industrialized countries, wastewater is transported to wastewater treatment plants where it is treated before being discharged into the environment or reused. The primary aims of wastewater treatment are to protect the environment from pollution and to safeguard public health, with a secondary aim being the generation of valuable end-products such as reusable water (16).

Wastewater treatment can be achieved using several physical, chemical, thermal and biological processes and is commonly divided into primary, secondary and tertiary treatment. An overview of commonly used wastewater treatment processes is provided in Table 1.1.1. Primary treatment is employed for removal of large solids, suspended solids and floating materials. Secondary treatment comprises biological processes to remove organic matter and nutrients. Tertiary treatment is intended for the elimination of pollutants or nutrients not removed by conventional biological treatment (8).

Nowadays, tertiary (or advanced) wastewater treatment is often considered necessary to protect ecosystems, as well as drinking water resources, from an ever-increasing number of anthropogenic chemicals of which wastewater treatment plants are a major source of emission (17, 18). This becomes especially important in wastewater reuse applications, where the treated effluent needs to meet strict quality standards (19). The DOM in wastewater effluent is termed effluent organic matter and consists of natural organic matter, soluble microbial products and trace chemicals (20). Among other technologies, chemical oxidation of secondary treated wastewater can degrade organics using permanganate, chlorine, chlorine dioxide, ozone, hydrogen peroxide and AOPs (21).

1.3 Ozonation processes

Ozone is a highly toxic, oxidizing gas, that is named after its strong smell. It is produced naturally by the discharge of lightning and artificially by the discharge of electricity in the presence of oxygen (22). Ozone was discovered in 1839, while the first full-scale water disinfection unit using ozone was installed in 1906 in Nice, France (23).

Ozonation is used in both water and wastewater treatment for disinfection, oxidation of inorganic compounds, oxidation of organic compounds (including improvement of taste, odour and colour and abatement of trace organic contaminants) and particle removal (22). An important difference of ozone from chlorine-based disinfectants is its short lifetime which means that it cannot be used to maintain a disinfectant residual in the water distribution network (24). The ozonation process can be located at different points of the treatment train (pre-ozonation, intermediate ozonation, post-ozonation) depending on the treatment goals and the other processes employed (22, 25). Two typical treatment trains that include ozonation are shown in Figure 1.3.1.

The primary operational costs of ozonation plants are energy and oxygen supply (26). Within the last thirty years, the cost efficiency of ozone production has improved and the worldwide ozone capacity for water and wastewater treatment has increased, with numerous facilities in France, Germany, the Netherlands, Switzerland, Japan, the USA and elsewhere (27).

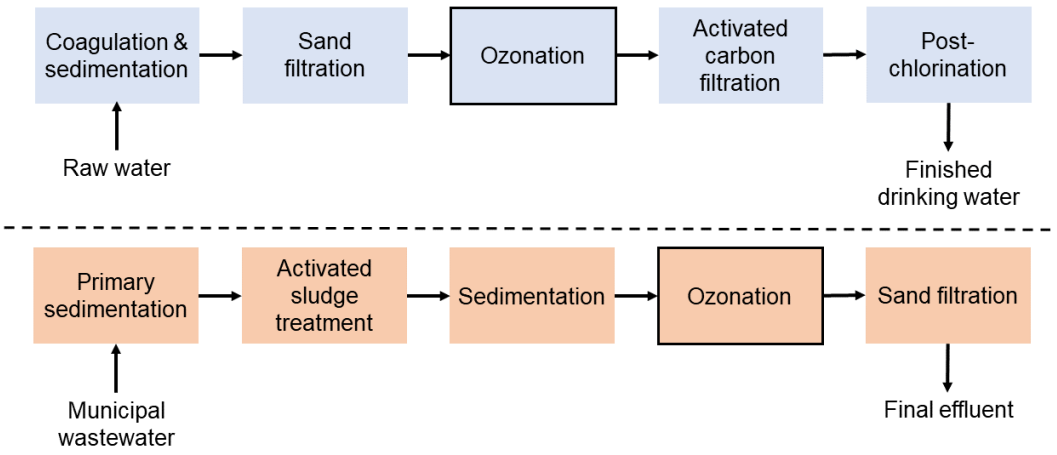

Figure 1.3.1. Example of a treatment train for drinking water production and of one for wastewater treatment, both including an ozonation step. Adapted from (22, 25).

Figure 1.3.2 demonstrates the main components of an ozone process. Since ozone is an unstable gas, it must be generated on-site from air or oxygen. After generation, ozone is transferred into the water. This is most commonly achieved either through counter-current multistage bubble contactors using gas diffusers, or through Venturi-type in-line gas injection systems (28). The off-gas is usually treated to destroy residual ozone and is then vented into the atmosphere or recycled, either in the ozonation process or in other processes of the treatment plant (29).

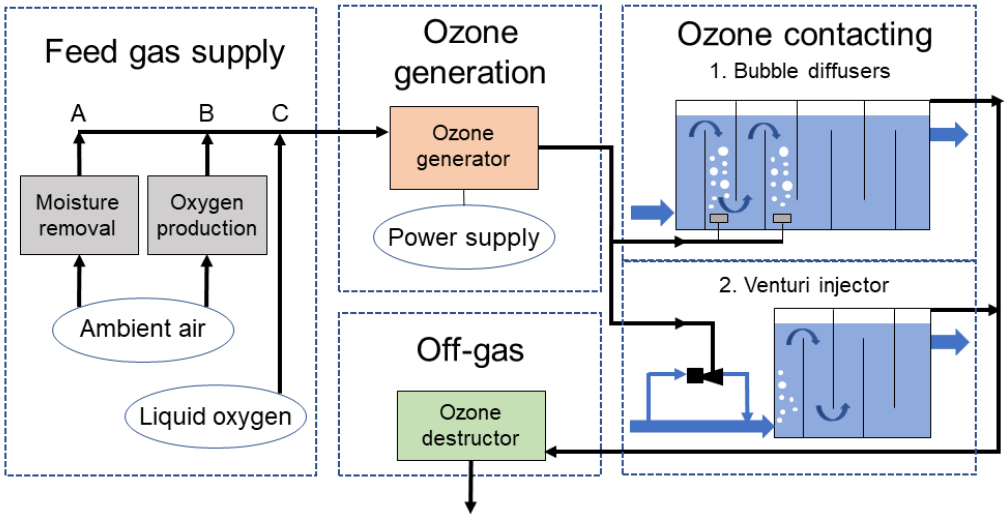

Figure 1.3.2. The primary components of an ozone process, adapted from (28). Three options for feed gas supply are shown (A, B and C), along with two alternatives for ozone contacting (1 and 2). Black arrows are gas flows and blue arrows are water flows.

Many parameters affect the transfer of ozone from the gas phase into the liquid phase. They include process parameters (e.g. gas and liquid flow rates), physical parameters (e.g. density, viscosity and surface tension of the liquid phase), reactor geometry (e.g. reactor dimensions and type of stirring) and reactions in the liquid phase (30). In conventional ozone contactors the mass transfer interface is in the form of bubbles, with smaller bubble sizes resulting in higher mass transfer rate, while also being more costly to achieve (31). An alternative approach, not yet implemented in large-scale applications, consists in bubble-free transfer of ozone by using membrane contactors equipped with ozone-permeable membranes (32).

Table 1.3.1 provides an overview of important parameters for ozonation processes. The applied ozone dose depends on the treatment objective and the water feed characteristics, and impacts the operational and capital costs of ozonation plants (26). The concept of *ct* (disinfectant concentration multiplied by the available contact time) is used to assess disinfection, based on reported *ct*-values for a given degree of inactivation of a specific microorganism (33).

Table 1.3.1. Important parameters in ozonation processes and the equations used for their calculation in continuous-flow systems. Adapted from (34).

Parameter	**Symbol (units)**	**Equation**	
Applied ozone dose	I (mg L^{-1})	$I = \frac{Q_G}{Q_L} \times c_{Go}$	(1.3.1)
Absorbed or transferred ozone dose	A (mg L^{-1})	$A = \frac{Q_G}{Q_L} \times (c_{Go} - c_{Ge})$	(1.3.2)
Consumed ozone dose	$D(O_3)$ (mg L^{-1})	$D(O_3) = A - c_{Le}$	(1.3.3)
Ozone transfer efficiency	$\eta(O_3)$ (%)	$\eta(O_3) = \frac{c_{Go} - c_{Ge}}{c_{Go}} = \frac{A}{I}$	(1.3.4)
ct-value	ct (mg L^{-1} s)	$ct = c_L \times t_H$	(1.3.5)

Q_G (L s^{-1}) gas flow rate; Q_L (L s^{-1}) liquid flow rate; c_{Go} (mg L^{-1}) influent-gas concentration; c_{Ge} (mg L^{-1}) effluent-gas concentration; c_L (mg L^{-1}) liquid concentration in reactor; c_{Le} (mg L^{-1}) effluent-liquid concentration; t_H (s) hydraulic retention time.

1.4 Ozonation chemistry

Ozone is unstable in water and decomposes into OH radicals via a radical chain mechanism. Different substances can initiate, promote or terminate the chain reaction

(e.g. hydroxide ions, humic acids and alcohols). The following overall reaction can be deduced from the complex radical pathway (35):

$$3\ O_3 + OH^- + H^+ \rightarrow 2\ OH\bullet + 4\ O_2 \qquad (1.4.1)$$

The R_{ct} value, corresponding to the ratio of the OH radicals concentration to the ozone concentration, depends on water properties, for example pH, alkalinity and concentration of DOM (36, 37). While disinfection occurs mainly through ozone, oxidation processes occur through both ozone and OH radicals (38). As an electrophile, ozone is a selective oxidant which reacts preferentially with electron-rich moieties, including activated aromatic rings, deprotonated amines and olefins. OH radicals react fast with almost all organic moieties (39). Ozone can be used with addition of hydrogen peroxide (peroxone process) or UV irradiation to increase the production of OH radicals in order to degrade ozone-resistant contaminants (38).

The ultimate goal of the oxidation of pollutants is to mineralise them, namely to convert them into simple inorganic molecules (carbon dioxide, water, etc.) (40). Ozonation treatment with typical ozone doses results in little mineralisation of DOM, however it does enhance its biodegradability (i.e. it increases the biodegradable dissolved organic carbon and the assimilable organic carbon) (41). The reactions of ozone with DOM generate low molecular weight, polar, oxygen-rich by-products, including aldehydes and carboxylic acids (42, 43). Ozonation is commonly followed by a polishing step or post-treatment (see Figure 1.3.1), such as sand filtration or biological activated carbon filtration (44). Thereby, most ozonation by-products can be removed through biodegradation, to minimise the risk of bacterial regrowth in drinking water distribution systems or effluent receiving waters (45, 46).

The main ozonation by-product of concern is bromate (BrO_3^-), which is subject to regulations and a drinking water guideline value of 10 μg L^{-1} set by the World Health Organization (WHO) (47). Bromate is formed in the ozonation of waters containing bromide, which stems from both natural and anthropogenic sources, such as industrial wastewater and landfill leachate (48). Bromate is hard to remove with filtration post-treatment, thus it is more economical to minimise its formation during ozonation. This can be achieved by addition of ammonia or hydrogen peroxide, or by pH depression (33). An alternative strategy is reducing the level of bromide prior to

ozonation (49, 50). Finally, optimizing the reactor configuration can help inhibit bromate formation by resolving flow issues and allowing the use of lower ozone doses or reaction times (51). A promising technology in this regard is the bubble-less transfer of ozone into the water using membrane contactors (52).

Another class of by-products of concern for ozonation are nitrosamines, especially *N*-nitrosodimethylamine (NDMA). The WHO drinking water guideline value for NDMA is 0.1 μg L^{-1} (47). NDMA is formed from the ozonation of several amine precursors, with high yields observed for hydrazines and sulfamides (53, 54). However, ozonation is usually not a major pathway of NDMA formation, since nitrosamines are mainly associated with chloramination (55). In addition, the NDMA formed in ozonation can be removed by sand filtration post-treatment (56).

Overall, as with other disinfection and chemical oxidation processes, ozonation needs to be optimized to achieve treatment goals whilst mitigating hazardous by-product formation (57).

1.5 Trace organic contaminants

Trace organic contaminants (TrOCs) or organic micropollutants (OMPs) are organic compounds which can be found at trace concentrations (ng L^{-1} to μg L^{-1}) in the influent and the effluent of wastewater treatment plants, as well as in the environment, and even in drinking water (58-60). Despite their very low concentrations, TrOCs pose a threat to organisms and entire ecosystems due to their endocrine-disrupting action and synergistic toxicity (61, 62). Many TrOCs are considered persistent because they are not readily attenuated by natural processes in the environment and the engineered processes of water and wastewater treatment (63). Those TrOCs that can be degraded are termed pseudo-persistent, because their continuous release from various sources can still lead to environmental occurrence (64). TrOCs are often considered contaminants of emerging concern (65), even though some of them have now been studied for several decades (66).

TrOCs include numerous classes of compounds: pharmaceuticals, personal care products, hormones, illicit drugs, pesticides, household chemicals and more. Pharmaceuticals have attracted particular attention because they are designed to have

biological action (67). They are present in crude wastewater due to incomplete metabolism in the human body and direct disposal of unused or expired substances into the sewer system (68). A related class of TrOCs gaining attention in recent years are illicit drugs, but there is still limited information on their fate in the water cycle (69-72).

Transformation products (TPs) of TrOCs are the compounds created as TrOCs are degraded via chemical and biological processes, including human metabolism, biotic and abiotic processes in the environment, and water and wastewater treatment (73, 74). Figure 1.5.1 shows the main transformation processes of TrOCs as part of their pathways from their major sources into environmental compartments and, potentially, into the water distribution network. These processes involve several types of reactions, such as conjugation, oxidation, reduction, hydrolysis and photolysis resulting in structurally diverse TPs (75). The contribution of TPs to the environmental risk posed by the parent compounds needs to be considered, taking into account their formation yield, potential toxicity, persistence and mobility (76). The current deficit regarding this information hinders the inclusion of TPs in environmental risk assessments and chemicals regulations (77), with a notable example being the REACH regulation of the European Union (EU) (78).

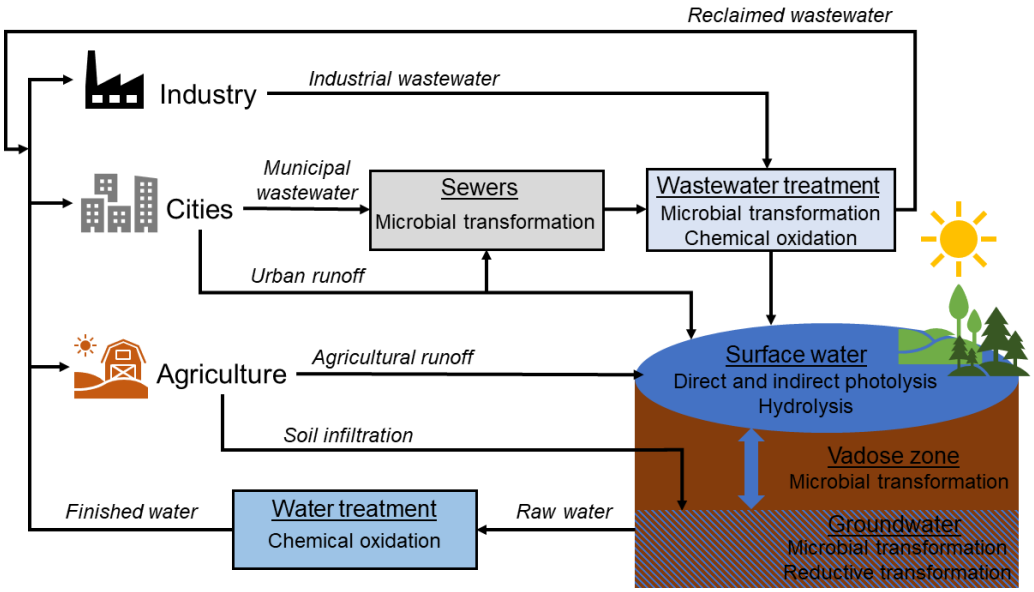

Figure 1.5.1. Major sources, pathways and transformation processes of trace organic contaminants in water and wastewater treatment and in the environment. Other sinks such as adsorption in soil are not shown.

1.6 Abatement of trace organic contaminants

The release of certain TrOCs into the environment can be mitigated through source control (or input prevention) strategies, such as changes in consumer behaviour and design of substances that can be easily removed with wastewater treatment ('benign by design') (79). However, source control is a long-term strategy, which needs to be complemented by effective end-of-pipe treatment. The fate of different TrOCs in conventional wastewater treatment plants depends on their physical, chemical and biological properties and ranges from no removal to complete removal (80). Upgrading treatment plants with advanced technologies for the elimination of TrOCs is widely investigated and has already been implemented in some countries, for example Switzerland (81). The main methods being considered are ozonation and other AOPs, activated carbon adsorption (powdered or granular) and membrane filtration (nanofiltration or reverse osmosis) (82-84).

Figure 1.6.1 presents the main criteria for the assessment of advanced treatment technologies for the removal of TrOCs from water or wastewater. Each technology has advantages and disadvantages, regarding its capital and operational costs, efficiency, feasibility and associated environmental effects. The high performance of a certain technology should not compromise the affordability of water or sanitation services, nor should it be outweighed by the negative effects of energy- and chemical-intensive treatment on the wider environment (85, 86). For example, nanofiltration and reverse osmosis are cost-intensive due to high energy consumption and generate a concentrated waste stream which needs to be treated (84). The main drawback of ozonation is the formation of known and unknown by-products, but it remains one of the best candidates for large-scale abatement of TrOCs (87).

The principle driver for the implementation of advanced treatment is or will be legislation that aims to protect human and environmental health. In 2015 the European Commission published its first Watch List of substances that may pose a significant risk to or via the aquatic environment for EU-wide monitoring (88), with an updated version in 2018 (89). The current list includes hormones, antibiotics and pesticides. Since 2016, Switzerland has implemented one of the most comprehensive management strategies for TrOCs worldwide, which involves relevant legislation and the upgrade of about 100 wastewater treatment plants (81). It is expected that future

regulations will become tighter in more countries, enforcing toxicologically-based limits for the concentration of TrOCs in aqueous matrices and further driving the implementation of mitigating measures, including advanced treatment (90, 91).

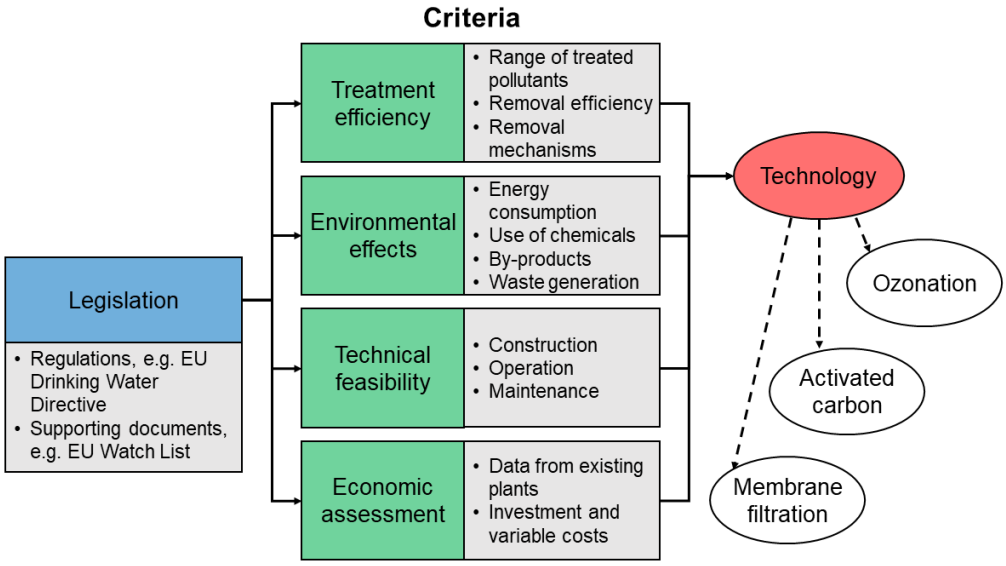

Figure 1.6.1. Criteria for the selection of advanced treatment technologies for the removal of trace organic contaminants from water or wastewater. Legislation is shown as the main driver of change. Adapted from (87).

1.7 Ozonation of trace organic contaminants

The reactivity of TrOCs with ozone is typically expressed with second order rate constants (k_{O3} in M^{-1} s^{-1}). Depending on the molecular structure of the compound, these vary over 10 orders of magnitude, while they are also affected by temperature and pH (92). Several compilations of rate constants for reactions of TrOCs with ozone exist in the literature, for example (93, 94), while more are constantly being reported. Kinetic parameters, combined with characteristics of the water matrix, can be used to predict the abatement of TrOCs in ozonation treatment (95, 96).

In addition to kinetics, the advancement of analytical techniques has enabled the development of a large dataset of ozonation products of TrOCs (97-99). Some examples of the products formed from compounds containing five major ozone-reactive functional groups are presented in Table 1.7.1. Ozonation products may have a structure very similar to that of the parent compound (e.g. containing just one additional oxygen atom) or may be substantially different (e.g. after cleavage of

carbon-carbon bonds). The formation and the potential removal through further reaction with ozone of ozonation products depend on the applied ozone dose (100).

Table 1.7.1. Main ozonation products of trace organic contaminants grouped according to their functional groups. Adapted from (97).

Compound group	Main ozonation products	Example trace organic contaminant
Olefins	Aldehydes, ketones and carboxylic acids formed from cleavage of the double bond	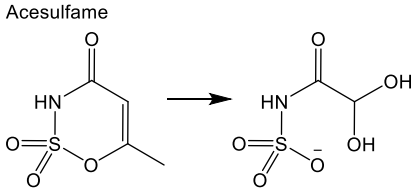
Tertiary aliphatic amines	*N*-oxides, dealkylated amines	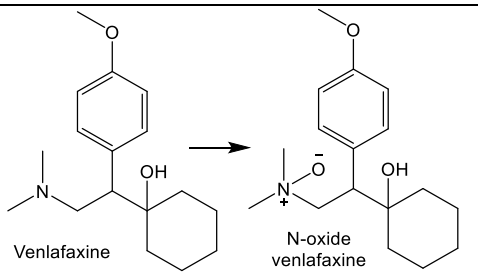
Secondary aliphatic amines	Hydroxylamines, dealkylated amines	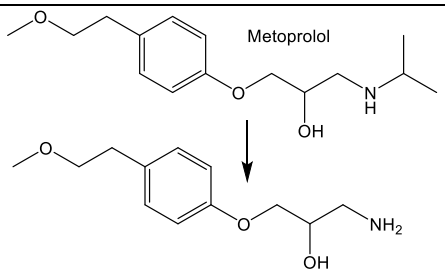
Activated aromatic compounds	Hydroxylated-ring compounds, aldehydes and carboxylic acids formed from ring cleavage	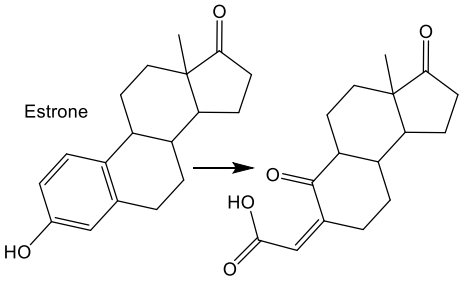
Sulfides	Sulfoxides	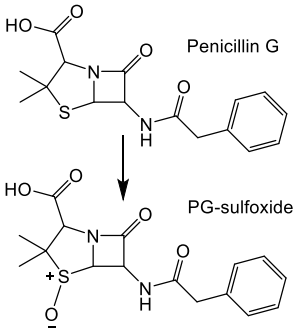

Despite the existing knowledge on ozonation products, certain compound classes of TrOCs were until recently overlooked or remain understudied. For example, the ozonation of five-membered heterocycles containing nitrogen (azoles) was only recently elucidated (101). The aqueous ozonation chemistry of five-membered heterocycles containing an oxygen atom (furans) is poorly understood. New information is still emerging on the oxidative transformation of well-investigated compounds, including phenols (102), and aliphatic amines (103).

Furthermore, the vast majority of relevant studies focus on the molecular structure of ozonation products, with only a few looking into their properties, such as toxicity, biodegradability and fate in post-ozonation processes (104-107). This information is crucial to assess the environmental risk posed by ozone TPs and whether mitigating measures are required. The levels of ozonation products of TrOCs could potentially be controlled either during the ozonation treatment (e.g. through optimisation of operational parameters or alternative ozone systems) or via ozonation post-treatment (e.g. sand filtration) (108, 109). Figure 1.7.1 summarises the different products formed in ozonation and some strategies which can be applied to manage the potential risk posed by them.

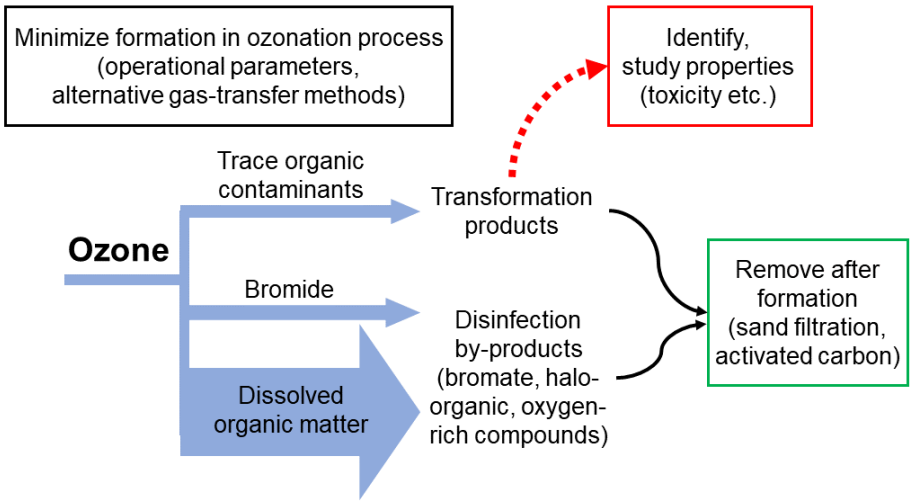

Figure 1.7.1. Formation of transformation products and disinfection by-products during ozonation, adapted from (110), alongside strategies to minimise their release into the environment.

1.8 Aims and objectives

The aim of this PhD thesis was to investigate the implications of trace organic contaminant degradation, ozonation product formation and ozone mass transfer for water and wastewater ozonation treatment. This aim was addressed through the following objectives:

- Conduct single and multi-compound ozonation studies focusing on trace organic contaminants whose ozone reactivity and transformation products were previously unknown or poorly understood.
- Investigate the properties of ozonation products of trace organic contaminants, focusing on biodegradability and toxicity.
- Develop a lab-based system to combine ozonation with continuous long-term biofiltration, which was previously only feasible at pilot- or large-scale plants.
- Investigate non-traditional methods for transferring ozone gas into the water, using porous and non-porous membranes.
- Explore the potential of biofiltration post-treatment and bubble-less ozone transfer to reduce the formation or discharge of ozone transformation products and by-products.

1.9 Outline of the thesis

This thesis was written in the alternative format. Chapter 1 provides a general introduction on ozonation and trace organic contaminants and presents the aims and objectives of the research. Chapters 2 to 5 consist of research results, presented either in paper format for publication in peer-reviewed journals (Chapters 2, 3 and 5), or in conventional thesis chapter format (Chapter 4). Each chapter contains an introductory section reviewing relevant literature, a methods section, a results and discussion section, a conclusions section and a Supplementary Information (SI) section or Appendix.

In Chapter 2 a large database of both literature and experimental data was compiled for 90 structurally diverse TrOCs, with a focus on less studied compound classes including illicit drugs and their metabolites.

Chapter 3 describes a novel laboratory setup that was designed to facilitate research on the fate of ozonation products of TrOCs in sand filtration post-treatment. Five selected TrOCs and their ozonation products were investigated in two case studies, one for tertiary wastewater treatment and one for water purification.

In Chapter 4 bubble-less ozonation using membrane contactors was investigated as an alternative to the traditional ozone bubbling approach. The mass transfer mechanisms of ozone, the abatement of trace organic contaminants and the formation of bromate were studied in two membrane ozonation setups: a single tube contactor with a non-porous membrane and a hollow fibre module with multiple porous membranes.

In Chapter 5 furan derivatives were targeted as a class of trace organic contaminants with poorly understood ozonation chemistry. Both the kinetics and the transformation products of the ozonation of furans were studied. Using a recently developed analytical approach, the formation of α,β-unsaturated dicarbonyls with ecotoxicological relevance was analysed.

Chapter 6 contains general conclusions drawn from the work presented in this thesis and recommendations for future research.

1.10 References

1. Crittenden JC, Trussell RR, Hand DW, Howe KJ, Tchobanoglous G. Introduction. In: Crittenden JC, Trussell RR, Hand DW, Howe KJ, Tchobanoglous G, editors. MWH's Water Treatment: Principles and Design, Third Edition: Wiley; 2012. p. 1-16.
2. Gray NF. Water Treatment and Distribution. In: Gray NF, editor. Water Technology (Third Edition). Oxford: Butterworth-Heinemann; 2010. p. 301-27.
3. Crittenden JC, Trussell RR, Hand DW, Howe KJ, Tchobanoglous G. Water Quality Management Strategies. In: Crittenden JC, Trussell RR, Hand DW, Howe KJ, Tchobanoglous G, editors. MWH's Water Treatment: Principles and Design, Third Edition: Wiley; 2012. p. 165-224.
4. Crittenden JC, Trussell RR, Hand DW, Howe KJ, Tchobanoglous G. Disinfection. In: Crittenden JC, Trussell RR, Hand DW, Howe KJ, Tchobanoglous G, editors. MWH's Water Treatment: Principles and Design, Third Edition: Wiley; 2012. p. 903-1032.
5. Singer PC, Reckhow DA. Chemical Oxidation. In: A.W.W. Association, Edzwald JK, editors. Water Quality & Treatment: A Handbook on Drinking Water: McGraw-Hill Education; 2010.
6. Miklos DB, Remy C, Jekel M, Linden KG, Drewes JE, Hubner U. Evaluation of advanced oxidation processes for water and wastewater treatment - A critical review. Water Res. 2018;139:118-31.
7. Comninellis C, Kapalka A, Malato S, Parsons SA, Poulios I, Mantzavinos D. Advanced oxidation processes for water treatment: advances and trends for R&D. Journal of Chemical Technology & Biotechnology. 2008;83(6):769-76.
8. Ramalho RS. Introduction. In: Ramalho RS, editor. Introduction to Wastewater Treatment Processes (Second Edition). San Diego: Academic Press; 1983. p. 1-23.
9. Leenheer JA, Croué J-P. Peer Reviewed: Characterizing Aquatic Dissolved Organic Matter. Environmental Science & Technology. 2003;37(1):18A-26A.
10. Rook JJ. Formation of haloforms during chlorination of natural waters. Water Treatment Exam. 1974;23:234–43.

11. Richardson SD, Plewa MJ. To regulate or not to regulate? What to do with more toxic disinfection by-products? Journal of Environmental Chemical Engineering. 2020;8(4).
12. Diana M, Felipe-Sotelo M, Bond T. Disinfection byproducts potentially responsible for the association between chlorinated drinking water and bladder cancer: A review. Water Res. 2019;162:492-504.
13. Sauvé S, Desrosiers M. A review of what is an emerging contaminant. Chemistry Central Journal. 2014;8(1):15.
14. Richardson SD, Ternes TA. Water Analysis: Emerging Contaminants and Current Issues. Anal Chem. 2018;90(1):398-428.
15. Tilley E, Ulrich L, Lüthi C, Reymond P, Schertenleib R, Zurbrügg C. Compendium of Sanitation Systems and Technologies 2nd Edition. Dübendorf, Switzerland: Swiss Federal Institute of Aquatic Science and Technology (Eawag); 2014.
16. Comeau Y. Microbial Metabolism. In: Henze M, van Loosdrecht MCM, Ekama GA, Brdjanovic D, editors. Biological Wastewater Treatment: IWA Publishing; 2008. p. 9-32.
17. Schwarzenbach RP, Egli T, Hofstetter TB, Gunten Uv, Wehrli B. Global Water Pollution and Human Health. Annual Review of Environment and Resources. 2010;35(1):109-36.
18. Escher BI, Stapleton HM, Schymanski EL. Tracking complex mixtures of chemicals in our changing environment. Science. 2020;367(6476):388-92.
19. Salgot M, Huertas E, Weber S, Dott W, Hollender J. Wastewater reuse and risk: definition of key objectives. Desalination. 2006;187(1):29-40.
20. Shon HK, Vigneswaran S, Snyder SA. Effluent Organic Matter (EfOM) in Wastewater: Constituents, Effects, and Treatment. Critical Reviews in Environmental Science and Technology. 2006;36(4):327-74.
21. Gupta VK, Ali I, Saleh TA, Nayak A, Agarwal S. Chemical treatment technologies for waste-water recycling - An overview. RSC Advances. 2012;2(16):6380-8.
22. Gottschalk C, Libra JA, Saupe A. Ozone Applications. In: Gottschalk C, Libra JA, Saupe A, editors. Ozonation of Water and Waste Water: Wiley; 2010. p. 27-65.
23. Le Paulouë J, Langlais B. State-of-the-Art of Ozonation in France. Ozone: Science & Engineering. 1999;21(2):153-62.

24. Rosario-Ortiz F, Rose J, Speight V, Gunten Uv, Schnoor J. How do you like your tap water? Science. 2016;351(6276):912-4.
25. Von Sonntag C, Von Gunten U. Integration of ozonation in drinking water and wastewater process trains. In: Von Sonntag C, Von Gunten U, editors. Chemistry of ozone in water and wastewater treatment: IWA publishing; 2012.
26. Mundy B, Kuhnel B, Hunter G, Jarnis R, Funk D, Walker S, Burns N, Drago J, Nezgod W, Huang J, Rakness K, Jasim S, Joost R, Kim R, Muri J, Nattress J, Oneby M, Sosebee A, Thompson C, Walsh M, Schulz C. A Review of Ozone Systems Costs for Municipal Applications. Report by the Municipal Committee – IOA Pan American Group. Ozone: Science & Engineering. 2018;40(4):266-74.
27. Loeb BL, Thompson CM, Drago J, Takahara H, Baig S. Worldwide Ozone Capacity for Treatment of Drinking Water and Wastewater: A Review. Ozone: Science & Engineering. 2012;34(1):64-77.
28. Rakness KL. Ozone Side-Stream Design Options and Operating Considerations. Ozone: Science & Engineering. 2007;29(4):231-44.
29. Oneby MA, Bromley CO, Borchardt JH, Harrison DS. Ozone Treatment of Secondary Effluent at U.S. Municipal Wastewater Treatment Plants. Ozone: Science & Engineering. 2010;32(1):43-55.
30. Gottschalk C, Libra JA, Saupe A. Mass Transfer. In: Gottschalk C, Libra JA, Saupe A, editors. Ozonation of Water and Waste Water: Wiley; 2010. p. 163-203.
31. Gottschalk C, Libra JA, Saupe A. Experimental Equipment and Analytical Methods. In: Gottschalk C, Libra JA, Saupe A, editors. Ozonation of Water and Waste Water2010. p. 113-62.
32. Pines DS, Min K-N, Ergas SJ, Reckhow DA. Investigation of an Ozone Membrane Contactor System. Ozone: Science & Engineering. 2005;27(3):209-17.
33. von Gunten U. Ozonation of drinking water: Part II. Disinfection and by-product formation in presence of bromide, iodide or chlorine. Water Research. 2003;37(7):1469-87.
34. Gottschalk C, Libra JA, Saupe A. Experimental Design. In: Gottschalk C, Libra JA, Saupe A, editors. Ozonation of Water and Waste Water: Wiley; 2010. p. 67-112.
35. Gottschalk C, Libra JA, Saupe A. Reaction Mechanism. In: Gottschalk C, Libra JA, Saupe A, editors. Ozonation of Water and Waste Water: Wiley; 2010. p. 13-26.

36. Elovitz MS, von Gunten U. Hydroxyl Radical/Ozone Ratios During Ozonation Processes. I. The R_{ct} Concept. Ozone: Science & Engineering. 1999;21(3):239-60.

37. Elovitz MS, von Gunten U, Kaiser H-P. Hydroxyl Radical/Ozone Ratios During Ozonation Processes. II. The Effect of Temperature, pH, Alkalinity, and DOM Properties. Ozone: Science & Engineering. 2000;22(2):123-50.

38. von Gunten U. Ozonation of drinking water: Part I. Oxidation kinetics and product formation. Water Research. 2003;37(7):1443-67.

39. Lee Y, von Gunten U. Oxidative transformation of micropollutants during municipal wastewater treatment: Comparison of kinetic aspects of selective (chlorine, chlorine dioxide, ferrate^{VI}, and ozone) and non-selective oxidants (hydroxyl radical). Water Research. 2010;44(2):555-66.

40. Parsons S. Advanced Oxidation Processes for Water and Wastewater Treatment: IWA Publishing; 2004.

41. Escobar IC, Randall AA. Assimilable organic carbon (AOC) and biodegradable dissolved organic carbon (BDOC): complementary measurements. Water Research. 2001;35(18):4444-54.

42. Richardson SD, Thruston AD, Caughran TV, Chen PH, Collette TW, Floyd TL, Schenck KM, Lykins BW, Sun G-r, Majetich G. Identification of New Ozone Disinfection Byproducts in Drinking Water. Environmental Science & Technology. 1999;33(19):3368-77.

43. Le Lacheur RM, Sonnenberg LB, Singer PC, Christman RF, Charles MJ. Identification of carbonyl compounds in environmental samples. Environmental Science & Technology. 1993;27(13):2745-53.

44. Hu JY, Wang ZS, Ng WJ, Ong SL. The effect of water treatment processes on the biological stability of potable water. Water Research. 1999;33(11):2587-92.

45. Papageorgiou A, Voutsa D, Papadakis N. Occurrence and fate of ozonation by-products at a full-scale drinking water treatment plant. Science of The Total Environment. 2014;481:392-400.

46. Yavich AA, Lee KH, Chen KC, Pape L, Masten SJ. Evaluation of biodegradability of NOM after ozonation. Water Research. 2004;38(12):2839-46.

47. World Health Organization. Guidelines for drinking-water quality, 4th edition, incorporating the 1st addendum. 2017.

48. Soltermann F, Abegglen C, Gotz C, von Gunten U. Bromide Sources and Loads in Swiss Surface Waters and Their Relevance for Bromate Formation during Wastewater Ozonation. Environ Sci Technol. 2016;50(18):9825-34.

49. Johnson CJ, Singer PC. Impact of a magnetic ion exchange resin on ozone demand and bromate formation during drinking water treatment. Water Research. 2004;38(17):3738-50.

50. Soltermann F, Abegglen C, Tschui M, Stahel S, von Gunten U. Options and limitations for bromate control during ozonation of wastewater. Water Research. 2017;116:76-85.

51. Yang J, Dong Z, Jiang C, Wang C, Liu H. An overview of bromate formation in chemical oxidation processes: Occurrence, mechanism, influencing factors, risk assessment, and control strategies. Chemosphere. 2019;237:124521.

52. Merle T, Pronk W, von Gunten U. MEMBRO$_3$X, a Novel Combination of a Membrane Contactor with Advanced Oxidation (O_3/H_2O_2) for Simultaneous Micropollutant Abatement and Bromate Minimization. Environmental Science & Technology Letters. 2017;4(5):180-5.

53. Andrzejewski P, Kasprzyk-Hordern B, Nawrocki J. *N*-nitrosodimethylamine (NDMA) formation during ozonation of dimethylamine-containing waters. Water Research. 2008;42(4–5):863-70.

54. Schmidt CK, Brauch H-J. N,N-Dimethylsulfamide as Precursor for *N*-Nitrosodimethylamine (NDMA) Formation upon Ozonation and its Fate During Drinking Water Treatment. Environmental Science & Technology. 2008;42(17):6340-6.

55. Krasner SW, Mitch WA, McCurry DL, Hanigan D, Westerhoff P. Formation, precursors, control, and occurrence of nitrosamines in drinking water: A review. Water Research. 2013;47(13):4433-50.

56. Hollender J, Zimmermann SG, Koepke S, Krauss M, McArdell CS, Ort C, Singer H, Von Gunten U, Siegrist H. Elimination of organic micropollutants in a municipal wastewater treatment plant upgraded with a full-scale post-ozonation followed by sand filtration. Environmental Science and Technology. 2009;43(20):7862-9.

57. Li X-F, Mitch WA. Drinking Water Disinfection Byproducts (DBPs) and Human Health Effects: Multidisciplinary Challenges and Opportunities. Environmental Science & Technology. 2018;52(4):1681-9.

58. Petrie B, Youdan J, Barden R, Kasprzyk-Hordern B. Multi-residue analysis of 90 emerging contaminants in liquid and solid environmental matrices by ultra-high-performance liquid chromatography tandem mass spectrometry. J Chromatogr A. 2016;1431:64-78.

59. Barbosa MO, Moreira NFF, Ribeiro AR, Pereira MFR, Silva AMT. Occurrence and removal of organic micropollutants: An overview of the watch list of EU Decision 2015/495. Water Res. 2016;94:257-79.

60. Benotti MJ, Trenholm RA, Vanderford BJ, Holady JC, Stanford BD, Snyder SA. Pharmaceuticals and Endocrine Disrupting Compounds in U.S. Drinking Water. Environmental Science & Technology. 2009;43(3):597-603.

61. Schwarzenbach RP, Escher BI, Fenner K, Hofstetter TB, Johnson CA, Von Gunten U, Wehrli B. The challenge of micropollutants in aquatic systems. Science. 2006;313(5790):1072-7.

62. Pal A, Gin KY, Lin AY, Reinhard M. Impacts of emerging organic contaminants on freshwater resources: review of recent occurrences, sources, fate and effects. Sci Total Environ. 2010;408(24):6062-9.

63. Luo Y, Guo W, Ngo HH, Nghiem LD, Hai FI, Zhang J, Liang S, Wang XC. A review on the occurrence of micropollutants in the aquatic environment and their fate and removal during wastewater treatment. Science of the Total Environment. 2014;473-474:619-41.

64. Margot J, Rossi L, Barry DA, Holliger C. A review of the fate of micropollutants in wastewater treatment plants. Wiley Interdisciplinary Reviews: Water. 2015;2(5):457-87.

65. Oberg G, Leopold A. On the role of review papers in the face of escalating publication rates - a case study of research on contaminants of emerging concern (CECs). Environ Int. 2019;131:104960.

66. Hignite C, Azarnoff DL. Drugs and drug metabolites as environmental contaminants: Chlorophenoxyisobutyrate and salicylic acid in sewage water effluent. Life Sci. 1977;20(2):337-41.

67. Kasprzyk-Hordern B. Pharmacologically active compounds in the environment and their chirality. Chemical Society Reviews. 2010;39(11):4466-503.

68. Petrie B, Youdan J, Barden R, Kasprzyk-Hordern B. New Framework To Diagnose the Direct Disposal of Prescribed Drugs in Wastewater - A Case Study of the Antidepressant Fluoxetine. Environ Sci Technol. 2016;50(7):3781-9.

69. Baker DR, Kasprzyk-Hordern B. Spatial and temporal occurrence of pharmaceuticals and illicit drugs in the aqueous environment and during wastewater treatment: New developments. Science of The Total Environment. 2013;454-455:442-56.

70. Pal R, Megharaj M, Kirkbride KP, Naidu R. Illicit drugs and the environment — A review. Science of The Total Environment. 2013;463-464:1079-92.

71. Subedi B, Kannan K. Mass Loading and Removal of Select Illicit Drugs in Two Wastewater Treatment Plants in New York State and Estimation of Illicit Drug Usage in Communities through Wastewater Analysis. Environmental Science & Technology. 2014;48(12):6661-70.

72. Peng Y, Gautam L, Hall SW. The detection of drugs of abuse and pharmaceuticals in drinking water using solid-phase extraction and liquid chromatography-mass spectrometry. Chemosphere. 2019;223:438-47.

73. Chibwe L, Titaley IA, Hoh E, Simonich SLM. Integrated Framework for Identifying Toxic Transformation Products in Complex Environmental Mixtures. Environmental Science & Technology Letters. 2017;4(2):32-43.

74. Evgenidou EN, Konstantinou IK, Lambropoulou DA. Occurrence and removal of transformation products of PPCPs and illicit drugs in wastewaters: a review. Sci Total Environ. 2015;505:905-26.

75. Wilkinson J, Hooda PS, Barker J, Barton S, Swinden J. Occurrence, fate and transformation of emerging contaminants in water: An overarching review of the field. Environmental Pollution. 2017;231:954-70.

76. Escher BI, Fenner K. Recent advances in environmental risk assessment of transformation products. Environ Sci Technol. 2011;45(9):3835-47.

77. Toolaram AP, Kümmerer K, Schneider M. Environmental risk assessment of anti-cancer drugs and their transformation products: A focus on their genotoxicity characterization-state of knowledge and short comings. Mutation Research/Reviews in Mutation Research. 2014;760:18-35.

78. Hernando Guil MD, Martínez-Bueno MJ, Duran L, Navas JM, Fernández-Alba AR. Steps Toward a Regulatory Framework for Transformation Products in Water. In: Lambropoulou DA, Nollet LML, editors. Transformation Products of Emerging Contaminants in the Environment: Wiley; 2014. p. 877-902.

79. Kümmerer K, Dionysiou DD, Olsson O, Fatta-Kassinos D. A path to clean water. Science. 2018;361(6399):222.

80. Tran NH, Reinhard M, Gin KY-H. Occurrence and fate of emerging contaminants in municipal wastewater treatment plants from different geographical regions-a review. Water Research. 2018;133:182-207.
81. Eggen RIL, Hollender J, Joss A, Schärer M, Stamm C. Reducing the Discharge of Micropollutants in the Aquatic Environment: The Benefits of Upgrading Wastewater Treatment Plants. Environmental Science & Technology. 2014;48(14):7683-9.
82. Joss A, Siegrist H, Ternes TA. Are we about to upgrade wastewater treatment for removing organic micropollutants? Water Science and Technology. 2008;57(2):251-5.
83. Margot J, Kienle C, Magnet A, Weil M, Rossi L, de Alencastro LF, Abegglen C, Thonney D, Chèvre N, Schärer M, Barry DA. Treatment of micropollutants in municipal wastewater: Ozone or powdered activated carbon? Science of the Total Environment. 2013;461-462:480-98.
84. Rizzo L, Malato S, Antakyali D, Beretsou VG, Dolic MB, Gernjak W, Heath E, Ivancev-Tumbas I, Karaolia P, Lado Ribeiro AR, Mascolo G, McArdell CS, Schaar H, Silva AMT, Fatta-Kassinos D. Consolidated vs new advanced treatment methods for the removal of contaminants of emerging concern from urban wastewater. Sci Total Environ. 2019;655:986-1008.
85. Jones OAH, Green PG, Voulvoulis N, Lester JN. Questioning the Excessive Use of Advanced Treatment to Remove Organic Micropollutants from Wastewater. Environmental Science & Technology. 2007;41(14):5085-9.
86. Rahman SM, Eckelman MJ, Onnis-Hayden A, Gu AZ. Comparative Life Cycle Assessment of Advanced Wastewater Treatment Processes for Removal of Chemicals of Emerging Concern. Environmental Science & Technology. 2018;52(19):11346-58.
87. Bui XT, Vo TP, Ngo HH, Guo WS, Nguyen TT. Multicriteria assessment of advanced treatment technologies for micropollutants removal at large-scale applications. Sci Total Environ. 2016;563-564:1050-67.
88. European Commission. Implementing decision (EU) 2015/495 of 20 March 2015 establishing a watch list of substances for Union-wide monitoring in the field of water policy pursuant to Directive 2008/105/EC of the European Parliament and of the Council. 2015.

89. European Commission. Implementing decision (EU) 2018/840 of 5 June 2018 establishing a watch list of substances for Union-wide monitoring in the field of water policy pursuant to Directive 2008/105/EC of the European Parliament and of the Council and repealing Commission Implementing Decision (EU) 2015/495. 2018.
90. Bieber S, Snyder SA, Dagnino S, Rauch-Williams T, Drewes JE. Management strategies for trace organic chemicals in water - A review of international approaches. Chemosphere. 2018;195:410-26.
91. Audenaert W, Chys M, Auvinen H, Dumoulin A, Rousseau D, Van Hulle S. (Future) regulation of trace organic compounds in WWTP effluents as a driver of advanced wastewater treatment. Ozone News. 2014;42(6):17-23.
92. Von Sonntag C, Von Gunten U. Physical and chemical properties of ozone. In: Von Sonntag C, Von Gunten U, editors. Chemistry of ozone in water and wastewater treatment: IWA publishing; 2012.
93. Ikehata K, Gamal El-Din M. Aqueous Pesticide Degradation by Ozonation and Ozone-Based Advanced Oxidation Processes: A Review (Part I). Ozone: Science & Engineering. 2005;27(2):83-114.
94. Ikehata K, Jodeiri Naghashkar N, Gamal El-Din M. Degradation of Aqueous Pharmaceuticals by Ozonation and Advanced Oxidation Processes: A Review. Ozone: Science & Engineering. 2006;28(6):353-414.
95. Lee Y, Gerrity D, Lee M, Bogeat AE, Salhi E, Gamage S, Trenholm RA, Wert EC, Snyder SA, von Gunten U. Prediction of Micropollutant Elimination during Ozonation of Municipal Wastewater Effluents: Use of Kinetic and Water Specific Information. Environmental Science & Technology. 2013;47(11):5872-81.
96. Liu Z, Yang Y, Shao C, Ji Z, Wang Q, Wang S, Guo Y, Demeestere K, Hulle SV. Ozonation of trace organic compounds in different municipal and industrial wastewaters: Kinetic-based prediction of removal efficiency and ozone dose requirements. Chemical Engineering Journal. 2020;387.
97. Hübner U, von Gunten U, Jekel M. Evaluation of the persistence of transformation products from ozonation of trace organic compounds – A critical review. Water Research. 2015;68:150-70.
98. Lee Y, von Gunten U. Advances in predicting organic contaminant abatement during ozonation of municipal wastewater effluent: reaction kinetics, transformation products, and changes of biological effects. Environmental Science: Water Research & Technology. 2016;2(3):421-42.

99. Deeb AA, Stephan S, Schmitz OJ, Schmidt TC. Suspect screening of micropollutants and their transformation products in advanced wastewater treatment. Sci Total Environ. 2017;601-602:1247-53.
100. Kharel S, Stapf M, Miehe U, Ekblad M, Cimbritz M, Falas P, Nilsson J, Sehlen R, Bester K. Ozone dose dependent formation and removal of ozonation products of pharmaceuticals in pilot and full-scale municipal wastewater treatment plants. Sci Total Environ. 2020;731:139064.
101. Tekle-Röttering A, Lim S, Reisz E, Lutze HV, Abdighahroudi MS, Willach S, Schmidt W, Tentscher PR, Rentsch D, McArdell CS, Schmidt TC, von Gunten U. Reactions of pyrrole, imidazole, and pyrazole with ozone: kinetics and mechanisms. Environmental Science: Water Research & Technology. 2020;6(4):976-92.
102. Prasse C, Ford B, Nomura DK, Sedlak DL. Unexpected transformation of dissolved phenols to toxic dicarbonyls by hydroxyl radicals and UV light. Proc Natl Acad Sci U S A. 2018;115(10):2311-6.
103. Lim S, McArdell CS, von Gunten U. Reactions of aliphatic amines with ozone: Kinetics and mechanisms. Water Research. 2019;157:514-28.
104. Zucker I, Mamane H, Riani A, Gozlan I, Avisar D. Formation and degradation of N-oxide venlafaxine during ozonation and biological post-treatment. Sci Total Environ. 2018;619-620:578-86.
105. Gartiser S, Hafner C, Kronenberger-Schäfer K, Happel O, Trautwein C, Kümmerer K. Approach for detecting mutagenicity of biodegraded and ozonated pharmaceuticals, metabolites and transformation products from a drinking water perspective. Environmental Science and Pollution Research. 2012;19(8):3597-609.
106. Han Y, Ma M, Li N, Hou R, Huang C, Oda Y, Wang Z. Chlorination, chloramination and ozonation of carbamazepine enhance cytotoxicity and genotoxicity: Multi-endpoint evaluation and identification of its genotoxic transformation products. J Hazard Mater. 2018;342:679-88.
107. Pohl J, Golovko O, Carlsson G, Eriksson J, Glynn A, Orn S, Weiss J. Carbamazepine Ozonation Byproducts: Toxicity in Zebrafish (Danio rerio) Embryos and Chemical Stability. Environ Sci Technol. 2020;54(5):2913-21.
108. Hübner U, Seiwert B, Reemtsma T, Jekel M. Ozonation products of carbamazepine and their removal from secondary effluents by soil aquifer treatment – Indications from column experiments. Water Research. 2014;49:34-43.

109. Bourgin M, Beck B, Boehler M, Borowska E, Fleiner J, Salhi E, Teichler R, von Gunten U, Siegrist H, McArdell CS. Evaluation of a full-scale wastewater treatment plant upgraded with ozonation and biological post-treatments: Abatement of micropollutants, formation of transformation products and oxidation by-products. Water Research. 2018;129:486-98.
110. von Gunten U. Oxidation Processes in Water Treatment: Are We on Track? Environ Sci Technol. 2018;52(9):5062-75.

Chapter 2: Simultaneous ozonation of 90 organic micropollutants including illicit drugs and their metabolites in different water matrices

This chapter is presented in publication format. This work was published in Environmental Science: Water Research & Technology (RSC) in April 2020 (DOI: https://doi.org/10.1039/D0EW00260G). An additional Supporting Information file in xlsx format was not included in the thesis but is available online.

Context: The number of chemical compounds that are classified as organic micropollutants is so large, that decades of research on their oxidation treatment have yet to elucidate the ozonation of all compound classes that are relevant for the water cycle. The group of Prof Kasprzyk-Hordern has developed a number of liquid chromatography-mass spectrometry (LC-MS) methods for the multi-residue analysis of organic micropollutants in different matrices. Using one of these methods for analysis allowed us to perform a multi-compound ozonation study for a set of 90 organic micropollutants. We thus compiled a large database of both literature and experimental data on the ozone reactivity of a high number of structurally diverse compounds, including several understudied micropollutants such as illicit drugs and their metabolites.

Note: The term ‘organic micropollutant’ is used in this chapter as synonymous to the term ‘trace organic contaminant’ that is used elsewhere in this thesis.

Contributions: The following work was performed by the author of this thesis under the supervision of Dr Jannis Wenk and the co-supervision of Prof Barbara Kasprzyk-Hordern:

- Literature research
- Analysis of experimental data

- Data interpretation and visualisation, and writing the manuscript

Fernanda Siqueira Souza performed the batch ozonation experiments. Liquid chromatography-mass spectrometry analysis of samples was conducted by the BKH group (Dr Bruce Petrie).

First authorship of the manuscript is shared between the author of this thesis and Fernanda Siqueira Souza.

Simultaneous ozonation of 90 organic micropollutants including illicit drugs and their metabolites in different water matrices

Garyfalia A. Zoumpouli[a,b,c], Fernanda Siqueira Souza[b,c,d,e], Bruce Petrie[c,f,g], Liliana Amaral Féris[d], Barbara Kasprzyk-Hordern[c,f], Jannis Wenk[b,c,*]

[a] Centre for Doctoral Training, Centre for Sustainable Chemical Technologies, University of Bath, Bath BA2 7AY, UK

[b] Department of Chemical Engineering, University of Bath, Bath BA2 7AY, UK.

[c] Water Innovation & Research Centre (WIRC), University of Bath, Bath BA2 7AY, UK

[d] Federal University of Rio Grande do Sul, Department of Chemical Engineering, Porto Alegre, Brazil.

[e] La Salle University, 2288 Victor Barreto Av, 92010-000 Canoas, Rio Grande do Sul, Brazil.

[f] Department of Chemistry, University of Bath, Bath BA2 7AY, Bath, UK

[g] School of Pharmacy and Life Sciences, Robert Gordon University, Aberdeen AB10 7GJ, UK

*Corresponding author

2.1 Abstract

The ozonation of 90 chemically diverse organic micropollutants (OMPs) including four classes of illicit drugs and their metabolites was studied in pure buffered water, tap water and wastewater effluent at three specific ozone doses and three pH levels. The second order rate constants for the reaction of 40 OMPs with ozone were known and span across 8 orders of magnitude, from below 1 M^{-1} s^{-1} to above 10^7 M^{-1} s^{-1}. 47 of the tested OMPs were removed to at least 90% at the highest specific ozone dose of 0.3 mM O_3 (mM C)$^{-1}$ at pH 7. However, most illicit drugs, including cocainics, amphetamines and ecstasy-group compounds, were ozone-resistant due to their lack of ozone-reactive functional groups. Exceptions included some opioids and the cocaine biomarker anhydroecgonine methylester which contain olefinic bonds and/or activated benzene rings. Different removal trends at different pH for OMPs were due to the combined effect of target compound speciation and ozone stability, leading to elimination of less than 70% for all OMPs at pH 11. In both tap water and wastewater

effluent scavenging by matrix components led to lower ozone exposure compared to pure buffered water and consequently lower removal of OMPs. This multi-compound ozonation study utilised liquid chromatography-mass spectrometry to provide a large dataset on the removal of environmentally relevant OMPs, including those of interest for drinking water regulations. Besides including pharmaceutically active compounds that have not been studied with ozone before (e.g. gliclazide, anhydroecgonine methylester, quetiapine, 6-monoacetylmorphine), this study simultaneously shows ozonation data for a wide range of illicit drugs.

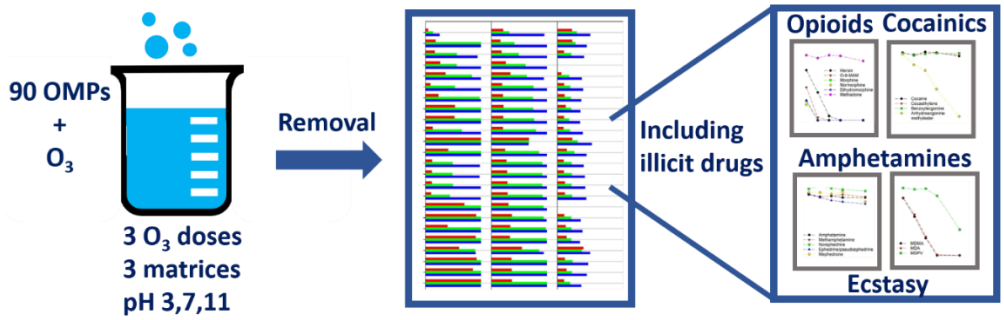

2.2 Water impact

Ozonation is a promising technology for the removal of organic micropollutants from water. Here, ozonation results for 90 chemically diverse micropollutants including illicit drugs are reported and interpreted based on compound chemical structure. The study provides a valuable ozonation database for a large variety of micropollutants with specific focus on occurrence and ozonation of illicit drugs in drinking water.

2.3 Introduction

Many different organic micropollutants (OMPs) including pharmaceuticals, personal care products, hormones and their transformation products can be found at trace concentrations in surface water, groundwater and finished drinking water (1-4). OMPs may reach drinking water resources through numerous routes, with their main sources being the discharge of wastewater effluent and diffuse pollution, such as agricultural and urban runoff (5, 6). OMPs have raised scientific and public concern regarding their impact on the environment and on human health, including short-term and long-

term toxicity, endocrine disruption, antibiotic resistance of microorganisms and accumulation in soils, plants and animals (7, 8). A group of OMPs of particular interest are illicit drugs and their metabolites (9-12), due to biological activity and largely unknown effects on the environment and on water quality (13, 14).

Ozonation is among the most effective methods for the abatement of OMPs in full-scale water treatment applications (15). Ozone is a strong oxidant which reacts with organic compounds in water either directly, or indirectly through free radicals produced from ozone decomposition (16). The ozonation of single compounds has been extensively studied in terms of degradation, reaction kinetics and identification of transformation products (17-20). Analytical advancements have also enabled the investigation of the simultaneous ozonation of mixtures of OMPs. Multi-component ozonation studies have been performed at lab-, pilot- and full-scale and have included a wide range of compounds (21-25). However, the ozonation of some classes of OMPs, including illicit drugs and their metabolites, remains less conclusively studied (11, 26-28).

The reactivity of organic compounds with ozone depends on their chemical structure, with second order rate constants reaching across several orders of magnitude (29). Kinetic parameters of ozonation reactions can be determined experimentally or calculated through QSAR (quantitative structure–activity relationship) models (30). In complex water matrices, such as surface water, the properties of the matrix affect the stability of dissolved ozone, while matrix components act as oxidant scavengers, increasing the required ozone dose for a desired extent of OMP abatement. Therefore, the abatement of OMPs by ozonation can be related to kinetic parameters, operational parameters (e.g. ozone dose, temperature) and water quality parameters (e.g. organic carbon concentration, pH, alkalinity) (31, 32).

The aim of this study was to gain insights into the simultaneous ozonation of 90 chemically diverse OMPs. The selection of the compounds was based on existing and proposed EU legislation, UK prescription data, metabolism and excretion from the human body, known environmental occurrence, persistence during wastewater treatment and toxicity to aquatic organisms (33). Ozonation experiments were conducted in three different water matrices (pure buffered water, tap water and wastewater effluent), at different ozone doses and pH levels. In contrast to the

majority of previous ozonation studies, several illicit drugs and illicit drug metabolites were investigated. For some compounds, the reactivity with ozone in water is investigated for the first time, including the diabetes drug gliclazide, the cocaine biomarker anhydroecgonine methylester, the antipsychotic drug quetiapine and the heroin metabolite 6-monoacetylmorphine (O-6-MAM).

2.4 Materials and Methods

2.4.1 Chemicals

OMPs were either purchased dissolved in 0.1 or 1.0 mg mL^{-1} solutions or as powder. Stock solutions from powders were prepared at 1 mg mL^{-1} in either acetonitrile or methanol and stored in the dark at −20°C. All aqueous solutions were made in ultrapure water (Milli-Q, Millipore, USA). Chemicals and solvents (purity 95% or higher) were used as received from various commercial suppliers. Methanol, ammonium acetate (NH_4OAc), ammonium fluoride (NH_4F) and acetic acid (CH_3COOH) for chromatographic analysis (all HPLC grade), phosphoric acid (H_3PO_4), disodium phosphate (Na_2HPO_4), monosodium phosphate (NaH_2PO_4) and sodium tetraborate ($Na_2B_4O_7$) were obtained from either Sigma-Aldrich or Fisher Scientific, sodium thiosulfate ($Na_2S_2O_3$) from Merck, sodium hydroxide (NaOH) from PanReac.

Table 2.4.1 provides a list of the 90 OMPs studied, including information about their estimated or known ozone reactivity. The referenced studies consist of both mechanistic single-compound studies and multi-compound studies. Table 2.9.1 (SI) provides CAS number, molecular weight, formula, structure, and instrument detection and quantification limit for each compound. Table 2.9.2 (SI) provides second order rate constants for the reactions of the compounds with OH radicals, when available.

Table 2.4.1. Studied organic micropollutants (in alphabetical order). k_{O3} values are experimental or calculated by QSAR as indicated. Estimated ozone reactivity is based on compound structure. Literature column shows reference for k_{O3} or other relevant study. pK_a values were obtained from (33).

Chemical	Mode of action/Use	pK_a (Most acidic)	pK_a (Most basic)	Ozone-(non) reactive functional groups	k_{O3} (M^{-1} s^{-1}) at pH 7 or estimated ozone reactivity	Literature
1,7-Dimethylxanthine	Human indicator	8.5	0.2	amide, imidazole	medium	(34)
10,11-Dihydro-10-ydroxycarbamazepine	Anti-epileptic metabolite	13.8	-0.5	amide, benzene ring	low	
Acetaminophen	NSAID	9.9	1.7	benzene ring	4.1×10^6	(35)
Amphetamine	Stimulant	-	9.9	(protonated) amine, benzene ring	low	(27)
Anhydroecgonine methylester	Stimulant metabolite	-	8.0	olefin, (protonated) amine	high	
Atenolol	Beta-blocker	13.9	9.4	amide, (protonated) amine, benzene ring	1.7×10^3	(36)
Atorvastatin	Lipid regulator	4.3	0.4	benzene ring	medium	
Azathioprine	Anti-cancer	-	7.5	(deactivated) thioether, imidazole	low	(37)
Azithromycin	Antibiotic	13.3	8.6	(protonated) amine	1.1×10^5	(38)
Benzophenone-1	UV filter	7.7	-	benzene ring	high	
Benzophenone-2	UV filter	7.0	-	benzene ring	high	(39)
Benzophenone-3	UV filter	7.6	-	benzene ring	6.9×10^5	(40)
Benzophenone-4	UV filter	-0.7	-	benzene ring	medium	(41)
Benzoylecgonine	Stimulant metabolite	3.4	10.8	(protonated) amine, deactivated benzene ring	low	(11, 27)
Bezafibrate	Lipid regulator	3.3	-2.1	amide, benzene ring	590	(18, 42)

Chemical	Mode of action/Use	pK_a (Most acidic)	pK_a (Most basic)	Ozone-(non) reactive functional groups	k_{O3} (M^{-1} s^{-1}) at pH 7 or estimated ozone reactivity	Literature
Bisphenol A	Plasticizer	10.3	-	phenol	1.1×10^6	(43)
Butylparaben	Parabens	8.2	-	phenol	7.9×10^7	(44)
Caffeine	Human indicator	-	0.5	amide, imidazole	673	(23, 45)
Carbamazepine	Anti-epileptic	13.9	-0.5	olefin, amide, benzene ring	3×10^5	(18, 46)
Carbamazepine-10,11-epoxide	Anti-epileptic metabolite	13.9	-0.5	amide, benzene ring	low	(24)
Cetirizine	Antihistamine	3.5	6.7	(protonated) amine, benzene ring	1.7×10^5	(47)
Cimetidine	H2 receptor antagonists	14.1	7.1	thioether, amidine, imidazole	high	
Citalopram	Anti-depressant	-	9.6	(protonated) amine, deactivated benzene ring	low	(48, 49)
Clarithromycin	Antibiotic	13.1	8.2	(protonated) amine	7×10^4	(50)
Cocaethylene	Stimulant metabolite	-	9.0	(protonated) amine, deactivated benzene ring	low	
Cocaine	Stimulant	-	9.0	(protonated) amine, deactivated benzene ring	low	(11, 27)
Codeine	Analgesic	13.4	8.2	olefin, (protonated) amine, benzene ring	high	(24)
Cotinine	Human indicator	-	4.7	amide, pyridine	low	(11, 24)
Creatinine	Human indicator	-	6.9	amide, (protonated) amine	2	(51)
Desmethylcitalopram	Anti-depressant metabolite	-	10.5	(protonated) amine, deactivated benzene ring	low	(48)
Desmethylvenlafaxine	Anti-depressant metabolite	10.0	9.3	phenol, (protonated) amine	high	(49)
Diclofenac	NSAID	4.9	-2.3	aniline	1×10^6	(18, 52)
Dihydrocodeine	Analgesic	14.2	8.4	(protonated) amine, benzene ring	medium	

Chemical	Mode of action/Use	pK_a (Most acidic)	pK_a (Most basic)	Ozone-(non) reactive functional groups	k_{O3} (M^{-1} s^{-1}) at pH 7 or estimated ozone reactivity	Literature
Dihydromorphine	Analgesic metabolite	9.6	8.4	(protonated) amine, benzene ring	high	
Diltiazem	Calcium channel blocker	-	8.9	(protonated) amine, benzene ring	high	
E1	Steroid estrogen	10.3	-	phenol	9.4×10^5	(43, 53)
E2	Steroid estrogen	10.3	-	phenol	2.2×10^6	(43, 53)
EDDP	Analgesic metabolite	-	7.7	olefin, (protonated) amine, benzene ring	high	(28)
EE2	Steroid estrogen	10.2	-	phenol	2.3×10^6	(43)
Ephedrine/pseudoephedrine	Drug precursor	14.0	9.4	(protonated) amine, benzene ring	low	
Ethylparaben	Parabens	8.3	-	phenol	5.5×10^7	(44)
Fexofenadine	Antihistamine	4.4	9.4	(protonated) amine, benzene ring	9.0×10^3	(47)
Fluoxetine	Anti-depressant	-	10.1	(protonated) amine, benzene ring	1.6×10^4	(54)
Gliclazide	Diabetes	6.1	3.9	amide, (protonated) amine, deactivated benzene ring	high	
Heroin	Opioid	-	7.9	olefin, (protonated) amine, benzene ring	high	
Ibuprofen	NSAID	4.4	-	benzene ring	9.6	(18)
Ifosfamide	Anti-cancer	-	1.4	phosphamide	<1 (QSAR)	(55)
Iopromide	X-ray contrast media	10.6	-2.6	amide, deactivated benzene ring	<0.8	(18)
Irbesartan	Hypertension	4.2	2.6	amide, (protonated) amine, benzene ring	24	(25)
Ketamine	Anaesthetic	-	6.5	(protonated) amine, deactivated benzene ring	medium	(27)
Ketoprofen	NSAID	4.2	-	deactivated benzene ring	0.40	(56)
Lisinopril	Hypertension	2.2	10.5	(protonated) amine, benzene ring	low	

Chemical	Mode of action/Use	pK_a (Most acidic)	pK_a (Most basic)	Ozone-(non) reactive functional groups	k_{O3} (M^{-1} s^{-1}) at pH 7 or estimated ozone reactivity	Literature
MDA	Stimulant	-	10.0	(protonated) amine, anisole	high	
MDMA	Stimulant	-	10.3	(protonated) amine, anisole	high	(11, 27)
MDPV	Stimulant	-	8.4	(protonated) amine, anisole	medium	
Mephedrone	Stimulant	-	7.4	(protonated) amine, deactivated benzene ring	medium	
Metformin	Diabetes	-	12.3	(protonated) amine	1.2	(19)
Methadone	Analgesic	-	9.5	(protonated) amine, benzene ring	low	(28)
Methamphetamine	Stimulant	-	10.4	(protonated) amine, benzene ring	low	(27)
Methotrexate	Anti-cancer	3.5	5.6	aniline, amide, (protonated) amine	high	(57)
Methylparaben	Parabens	8.3	-	phenol	4.8×10^7	(44)
Metoprolol	Beta-blocker	13.9	9.4	(protonated) amine, benzene ring	2.0×10^3	(36)
Mirtazapine	Anti-depressant	-	8.1	(protonated) amine, benzene ring, pyridine	medium	(49)
Morphine	Analgesic	9.5	8.3	olefin, (protonated) amine, benzene ring	6.4×10^6 (QSAR)	(55)
Naproxen	NSAID	4.8	-	naphthalene	2×10^5	(58)
N-desmethyltramadol	Analgesic metabolite	14.5	10.6	(protonated) amine, anisole	medium	
Nicotine	Human indicator	-	8.0	(protonated) amine, pyridine	medium	(11, 24)
Norcodeine	Analgesic metabolite	13.3	9.3	olefin, (protonated) amine, benzene ring	high	(26)
Norephedrine	Stimulant metabolite	12.1	8.5	(protonated) amine, benzene ring	low	
Norfluoxetine	Anti-depressant metabolite	-	9.1	(protonated) amine, benzene ring	65	(54)
Norketamine	Anaesthetic metabolite	-	6.3	(protonated) amine, deactivated benzene ring	medium	

Chemical	Mode of action/Use	pK_a (Most acidic)	pK_a (Most basic)	Ozone-(non) reactive functional groups	k_{O3} (M^{-1} s^{-1}) at pH 7 or estimated ozone reactivity	Literature
Normorphine	Analgesic metabolite	9.2	9.5	olefin, (protonated) amine, benzene ring	high	
O-6-MAM	Opioid metabolite	9.4	8.0	olefin, (protonated) amine, benzene ring	high	
O-desmethyltramadol	Analgesic metabolite	10.0	9.6	(protonated) amine, phenol	high	
Pholcodine	Cough suppressant	13.4	8.2	olefin, (protonated) amine, benzene ring	high	
Propranolol	Beta-blocker	13.8	9.5	naphthalene, (protonated) amine	1×10^5	(36)
Propylparaben	Parabens	8.2	-	phenol	7.0×10^7	(44)
Quetiapine	Anti-psychotic	14.4	6.7	amidine, benzene ring, thioether	high	
Ranitidine	H2 receptor antagonists	-	8.4	amidine, furan, thioether	2.1×10^6	(59)
Sertraline	Anti-depressant	-	9.5	(protonated) amine, benzene ring	medium	(49)
Sulfamethoxazole	Antibiotic	5.8	1.4	aniline, sulfonamide	2.6×10^6	(18, 60)
Sulfasalazine	Antibacterial	2.7	0.9	benzene ring, sulfonamide	high	
Tamoxifen	Anti-cancer	-	8.7	olefin, benzene ring	high	(61)
Temazepam	Hypnotic	11.7	1.6	amide, deactivated benzene ring	low	(62)
Tramadol	Analgesic	14.5	9.6	(protonated) amine, anisole	2.2×10^3	(63)
Triclosan	Antibacterial	7.8	-	benzene ring	3.8×10^7	(64, 65)
Trimethoprim	Antibiotic	-	7.0	(protonated) amine, pyrimidine, benzene ring	2.7×10^5	(38, 66)
Tylosin	Veterinary	13.1	7.4	olefin, (protonated) amine	5.1×10^5	(38)
Valsartan	Hypertension	3.6	0.6	amide, benzene ring	38 (QSAR)	(55, 67)
Venlafaxine	Anti-depressant	14.8	9.3	(protonated) amine, anisole	1.3×10^3	(49, 68)

2.4.2 Ozonation experiments

All reactions were conducted in 10 mL glass flasks. Freshly prepared methanol stock solution containing all 90 compounds at equal mass concentration was spiked into empty flasks. The solvent was evaporated under a gentle stream of nitrogen followed by re-dissolution with the aqueous phase, which consisted of either buffered ultrapure water at pH 3 (10 mM H_3PO_4/H_2NaPO_4), pH 7 (10 mM H_2NaPO_4/HNa_2PO_4) or pH 11 (10 mM H_3BO_3), tap water (total organic carbon (TOC) 1.5 mg C L^{-1}, pH 7.5) or secondary wastewater effluent (TOC 7.1 mg C L^{-1}, pH 7.8) from a wastewater treatment plant in the Southwest of England. The concentration of each OMP in the final reaction solution was approximately 100 µg L^{-1}, which translated into a TOC of 6 mg C L^{-1} added to the TOC of the matrix. A high initial concentration of each OMP was chosen to avoid an analyte concentration step prior to LC-MS (liquid chromatography coupled with tandem mass spectrometry) analysis.

Ozone was produced with a BMT 803N ozone generator (BMT Messtechnik, Berlin, Germany). Stock solutions (1.3-1.5 mM, 62-72 mg L^{-1}) were made by sparging ozone gas through ultrapure water (≤4°C) that was cooled in an ice bath. The dissolved ozone concentration of stock solutions was quantified directly spectrophotometrically using a molar absorption coefficient of $\epsilon = 3000\ M^{-1}cm^{-1}$ at an absorption wavelength of $\lambda = 258$ nm (69).

The ozone stock solution was added under vigorous stirring to each flask to achieve ozone doses on a carbon basis of 0.05 mM O_3 (mM C)$^{-1}$ (0.2 g O_3 (g C)$^{-1}$), 0.15 mM O_3 (mM C)$^{-1}$ (0.6 g O_3 (g C)$^{-1}$) and 0.3 mM O_3 (mM C)$^{-1}$ (1.2 g O_3 (g C)$^{-1}$), to cover the range used for water treatment. Specific ozone doses on a molar basis are hereafter used. After 5 min reaction time, the samples were quenched with 0.1 M sodium thiosulfate ($Na_2S_2O_3$) and analysed within 24 h.

2.4.3 Analytical methods

A detailed description of the analytical method used for the OMPs can be found elsewhere (33). Briefly, the target compounds were analysed by liquid chromatography-tandem mass spectrometry (LC-MS) using a Waters Acquity UPLC system (Waters, Manchester, UK) coupled to a Xevo TQD (Triple Quadrupole Mass

Spectrometer, Waters, Manchester, UK) equipped with an electrospray ionisation source. The determination of acidic and basic compounds was performed in negative and positive ionisation mode, respectively. Limits of quantification and detection for individual analytes are presented in Table 2.9.1 (SI). Each sample was analysed in duplicate. Method performance is described in detail elsewhere (33).

Total organic carbon was analysed with a Shimadzu TOC-VCPN Analyzer (Shimadzu, Kyoto, Japan). Spectroscopic measurements were conducted with a Cary 100 UV-Vis Spectrometer (Agilent Technologies, Santa Clara, California, USA)

2.4.4 Ozone and OH radical exposures

The exposure (time-integrated concentration) of OH radicals was estimated from the elimination percentage of ketoprofen (KET). Ketoprofen was selected because it is the compound with the lowest ozonation second order rate constant (0.4 M^{-1} s^{-1}) among the compounds included in this study (see Table 2.4.1). Additionally, ketoprofen has a known and high second order rate constant for its reaction with OH radicals (see SI, Table 2.9.2). Therefore, its reaction with ozone can be considered negligible, while the OH radical exposure was calculated based on equation 2.4.1:

$$k_{OH/KET} \int [OH]dt = -\ln\left(\frac{[KET]}{[KET]_0}\right) \qquad (2.4.1)$$

The ozone exposure was then estimated from the elimination percentage of carbamazepine (CBZ), or tramadol (TRA) in cases when carbamazepine was below the limit of quantification after ozonation. Carbamazepine has a high ozone reactivity that does not depend on the pH, while tramadol has a moderate ozone reactivity that does depend on the pH, which was considered (see Table 2.4.1). The ozone exposure was calculated from equation 2.4.2:

$$k_{OH/CBZ\ or\ TRA} \int [OH]dt + k_{O_3/CBZ\ or\ TRA} \int [O_3]dt = -\ln\left(\frac{[CBZ\ or\ TRA]}{[CBZ\ or\ TRA]_0}\right) \qquad (2.4.2)$$

2.5 Results and Discussion

2.5.1 Abatement by ozonation of organic micropollutants including illicit drugs added to pure water at pH 7

An overview of the elimination of the 90 OMPs by ozonation in pure buffered water at three different pH values and at three specific ozone doses is shown in Figure 2.5.1. As expected by the chemical diversity of the OMPs (see Table 2.4.1 and SI, Table 2.9.1), the results range from no removal to complete removal. At the highest ozone dose of 0.3 mM O_3 (mM C)$^{-1}$ and at pH 7 almost half of all compounds were removed to below the limit of detection. The medium ozone dose of 0.15 mM O_3 (mM C)$^{-1}$ at pH 7 led to 80% or higher removal for more than a third of compounds. At the lowest ozone dose of 0.05 mM O_3 (mM C)$^{-1}$ at pH 7 partial removal occurred for most compounds.

The OMPs may be classified into three groups according to their attenuation at the highest specific ozone dose at pH 7: Group I compounds were readily removed by more than 90%, Group II compounds had a moderate removal of 50 to 90% and Group III compounds were hard to remove with less than 50% removal. Group I consisted of 47 (52%) of the tested compounds, 10 compounds (11%) were in Group II, while 33 (37%) were in Group III. Similar classifications of OMPs have been used in previous studies, with comparable elimination observed in municipal and hospital wastewater effluent at the same specific ozone doses (32, 55). However, it should be noted that high concentrations of OMPs in waters with a low scavenger concentration (in this case pure buffered water) may affect the ozone and OH radical exposures (70), and therefore the observed OMP elimination (see also below discussion on ozone and OH radical exposures).

Group III included most illicit stimulants, antidepressants and their metabolites. These compounds exhibit no functional groups that are readily reactive with ozone. As an electrophile, ozone reacts selectively with electron-rich moieties, such as neutral amines, activated benzene rings and olefins (16). Compounds in Group III include deactivated benzene rings (e.g. ketoprofen, cocaine), amides (e.g. cotinine, ifosfamide) and protonated amines (e.g. citalopram, metformin), which have second order rate constants with ozone <10 M^{-1} s^{-1} (see Table 2.4.1). Their elimination can be attributed to reaction with less selective OH radicals. The OH radical second order

rate constants (k_{OH}) of most OMPs vary by only one order of magnitude, between 10^9 M^{-1} s^{-1} and diffusion-controlled values of 10^{10} M^{-1} s^{-1} (see SI, Table 2.9.2). Group III compounds can be more effectively attenuated with advanced oxidation processes (AOPs) that aim to increase the concentration of OH radicals, such as the peroxone process (O_3/H_2O_2) or ultraviolet (UV) light combined with hydrogen peroxide (UV/H_2O_2) (15).

Few compounds such as the carbamazepine metabolites carbamazepine-10,11-epoxide and 10,11-dihydro-10-hydroxycarbamazepine, exhibited unclear elimination trends with increasing ozone dose, which may be ascribed to simultaneous degradation and formation from the oxidation of structurally similar compounds. Azathioprine had the lowest removal of all compounds in this study, and there is only limited information about its ozone reactivity in the literature (37).

Most antibacterial agents and antibiotics, analgesics and their metabolites, UV filters, parabens and steroid estrogens belong to Group I and exhibit high elimination with ozone. Group I compounds contain moieties known to react fast with ozone: activated benzene rings, such as phenols (e.g. methylparaben, estrone, bisphenol A) and anilines (e.g. methotrexate, diclofenac), amines (e.g. mirtazapine, gliclazide), olefins (e.g. morphine, pholcodine) and thioethers (e.g. ranitidine). Note that several compounds contain more than one ozone-reactive sites.

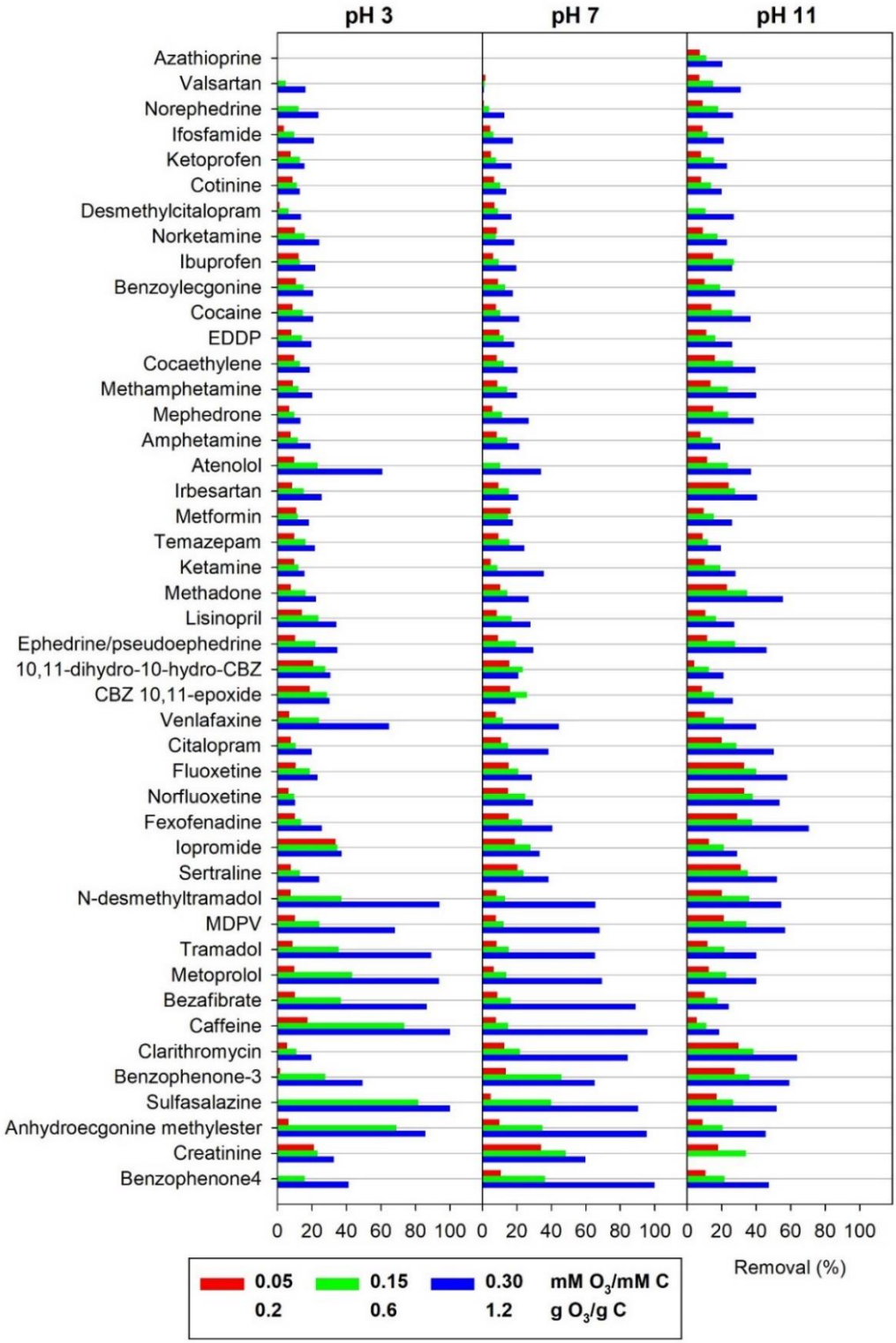

Figure 2.5.1.a Simultaneous removal of 90 organic micropollutants added to pure buffered water as a function of the specific ozone dose and the pH (arranged with increasing average removal at pH 7). Error bars from duplicate analysis of samples were omitted for figure overview and are provided in the SI xlsx-data file. CBZ: carbamazepine.

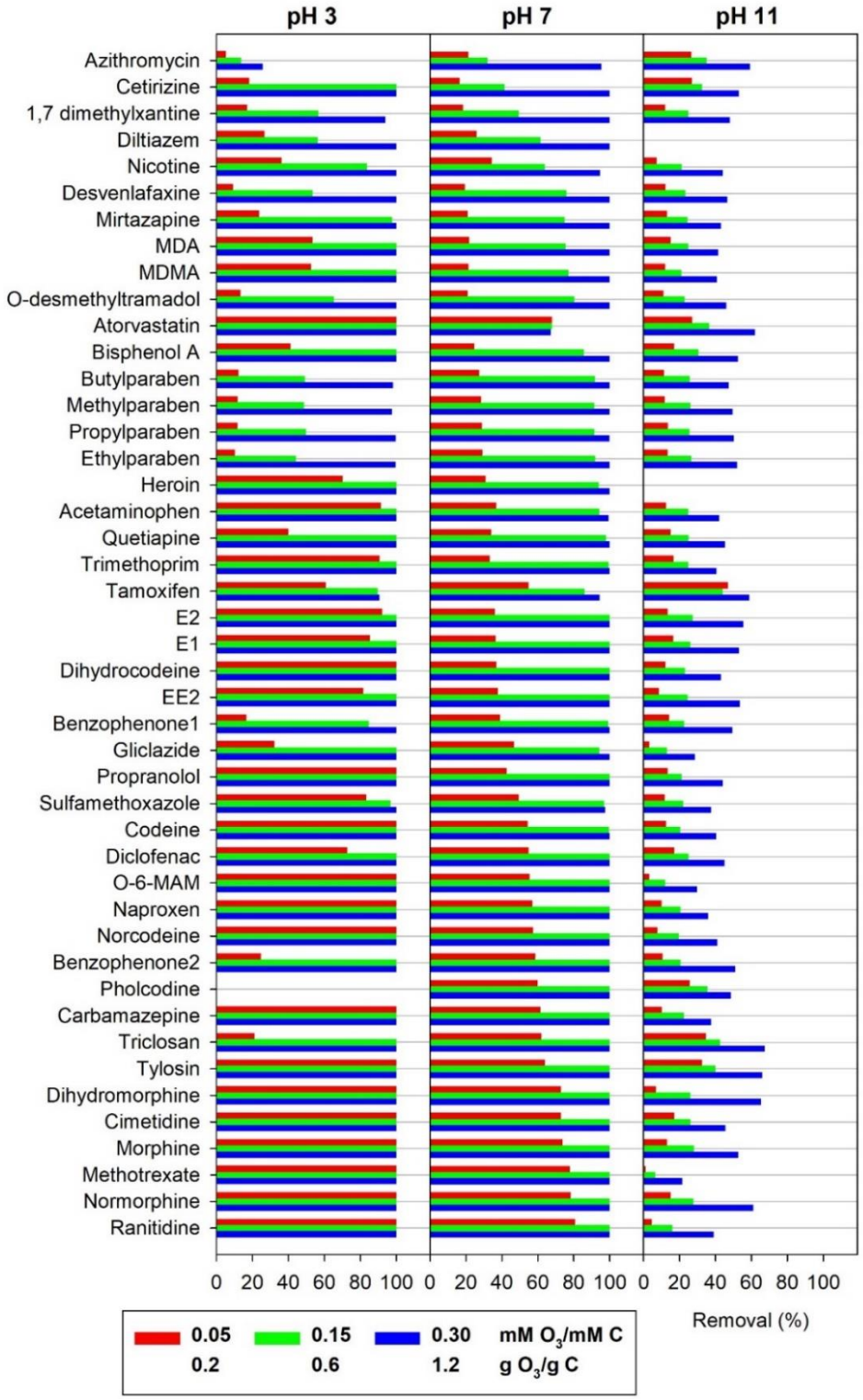

Figure 2.5.1.b Simultaneous removal of 90 organic micropollutants added to pure buffered water as a function of the specific ozone dose and the pH (arranged with increasing average removal at pH 7). Error bars from duplicate analysis of samples were omitted for figure overview and are provided in the SI xlsx-data file.

The illicit drugs and illicit drug metabolites included in this study fall into four categories: opioids (heroin, O-6-MAM, morphine, normorphine, dihydromorphine, methadone, EDDP), cocainics (cocaine, cocaethylene, benzoylecgonine, anhydroecgonine methylester), amphetamine-type (amphetamine, methamphetamine, mephedrone, norephedrine, ephedrine/pseudoephedrine [a precursor]) and ecstasy group (MDMA, MDA, MDPV). Figure 2.5.2 provides an overview on the elimination of the four substance categories at five different specific ozone doses in pure buffered water at pH 7.

Five of the opioids (heroin, O-6-MAM, morphine, normorphine, dihydromorphine) have a similar molecular structure. They contain an activated benzene ring (phenol or anisole), a tertiary or secondary amine (pK_a=7.9-9.6) and, apart from dihydromorphine, a carbon double bond. These opioids are efficiently removed by ozonation at pH 7. Second order rate constants for reactions of opioids with ozone have not been determined experimentally, while for morphine the rate constant has been estimated with a QSAR approach as $6.4 \times 10^6\ M^{-1}\ s^{-1}$ (55). Second order rate constants of other structurally similar opioids can be expected to be close to this value. Since dihydromorphine appears to have the same ozone reactivity as morphine, the primary site of ozone attack at pH 7 is likely the activated benzene ring rather than the olefinic bond. In contrast, methadone and its metabolite EDDP were both poorly removed by ozonation at pH 7, despite EDDP having a carbon double bond. Only partial removal of these two compounds has been observed in waterworks employing different treatment methods, while trace concentrations of both compounds have been detected in finished drinking water (28, 71).

Cocaine and two of its metabolites (cocaethylene and benzoylecgonine) have similar structures containing a deactivated benzene ring (carbonyl-substituted) and a protonated amine (pK_a=9-10.8). As a result, their reactivity with ozone is low and minimal removal at pH 7 was observed. Cocaine has been shown to be more ozone reactive than benzoylecgonine (27), which was not observed in this study, due to the very low removal of both compounds. These three cocainics have been found as traces in tap water of different countries (71, 72). In contrast, anhydroecgonine methylester (a biomarker for the use of crack cocaine) contains an olefinic bond and has a lower pK_a of 8. Accordingly, as shown in Figure 2.5.2, this compound has a much higher ozonation removal than the other compounds in this category.

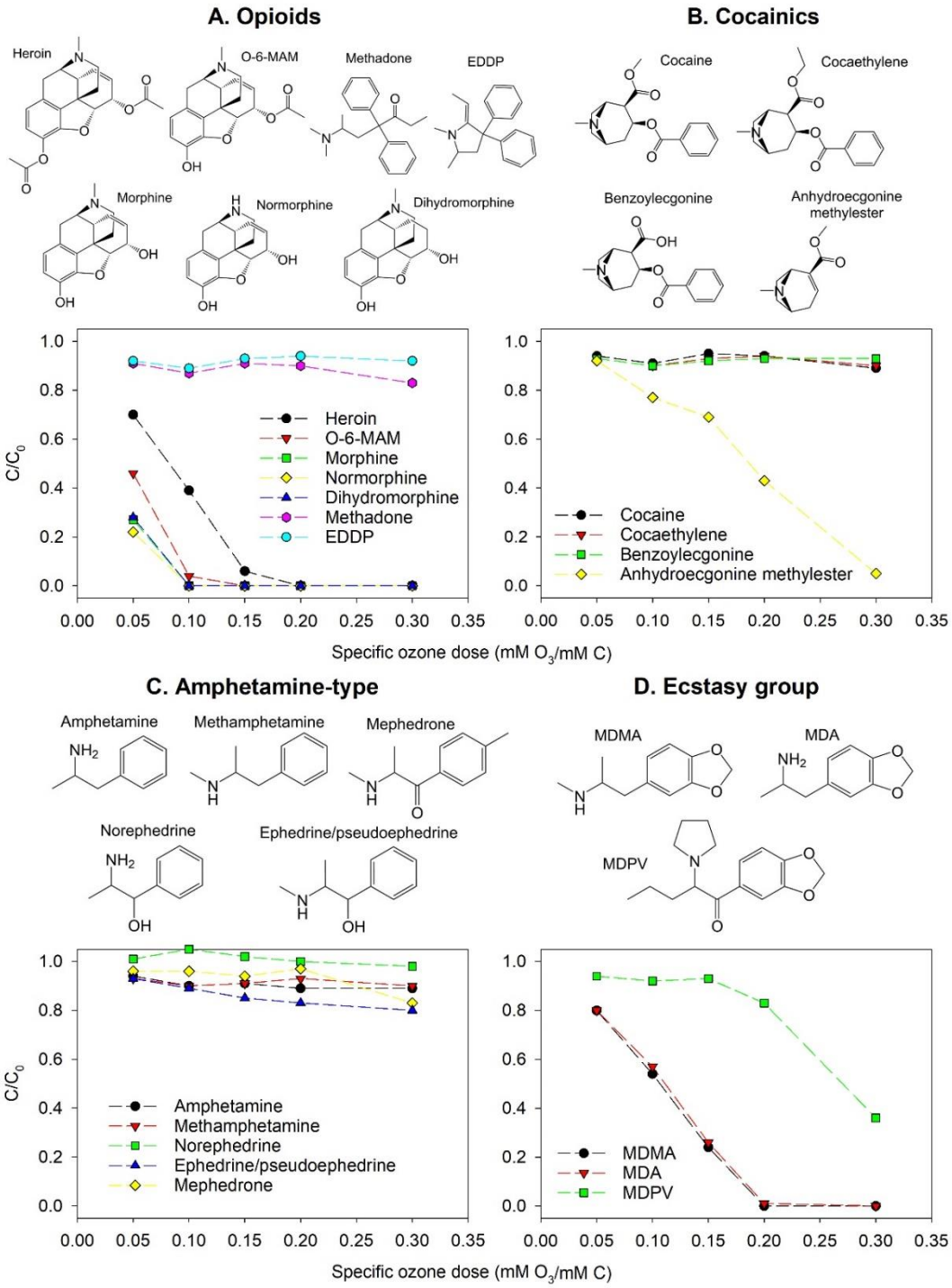

Figure 2.5.2. Abatement of illicit drugs and their metabolites as a function of the specific ozone dose in pure buffered water at pH 7. All compounds were added as a mixture of 90 OMPs in total. Error bars from duplicate analysis of samples were omitted for figure overview and are provided in the SI xlsx-data file.

The amphetamine-type compounds contain a deactivated or slightly activated benzene ring and an amine (pK_a=7.4-10.4). Figure 2.5.2 shows that all amphetamine-type compounds were ozone-resistant at pH 7. Mephedrone and methamphetamine have been detected in drinking water samples from the UK, which had undergone treatment

including ozonation (12). Methamphetamine is reported to be more ozone-reactive than amphetamine due to the presence of a secondary rather than a primary amine (27). This was not observed in this study due to the very low removal of both compounds under the employed conditions. However, this effect could be observed for ephedrine/pseudoephedrine which had a higher elimination than norephedrine.

Drugs of the ecstasy group contain a benzene ring activated by two anisole substituents, and an amine with pK_a of 8.4-10.3 (primary-MDA, secondary-MDMA, tertiary-MDPV). The main reactive site is expected to be the benzene ring leading to high removal. MDA and MDMA differ by only one methyl group attached to the amine and showed the same ozone reactivity, while MDPV contains an additional carbonyl substituent on the benzene ring, inducing partial deactivation and lower reactivity. MDMA has been detected in surface water and was only partly removed during the ozonation step of drinking water production (11).

2.5.2 Effect of pH on micropollutant abatement by ozone in pure buffered water

Changes in pH strongly affect ozone chemistry in water. An elevated pH leads to faster ozone decay due to two phenomena: hydroxide ions initiate the chain reaction of ozone decomposition and at the same time electrophilic ozone reacts faster with deprotonated or dissociated species of the dissolved organic matter (73, 74). In the experimental system of this study the latter phenomenon is expected to be more important due to the increased concentrations of OMPs. Deprotonated alkylamines (typical pK_a=9-11) have up to six orders of magnitude higher reactivity with ozone than the protonated species (29). The second order rate constant for the reaction of ozone with dissociated phenolic compounds is five orders of magnitude higher compared to the corresponding non-dissociated species (30). Despite lower ozone exposure at higher pH, the OH radical exposure remains roughly constant with pH in natural waters (73).

The estimated ozone and OH radical exposures in pure buffered water under each set of conditions are shown in Table 2.5.1 (tap water and wastewater effluent are discussed in the next section). At a given specific ozone dose, the ozone exposure increased by two orders of magnitude as the pH decreased by 4 units. The OH radical exposure remained roughly constant within the uncertainty of the employed

estimation method (approximately accurate within an order of magnitude). The ozone exposure values at pH 3 and 7 were of the same order of magnitude as those measured in natural waters (73), while those at pH 11 were lower and accompanied by slightly higher OH radical exposures. It should be noted that samples were quenched of residual ozone after 5 minutes of reaction, which may have resulted in lower ozone exposure than the maximum possible. The ratio of OH radical exposure to ozone exposure, i.e. the R_{ct} value (75), was in the range of 10^{-4} to 10^{-10} across the three pH levels.

Table 2.5.1. Estimated ozone and OH radical exposures in each water matrix and specific ozone dose, calculated from the elimination of carbamazepine/tramadol and ketoprofen, respectively.

	OH radical exposure (M s)			**Ozone exposure (M s)**		
Specific ozone dose (mM O_3 (mM C)$^{-1}$)	**0.05**	**0.15**	**0.30**	**0.05**	**0.15**	**0.30**
Buffered at pH 3	7×10^{-12}	9×10^{-12}	6×10^{-12}	3×10^{-4}	4×10^{-3}	3×10^{-2}
Buffered at pH 7	4×10^{-12}	3×10^{-12}	8×10^{-12}	3×10^{-6}	4×10^{-5}	4×10^{-4}
Buffered at pH 11	8×10^{-12}	1×10^{-11}	2×10^{-11}	6×10^{-8}	3×10^{-7}	7×10^{-7}
Tap water	1×10^{-13}	6×10^{-12}	1×10^{-11}	5×10^{-7}	1×10^{-6}	5×10^{-6}
Wastewater effluent	1×10^{-11}	7×10^{-12}	2×10^{-11}	3×10^{-7}	1×10^{-6}	3×10^{-6}

The combined effect of different ozone exposure and target compound speciation has led to different removal trends among the 90 OMPs (Figure 2.5.1). The amines fluoxetine (pK_a=10.1) and sertraline (pK_a=9.5) were better removed at higher pH due to deprotonation. In contrast, the four parabens (phenols with pK_a of 8.2 to 8.3) followed a distinct trend: their removal increased with a change of pH from 3 to 7 (due to increased dissociation of the phenols which enhanced their ozone reactivity) and then decreased at pH 11 (due to lower ozone exposure). The four benzophenones followed the same trend. However, the removal of the phenolic hormones E1, E2 and EE2 and the plasticizer bisphenol A decreased with higher pH, indicating that the increased reactivity of the dissociated form was outweighed by the lower ozone exposure. For olefins, such as carbamazepine and tamoxifen, a sharp drop of removal was observed at pH 11. In these cases, the effect of the pH is only due to the different ozone and OH radical exposures.

The effect of the pH on the ozonation of illicit drugs and their metabolites was also examined. Four of the opioids with structure similar to morphine have a phenolic moiety with pK_a>9. However, the effect of the pH change on their removal seems to be mainly due to the different ozone exposure rather than the dissociation of the phenolic moiety. Decreased elimination was observed with an increase of pH from 3 to 7 but only at the lowest ozone dose. At pH 11 removals were markedly lower than those at pH 3 and 7, with the highest one being 61% for dihydromorphine and the lowest being 21% for O-6-MAM. In contrast, methadone was better removed at higher pH due to deprotonation of its amine moiety (pK_a=9.5) and reached 50% removal at pH 11 with the highest ozone dose. The removal of EDDP also slightly increased with pH but remained poor (<20%) under all conditions.

Cocaine, cocaethylene and benzoylecgonine showed enhanced removal at pH 11, since their main ozone-reactive moiety is an amine (pK_a=9-10.8). Despite this increase, their removal was still below 35%. The fourth compound of the cocainics class, anhydroecgonine methylester, is an olefin and showed decreased elimination at pH 11 due to lower ozone exposure. The amphetamine-type compounds were ozone-resistant at all pH values (removal below 35%), but an increase of removal was observed at pH 11 due to deprotonation of the amine (pK_a=7.4-10.4). The removal of MDA and MDMA decreased at higher pH due to the lower ozone exposure, as their main ozone-reactive site is an activated benzene ring. The less reactive MDPV showed a slight increase of removal at pH 11, indicating that the amine (pK_a=8.4) plays a more important role in its reaction with ozone due to partial deactivation of its benzene ring.

An overview of the complete dataset is presented as box and whisker plots in Figure 2.5.3. Since a similar broad range of compounds can be expected in real water matrices, such as river water (33), the box and whisker plots provide a rough estimation on ozonation performance for multi-compound mixtures. Overall, the optimal pH for the elimination of the selected OMPs was 3 and 7. At pH 3 higher removal compared to pH 7 was observed at the lowest ozone dose, while the removal was similar at the other two applied ozone doses. Ozonation at pH 11 was ineffective and would require higher ozone doses to yield results like those of the lower pH values. The only compounds whose removal improved at pH 11 were Group II and

III compounds, including amines with pK_a>7. Typical pH for ozonation in treatment practice is 7 to 8.5.

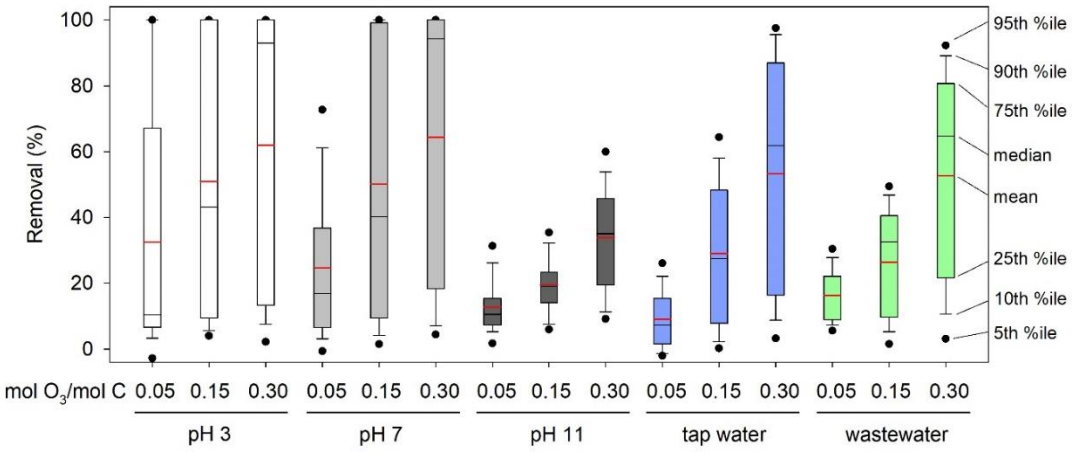

Figure 2.5.3. Box and whisker plots of the removal of the 90 OMPs under the different conditions used in this study. %ile: percentile.

2.5.3 Removal in tap water and wastewater effluent

Although the ozone dose was normalised to the TOC concentration, the dissolved organic carbon in each water matrix used has different characteristics. In pure buffered water, the organic matter consists of the added OMPs, while in tap water and wastewater effluent it also includes the bulk organic matter. The bulk organic matter was 20% of the total TOC in tap water and 54% in wastewater effluent (on a mass basis). The ozone reactivity of bulk organic matter varies depending on the origin and characteristics of the sample, and typically covers a range of several orders of magnitude (76). Different fractions of dissolved organic matter promote or inhibit ozone decay and the production of OH radicals, leading to different ozone and OH radical exposures (16, 77). The characteristics of the organic matrix, such as aromaticity, protein and humic acid content, were not determined in this study.

As shown in Table 2.5.1, the ozone exposure in tap water (pH 7.5) and wastewater effluent (pH 7.8) was one to two orders of magnitude lower than the one in pure buffered water at pH 7, but higher than that at pH 11. For most of the compounds that react fast with ozone, the removal in tap water or wastewater effluent decreased compared to pure buffered water at pH 7 (see SI xlsx-data file). This matrix effect is also evident in Figure 2.5.3, especially at the intermediate ozone dose

(0.15 mM O_3 (mM C)$^{-1}$) and can be attributed to partial ozone consumption by the bulk organic matter. With 0.15 mM O_3 (mM C)$^{-1}$, no compound was removed by more than 90% in tap water or wastewater effluent. The maximum removal in tap water at this ozone dose was 79% (cimetidine), while in wastewater effluent it was 60% (triclosan). At the highest ozone dose (0.30 mM O_3 (mM C)$^{-1}$) removal of cimetidine and normorphine to below the limit of detection was achieved in tap water, but removal was partial for all compounds in wastewater effluent.

The water matrix had a smaller effect on the OH radical exposure and the elimination of ozone-resistant compounds (Table 2.5.1 and SI xlsx-data file). Due to their high concentrations, the OMPs already reacted very fast with OH radicals in pure buffered water. Therefore, no additional scavenging of OH radicals by the bulk organic matter in tap water and wastewater effluent was observed. For a few compounds, such as citalopram, ibuprofen and valsartan, even an enhanced elimination in tap water or wastewater effluent was noticed as a result of a slightly increased OH radical exposure. The average R_{ct} value was 2×10^{-5} in wastewater effluent and 2×10^{-6} in tap water, which was higher compared to previously reported values for wastewater effluent (78, 79).

Figure 2.5.4 shows the elimination of 40 OMPs with known second order rate constants for their reaction with ozone, added in tap water and wastewater effluent. Data including compound names are provided in the SI. Overall, at the lowest specific ozone dose, ozone reactivity had a small effect on the removal of the OMPs in tap water or wastewater effluent, as all 40 compounds were poorly removed (<50% removal). The effect of ozone reactivity became obvious at the intermediate and the highest ozone dose.

2.6 Conclusions

We conducted the simultaneous ozonation of 90 OMPs including illicit drugs and their metabolites in different aqueous matrices. Target compounds were chosen based on their relevance for current and future legislation and their environmental occurrence, persistence and toxicity. Forty-seven of the tested compounds were readily removed by ozone, including most antibacterials, antibiotics, analgesics, UV filters, parabens

and steroids since these compounds contained moieties that are highly reactive with ozone. Compounds that were hard to remove with ozone contained deactivated benzene rings, amide and protonated amine moieties that are unreactive with ozone and included most illicit stimulants, antidepressants and their metabolites. This study provides a valuable database of both literature and experimental results on a wide range of OMPs, including some compounds not studied with ozone before. We specifically focused on discussing results for illicit drugs, including their occurrence in drinking water, because ozonation of illicit drugs and their metabolites is significantly less studied compared to the pharmaceuticals and other compounds investigated here. The results of this study are important to predict the performance of ozonation for the removal of trace organic contaminants during water treatment.

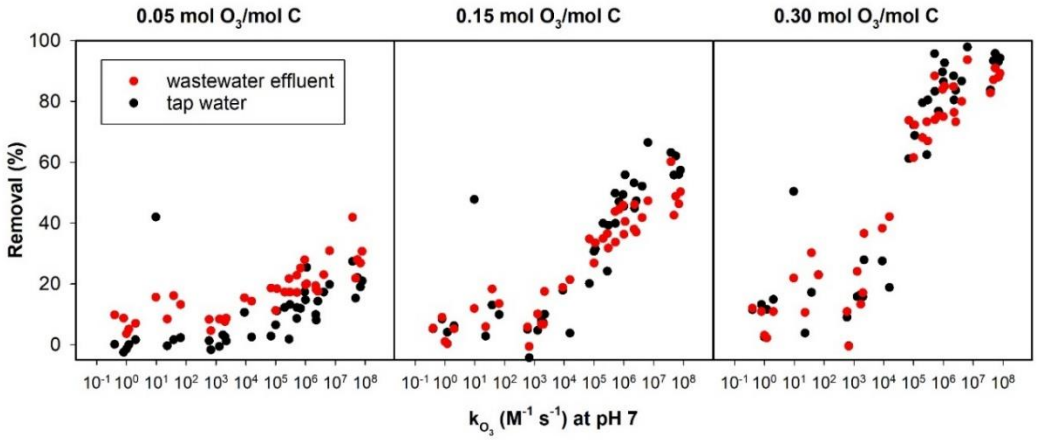

Figure 2.5.4. Removal of 40 OMPs in wastewater effluent and tap water versus their known from the literature ozonation second order rate constants.

2.7 Acknowledgements

FSS and GAZ contributed equally to this study. FSS was supported by a scholarship of the PDSE/CAPES Sandwich PhD Program: Process PDSE 99999.006445/2015-02. The support of Wessex Water and the University of Bath's EPSRC Impact Acceleration Account; Project number: EP/K503897/1 and ZR-Z0248 is greatly appreciated. GAZ was supported by a University of Bath research scholarship and an EPSRC funded integrated PhD studentship in Sustainable Chemical Technologies: EP/ L016354/1. JW research group was supported by a Royal Society equipment grant (RG2016-150544). Infrastructure and technical support by the Departments of Chemical Engineering and Chemistry and the Faculty of Engineering & Design is

appreciated. We would like to thank Urs von Gunten for his valuable comments that helped to improve this manuscript. All data supporting this study is provided as supplementary information accompanying this paper.

2.8 References

1. Petrie B, Barden R, Kasprzyk-Hordern B. A review on emerging contaminants in wastewaters and the environment: Current knowledge, understudied areas and recommendations for future monitoring. Water Research. 2015;72:3-27.

2. Benotti MJ, Trenholm RA, Vanderford BJ, Holady JC, Stanford BD, Snyder SA. Pharmaceuticals and Endocrine Disrupting Compounds in U.S. Drinking Water. Environmental Science & Technology. 2009;43(3):597-603.

3. Vulliet E, Cren-Olivé C, Grenier-Loustalot M-F. Occurrence of pharmaceuticals and hormones in drinking water treated from surface waters. Environmental Chemistry Letters. 2011;9(1):103-14.

4. Fram MS, Belitz K. Occurrence and concentrations of pharmaceutical compounds in groundwater used for public drinking-water supply in California. Sci Total Environ. 2011;409(18):3409-17.

5. Kasprzyk-Hordern B, Dinsdale RM, Guwy AJ. The removal of pharmaceuticals, personal care products, endocrine disruptors and illicit drugs during wastewater treatment and its impact on the quality of receiving waters. Water Research. 2009;43(2):363-80.

6. Lapworth DJ, Baran N, Stuart ME, Ward RS. Emerging organic contaminants in groundwater: A review of sources, fate and occurrence. Environmental Pollution. 2012;163:287-303.

7. Bouki C, Venieri D, Diamadopoulos E. Detection and fate of antibiotic resistant bacteria in wastewater treatment plants: A review. Ecotoxicology and Environmental Safety. 2013;91:1-9.

8. Jobling S, Nolan M, Tyler CR, Brighty G, Sumpter JP. Widespread Sexual Disruption in Wild Fish. Environmental Science & Technology. 1998;32(17):2498-506.

9. Baker DR, Kasprzyk-Hordern B. Spatial and temporal occurrence of pharmaceuticals and illicit drugs in the aqueous environment and during wastewater

treatment: New developments. Science of The Total Environment. 2013;454-455:442-56.

10. Subedi B, Kannan K. Mass Loading and Removal of Select Illicit Drugs in Two Wastewater Treatment Plants in New York State and Estimation of Illicit Drug Usage in Communities through Wastewater Analysis. Environmental Science & Technology. 2014;48(12):6661-70.

11. Huerta-Fontela M, Galceran MT, Ventura F. Stimulatory Drugs of Abuse in Surface Waters and Their Removal in a Conventional Drinking Water Treatment Plant. Environmental Science & Technology. 2008;42(18):6809-16.

12. Peng Y, Gautam L, Hall SW. The detection of drugs of abuse and pharmaceuticals in drinking water using solid-phase extraction and liquid chromatography-mass spectrometry. Chemosphere. 2019;223:438-47.

13. Pal R, Megharaj M, Kirkbride KP, Naidu R. Illicit drugs and the environment — A review. Science of The Total Environment. 2013;463-464:1079-92.

14. Evgenidou EN, Konstantinou IK, Lambropoulou DA. Occurrence and removal of transformation products of PPCPs and illicit drugs in wastewaters: a review. Sci Total Environ. 2015;505:905-26.

15. von Gunten U. Oxidation Processes in Water Treatment: Are We on Track? Environ Sci Technol. 2018;52(9):5062-75.

16. von Gunten U. Ozonation of drinking water: Part I. Oxidation kinetics and product formation. Water Research. 2003;37(7):1443-67.

17. Ikehata K, Jodeiri Naghashkar N, Gamal El-Din M. Degradation of Aqueous Pharmaceuticals by Ozonation and Advanced Oxidation Processes: A Review. Ozone: Science & Engineering. 2006;28(6):353-414.

18. Huber MM, Canonica S, Park G-Y, von Gunten U. Oxidation of Pharmaceuticals during Ozonation and Advanced Oxidation Processes. Environmental Science & Technology. 2003;37(5):1016-24.

19. Jin X, Peldszus S, Huck PM. Reaction kinetics of selected micropollutants in ozonation and advanced oxidation processes. Water Research. 2012;46(19):6519-30.

20. Lee Y, von Gunten U. Advances in predicting organic contaminant abatement during ozonation of municipal wastewater effluent: reaction kinetics, transformation products, and changes of biological effects. Environmental Science: Water Research & Technology. 2016;2(3):421-42.

21. Kovalova L, Siegrist H, Von Gunten U, Eugster J, Hagenbuch M, Wittmer A, Moser R, McArdell CS. Elimination of micropollutants during post-treatment of hospital wastewater with powdered activated carbon, ozone, and UV. Environmental Science and Technology. 2013;47(14):7899-908.

22. Wert EC, Rosario-Ortiz FL, Snyder SA. Effect of ozone exposure on the oxidation of trace organic contaminants in wastewater. Water Research. 2009;43(4):1005-14.

23. Broséus R, Vincent S, Aboulfadl K, Daneshvar A, Sauvé S, Barbeau B, Prévost M. Ozone oxidation of pharmaceuticals, endocrine disruptors and pesticides during drinking water treatment. Water Research. 2009;43(18):4707-17.

24. Rosal R, Rodríguez A, Perdigón-Melón JA, Petre A, García-Calvo E, Gómez MJ, Agüera A, Fernández-Alba AR. Occurrence of emerging pollutants in urban wastewater and their removal through biological treatment followed by ozonation. Water Research. 2010;44(2):578-88.

25. Bourgin M, Beck B, Boehler M, Borowska E, Fleiner J, Salhi E, Teichler R, von Gunten U, Siegrist H, McArdell CS. Evaluation of a full-scale wastewater treatment plant upgraded with ozonation and biological post-treatments: Abatement of micropollutants, formation of transformation products and oxidation by-products. Water Research. 2018;129:486-98.

26. Boleda MR, Galceran MT, Ventura F. Behavior of pharmaceuticals and drugs of abuse in a drinking water treatment plant (DWTP) using combined conventional and ultrafiltration and reverse osmosis (UF/RO) treatments. Environmental Pollution. 2011;159(6):1584-91.

27. Rodayan A, Segura PA, Yargeau V. Ozonation of wastewater: Removal and transformation products of drugs of abuse. Science of The Total Environment. 2014;487:763-70.

28. Boleda MR, Galceran MT, Ventura F. Monitoring of opiates, cannabinoids and their metabolites in wastewater, surface water and finished water in Catalonia, Spain. Water Research. 2009;43(4):1126-36.

29. Von Sonntag C, Von Gunten U. Chemistry of ozone in water and wastewater treatment: IWA publishing; 2012.

30. Lee Y, von Gunten U. Quantitative structure–activity relationships (QSARs) for the transformation of organic micropollutants during oxidative water treatment. Water Research. 2012;46(19):6177-95.

31. Bourgin M, Borowska E, Helbing J, Hollender J, Kaiser HP, Kienle C, McArdell CS, Simon E, von Gunten U. Effect of operational and water quality parameters on conventional ozonation and the advanced oxidation process O_3/H_2O_2: Kinetics of micropollutant abatement, transformation product and bromate formation in a surface water. Water Res. 2017;122:234-45.

32. Lee Y, Gerrity D, Lee M, Bogeat AE, Salhi E, Gamage S, Trenholm RA, Wert EC, Snyder SA, von Gunten U. Prediction of Micropollutant Elimination during Ozonation of Municipal Wastewater Effluents: Use of Kinetic and Water Specific Information. Environmental Science & Technology. 2013;47(11):5872-81.

33. Petrie B, Youdan J, Barden R, Kasprzyk-Hordern B. Multi-residue analysis of 90 emerging contaminants in liquid and solid environmental matrices by ultra-high-performance liquid chromatography tandem mass spectrometry. J Chromatogr A. 2016;1431:64-78.

34. Prieto-Rodríguez L, Oller I, Klamerth N, Agüera A, Rodríguez EM, Malato S. Application of solar AOPs and ozonation for elimination of micropollutants in municipal wastewater treatment plant effluents. Water Research. 2013;47(4):1521-8.

35. Andreozzi R, Caprio V, Marotta R, Vogna D. Paracetamol oxidation from aqueous solutions by means of ozonation and H_2O_2/UV system. Water Research. 2003;37(5):993-1004.

36. Benner J, Salhi E, Ternes T, von Gunten U. Ozonation of reverse osmosis concentrate: Kinetics and efficiency of beta blocker oxidation. Water Research. 2008;42(12):3003-12.

37. Pérez Rey R, Padrón AS, García León L, Martínez Pozo M, Baluja C. Ozonation of Cytostatics in Water Medium. Nitrogen Bases. Ozone: Science & Engineering. 1999;21(1):69-77.

38. Dodd MC, Buffle M-O, von Gunten U. Oxidation of Antibacterial Molecules by Aqueous Ozone: Moiety-Specific Reaction Kinetics and Application to Ozone-Based Wastewater Treatment. Environmental Science & Technology. 2006;40(6):1969-77.

39. Wang S, Wang X, Chen J, Qu R, Wang Z. Removal of the UV Filter Benzophenone-2 in Aqueous Solution by Ozonation: Kinetics, Intermediates, Pathways and Toxicity. Ozone: Science & Engineering. 2018;40(2):122-32.

40. Hopkins ZR, Snowberger S, Blaney L. Ozonation of the oxybenzone, octinoxate, and octocrylene UV-filters: Reaction kinetics, absorbance characteristics, and transformation products. Journal of Hazardous Materials. 2017;338:23-32.

41. Liu H, Sun P, He Q, Feng M, Liu H, Yang S, Wang L, Wang Z. Ozonation of the UV filter benzophenone-4 in aquatic environments: Intermediates and pathways. Chemosphere. 2016;149:76-83.

42. Dantas RF, Canterino M, Marotta R, Sans C, Esplugas S, Andreozzi R. Bezafibrate removal by means of ozonation: Primary intermediates, kinetics, and toxicity assessment. Water Research. 2007;41(12):2525-32.

43. Deborde M, Rabouan S, Duguet J-P, Legube B. Kinetics of Aqueous Ozone-Induced Oxidation of Some Endocrine Disruptors. Environmental Science & Technology. 2005;39(16):6086-92.

44. Tay KS, Rahman NA, Abas MRB. Ozonation of parabens in aqueous solution: Kinetics and mechanism of degradation. Chemosphere. 2010;81(11):1446-53.

45. Rosal R, Rodríguez A, Perdigón-Melón JA, Petre A, García-Calvo E, Gómez MJ, Agüera A, Fernández-Alba AR. Degradation of caffeine and identification of the transformation products generated by ozonation. Chemosphere. 2009;74(6):825-31.

46. McDowell DC, Huber MM, Wagner M, von Gunten U, Ternes TA. Ozonation of Carbamazepine in Drinking Water: Identification and Kinetic Study of Major Oxidation Products. Environmental Science & Technology. 2005;39(20):8014-22.

47. Borowska E, Bourgin M, Hollender J, Kienle C, McArdell CS, von Gunten U. Oxidation of cetirizine, fexofenadine and hydrochlorothiazide during ozonation: Kinetics and formation of transformation products. Water Research. 2016;94:350-62.

48. Horsing M, Kosjek T, Andersen HR, Heath E, Ledin A. Fate of citalopram during water treatment with O_3, ClO_2, UV and Fenton oxidation. Chemosphere. 2012;89(2):129-35.

49. Lajeunesse A, Blais M, Barbeau B, Sauvé S, Gagnon C. Ozone oxidation of antidepressants in wastewater –Treatment evaluation and characterization of new by-products by LC-QToFMS. Chemistry Central Journal. 2013;7(1):15.

50. Lange F, Cornelissen S, Kubac D, Sein MM, von Sonntag J, Hannich CB, Golloch A, Heipieper HJ, Möder M, von Sonntag C. Degradation of macrolide antibiotics by ozone: A mechanistic case study with clarithromycin. Chemosphere. 2006;65(1):17-23.

51. Hoigné J, Bader H. Rate constants of reactions of ozone with organic and inorganic compounds in water—II: Dissociating organic compounds. Water Research. 1983;17(2):185-94.
52. Sein MM, Zedda M, Tuerk J, Schmidt TC, Golloch A, Sonntag Cv. Oxidation of Diclofenac with Ozone in Aqueous Solution. Environmental Science & Technology. 2008;42(17):6656-62.
53. Pereira RdO, de Alda ML, Joglar J, Daniel LA, Barceló D. Identification of new ozonation disinfection byproducts of 17β-estradiol and estrone in water. Chemosphere. 2011;84(11):1535-41.
54. Zhao Y, Yu G, Chen S, Zhang S, Wang B, Huang J, Deng S, Wang Y. Ozonation of antidepressant fluoxetine and its metabolite product norfluoxetine: Kinetics, intermediates and toxicity. Chemical Engineering Journal. 2017;316:951-63.
55. Lee Y, Kovalova L, McArdell CS, von Gunten U. Prediction of micropollutant elimination during ozonation of a hospital wastewater effluent. Water Research. 2014;64:134-48.
56. Real FJ, Benitez FJ, Acero JL, Sagasti JJP, Casas F. Kinetics of the Chemical Oxidation of the Pharmaceuticals Primidone, Ketoprofen, and Diatrizoate in Ultrapure and Natural Waters. Industrial & Engineering Chemistry Research. 2009;48(7):3380-8.
57. Garcia-Ac A, Broséus R, Vincent S, Barbeau B, Prévost M, Sauvé S. Oxidation kinetics of cyclophosphamide and methotrexate by ozone in drinking water. Chemosphere. 2010;79(11):1056-63.
58. Huber MM, Göbel A, Joss A, Hermann N, Löffler D, McArdell CS, Ried A, Siegrist H, Ternes TA, von Gunten U. Oxidation of Pharmaceuticals during Ozonation of Municipal Wastewater Effluents: A Pilot Study. Environmental Science & Technology. 2005;39(11):4290-9.
59. Jeon D, Kim J, Shin J, Hidayat ZR, Na S, Lee Y. Transformation of ranitidine during water chlorination and ozonation: Moiety-specific reaction kinetics and elimination efficiency of NDMA formation potential. Journal of Hazardous Materials. 2016;318:802-9.
60. Gómez-Ramos MdM, Mezcua M, Agüera A, Fernández-Alba AR, Gonzalo S, Rodríguez A, Rosal R. Chemical and toxicological evolution of the antibiotic

sulfamethoxazole under ozone treatment in water solution. Journal of Hazardous Materials. 2011;192(1):18-25.

61. Ferrando-Climent L, Gonzalez-Olmos R, Anfruns A, Aymerich I, Corominas L, Barceló D, Rodriguez-Mozaz S. Elimination study of the chemotherapy drug tamoxifen by different advanced oxidation processes: Transformation products and toxicity assessment. Chemosphere. 2017;168:284-92.

62. Blackbeard J, Lloyd J, Magyar M, Mieog J, Linden KG, Lester Y. Demonstrating organic contaminant removal in an ozone-based water reuse process at full scale. Environ Sci: Water Res Technol. 2016;2(1):213-22.

63. Zimmermann SG, Schmukat A, Schulz M, Benner J, Gunten Uv, Ternes TA. Kinetic and Mechanistic Investigations of the Oxidation of Tramadol by Ferrate and Ozone. Environmental Science & Technology. 2012;46(2):876-84.

64. Suarez S, Dodd MC, Omil F, von Gunten U. Kinetics of triclosan oxidation by aqueous ozone and consequent loss of antibacterial activity: Relevance to municipal wastewater ozonation. Water Research. 2007;41(12):2481-90.

65. Chen X, Richard J, Liu Y, Dopp E, Tuerk J, Bester K. Ozonation products of triclosan in advanced wastewater treatment. Water Research. 2012;46(7):2247-56.

66. Kuang J, Huang J, Wang B, Cao Q, Deng S, Yu G. Ozonation of trimethoprim in aqueous solution: Identification of reaction products and their toxicity. Water Research. 2013;47(8):2863-72.

67. Diehle M, Gebhardt W, Pinnekamp J, Schäffer A, Linnemann V. Ozonation of valsartan: Structural elucidation and environmental properties of transformation products. Chemosphere. 2019;216:437-48.

68. Zucker I, Mamane H, Riani A, Gozlan I, Avisar D. Formation and degradation of N-oxide venlafaxine during ozonation and biological post-treatment. Sci Total Environ. 2018;619-620:578-86.

69. Gottschalk C, Libra JA, Saupe A. Ozonation of water and waste water: A practical guide to understanding ozone and its applications: John Wiley & Sons; 2009.

70. Pi Y, Schumacher J, Jekel M. The Use of para-Chlorobenzoic Acid (pCBA) as an Ozone/Hydroxyl Radical Probe Compound. Ozone: Science & Engineering. 2005;27(6):431-6.

71. Mendoza A, Zonja B, Mastroianni N, Negreira N, Lopez de Alda M, Perez S, Barcelo D, Gil A, Valcarcel Y. Drugs of abuse, cytostatic drugs and iodinated contrast media in tap water from the Madrid region (central Spain):A case study to analyse

their occurrence and human health risk characterization. Environ Int. 2016;86:107-18.

72. Rosa Boleda M, Huerta-Fontela M, Ventura F, Galceran MT. Evaluation of the presence of drugs of abuse in tap waters. Chemosphere. 2011;84(11):1601-7.

73. Elovitz MS, von Gunten U, Kaiser H-P. Hydroxyl Radical/Ozone Ratios During Ozonation Processes. II. The Effect of Temperature, pH, Alkalinity, and DOM Properties. Ozone: Science & Engineering. 2000;22(2):123-50.

74. Buffle M-O, Schumacher J, Meylan S, Jekel M, von Gunten U. Ozonation and Advanced Oxidation of Wastewater: Effect of O_3 Dose, pH, DOM and HO•-Scavengers on Ozone Decomposition and HO• Generation. Ozone: Science & Engineering. 2006;28(4):247-59.

75. Elovitz MS, von Gunten U. Hydroxyl Radical/Ozone Ratios During Ozonation Processes. I. The R_{ct} Concept. Ozone: Science & Engineering. 1999;21(3):239-60.

76. Mandel P, Roche P, Wolbert D. Large-Scale Experimental Validation of a Model for the Kinetics of Ozone and Hydroxyl Radicals with Natural Organic Matter. Ozone: Science & Engineering. 2014;36(1):73-85.

77. Staehelin J, Hoigne J. Decomposition of ozone in water in the presence of organic solutes acting as promoters and inhibitors of radical chain reactions. Environmental Science & Technology. 1985;19(12):1206-13.

78. Hollender J, Zimmermann SG, Koepke S, Krauss M, McArdell CS, Ort C, Singer H, Von Gunten U, Siegrist H. Elimination of organic micropollutants in a municipal wastewater treatment plant upgraded with a full-scale post-ozonation followed by sand filtration. Environmental Science and Technology. 2009;43(20):7862-9.

79. Gonzales S, Peña A, Rosario-Ortiz FL. Examining the Role of Effluent Organic Matter Components on the Decomposition of Ozone and Formation of Hydroxyl Radicals in Wastewater. Ozone: Science & Engineering. 2012;34(1):42-8.

2.9 Supplementary information

Table 2.9.1. Molecular structure and additional information about the 90 OMPs (in alphabetical order). LC-MS performance data was obtained from Petrie et al. (1), where more parameters can also be found (linearity range, precision, accuracy).

Chemical	CAS number	Molecular weight (g mol^{-1})	Molecular formula	Molecular structure	Instrument detection limit (ng mL^{-1})	Instrument quantification limit (ng mL^{-1})
1,7-Dimethylxanthine	611-59-6	180.15	$C_7H_8N_4O_2$	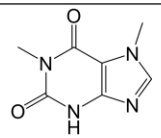	0.30	1.00
10,11-Dihydro-10-hydroxycarbamazepine	29331-92-8	254.28	$C_{15}H_{14}N_2O_2$	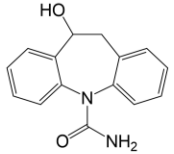	0.05	0.50
Acetaminophen	103-90-2	151.17	$C_8H_9NO_2$	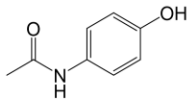	0.11	0.54
Amphetamine	300-62-9	135.21	$C_9H_{13}N$	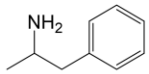	0.03	0.10

Chemical	CAS number	Molecular weight (g mol^{-1})	Molecular formula	Molecular structure	Instrument detection limit (ng mL^{-1})	Instrument quantification limit (ng mL^{-1})
Anhydroecgonine methylester	43021-26-7	181.23	$C_{10}H_{15}NO_2$	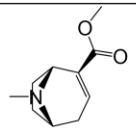	0.10	0.50
Atenolol	29122-68-7	266.34	$C_{14}H_{22}N_2O_3$	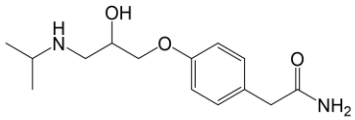	0.03	0.10
Atorvastatin	134523-00-5	558.64	$C_{33}H_{35}FN_2O_5$	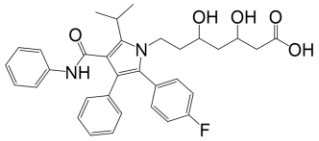	0.01	0.05
Azathioprine	446-86-6	277.26	$C_9H_7N_7O_2S$	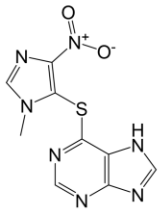	0.03	0.10
Azithromycin	83905-01-5	749	$C_{38}H_{72}N_2O_{12}$	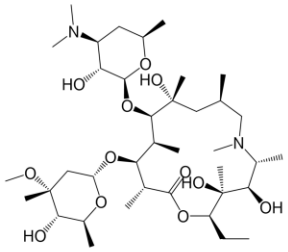	0.03	0.11

Chemical	CAS number	Molecular weight (g mol^{-1})	Molecular formula	Molecular structure	Instrument detection limit (ng mL^{-1})	Instrument quantification limit (ng mL^{-1})
Benzophenone-1	131-56-6	214.22	$C_{13}H_{10}O_3$	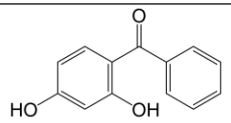	0.01	0.06
Benzophenone-2	131-55-5	246.22	$C_{13}H_{10}O_5$	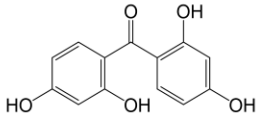	0.01	0.05
Benzophenone-3	131-57-7	228.25	$C_{14}H_{12}O_3$	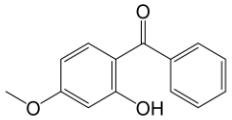	0.01	0.05
Benzophenone-4	4065-45-6	308.31	$C_{14}H_{12}O_6S$	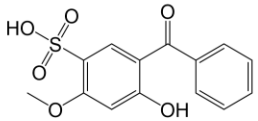	0.31	1.01
Benzoylecgonine	519-09-5	289.33	$C_{16}H_{19}NO_4$	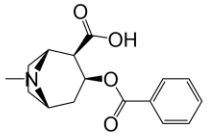	0.01	0.05
Bezafibrate	41859-67-0	361.83	$C_{19}H_{20}ClNO_4$	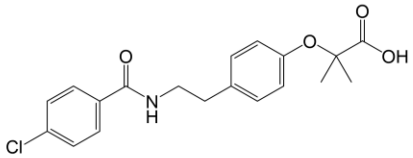	0.03	0.10

Chemical	CAS number	Molecular weight (g mol^{-1})	Molecular formula	Molecular structure	Instrument detection limit (ng mL^{-1})	Instrument quantification limit (ng mL^{-1})
Bisphenol A	80-05-7	228.29	$C_{15}H_{16}O_2$	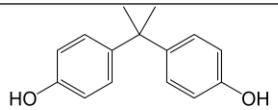	0.03	0.10
Butylparaben	94-26-8	194.23	$C_{11}H_{14}O_3$	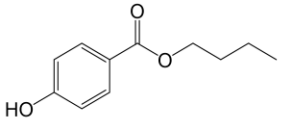	0.01	0.06
Caffeine	58-08-2	194.19	$C_8H_{10}N_4O_2$	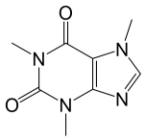	0.10	0.50
Carbamazepine	298-46-4	236.28	$C_{15}H_{12}N_2O$	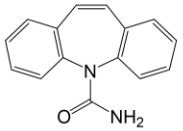	0.01	0.05
Carbamazepine-10,11-epoxide	36507-30-9	252.27	$C_{15}H_{12}N_2O_2$	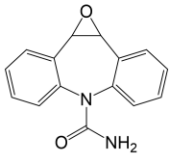	0.03	0.10
Cetirizine	83881-51-0	388.9	$C_{21}H_{25}ClN_2O_3$	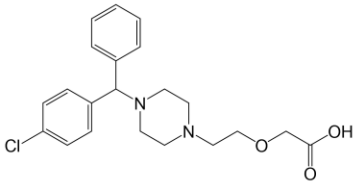	0.02	0.08

Chemical	CAS number	Molecular weight (g mol^{-1})	Molecular formula	Molecular structure	Instrument detection limit (ng mL^{-1})	Instrument quantification limit (ng mL^{-1})
Cimetidine	51481-61-9	252.34	$C_{10}H_{16}N_6S$	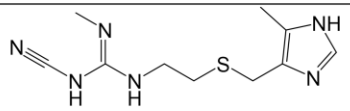	0.10	0.52
Citalopram	59729-33-8	324.4	$C_{20}H_{21}FN_2O$	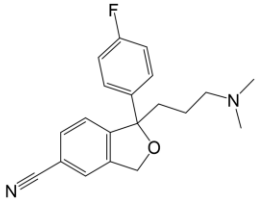	0.05	0.50
Clarithromycin	81103-11-9	747.97	$C_{38}H_{69}NO_{13}$	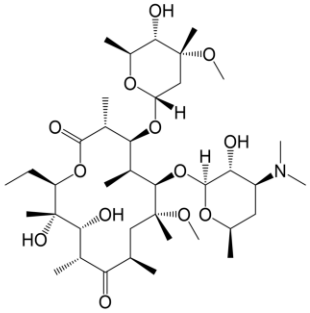	0.01	0.06
Cocaethylene	529-38-4	317.38	$C_{18}H_{23}NO_4$	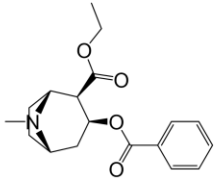	0.01	0.05

Chemical	CAS number	Molecular weight (g mol^{-1})	Molecular formula	Molecular structure	Instrument detection limit (ng mL^{-1})	Instrument quantification limit (ng mL^{-1})
Cocaine	50-36-2	303.36	$C_{17}H_{21}NO_4$	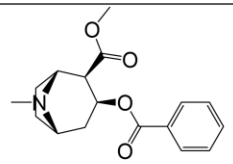	0.01	0.05
Codeine	76-57-3	299.37	$C_{18}H_{21}NO_3$	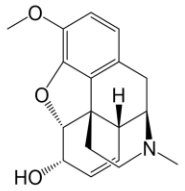	0.10	0.50
Cotinine	486-56-6	176.22	$C_{10}H_{12}N_2O$	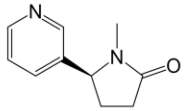	0.01	0.05
Creatinine	60-27-5	113.12	$C_4H_7N_3O$	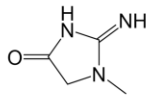	0.30	1.00
Desmethylcitalopram	62498-67-3	310.37	$C_{19}H_{19}FN_2O$	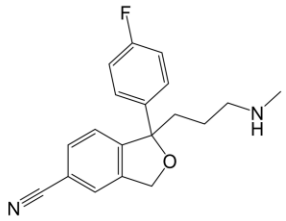	0.01	0.05

Chemical	CAS number	Molecular weight (g mol^{-1})	Molecular formula	Molecular structure	Instrument detection limit (ng mL^{-1})	Instrument quantification limit (ng mL^{-1})
Desmethylvenlafaxine	93413-62-8	263.38	$C_{16}H_{25}NO_2$	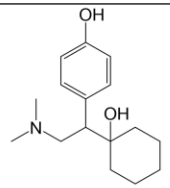	0.03	0.10
Diclofenac	15307-86-5	296.15	$C_{14}H_{11}Cl_2NO_2$	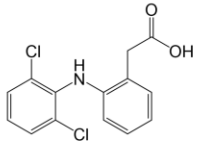	0.03	0.10
Dihydrocodeine	125-28-0	301.39	$C_{18}H_{23}NO_3$	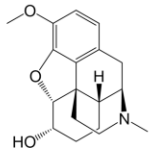	0.03	0.10
Dihydromorphine	509-60-4	287.36	$C_{17}H_{21}NO_3$	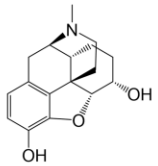	0.01	0.05
Diltiazem	42399-41-7	414.52	$C_{22}H_{26}N_2O_4S$	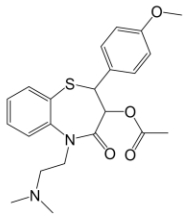	0.01	0.05

Chemical	CAS number	Molecular weight (g mol^{-1})	Molecular formula	Molecular structure	Instrument detection limit (ng mL^{-1})	Instrument quantification limit (ng mL^{-1})
E1	53-16-7	270.37	$C_{18}H_{22}O_2$	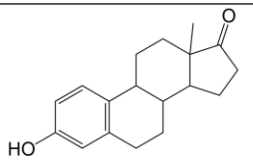	0.10	0.49
E2	50-28-2	272.39	$C_{18}H_{24}O_2$	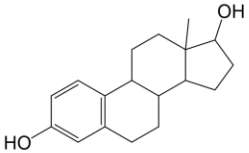	0.09	0.47
EDDP	30223-73-5	277.4	$C_{20}H_{23}N$	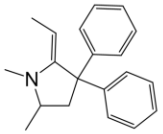	0.01	0.05
EE2	57-63-6	296.41	$C_{20}H_{24}O_2$	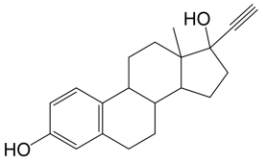	0.10	0.48
Ephedrine/pseudoephedrine	299-42-3	165.24	$C_{10}H_{15}NO$	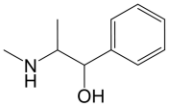	0.03	0.10
Ethylparaben	120-47-8	166.18	$C_9H_{10}O_3$	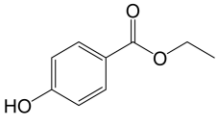	0.03	0.11

Chemical	CAS number	Molecular weight (g mol^{-1})	Molecular formula	Molecular structure	Instrument detection limit (ng mL^{-1})	Instrument quantification limit (ng mL^{-1})
Fexofenadine	83799-24-0	501.67	$C_{32}H_{39}NO_4$	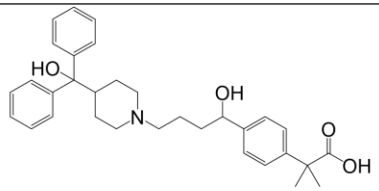	0.03	0.09
Fluoxetine	54910-89-3	309.33	$C_{17}H_{18}F_3NO$	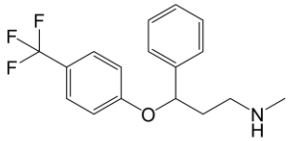	0.01	0.05
Gliclazide	21187-98-4	323.41	$C_{15}H_{21}N_3O_3S$	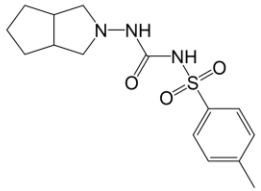	0.01	0.05
Heroin	561-27-3	369.42	$C_{21}H_{23}NO_5$	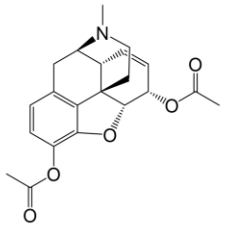	0.10	0.50
Ibuprofen	15687-27-1	206.29	$C_{13}H_{18}O_2$	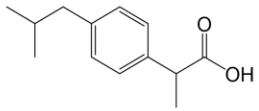	0.01	0.05

Chemical	CAS number	Molecular weight (g mol^{-1})	Molecular formula	Molecular structure	Instrument detection limit (ng mL^{-1})	Instrument quantification limit (ng mL^{-1})
Ifosfamide	3778-73-2	261.09	$C_7H_{15}Cl_2N_2O_2P$	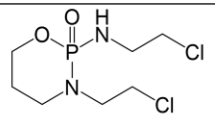	0.01	0.05
Iopromide	73334-07-3	791.12	$C_{18}H_{24}I_3N_3O_8$	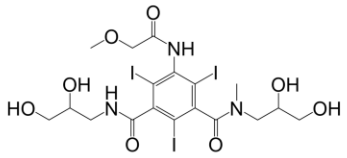	1.16	5.79
Irbesartan	138402-11-6	428.53	$C_{25}H_{28}N_6O$	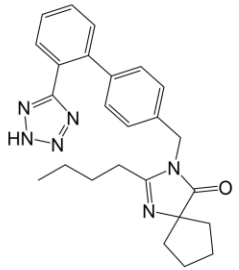	0.10	0.50
Ketamine	6740-88-1	237.73	$C_{13}H_{16}ClNO$	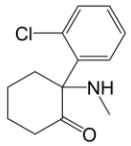	0.01	0.05
Ketoprofen	22071-15-4	254.29	$C_{16}H_{14}O_3$	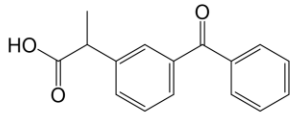	0.11	0.54

Chemical	CAS number	Molecular weight (g mol^{-1})	Molecular formula	Molecular structure	Instrument detection limit (ng mL^{-1})	Instrument quantification limit (ng mL^{-1})
Lisinopril	76547-98-3	405.5	$C_{21}H_{31}N_3O_5$	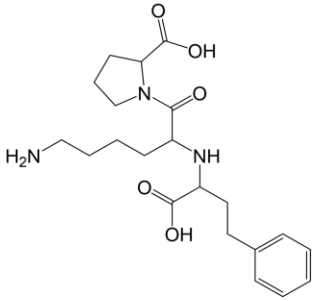	0.09	0.93
MDA	4764-17-4	179.22	$C_{10}H_{13}NO_2$	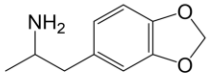	0.03	0.10
MDMA	42542-10-9	193.25	$C_{11}H_{15}NO_2$	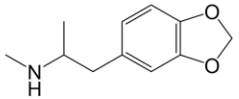	0.01	0.05
MDPV	687603-66-3	275.34	$C_{16}H_{21}NO_3$	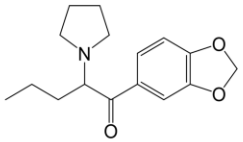	0.01	0.50
Mephedrone	1189805-46-6	177.24	$C_{11}H_{15}NO$	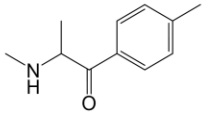	0.01	0.05
Metformin	657-24-9	129.17	$C_4H_{11}N_5$	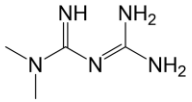	0.09	0.43

Chemical	CAS number	Molecular weight (g mol^{-1})	Molecular formula	Molecular structure	Instrument detection limit (ng mL^{-1})	Instrument quantification limit (ng mL^{-1})
Methadone	76-99-3	309.46	$C_{21}H_{27}NO$	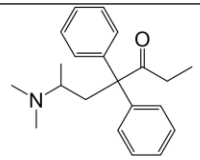	0.11	0.56
Methamphetamine	537-46-2	149.24	$C_{10}H_{15}N$	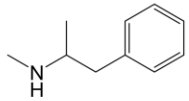	0.03	0.10
Methotrexate	59-05-2	454.45	$C_{20}H_{22}N_8O_5$	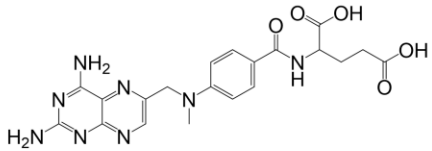	0.28	0.92
Methylparaben	99-76-3	152.15	$C_8H_8O_3$	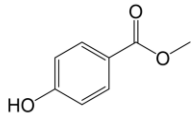	0.01	0.06
Metoprolol	51384-51-1	267.37	$C_{15}H_{25}NO_3$	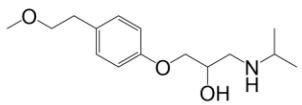	0.01	0.05
Mirtazapine	85650-52-8	265.35	$C_{17}H_{19}N_3$	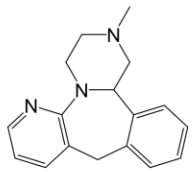	0.01	0.05

Chemical	CAS number	Molecular weight (g mol^{-1})	Molecular formula	Molecular structure	Instrument detection limit (ng mL^{-1})	Instrument quantification limit (ng mL^{-1})
Morphine	57-27-2	285.35	$C_{17}H_{19}NO_3$	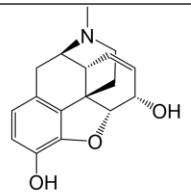	0.30	1.00
Naproxen	22204-53-1	230.27	$C_{14}H_{14}O_3$	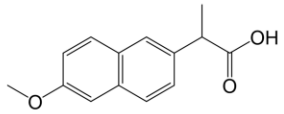	0.10	0.49
N-desmethyltramadol	75377-45-6	249.35	$C_{15}H_{23}NO_2$	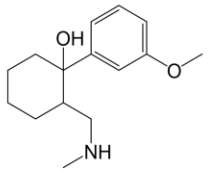	0.01	0.05
Nicotine	54-11-5	162.24	$C_{10}H_{14}N_2$	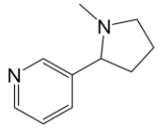	0.30	1.00
Norcodeine	467-15-2	285.35	$C_{17}H_{19}NO_3$	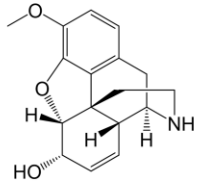	0.30	1.00

Chemical	CAS number	Molecular weight (g mol^{-1})	Molecular formula	Molecular structure	Instrument detection limit (ng mL^{-1})	Instrument quantification limit (ng mL^{-1})
Norephedrine	492-39-7	151.21	$C_9H_{13}NO$	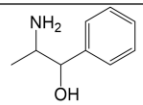	0.01	0.50
Norfluoxetine	83891-03-6	295.3	$C_{16}H_{16}F_3NO$	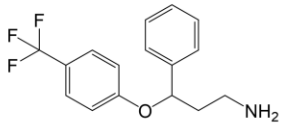	0.01	0.05
Norketamine	35211-10-0	233.7	$C_{15}H_{11}ClN_2O$	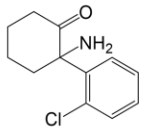	0.03	0.10
Normorphine	466-97-7	271.32	$C_{16}H_{17}NO_3$	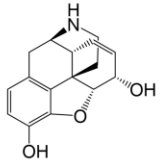	0.30	1.00
O-6-MAM	2784-73-8	327.37	$C_{19}H_{21}NO_4$	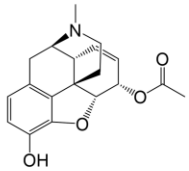	0.03	0.10
O-desmethyltramadol	185453-02-5	249.35	$C_{15}H_{23}NO_2$	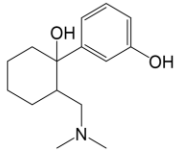	0.01	1.00

Chemical	CAS number	Molecular weight (g mol^{-1})	Molecular formula	Molecular structure	Instrument detection limit (ng mL^{-1})	Instrument quantification limit (ng mL^{-1})
Pholcodine	509-67-1	398.51	$C_{23}H_{30}N_2O_4$	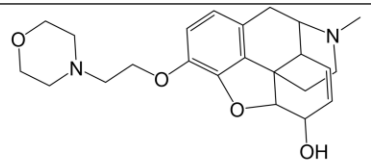	0.35	1.14
Propranolol	525-66-6	259.35	$C_{16}H_{21}NO_2$	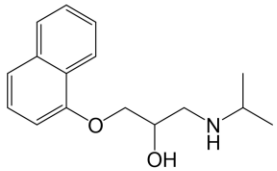	0.03	0.09
Propylparaben	94-13-3	180.21	$C_{10}H_{12}O_3$	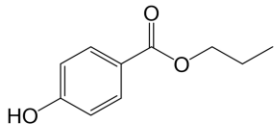	0.04	0.12
Quetiapine	111974-69-7	384.52	$C_{21}H_{25}N_3O_2S$	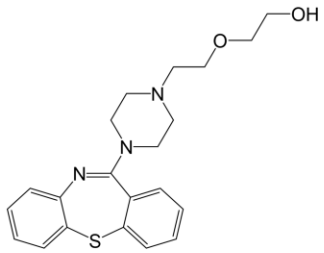	0.01	0.05
Ranitidine	66357-35-5	314.41	$C_{13}H_{22}N_4O_3S$	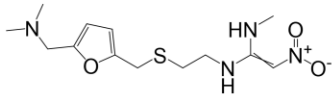	1.03	5.17

Chemical	CAS number	Molecular weight (g mol^{-1})	Molecular formula	Molecular structure	Instrument detection limit (ng mL^{-1})	Instrument quantification limit (ng mL^{-1})
Sertraline	79617-96-2	306.24	$C_{17}H_{17}Cl_2N$	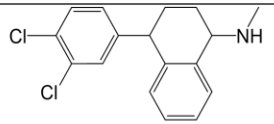	0.01	0.05
Sulfamethoxazole	723-46-6	253.28	$C_{10}H_{11}N_3O_3S$	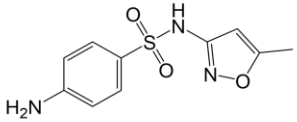	0.03	0.10
Sulfasalazine	599-79-1	398.4	$C_{18}H_{14}N_4O_5S$	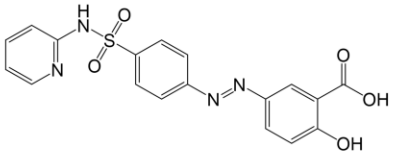	0.27	0.90
Tamoxifen	10540-29-1	371.53	$C_{26}H_{29}NO$	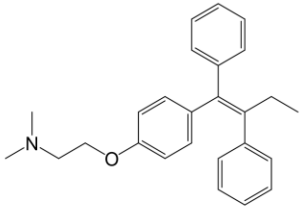	0.01	0.03
Temazepam	846-50-4	300.75	$C_{16}H_{13}ClN_2O_2$	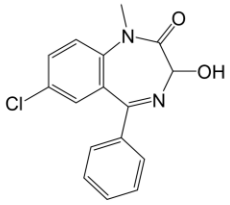	0.01	0.05

Chemical	CAS number	Molecular weight (g mol^{-1})	Molecular formula	Molecular structure	Instrument detection limit (ng mL^{-1})	Instrument quantification limit (ng mL^{-1})
Tramadol	27203-92-5	263.38	$C_{16}H_{25}NO_2$	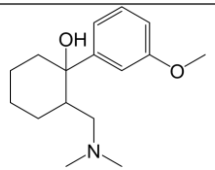	0.01	1.00
Triclosan	3380-34-5	289.55	$C_{12}H_7Cl_3O_2$	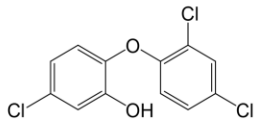	0.34	1.13
Trimethoprim	738-70-5	290.32	$C_{14}H_{18}N_4O_3$	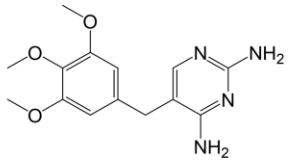	0.03	0.10
Tylosin	1401-69-0	916.12	$C_{46}H_{77}NO_{17}$	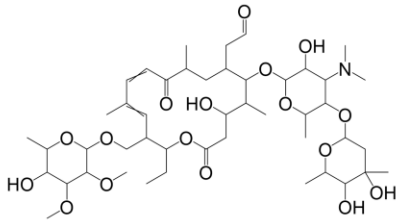	0.01	0.10

Chemical	CAS number	Molecular weight (g mol^{-1})	Molecular formula	Molecular structure	Instrument detection limit (ng mL^{-1})	Instrument quantification limit (ng mL^{-1})
Valsartan	137862-53-4	435.53	$C_{24}H_{29}N_5O_3$	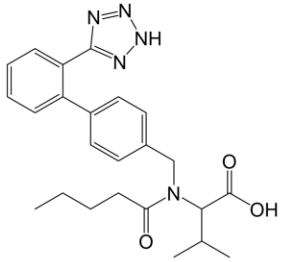	0.34	1.12
Venlafaxine	93413-69-5	277.41	$C_{17}H_{27}NO_2$	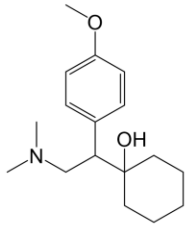	0.01	0.04

Table 2.9.2. Second order rate constants for the reaction of 40 OMPs with OH radicals. Experimentally determined, unless otherwise specified (QSAR: Quantitative structure–activity relationship).

Compound	k_{OH} (M^{-1} s^{-1})	Reference
Acetaminophen	2.2×10^9	(2)
Atenolol	8.0×10^9	(3)
Atorvastatin	1.9×10^{10}	(4)
Azathioprine	1.86×10^9	(5)
Azithromycin	2.9×10^9	(6)
Benzophenone-3	2.97×10^{10}	(7)
Benzoylecgonine	5.13×10^9	(8)
Bezafibrate	7.4×10^9	(9)
Bisphenol A	1.02×10^{10}	(10)
Butylparaben	9.2×10^9	(11)
Caffeine	5.9×10^9	(12)
Carbamazepine	8.8×10^9	(9)
Cimetidine	6.5×10^9	(13)
Diclofenac	7.5×10^9	(9)
E1	2.6×10^{10}	(14)
E2	1.41×10^{10}	(10)
EE2	1.08×10^{10}	(10)
Ethylparaben	7.7×10^9	(11)
Fluoxetine	9×10^9	(15)
Ibuprofen	7.4×10^9	(9)
Ifosfamide	3.6×10^9	(16)
Iopromide	3.3×10^9	(9)
Ketoprofen	8.4×10^9	(17)
Metformin	1.4×10^9	(16)
Methamphetamine	7.9×10^9	(18)
Methotrexate	8.7×10^9	(19)
Methylparaben	6.8×10^9	(11)
Metoprolol	7.3×10^9	(3)
Morphine	10^{10} (QSAR)	(20)
Naproxen	9.6×10^9	(21)
Propranolol	1.0×10^{10}	(3)
Propylparaben	8.6×10^9	(11)
Ranitidine	1.5×10^{10}	(13)
Sulfamethoxazole	5.5×10^9	(9)
Tramadol	6.3×10^9	(22)
Triclosan	5.4×10^9	(23)
Trimethoprim	6.9×10^9	(6)
Tylosin	8.2×10^9	(6)
Valsartan	10^{10} (QSAR)	(20)
Venlafaxine	8.8×10^9	(16)

References

1. Petrie B, Youdan J, Barden R, Kasprzyk-Hordern B. Multi-residue analysis of 90 emerging contaminants in liquid and solid environmental matrices by ultra-high-performance liquid chromatography tandem mass spectrometry. J Chromatogr A. 2016;1431:64-78.

2. Andreozzi R, Caprio V, Marotta R, Vogna D. Paracetamol oxidation from aqueous solutions by means of ozonation and H_2O_2/UV system. Water Research. 2003;37(5):993-1004.

3. Benner J, Salhi E, Ternes T, von Gunten U. Ozonation of reverse osmosis concentrate: Kinetics and efficiency of beta blocker oxidation. Water Research. 2008;42(12):3003-12.

4. Lam MW, Mabury SA. Photodegradation of the pharmaceuticals atorvastatin, carbamazepine, levofloxacin, and sulfamethoxazole in natural waters. Aquatic Sciences. 2005;67(2):177-88.

5. Zhang Y, Zhang J, Xiao Y, Chang VWC, Lim T-T. Kinetic and mechanistic investigation of azathioprine degradation in water by UV, UV/H_2O_2 and UV/persulfate. Chemical Engineering Journal. 2016;302:526-34.

6. Dodd MC, Buffle M-O, von Gunten U. Oxidation of Antibacterial Molecules by Aqueous Ozone: Moiety-Specific Reaction Kinetics and Application to Ozone-Based Wastewater Treatment. Environmental Science & Technology. 2006;40(6):1969-77.

7. Gong P, Yuan H, Zhai P, Xue Y, Li H, Dong W, Mailhot G. Investigation on the degradation of benzophenone-3 by UV/H_2O_2 in aqueous solution. Chemical Engineering Journal. 2015;277:97-103.

8. Spasiano D, Russo D, Vaccaro M, Siciliano A, Marotta R, Guida M, Reis NM, Li Puma G, Andreozzi R. Removal of benzoylecgonine from water matrices through UV_{254}/H_2O_2 process: Reaction kinetic modeling, ecotoxicity and genotoxicity assessment. Journal of Hazardous Materials. 2016;318:515-25.

9. Huber MM, Canonica S, Park G-Y, von Gunten U. Oxidation of Pharmaceuticals during Ozonation and Advanced Oxidation Processes. Environmental Science & Technology. 2003;37(5):1016-24.

10. Rosenfeldt EJ, Linden KG. Degradation of Endocrine Disrupting Chemicals Bisphenol A, Ethinyl Estradiol, and Estradiol during UV Photolysis and Advanced Oxidation Processes. Environmental Science & Technology. 2004;38(20):5476-83.
11. Tay KS, Rahman NA, Abas MRB. Ozonation of parabens in aqueous solution: Kinetics and mechanism of degradation. Chemosphere. 2010;81(11):1446-53.
12. Shi X, Dalal NS, Jain AC. Antioxidant behaviour of caffeine: Efficient scavenging of hydroxyl radicals. Food Chem Toxicol. 1991;29(1):1-6.
13. Latch DE, Stender BL, Packer JL, Arnold WA, McNeill K. Photochemical Fate of Pharmaceuticals in the Environment: Cimetidine and Ranitidine. Environmental Science & Technology. 2003;37(15):3342-50.
14. Nakonechny M, Ikehata K, Gamal El-Din M. Kinetics of Estrone Ozone/Hydrogen Peroxide Advanced Oxidation Treatment. Ozone: Science & Engineering. 2008;30(4):249-55.
15. Lam MW, Young CJ, Mabury SA. Aqueous Photochemical Reaction Kinetics and Transformations of Fluoxetine. Environmental Science & Technology. 2005;39(2):513-22.
16. Wols BA, Hofman-Caris CHM, Harmsen DJH, Beerendonk EF. Degradation of 40 selected pharmaceuticals by UV/H_2O_2. Water Research. 2013;47(15):5876-88.
17. Real FJ, Benitez FJ, Acero JL, Sagasti JJP, Casas F. Kinetics of the Chemical Oxidation of the Pharmaceuticals Primidone, Ketoprofen, and Diatrizoate in Ultrapure and Natural Waters. Industrial & Engineering Chemistry Research. 2009;48(7):3380-8.
18. Gu D, Guo C, Lv J, Hou S, Zhang Y, Feng Q, Zhang Y, Xu J. Removal of methamphetamine by UV-activated persulfate: Kinetics and mechanisms. Journal of Photochemistry and Photobiology A: Chemistry. 2019;379:32-8.
19. Lai WW-P, Hsu M-H, Lin AY-C. The role of bicarbonate anions in methotrexate degradation via UV/TiO_2: Mechanisms, reactivity and increased toxicity. Water Research. 2017;112:157-66.
20. Lee Y, Kovalova L, McArdell CS, von Gunten U. Prediction of micropollutant elimination during ozonation of a hospital wastewater effluent. Water Research. 2014;64:134-48.
21. Packer JL, Werner JJ, Latch DE, McNeill K, Arnold WA. Photochemical fate of pharmaceuticals in the environment: Naproxen, diclofenac, clofibric acid, and ibuprofen. Aquatic Sciences. 2003;65(4):342-51.

22. Zimmermann SG, Schmukat A, Schulz M, Benner J, Gunten Uv, Ternes TA. Kinetic and Mechanistic Investigations of the Oxidation of Tramadol by Ferrate and Ozone. Environmental Science & Technology. 2012;46(2):876-84.

23. Latch DE, Packer JL, Stender BL, VanOverbeke J, Arnold WA, McNeill K. Aqueous photochemistry of triclosan: Formation of 2,4-dichlorophenol, 2,8-dichlorodibenzo-p-dioxin, and oligomerization products. Environmental Toxicology and Chemistry. 2005;24(3):517-25.

Chapter 3: Continuous ozonation merged with biofiltration to study oxidative and microbial transformation of trace organic contaminants

This chapter is presented in publication format. This work was published in Environmental Science: Water Research & Technology (RSC) in January 2019 (DOI: https://doi.org/10.1039/C8EW00855H).

Context: Ozonation is commonly followed by a biofiltration step for polishing of the ozonated water, namely for removal of biodegradable organic matter that was generated from ozone-induced oxidation reactions. With an ever-increasing number of ozone applications for the abatement of trace organic contaminants, the question arises whether biofiltration post-treatment can also remove the ozonation products of these contaminants. Studies of the ozonation-biofiltration treatment scheme are usually performed at large-scale or pilot-scale treatment plants, which require significant infrastructure and entail a high cost. Through a collaboration with DVGW-Technologiezentrum Wasser we developed and tested a low-cost and easy to build lab-scale setup to conduct continuous long-term studies on ozonation-biofiltration of trace organic contaminants.

Contributions: The following work was performed by the author of this thesis under the supervision of Dr Jannis Wenk and the co-supervision of Prof Barbara Kasprzyk-Hordern:

- Building and testing the COMBI system in Bath
- Experiments with carbamazepine, diclofenac and fluoxetine and related analysis
- Literature research and writing the manuscript

Dr Oliver Happel and Dr Marco Scheurer from DVGW-Technologiezentrum Wasser performed the following:

- Building and testing the COMBI system in Karlsruhe
- Experiments with acesulfame and dimethylsulfamide and related analysis, in addition to TFA measurements for samples from Bath
- Offering input for the manuscript

COMBI, continuous ozonation merged with biofiltration to study oxidative and microbial transformation of trace organic contaminants

Garyfalia A. Zoumpouli[a,d,e], Marco Scheurer[b], Heinz-Jürgen Brauch[b], Barbara Kasprzyk-Hordern[c,e], Jannis Wenk[d,e,*], Oliver Happel[b]

[a] Centre for Doctoral Training, Centre for Sustainable Chemical Technologies, University of Bath, BA2 7AY, UK.

[b] DVGW-Technologiezentrum Wasser (TZW), Karlsruher Straße 84, 76139 Karlsruhe, Germany.

[c] Department of Chemistry, University of Bath, BA2 7AY, UK.

[d] Department of Chemical Engineering, University of Bath, BA2 7AY, UK.

[e] Water Innovation and Research Centre (WIRC), University of Bath, BA2 7AY, UK.

*Corresponding author

3.1 Abstract

Investigating the biodegradation of ozonation products of trace organic contaminants is important to further elucidate their fate and to assess the efficiency of advanced water treatment processes. In this study, a Continuous Ozonation merged with Biofiltration (COMBI) laboratory system based on an electrochemical ozone generation method was developed. The system can be operated continuously and resource-efficiently over several months by supplying ozone doses typically used for water treatment and providing stable conditions for the establishment of microbial communities in biofiltration columns. Five trace organic contaminants, acesulfame, carbamazepine, diclofenac, dimethylsulfamide and fluoxetine, were investigated under drinking water and secondary treated wastewater ozonation conditions. After an equilibration time of three weeks, biodegradable ozonation products, for example *N*-nitrosodimethylamine (NDMA) and an acesulfame product, were removed in the filtration columns. Recalcitrant oxidation products such as trifluoroacetic acid (TFA) and two products of diclofenac either passed through the columns at unchanged concentration or were removed to a minor extent. The formation of a secondary biotransformation product from carbamazepine ozonation products could be also observed. In summary, the results show that the developed system is a valuable tool

to investigate complex transformation processes of ozonation products during biofiltration. COMBI will simplify future ozonation-biotransformation studies and enable more comprehensive investigations with a wider range of contaminants under different conditions.

3.2 Water impact

A continuously operating ozonation biofiltration system was developed and tested in a proof-of-concept study by following the fate of ozonation products of five exemplary trace organic contaminants during both a drinking water and a wastewater effluent ozonation scenario. The resourceful and flexible lab-scale system will lead to a better understanding of complex contaminant transformation processes during advanced water treatment schemes.

3.3 Introduction

Trace organic contaminants (TrOCs) are a diverse class of organic compounds comprising pharmaceuticals, personal care products, hormones, pesticides and specialty chemicals that are frequently present at nanogram to microgram per liter concentrations in surface water, ground water and drinking water (1-4). The main entry pathways for TrOCs into water bodies are direct sources from agriculture, aquaculture and urban stormwater runoff (5, 6), and indirectly through wastewater treatment plants (7-9). The occurrence of TrOCs in the aquatic environment poses a threat to various sensitive organisms (10, 11) and may adversely affect whole ecosystems (12). Furthermore, the detection of TrOCs in drinking water (13, 14) has raised public concerns (15, 16). In 2015 the European Commission published a first watch list of emerging water contaminants with the aim to create a reliable information base on the occurrence of selected substances across the EU (17). As a consequence, more stringent measures to reduce concentrations of TrOCs in water bodies can be expected, including the widespread application of advanced water treatment approaches.

Ozone is a traditional drinking water disinfectant (18) and ozonation is among the most promising technologies to degrade TrOCs during advanced wastewater

treatment, water recycling and for drinking water production (19-22). Ozone attacks electron rich moieties of organic substrates such as double bonds, tertiary amines, organosulfur compounds and activated aromatic systems (23). Secondary oxidants derived from ozone decomposition, in particular hydroxyl radicals, react less selectively mainly by hydroxylation, hydrogen abstraction and electron transfer (24). At ozone doses typically applied for water treatment, primary and secondary oxidation reactions do not lead to significant mineralization but generate biodegradable assimilable organic carbon (25-28) and transformation products of TrOCs (29). Some products are recalcitrant to further degradation (30). Ozonation is usually combined with a biofiltration step such as sand filtration to remove biodegradable organic carbon and to further break down transformation products (31). Ozonation can be also applied prior to natural engineered water treatment, including constructed wetlands, soil aquifer treatment and riverbank filtration (32).

Biofiltration and post-ozonation engineered natural treatment stages contribute to reducing ecotoxicity indicators of the treated water, which in some cases have been found to increase after ozonation (30, 33), depending on treatment conditions (34). Therefore, the combined effect of ozonation and subsequent biofiltration leads to significant reduction of the ecotoxicity of the treated water (35-40). The degradation of TrOCs during biofiltration depends on several factors, such as contaminant concentration (41), retention time (42, 43), age, diversity and adaptation of the microbial community (44, 45), substrate availability and composition for microbial metabolic processes (46, 47), redox conditions (48, 49), and temperature (50). Similar relationships during biofiltration can be expected for the removal of transformation products. However, extended studies are needed to further understand the fate of transformation products during biofiltration and to optimize removal efficiency under different conditions. A recent review concluded that the biodegradability of ozonation products of TrOCs depends on the reactive site of the target contaminant and on its reaction mechanism with ozone (51). Although ozonation products of numerous TrOCs have been identified, there are currently only a limited number of studies that investigate the biodegradability of ozonation products such as *N*-oxides (52-54).

In the lab, ozonation of a water sample can be readily performed, while biological treatment processes following ozonation must be continuous to provide a stable and adapted microbiological community. The available studies have therefore employed

batch ozonation followed by biofiltration or were carried out in pilot-scale and full-scale systems. These approaches have disadvantages because they are either laborious or require access to large infrastructure. An alternative is to perform batch biodegradation tests with ozonation products. However, the results of batch experiments might not be transferrable to continuous processes used in water and wastewater treatment. The kinetics in batch processes are different, the water matrix changes over time, and short-lifetime transformation products can only be studied through the online coupling of ozonation and biofiltration.

The goal of this study was to develop a cost-efficient continuously operating lab-scale system for the investigation of the ozonation of TrOCs and the fate of their ozonation and bio-transformation products during subsequent biological treatment steps. Two equivalent continuous ozonation systems with miniaturized electrochemical ozone generators followed by biologically active sand filtration columns were used, to test both a drinking water production scenario and a tertiary wastewater treatment scenario, which are two of the main applications of this treatment scheme. The selection of the target TrOCs was based on their diverse physicochemical properties and their relevance for drinking water (dimethylsulfamide, a pesticide metabolite, and acesulfame, an artificial sweetener), and wastewater (the pharmaceuticals carbamazepine, diclofenac, and fluoxetine). Through the analysis of literature-known transformation products the results could be compared with the ones from full-scale treatment plants and the capability of the COMBI setup could be proven.

3.4 Materials and Methods

3.4.1 Chemicals

All chemicals, including solvents, analytical consumables, TrOCs and ingredients for the preparation of synthetic wastewater were purchased from commercial sources. A list for TrOCs and analytical standards is provided in the supplementary information (SI, Text 3.9.2), including a table of molecular and structural data of parent compounds and their investigated ozonation products (SI, Table 3.9.2). Aqueous stock solutions were prepared from ultrapure water (resistivity >18 MΩ cm^{-1}) from Milli-Q (Merck) or ELGA (Veolia) water purification systems. Synthetic wastewater (SI,

Table 3.9.5) was prepared from tap water or deionized water according to OECD guidelines for synthetic sewage (55).

3.4.2 Experimental setup

The initial small-scale column setup for studying continuous ozonation merged with biofiltration (COMBI) was designed and built at DVGW-Technologiezentrum Wasser, Germany (System 1). This setup was used to investigate dimethylsulfamide (DMS) and acesulfame (ACE) in a waterworks scenario. A similar setup was built at the University of Bath, UK (System 2) and used to investigate the fate of carbamazepine (CBZ), diclofenac (DF) and fluoxetine (FLX) in a wastewater effluent ozonation scenario.

A schematic of the setup is shown in Figure 3.4.1. Photographs are shown in SI, Figure 3.9.1 and a summary of costs for parts is listed in SI, Table 3.9.1. The setup consisted of an ozonation column and three post-ozonation filtration columns, feed and effluent storage tanks, a pump and an ozone generation vessel. An ozone micro-cell (Innovatec Gerätetechnik GmbH, Germany) was used to generate ozone by electrolysis of demineralized water. The cell consists of porous stainless-steel frits that are used as electrodes, which are contacted with an ion-conducting membrane (solid electrolyte of a polymer, <0.2 mm). The amount of ozone generated is determined by the number of electrolysis cells and the DC current applied. Head-space ozone, including oxygen and hydrogen as by-products, flowed continuously *via* the intrinsic pressure of the electrochemical gas production through a tube connected to a sparger into the ozonation column. Water was delivered from the storage tank into the ozonation column using adjustable membrane pumps or gear pumps. The water was then gravity-fed from the ozonation column into the subsequent filtration columns.

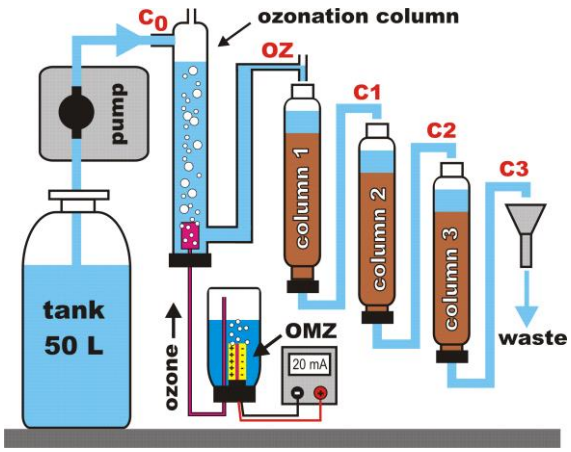

Figure 3.4.1. Schematic of the continuous small-scale ozonation/biofiltration setup. Sampling points are shown as C_0, OZ, C1, C2 and C3.

3.4.3 Operational parameters

The operational parameters of both systems are summarized in Table 3.4.1. System 1 used anthracite (Everzit) as filtration medium for the first column C1, and sand from a drinking water treatment plant for columns C2 and C3. The sand had been used for several years in a sand filter after an ozone treatment, and was used in the COMBI columns without any cleaning. For System 2 water filtration sand (0.7 mm to 1.2 mm, 1.0 to 2.0 mm, Long Rake Spar, UK) was used as purchased. A 1 cm-layer of the coarser sand served as bottom support over a metal mesh in each column. System 2 was inoculated with secondary treated wastewater effluent, while System 1 was not specifically inoculated. Both systems had been operating continuously at room temperature in the presence of target trace contaminants for at least three weeks before sampling first occurred. The columns were covered with aluminum foil to prevent photolysis, and sand is a non-adsorptive filtration medium.

The drinking water used for operating System 1 was obtained from groundwater, which is only treated by aeration. In a single combined experiment, 100 L of feed water were spiked with the target compounds (DMS = 16 nmol L^{-1} and ACE = 0.6 µmol L^{-1} to 1 µmol L^{-1}), and refilled weekly. Due to the persistence and high solubility of both ACE and DMS in water, no removal by degradation or significant adsorption to the feed tank was observed. Samples were collected on days 7, 24 and 97 for DMS and 24, 27 and 93 for ACE.

Table 3.4.1. Operational parameters.

Parameter	System 1 (Karlsruhe)	System 2 (Bath)
Ozone generation	Ozone-Microcell with 4 cell hearts (Innovatec)	
Voltage of microcell/V	24	
Current of microcell/mA	10 to 200	
Ozone output/(mg min^{-1})	0.01 to 1	
Pump	Solenoid diaphragm pump (e.g. FMM 20, KNF) or gear pump (e.g. REGLO-Z digital, Ismatec)	
Flow rate used for long-term operation/(mL min^{-1})	6	3
Diameter, length of the ozonation column/cm	1.8, 17.5	2, 20
Volume of ozonation column/mL	45	60
Diameter, length of each filtration column/cm	6.5, 20	4, 30
Volume of each filtration column/mL	660	375
Filtration medium/mm	Everzit®N (C1) and sand from a water treatment plant (C2/C3)	Quartz sand, 0.7 to 1.2/1.0 to 2.0 (Long Rake Spar)
Water type	Drinking water	Synthetic wastewater
Water characteristics	pH 7.2, conductivity 610 µS cm^{-1}, TOC ~ 0.9 mg L^{-1}, calcium carbonate hardness 3.2 mmol L^{-1}	pH 7.4, conductivity 800 µS cm^{-1}, TOC ~ 7 mg L^{-1}, TN ~ 7.5 mg L^{-1}
Target contaminants	Dimethylsulfamide (DMS), acesulfame (ACE)	Carbamazepine (CBZ), diclofenac (DF), fluoxetine (FLX)

The synthetic wastewater for System 2 was prepared freshly three times a week according to OECD guidelines for synthetic sewage (55) at 10-fold dilution to yield an initial total organic carbon (TOC) concentration of 10 mg L^{-1} (SI, Table 3.9.5). The easily biodegradable organic matter contained in this mixture led to biofilm growth and occasional clogging of the first column, which was resolved by scraping or manually removing the upper sand layer. The TrOCs CBZ, DF and FLX were spiked simultaneously into the influent tank (a range of 10 L to 15 L of synthetic wastewater) at a concentration of 1 µmol L^{-1} to 3 µmol L^{-1} two weeks after

continuous operation had started, to allow time for a microbial community to grow. The measured concentration in the influent tank fluctuated slightly due to the relatively large volume prepared for each refill, and sorption or slow microbial decomposition occurring in the tank. Samples were collected on days 22, 28, 42 and 54, where day 1 is the first day when trace contaminants were spiked. All samples were collected and analyzed in duplicate.

To enable detection of transformation products without pre-concentration, spiked levels of ACE, CBZ, DF and FLX were higher than those typically found in wastewater effluent (7). The microbial characterization of the sand columns was not the scope of this study, while known transformation pathways were consulted to interpret results.

3.4.4 Analysis

A description of analytical methods for all target compounds and their transformation products is provided in SI Section 3.9.3. Briefly, ultra high performance liquid chromatography-mass spectrometry (UHPLC-MS) analysis for CBZ, DF and FLX was performed with a Thermo Scientific Dionex UltiMate 3000 system coupled to a Bruker Daltonics maXis HD electrospray ionization quadrupole time-of-flight (ESI-QTOF) mass spectrometer. Transformation products of CBZ and DF were identified based on literature data, mass accuracy, consistent retention time and MS/MS analysis in MRM (multiple reaction monitoring) mode. Fragmentation patterns are provided in SI, Section 3.9.8. Direct injection was used for the analysis of trifluoroacetic acid (TFA), ACE and its ozonation product OP168. DMS and *N*-nitrosodimethylamine (NDMA) samples were pre-concentrated with solid phase extraction (SPE) prior the analysis (56). Analysis was performed on an API 5500 Q-Trap triple quadrupole mass spectrometer (Applied Biosystems/MDS Sciex Instruments, Concord, ON, Canada). TFA analysis was performed using ion exchange liquid chromatography-electrospray tandem mass spectrometry (LC-ESI-MS/MS) according to a recently developed method (57). GC analysis for NDMA was carried out with a series 6890 gas chromatograph connected to a MSD 5973 inert mass spectrometer (both Agilent, Waldbronn, Germany).

UV/Vis absorption for the determination of dissolved ozone in water with the indigo method (58), and for tracer tests with fluorescein to determine hydraulic residence times (HRTs), were conducted with stationary devices (e.g. Cary 100, Agilent; FP 8200, Jasco; EVO300, Thermo Scientific) or a self-built portable LED photometer. In System 2, the dissolved ozone concentration was measured in pure water (no reactions present) by sampling the water inside the ozonation column. In System 1, the ozone dose was measured by feeding an indigo solution through the ozonation column, which captured directly the ozone transferred. More details are provided in the SI Section 3.9.4.

3.5 Results and discussion

3.5.1 Determination of operational range

Initial tests determined ozone contact time and HRTs. Fluorescein breakthrough curves for both systems are shown in Figure 3.5.1A and B. Further details are provided in SI Section 3.9.6. The HRT was assumed to be equal to the time of maximum (complete) tracer breakthrough. At a flow rate of 6 mL min^{-1}, the ozonation contact time in System 1 was 30 min and the total HRT was approximately 5 h. For System 2 the ozonation contact time at a flow rate of 3 mL min^{-1} was 10 min and the HRT was approximately 4 h. A wide range of operational parameters can be achieved by varying the flow rate. For instance, in System 2 a change of flow rate from 2 mL min^{-1} to 12 mL min^{-1}, results in the single column HRT changing from 150 min to 15 min (SI, Figure 3.9.6), with the total HRT decreasing from approximately 8 h to 1 h.

The relationship of the applied electrical current of the electrochemical cell and the ozone dose is presented in Figure 3.5.1C. The change in ozone concentration for a single cell over time is shown in Figure 3.5.1D. The decreasing efficiency of ozone production is due to aging of the ozone micro-cells. The difference between the two systems can be attributed to design differences, such as the length of the tubing connecting the microcell vessel and the ozonation column, the height and volume of the ozonation column, and the hydrostatic pressure which must be overcome by the gas. To further characterize the mass transfer of ozone in the system, analysis of the ozone concentration in the inlet gas and the off-gas would need to be conducted.

Long-term experiments were conducted at conditions similar to those of other ozonation-biofiltration systems (ozone dose of 1 mg L^{-1} to 10 mg L^{-1}, ozonation HRT of 30 min or less, filtration HRT of 10 min to 30 min) (21, 52) without further optimization of the operational parameters. A longer filtration HRT was chosen to elucidate the fate of compounds that are not easily biodegradable.

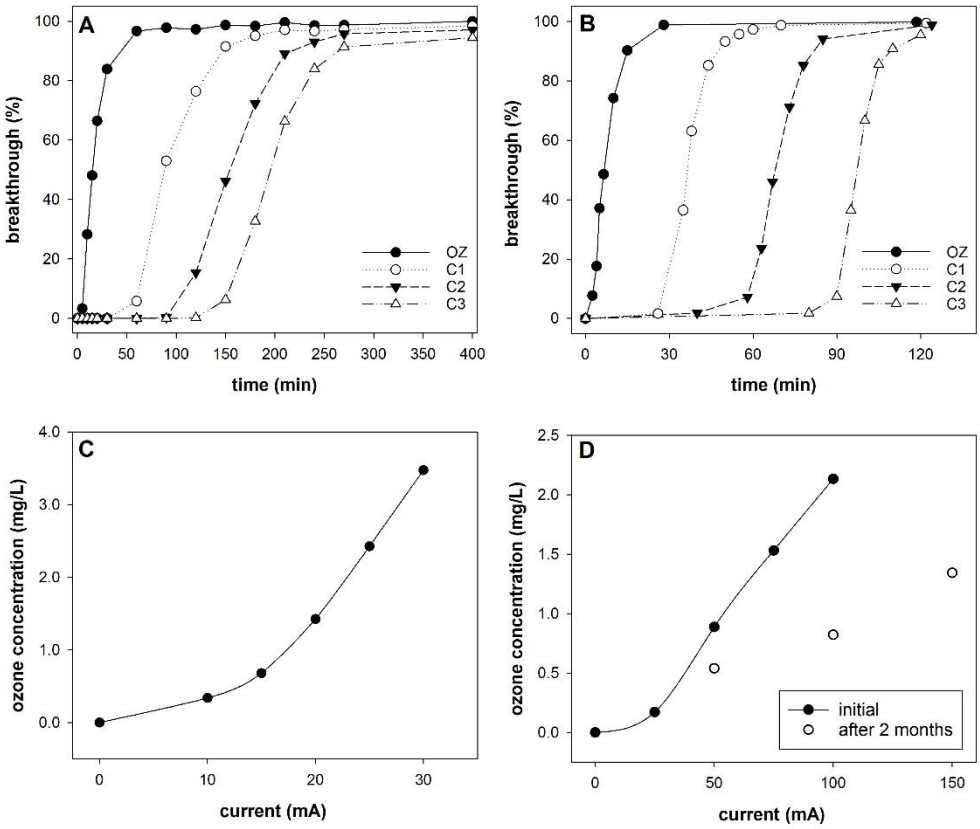

Figure 3.5.1. Fluorescein breakthrough curves for A) System 1 (flow rate of 6 mL min^{-1} and nitrogen flowing in the ozonation column), and B) System 2 (flow rate of 5 mL min^{-1}, without substitute gas sparging through in the ozonation column). Ozone dose or concentration depending on the current intensity at constant flow rates of C) 6 mL min^{-1} in System 1, and D) 3 mL min^{-1} in System 2.

3.5.2 Removal and transformation of trace contaminants in a drinking water treatment scenario

Dimethylsulfamide: The oxidative transformation of DMS to NDMA during ozonation was examined as a first example. Figure 3.5.2 shows the evolution of DMS and NDMA in the COMBI system at three sampling events during three months of continuous operation. The reactivity of DMS with ozone is important for waterworks

as both DMS sorption and biological degradation during riverbank filtration are limited, while filtration over activated carbon, sand filtration, disinfection by chlorine and nanofiltration cannot completely remove DMS if present in raw waters (59). Oxidative treatment followed by a biological treatment step seems to be one of the very few promising treatment combinations for waterworks to remove DMS (59). DMS was almost completely oxidized (to below 0.2 nmol L^{-1}, corresponding to at least 99% removal) under the applied conditions (ozone dose approx. 3 mg L^{-1}, contact time 30 min). The reaction of DMS with ozone is slow (rate constant of 20 M^{-1} s^{-1}) and leads to the formation of NDMA in the presence of bromide (60). The maximum NDMA yield is reached for bromide levels of 15 µg L^{-1} to 20 µg L^{-1} which are typical for drinking waters (60). The bromide level of the used tap water was about 35 µg L^{-1}. During the four-month experiment, the NDMA formation was reproducible, with an average molar yield of NDMA of approximately 50%. In full-scale waterworks similar DMS transformation rates of 73% to 100% were observed, while DMS to NDMA conversion rates were between 30% and 50% for spiked drinking water (59).

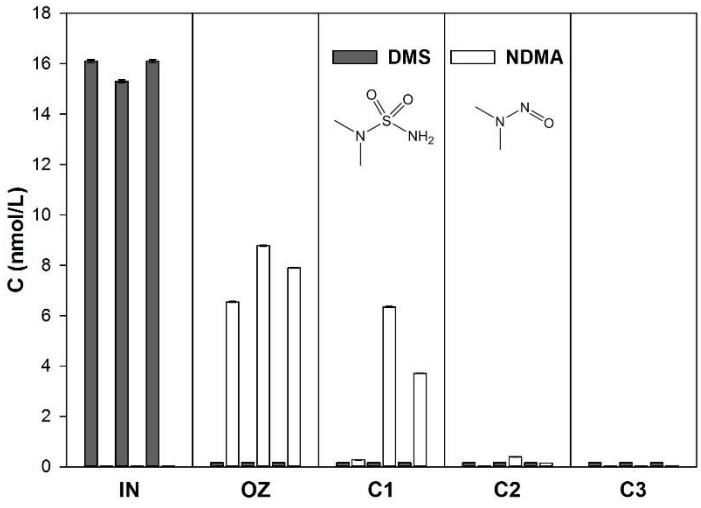

Figure 3.5.2. Conversion of DMS to NDMA by ozonation in drinking water matrix and subsequent degradation in biologically active sand columns in the COMBI set-up. The samples were taken on days 7, 24 and 97.

Only traces of NDMA were detected after the water had passed Column 2, while NDMA was absent (below 0.03 nmol L^{-1}) in the effluent of Column 3 (total HRT of approximately 5 h). NDMA has been shown to be biodegradable in sand filtration (59) and managed aquifer recharge (61). The high removal observed in this study

demonstrates the presence of a well-developed microbial community in the sand columns. Overall, both DMS and NDMA concentrations were below the detection limit in the final effluent of the system.

Acesulfame (ACE): The transformation of ACE to OP168 by ozone and its subsequent fate were also examined (Figure 3.5.3). ACE reacts with ozone with a rate constant of 88 M^{-1} s^{-1} (62), according to the Criegee mechanism, leading to ozonation products such as ACE OP170 and to a minor extent ACE OP168 (63). ACE was almost completely removed (at least 97% removal) under the applied conditions (ozone dose approx. 3 mg L^{-1}, contact time 30 min). OP168 was chosen for further investigation. As the ozonation products of ACE can be further oxidized, the yield at the effluent of the ozonation column (approximately 50% on the first two sampling days) may represent only a fraction of the initially formed OP168. However, the yield on the last sampling day was almost 100%.

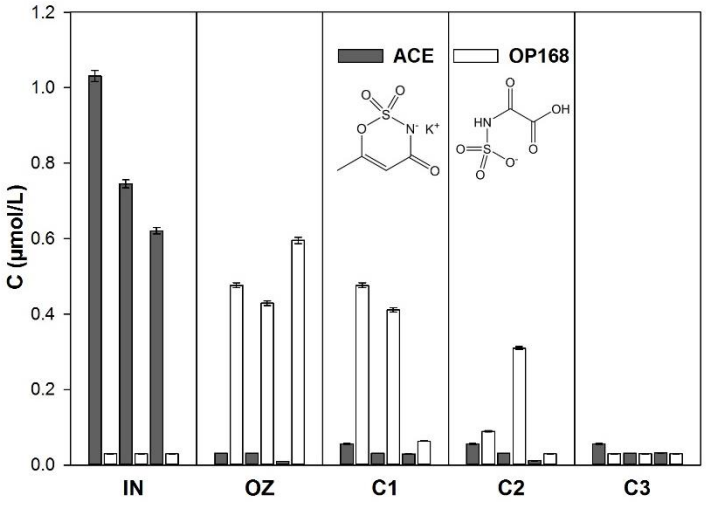

Figure 3.5.3. Conversion of ACE to OP168 in drinking water matrix by ozonation and subsequent degradation in biologically active sand columns in the COMBI set-up. The samples were taken on days 24, 27 and 93.

No further removal of unreacted residual ACE during column passage occurred. ACE was recently reported to be biodegradable during activated sludge treatment (64, 65) but has also been shown to persist in wastewater treatment, including riverbank filtration (63, 66). No biodegradation occurred over several months of operation and we suggest that the necessary biological community was absent. Breakthrough of OP168 through Columns 1 and 2 was observed during the first two sampling events,

but OP168 was not detected in the effluent of Column 3 (concentration below 0.03 µmol L^{-1}). This indicates that OP168 is biodegradable. Overall, removal of OP168 was highest at the last sampling date, which could be due to the maturation of the microbial community leading to an improved ability to degrade the transformation product. The structurally related compound ACE OP170 can be removed with activated carbon filtration, likely as a result of biodegradation (67). The fate of ACE OP168 in sand filtration has not been investigated before to the knowledge of the authors.

3.5.3 Removal and transformation of trace contaminants in a wastewater effluent ozonation scenario

Carbamazepine (CBZ): At ozone concentrations of 1 mg L^{-1} to 2 mg L^{-1} and a contact time of 10 min in the ozonation column more than 99% of CBZ (C_0 = 2.5 µmol L^{-1} ± 0.2 µmol L^{-1}) was removed (final concentration below 0.03 µmol L^{-1}). CBZ reacts with ozone at the double bond of its heterocyclic centre with a rate constant equal to 3×10^5 $M^{-1}s^{-1}$ (68). The main ozonation product is BQM (1-(2-benzaldehyde)-4-hydro-(1H,3H)-quinazoline-2-one) (69). Minor ozonation products are BaQD (1-(2-benzoic acid)-(1H,3H)-quinazoline-2,4-one), BQD (1-(2-benzaldehyde)-(1H,3H)-quinazoline-2,4-one) (69) and BaQM (1-(2-benzoic acid)-4-hydro-(1H,3H)-quinazoline-2-one) (70).

Figure 3.5.4 shows the evolution of the transformation products BQM and BaQD after ozonation at four sampling events during two months of continuous operation. Results are shown semi-quantitatively because analytical standards were not available. The variation in the formation of BQM and BaQD during ozonation on the four sampling days is shown in the SI, Figure 3.9.8. General trends were consistent over the observation period despite fluctuations in the concentration of BQM and BaQD after the filtration column passage. BQM concentrations decreased continuously during passage through the filtration columns, in agreement with a previous study (70). BQM removal occurred predominantly in the first column, while consecutive columns had modest additional effect. The high rate of BQM removal in the first column can be ascribed to an increased biological activity in the first few centimetres of the filter sand. The biological activity is slightly enhanced by additional oxygen following the

decomposition of ozone (32, 71), and also by the higher availability of biodegradable TOC after ozonation. Although the redox conditions were not measured, oxygen concentrations slightly above atmospheric equilibrium can be expected at the top of the first column. The increased biological activity in the first column was also evident by biofilm formation and occasional clogging during operation.

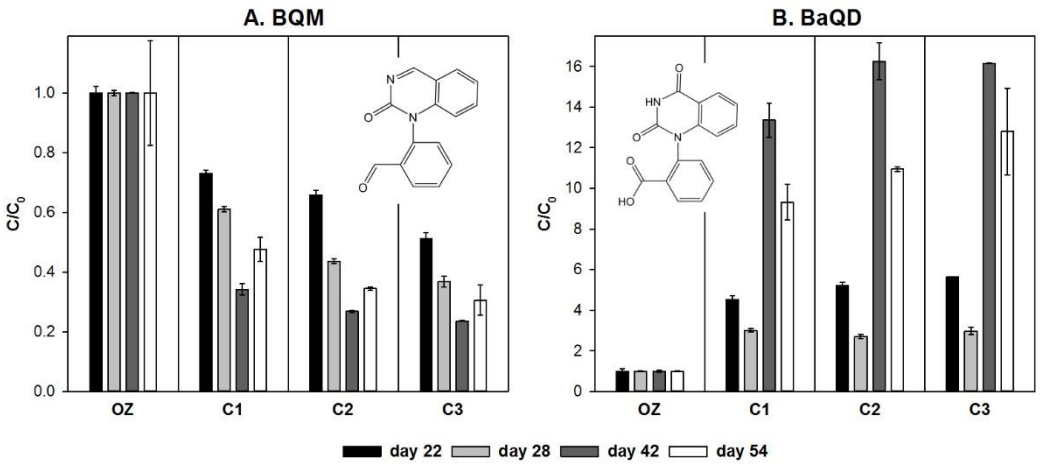

Figure 3.5.4. Evolution of carbamazepine transformation products BQM (A) and BaQD (B) during passage through the sand columns on four different days. The ratio C/C_0 was calculated by dividing each signal (peak area of target compound/peak area of internal standard) by the average signal after ozonation.

Overall removal of BQM during column passage was between 50% and 75%, which is high considering the HRT of 4 hours and shows that BQM is readily biodegradable, in contrast to its parent compound CBZ. Improved BQM removal towards later sampling dates could be due to the adaptation of the microbial community (72). Removal by adsorption was considered negligible, since the system was equilibrated for 3 weeks before sampling occurred and sand is a non-adsorptive filtration medium. An adsorption experiment with the parent compound CBZ showed no retardation in comparison to the tracer fluorescein or loss due to abiotic processes (SI, Figure 3.9.7). In addition, the ozonation products of CBZ have been shown to be less adsorptive to activated carbon than the parent compound (73).

Toxicity studies suggest that increased chromosomal damage of test organisms induced by ozonated CBZ solutions can be partially attributed to the formation of BQM (74). The results presented here indicate that BQM is readily biodegradable and unlikely to persist in surface water or groundwater.

BaQD concentration increased or remained unchanged during passage through the filtration columns. Higher BaQD formation roughly corresponded with higher removal of BQM, indicating that BaQD was microbially generated from BQM and other ozonation products of CBZ. BaQD can be formed directly by ozonation or by consecutive microbial transformation of ozonation products of CBZ and structurally similar compounds (70, 75). BaQD has been found to be slowly biodegradable and persistent in sand filtration experiments with an HRT of 12 days (70). In a pilot scale wastewater treatment plant, partial removal of BaQD was achieved during GAC filtration but not during passage through a clay biofilter (76).

BaQD has been detected in wastewater effluent, surface water, groundwater and drinking water (21, 75-77) and has potentially ecotoxicological relevance (78). The results of this study indicate that microbial transformation during biofiltration is a more important formation pathway of BaQD than ozonation itself. Monitoring BaQD in addition to BQM is important to fully understand the fate of CBZ during ozonation and subsequent treatment processes.

Diclofenac (DF): Under the applied conditions (C_0(DF) = 2.7 µmol L^{-1} ± 0.1 µmol L^{-1}, β_0(ozone) = 1°mg L^{-1} to 2 mg L^{-1}, contact time = 10 min) DF was removed to more than 99% during ozonation (final concentration below 0.03 µmol L^{-1}). DF has a high reaction rate constant with ozone (10^6 $M^{-1}s^{-1}$), due to the presence of two aromatic amino groups that are deprotonated at neutral pH (pK_a = 4) (68). The main ozonation products of DF are DF-IQ (diclofenac-2,5-iminoquinone), OH-DF (5-hydroxydiclofenac) and 2,6-dichloroaniline, while other minor ozonation products have also been detected (79, 80). Both DF-IQ and OH-DF have been found as microbial degradation products of DF in activated sludge (81). This study focussed on the fate of DF-IQ and OH-DF during column passage after ozonation. Other known DF ozonation products such as 2,6-dichloroaniline were either not detected or were only found in traces.

As shown in Figure 3.5.5, both DF-IQ and OH-DF were persistent during column passage. A slightly decreasing trend was observed for DF-IQ, while for OH-IF a slightly increasing trend was found. Biological and abiotic processes might affect the equilibrium between these two compounds (82), while DF-IQ has also been shown to adsorb on sediment (83). However, experiments with higher initial concentrations of

DF would be required to yield sufficient amounts of DF-IQ and OH-DF to investigate subtle concentration changes. In ozonation experiments with DF in deionized water, a maximum yield of 2.7% for DF-IQ and 4.5% for OH-IF on a molar basis was found, respectively (79).

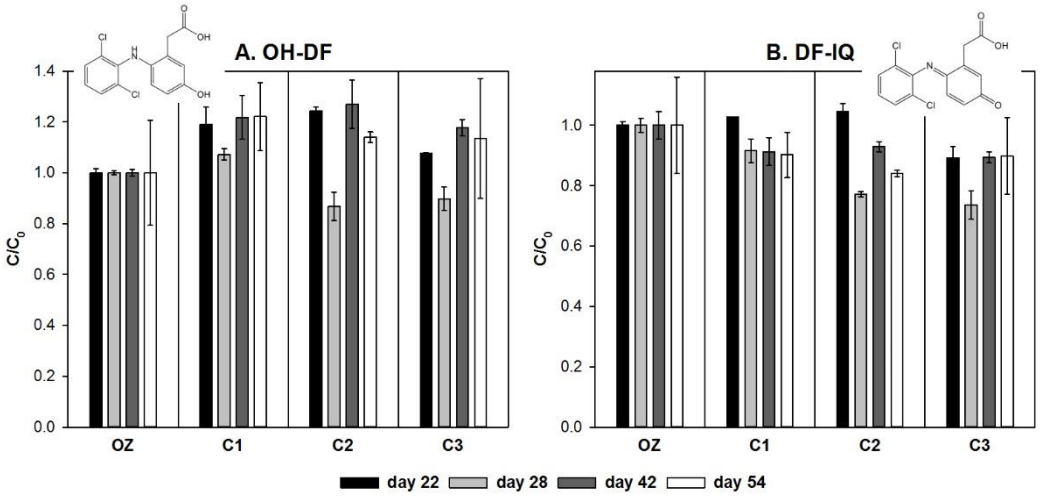

Figure 3.5.5. Evolution of diclofenac transformation products OH-DF (A) and DF-IQ (B) during passage through the sand columns on four different days. The ratio C/C_0 was calculated by dividing each signal (peak area of target compound/peak area of internal standard) by the average signal after ozonation.

The observed persistence of ozonation products of DF is in agreement with experiments in moving bed biofilm reactors (MBBRs), where the removal of DF-IQ reached 37% and that of OH-DF 27% after incubation for 150 h (84). Therefore, a longer filtration residence time might be necessary for the degradation of DF-IQ and OH-DF. The results show that sand filtration which is commonly employed after ozonation might not be a sufficient barrier to remove the main ozonation products of diclofenac.

Fluoxetine (FLX): FLX was chosen for investigation because it has recently been identified as a precursor of TFA in wastewater and drinking water treatment processes (57). The removal of FLX during ozonation at a concentration of $C_0(FLX) = 1.2\ \mu mol\ L^{-1} \pm 0.1\ \mu mol\ L^{-1}$ and $\beta_0(ozone) = 1\ mg\ L^{-1}$ to $2\ mg\ L^{-1}$, a contact time of 10 minutes and a pH of 7.5 was 70% to 95% (Figure 3.5.6). The ozonation rate constant of FLX is pH dependent, due to the presence of an amine moiety which is deprotonated at higher pH ($pK_a = 10$) and therefore more reactive. Several ozonation products of fluoxetine are known (33). TFA was targeted as a major

ozonation product of fluoxetine. Other known transformation products of FLX were either not detected or only found at trace levels. The formation of TFA during ozonation varied from 8% to 26% on a molar base. Despite this variation, higher TFA formation correlated with higher FLX removal (Figure 3.5.6).

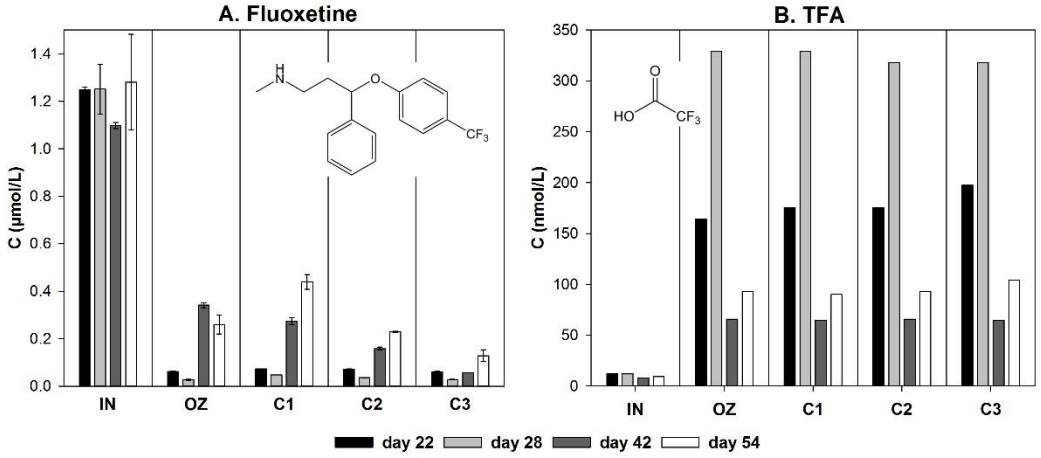

Figure 3.5.6. Evolution of fluoxetine (A) and TFA (B) during passage through the sand columns. Error bars for fluoxetine refer to the standard deviation of duplicate samples. For TFA, one sample was analysed for each sampling point on each day.

A small amount of TFA (approximately 10 nmol L^{-1}) was present in the influent, likely due to the presence of TFA in the tap water that was used to prepare the synthetic wastewater. A similar amount was formed due to the ozonation of other matrix components, based on the analysis of samples that were not spiked with FLX. The formation of TFA is likely mostly due to reactions mediated by OH-radicals, rather than direct reaction with ozone, considering the electron-withdrawing effect of the trifluoromethyl substituent of the aromatic ring.

Little to no removal of unreacted FLX was observed during passage through the sand columns. Minor changes in the concentration of FLX during its passage through sand filters might be due to ionic interactions with silica sand (85), since the silica surface is negatively charged at circumneutral pH (86), while FLX is a positively charged amine. The concentration of TFA was stable during passage through the sand filters. Evidence supporting both the persistence (87, 88) and the biodegradability of TFA (89, 90) can be found in the literature. In general, microbial defluorination is difficult to occur due to the low reduction potential of the C-F bond (91). Results are in agreement with a recent study, where no removal of TFA was observed at three

different waterworks that used filtration over biologically active or adsorptive media (57). Overall, TFA that is formed during ozonation of fluoxetine will likely persist during subsequent sand filtration.

3.6 Conclusions

A continuously operating laboratory system (COMBI) was developed to investigate the ozonation of TrOCs in water coupled with subsequent biologically active sand filtration. The system was used for both a drinking water treatment scenario and an advanced wastewater treatment scenario for five selected TrOCs and included fate analysis of ozonation products. After three weeks of operation, microbial degradation processes occurred in the filtration columns, while removal further increased over time. The microbial community is expected to be different in the two systems, as a result of the different filtration media and substrate compositions, although this was not further examined in this study.

Moderate to high removal was observed for the main ozonation product of carbamazepine, an ozonation product of acesulfame, as well as for NDMA, produced *via* ozonation through its precursor DMS. On the other hand, an ozonation product of carbamazepine, two ozonation products of diclofenac, and TFA from ozonation of fluoxetine persisted microbial degradation. Good agreement with the results of large-scale and pilot-scale studies was found (21, 57, 59), implying that the developed experimental setup can offer reliable predictions.

The developed system is a useful tool to provide reliable predictions on the fate of ozonation products for different treatment conditions and process configurations. The COMBI system has a small footprint, while the total cost of parts for a complete system is approximately 660 € (SI, Table 3.9.1). Based on these attributes COMBI will simplify studies on ozonation-biofiltration, ultimately leading to a better understanding of complex contaminant transformation processes during advanced water treatment schemes.

3.7 Acknowledgements

We would like to acknowledge Paula Brendel and Beat Schmutz for assistance in the lab and Shaun Reeksting for assistance with analysis. GAZ was supported by a University of Bath research scholarship and an EPSRC funded integrated PhD studentship in Sustainable Chemical Technologies (EP/L016354/1). Start-up infrastructure funding by the Faculty of Engineering & Design for JW research group is appreciated. This research was supported by a Royal Society equipment grant (RG2016-150544): Clean water technologies - Low-dosed oxidants to improve low-energy natural engineered water treatment systems.

3.8 References

1. Houtman CJ. Emerging contaminants in surface waters and their relevance for the production of drinking water in Europe. Journal of Integrative Environmental Sciences. 2010;7(4):271-95.
2. Hughes SR, Kay P, Brown LE. Global synthesis and critical evaluation of pharmaceutical data sets collected from river systems. Environ Sci Technol. 2013;47(2):661-77.
3. Stuart M, Lapworth D, Crane E, Hart A. Review of risk from potential emerging contaminants in UK groundwater. Science of The Total Environment. 2012;416:1-21.
4. Fram MS, Belitz K. Occurrence and concentrations of pharmaceutical compounds in groundwater used for public drinking-water supply in California. Sci Total Environ. 2011;409(18):3409-17.
5. Pal A, Gin KY, Lin AY, Reinhard M. Impacts of emerging organic contaminants on freshwater resources: review of recent occurrences, sources, fate and effects. Sci Total Environ. 2010;408(24):6062-9.
6. Lapworth DJ, Baran N, Stuart ME, Ward RS. Emerging organic contaminants in groundwater: A review of sources, fate and occurrence. Environmental Pollution. 2012;163:287-303.
7. Petrie B, Youdan J, Barden R, Kasprzyk-Hordern B. Multi-residue analysis of 90 emerging contaminants in liquid and solid environmental matrices by ultra-high-performance liquid chromatography tandem mass spectrometry. J Chromatogr A. 2016;1431:64-78.
8. Schröder P, Helmreich B, Škrbić B, Carballa M, Papa M, Pastore C, Emre Z, Oehmen A, Langenhoff A, Molinos M, Dvarioniene J, Huber C, Tsagarakis KP, Martinez-Lopez E, Pagano SM, Vogelsang C, Mascolo G. Status of hormones and painkillers in wastewater effluents across several European states—considerations for the EU watch list concerning estradiols and diclofenac. Environmental Science and Pollution Research. 2016;23(13):12835-66.
9. Tran NH, Reinhard M, Gin KY-H. Occurrence and fate of emerging contaminants in municipal wastewater treatment plants from different geographical regions-a review. Water Research. 2018;133:182-207.

10. Sanchez W, Sremski W, Piccini B, Palluel O, Maillot-Marechal E, Betoulle S, Jaffal A, Ait-Aissa S, Brion F, Thybaud E, Hinfray N, Porcher JM. Adverse effects in wild fish living downstream from pharmaceutical manufacture discharges. Environ Int. 2011;37(8):1342-8.
11. Brodin T, Piovano S, Fick J, Klaminder J, Heynen M, Jonsson M. Ecological effects of pharmaceuticals in aquatic systems—impacts through behavioural alterations. Philosophical Transactions of the Royal Society B: Biological Sciences. 2014;369(1656).
12. González S, López-Roldán R, Cortina J-L. Presence and biological effects of emerging contaminants in Llobregat River basin: A review. Environmental Pollution. 2012;161:83-92.
13. Klarich KL, Pflug NC, DeWald EM, Hladik ML, Kolpin DW, Cwiertny DM, LeFevre GH. Occurrence of Neonicotinoid Insecticides in Finished Drinking Water and Fate during Drinking Water Treatment. Environmental Science & Technology Letters. 2017;4(5):168-73.
14. Huerta-Fontela M, Galceran MT, Ventura F. Occurrence and removal of pharmaceuticals and hormones through drinking water treatment. Water Research. 2011;45(3):1432-42.
15. Schriks M, Heringa MB, van der Kooi MME, de Voogt P, van Wezel AP. Toxicological relevance of emerging contaminants for drinking water quality. Water Research. 2010;44(2):461-76.
16. de Jesus Gaffney V, Almeida CMM, Rodrigues A, Ferreira E, Benoliel MJ, Cardoso VV. Occurrence of pharmaceuticals in a water supply system and related human health risk assessment. Water Research. 2015;72:199-208.
17. European Commission. Implementing decision (EU) 2015/495 of 20 March 2015 establishing a watch list of substances for Union-wide monitoring in the field of water policy pursuant to Directive 2008/105/EC of the European Parliament and of the Council. 2015.
18. Gottschalk C, Libra JA, Saupe A. Ozonation of water and waste water: A practical guide to understanding ozone and its applications: John Wiley & Sons; 2009.
19. Eggen RIL, Hollender J, Joss A, Schärer M, Stamm C. Reducing the Discharge of Micropollutants in the Aquatic Environment: The Benefits of Upgrading Wastewater Treatment Plants. Environmental Science & Technology. 2014;48(14):7683-9.

20. Hollender J, Zimmermann SG, Koepke S, Krauss M, McArdell CS, Ort C, Singer H, von Gunten U, Siegrist H. Elimination of organic micropollutants in a municipal wastewater treatment plant upgraded with a full-scale post-ozonation followed by sand filtration. Environmental Science and Technology. 2009;43(20):7862-9.

21. Bourgin M, Beck B, Boehler M, Borowska E, Fleiner J, Salhi E, Teichler R, von Gunten U, Siegrist H, McArdell CS. Evaluation of a full-scale wastewater treatment plant upgraded with ozonation and biological post-treatments: Abatement of micropollutants, formation of transformation products and oxidation by-products. Water Research. 2018;129:486-98.

22. Blackbeard J, Lloyd J, Magyar M, Mieog J, Linden KG, Lester Y. Demonstrating organic contaminant removal in an ozone-based water reuse process at full scale. Environ Sci: Water Res Technol. 2016;2(1):213-22.

23. von Sonntag C, von Gunten U. Chemistry of ozone in water and wastewater treatment: IWA publishing; 2012.

24. von Sonntag C. Free-radical-induced DNA damage and its repair: Springer; 2006.

25. Ramseier MK, Peter A, Traber J, von Gunten U. Formation of assimilable organic carbon during oxidation of natural waters with ozone, chlorine dioxide, chlorine, permanganate, and ferrate. Water Research. 2011;45(5):2002-10.

26. Drewes JE, Jekel M. Behavior of DOC and AOX using advanced treated wastewater for groundwater recharge. Water Research. 1998;32(10):3125-33.

27. Yavich AA, Lee KH, Chen KC, Pape L, Masten SJ. Evaluation of biodegradability of NOM after ozonation. Water Research. 2004;38(12):2839-46.

28. Schumacher J, Pi YZ, Jekel M. Ozonation of persistent DOC in municipal WWTP effluent for groundwater recharge. Water Science and Technology2004. p. 305-10.

29. Merel S, Lege S, Yanez Heras JE, Zwiener C. Assessment of *N*-Oxide Formation during Wastewater Ozonation. Environ Sci Technol. 2017;51(1):410-7.

30. Schlüter-Vorberg L, Prasse C, Ternes TA, Mückter H, Coors A. Toxification by Transformation in Conventional and Advanced Wastewater Treatment: The Antiviral Drug Acyclovir. Environmental Science & Technology Letters. 2015;2(12):342-6.

31. Gerrity D, Arnold M, Dickenson E, Moser D, Sackett JD, Wert EC. Microbial community characterization of ozone-biofiltration systems in drinking water and potable reuse applications. Water Research. 2018;135:207-19.
32. Zucker I, Mamane H, Cikurel H, Jekel M, Hübner U, Avisar D. A hybrid process of biofiltration of secondary effluent followed by ozonation and short soil aquifer treatment for water reuse. Water Research. 2015;84:315-22.
33. Zhao Y, Yu G, Chen S, Zhang S, Wang B, Huang J, Deng S, Wang Y. Ozonation of antidepressant fluoxetine and its metabolite product norfluoxetine: Kinetics, intermediates and toxicity. Chemical Engineering Journal. 2017;316:951-63.
34. Petala M, Samaras P, Zouboulis A, Kungolos A, Sakellaropoulos GP. Influence of ozonation on the in vitro mutagenic and toxic potential of secondary effluents. Water Res. 2008;42(20):4929-40.
35. Bundschuh M, Pierstorf R, Schreiber WH, Schulz R. Positive effects of wastewater ozonation displayed by in situ bioassays in the receiving stream. Environ Sci Technol. 2011;45(8):3774-80.
36. Misik M, Knasmueller S, Ferk F, Cichna-Markl M, Grummt T, Schaar H, Kreuzinger N. Impact of ozonation on the genotoxic activity of tertiary treated municipal wastewater. Water Res. 2011;45(12):3681-91.
37. Altmann D, Schaar H, Bartel C, Schorkopf DL, Miller I, Kreuzinger N, Mostl E, Grillitsch B. Impact of ozonation on ecotoxicity and endocrine activity of tertiary treated wastewater effluent. Water Res. 2012;46(11):3693-702.
38. Stalter D, Magdeburg A, Weil M, Knacker T, Oehlmann J. Toxication or detoxication? In vivo toxicity assessment of ozonation as advanced wastewater treatment with the rainbow trout. Water Res. 2010;44(2):439-48.
39. Magdeburg A, Stalter D, Oehlmann J. Whole effluent toxicity assessment at a wastewater treatment plant upgraded with a full-scale post-ozonation using aquatic key species. Chemosphere. 2012;88(8):1008-14.
40. Yan Z, Zhang Y, Yuan H, Tian Z, Yang M. Fish larval deformity caused by aldehydes and unknown byproducts in ozonated effluents from municipal wastewater treatment systems. Water Res. 2014;66:423-9.
41. Onesios-Barry KM, Berry D, Proescher JB, Sivakumar IA, Bouwer EJ. Removal of pharmaceuticals and personal care products during water recycling:

microbial community structure and effects of substrate concentration. Applied and environmental microbiology. 2014;80(8):2440-50.

42. Paredes L, Fernandez-Fontaina E, Lema JM, Omil F, Carballa M. Understanding the fate of organic micropollutants in sand and granular activated carbon biofiltration systems. Sci Total Environ. 2016;551-552:640-8.

43. Escola Casas M, Bester K. Can those organic micro-pollutants that are recalcitrant in activated sludge treatment be removed from wastewater by biofilm reactors (slow sand filters)? Sci Total Environ. 2015;506-507:315-22.

44. Zearley TL, Summers RS. Removal of trace organic micropollutants by drinking water biological filters. Environ Sci Technol. 2012;46(17):9412-9.

45. Kim S, Rossmassler K, Broeckling CD, Galloway S, Prenni J, De Long SK. Impact of inoculum sources on biotransformation of pharmaceuticals and personal care products. Water Res. 2017;125:227-36.

46. Onesios KM, Bouwer EJ. Biological removal of pharmaceuticals and personal care products during laboratory soil aquifer treatment simulation with different primary substrate concentrations. Water Res. 2012;46(7):2365-75.

47. Alidina M, Li D, Ouf M, Drewes JE. Role of primary substrate composition and concentration on attenuation of trace organic chemicals in managed aquifer recharge systems. J Environ Manage. 2014;144:58-66.

48. Banzhaf S, Nödler K, Licha T, Krein A, Scheytt T. Redox-sensitivity and mobility of selected pharmaceutical compounds in a low flow column experiment. Science of the Total Environment. 2012;438:113-21.

49. Baumgarten B, Jährig J, Reemtsma T, Jekel M. Long term laboratory column experiments to simulate bank filtration: Factors controlling removal of sulfamethoxazole. Water Research. 2011;45(1):211-20.

50. Alidina M, Shewchuk J, Drewes JE. Effect of temperature on removal of trace organic chemicals in managed aquifer recharge systems. Chemosphere. 2015;122:23-31.

51. Hübner U, von Gunten U, Jekel M. Evaluation of the persistence of transformation products from ozonation of trace organic compounds – A critical review. Water Research. 2015;68:150-70.

52. Knopp G, Prasse C, Ternes TA, Cornel P. Elimination of micropollutants and transformation products from a wastewater treatment plant effluent through pilot scale

ozonation followed by various activated carbon and biological filters. Water Research. 2016;100:580-92.

53. Bollmann AF, Seitz W, Prasse C, Lucke T, Schulz W, Ternes T. Occurrence and fate of amisulpride, sulpiride, and lamotrigine in municipal wastewater treatment plants with biological treatment and ozonation. J Hazard Mater. 2016;320:204-15.

54. Zucker I, Mamane H, Riani A, Gozlan I, Avisar D. Formation and degradation of N-oxide venlafaxine during ozonation and biological post-treatment. Sci Total Environ. 2018;619-620:578-86.

55. OECD. OECD Guideline for the Testing of Chemicals. Section 3, Test No. 303. 2001.

56. Lee C, Schmidt C, Yoon J, von Gunten U. Oxidation of *N*-Nitrosodimethylamine (NDMA) Precursors with Ozone and Chlorine Dioxide: Kinetics and Effect on NDMA Formation Potential. Environmental Science & Technology. 2007;41(6):2056-63.

57. Scheurer M, Nodler K, Freeling F, Janda J, Happel O, Riegel M, Muller U, Storck FR, Fleig M, Lange FT, Brunsch A, Brauch HJ. Small, mobile, persistent: Trifluoroacetate in the water cycle - Overlooked sources, pathways, and consequences for drinking water supply. Water Res. 2017;126:460-71.

58. Bader H, Hoigné J. Determination of ozone in water by the indigo method. Water Research. 1981;15(4):449-56.

59. Schmidt CK, Brauch H-J. *N*,*N*-Dimethylsulfamide as Precursor for *N*-Nitrosodimethylamine (NDMA) Formation upon Ozonation and its Fate During Drinking Water Treatment. Environmental Science & Technology. 2008;42(17):6340-6.

60. von Gunten U, Salhi E, Schmidt CK, Arnold WA. Kinetics and Mechanisms of *N*-Nitrosodimethylamine Formation upon Ozonation of *N*,*N*-Dimethylsulfamide-Containing Waters: Bromide Catalysis. Environmental Science & Technology. 2010;44(15):5762-8.

61. Patterson BM, Pitoi MM, Furness AJ, Bastow TP, McKinley AJ. Fate of *N*-Nitrosodimethylamine in recycled water after recharge into anaerobic aquifer. Water Research. 2012;46(4):1260-72.

62. Kaiser H-P, Köster O, Gresch M, Périsset PMJ, Jäggi P, Salhi E, von Gunten U. Process Control For Ozonation Systems: A Novel Real-Time Approach. Ozone: Science & Engineering. 2013;35(3):168-85.

63. Scheurer M, Storck FR, Brauch H-J, Lange FT. Performance of conventional multi-barrier drinking water treatment plants for the removal of four artificial sweeteners. Water Research. 2010;44(12):3573-84.
64. Castronovo S, Wick A, Scheurer M, Nodler K, Schulz M, Ternes TA. Biodegradation of the artificial sweetener acesulfame in biological wastewater treatment and sandfilters. Water Res. 2017;110:342-53.
65. Kahl S, Kleinsteuber S, Nivala J, van Afferden M, Reemtsma T. Emerging Biodegradation of the Previously Persistent Artificial Sweetener Acesulfame in Biological Wastewater Treatment. Environmental Science & Technology. 2018;52(5):2717-25.
66. Buerge IJ, Buser H-R, Kahle M, Müller MD, Poiger T. Ubiquitous Occurrence of the Artificial Sweetener Acesulfame in the Aquatic Environment: An Ideal Chemical Marker of Domestic Wastewater in Groundwater. Environmental Science & Technology. 2009;43(12):4381-5.
67. Scheurer M, Godejohann M, Wick A, Happel O, Ternes TA, Brauch H-J, Ruck WKL, Lange FT. Structural elucidation of main ozonation products of the artificial sweeteners cyclamate and acesulfame. Environmental Science and Pollution Research. 2012;19(4):1107-18.
68. Huber MM, Canonica S, Park G-Y, von Gunten U. Oxidation of Pharmaceuticals during Ozonation and Advanced Oxidation Processes. Environmental Science & Technology. 2003;37(5):1016-24.
69. McDowell DC, Huber MM, Wagner M, von Gunten U, Ternes TA. Ozonation of Carbamazepine in Drinking Water: Identification and Kinetic Study of Major Oxidation Products. Environmental Science & Technology. 2005;39(20):8014-22.
70. Hübner U, Seiwert B, Reemtsma T, Jekel M. Ozonation products of carbamazepine and their removal from secondary effluents by soil aquifer treatment – Indications from column experiments. Water Research. 2014;49:34-43.
71. Hellauer K, Mergel D, Ruhl A, Filter J, Hübner U, Jekel M, Drewes J. Advancing Sequential Managed Aquifer Recharge Technology (SMART) Using Different Intermediate Oxidation Processes. Water. 2017;9(12):221.
72. Bertelkamp C, Verliefde AR, Schoutteten K, Vanhaecke L, Vanden Bussche J, Singhal N, van der Hoek JP. The effect of redox conditions and adaptation time on organic micropollutant removal during river bank filtration: A laboratory-scale column study. Sci Total Environ. 2016;544:309-18.

73. Schoutteten K, Hennebel T, Dheere E, Bertelkamp C, De Ridder DJ, Maes S, Chys M, Van Hulle SWH, Vanden Bussche J, Vanhaecke L, Verliefde ARD. Effect of oxidation and catalytic reduction of trace organic contaminants on their activated carbon adsorption. Chemosphere. 2016;165:191-201.

74. Han Y, Ma M, Li N, Hou R, Huang C, Oda Y, Wang Z. Chlorination, chloramination and ozonation of carbamazepine enhance cytotoxicity and genotoxicity: Multi-endpoint evaluation and identification of its genotoxic transformation products. J Hazard Mater. 2018;342:679-88.

75. Kaiser E, Prasse C, Wagner M, Broder K, Ternes TA. Transformation of oxcarbazepine and human metabolites of carbamazepine and oxcarbazepine in wastewater treatment and sand filters. Environ Sci Technol. 2014;48(17):10208-16.

76. Brezina E, Prasse C, Meyer J, Muckter H, Ternes TA. Investigation and risk evaluation of the occurrence of carbamazepine, oxcarbazepine, their human metabolites and transformation products in the urban water cycle. Environ Pollut. 2017;225:261-9.

77. Li Z, Fenet H, Gomez E, Chiron S. Transformation of the antiepileptic drug oxcarbazepine upon different water disinfection processes. Water Res. 2011;45(4):1587-96.

78. Azais A, Mendret J, Cazals G, Petit E, Brosillon S. Ozonation as a pretreatment process for nanofiltration brines: Monitoring of transformation products and toxicity evaluation. J Hazard Mater. 2017;338:381-93.

79. Sein MM, Zedda M, Tuerk J, Schmidt TC, Golloch A, Sonntag Cv. Oxidation of Diclofenac with Ozone in Aqueous Solution. Environmental Science & Technology. 2008;42(17):6656-62.

80. Coelho AD, Sans C, Aguera A, Gomez MJ, Esplugas S, Dezotti M. Effects of ozone pre-treatment on diclofenac: intermediates, biodegradability and toxicity assessment. Sci Total Environ. 2009;407(11):3572-8.

81. Kosjek T, Zigon D, Kralj B, Heath E. The use of quadrupole-time-of-flight mass spectrometer for the elucidation of diclofenac biotransformation products in wastewater. J Chromatogr A. 2008;1215(1-2):57-63.

82. Forrez I, Carballa M, Verbeken K, Vanhaecke L, Ternes T, Boon N, Verstraete W. Diclofenac oxidation by biogenic manganese oxides. Environ Sci Technol. 2010;44(9):3449-54.

83. Groning J, Held C, Garten C, Claussnitzer U, Kaschabek SR, Schlomann M. Transformation of diclofenac by the indigenous microflora of river sediments and identification of a major intermediate. Chemosphere. 2007;69(4):509-16.

84. El-Taliawy H, Casas ME, Bester K. Removal of ozonation products of pharmaceuticals in laboratory Moving Bed Biofilm Reactors (MBBRs). J Hazard Mater. 2018;347:288-98.

85. Tolls J. Sorption of Veterinary Pharmaceuticals in Soils: A Review. Environmental Science & Technology. 2001;35(17):3397-406.

86. Kosmulski M. The pH-Dependent Surface Charging and the Points of Zero Charge. Journal of Colloid and Interface Science. 2002;253(1):77-87.

87. Benesch JA, Gustin MS, Cramer GR, Cahill TM. Investigation of effects of trifluoroacetate on vernal pool ecosystems. Environmental toxicology and chemistry. 2002;21(3):640-7.

88. Ellis DA, Hanson ML, Sibley PK, Shahid T, Fineberg NA, Solomon KR, Muir DC, Mabury SA. The fate and persistence of trifluoroacetic and chloroacetic acids in pond waters. Chemosphere. 2001;42(3):309-18.

89. Visscher PT, Culbertson CW, Oremland RS. Degradation of trifluoroacetate in oxic and anoxic sediments. Nature. 1994;369(6483):729-31.

90. Kim B, Suidan M, Wallington T, Du X. Biodegradability of trifluoroacetic acid. Environmental Engineering Science. 2000;17(6):337-42.

91. Boutonnet JC, Bingham P, Calamari D, Rooij Cd, Franklin J, Kawano T, Libre J-M, McCul-loch A, Malinverno G, Odom JM, Rusch GM, Smythe K, Sobolev I, Thompson R, Tiedje JM. Environmental Risk Assessment of Trifluoroacetic Acid. Human and Ecological Risk Assessment: An International Journal. 1999;5(1):59-124.

3.9 Supplementary information

3.9.1 COMBI system

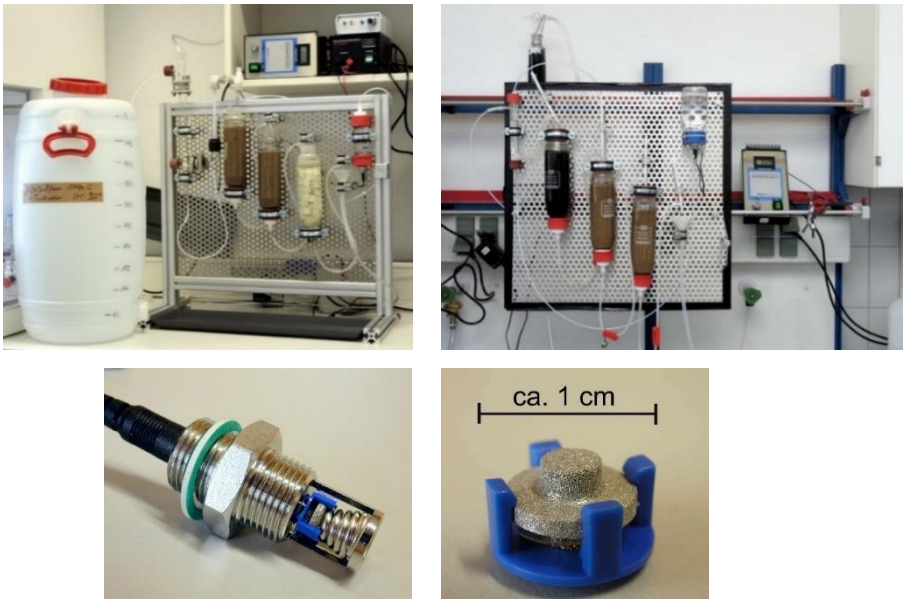

Figure 3.9.1. Top: Photographs of the COMBI System 1. Bottom: Photographs of the ozone micro cell holder with one electrolysis system (left-hand side), and a close-up of the electrolysis unit (right-hand side).

Table 3.9.1. Approximate cost of the parts needed to build a COMBI system (2017).

	Cost/€
Pump (e.g. KNF IP54 24V FMM 20 KPDC-P, including house-built controller)	215
Ozone micro-cell (including control box and power supply)	265
Glassware (glass tubing with added standard threads, standard thread bottles for System 2 & standard thread bottles, columns for System 1)	90
Tubing	20
Fittings	40
Storage tank	30
Total	**660**

3.9.2 Trace organic contaminants

Carbamazepine, diclofenac sodium salt and fluoxetine hydrochloride in solid form (purity ≥98%) were purchased from Sigma-Aldrich. Stock solutions used to spike the synthetic wastewater were regularly prepared in Milli-Q water. Diclofenac sodium

analytical standard was purchased from Sigma-Aldrich. Fluoxetine hydrochloride solution (1 mg mL^{-1} in methanol) used as a standard, fluoxetine-d_5 solution (1 mg mL^{-1} in methanol) used as an internal standard, carbamazepine solution (1 mg mL^{-1} in methanol) used as a standard, and carbamazepine-$^{13}C_6$ solution (100 µg mL^{-1} in methanol) used as an internal standard, were purchased from Sigma Aldrich.

Acesulfame potassium and *N*,*N*-dimethylsulfamide (DMS) were provided by LGC (formerly Dr. Ehrenstorfer, Wesel, Germany). Acesulfame-d_4 was purchased from Campro Scientific (Berlin, Germany) and DMS-d_6 from Bayer (Leverkusen, Germany). *N*-Nitrosodimethylamine (NDMA) was provided by Supelco (now Sigma-Aldrich, St.Louis, USA) and NDMA-d_6 by CDN Isotopes (Pointe-Claire, Canada).

The reference standard of OP168 was produced in the TZW lab as follows: Acesulfame (5 g, 25 mmol) was dissolved in 1000 mL distilled water and treated with ozone gas for 3 h. The resulting reaction solution was concentrated at a rotary evaporator. Hereby water and a part of semi-volatile acids (acetic acid and formic acid) can be removed from the mixture. The highly concentrated reaction mixture was neutralized with potassium hydroxide solution to pH 7. Crystal growth of the potassium salt of OP168 took place within a few days. For further purification a re-crystallization from water was performed. The confirmation of the anionic species OP168 (m/z = 167.9608) was done by ion exchange chromatography coupled to an accurate time of flight mass spectrometer after electrospray ionization (IC-ESI-TOF). The salt-composition was confirmed by elemental analyses using inductively coupled plasma coupled to mass spectrometry (ICP-MS): sulfur (calculated 13.1%, found 14.0%); potassium (calculated 31.9%, found 29.9%).

Sodium trifluoroacetate, was purchased from Sigma Aldrich (Steinheim, Germany) and the respective isotopically labeled internal standard sodium trifluoroacetate-$^{13}C_2$ was obtained from TRC (Toronto, Canada).

Table 3.9.2. Trace organic contaminants and ozonation products investigated in this study.

Parent compounds			Ozonation products		
Compound (Abbreviation)	**[CAS] Molecular formula MW/(g mol^{-1})**	**Structure**	**Compound (Abbreviation)**	**[CAS] Molecular formula MW/(g mol^{-1})**	**Structure**
N,*N*-Dimethylsulfamide (DMS)	[3984-14-3] $C_2H_8N_2O_2S$ 124.16	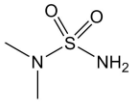	*N*-nitrosodimethylamine (NDMA)	[62-75-9] $C_2H_6N_2O$ 74.08	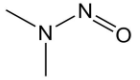
Acesulfame potassium (ACE)	[55589-62-3] $C_4H_4KNO_4S$ 201.24	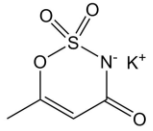	ACE OP168	[1403502-37-3] $C_2H_2NO_6S$ 167.96	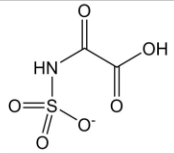
Carbamazepine (CBZ)	[298-46-4] $C_{15}H_{12}N_2O$ 236.27	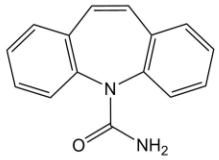	1-(2-benzaldehyde)-4-hydro-(1H,3H)-quinazoline-2-one (BQM)	[1401112-00-2] $C_{15}H_{10}N_2O_2$ 250.25	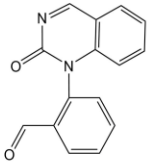
			1-(2-benzoic acid)-(1H,3H)-quinazoline-2,4-one (BaQD)	[n/a] $C_{15}H_{10}N_2O_4$ 282.25	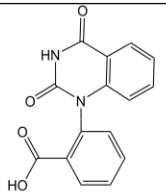

Parent compounds			Ozonation products		
Compound (Abbreviation)	**[CAS] Molecular formula MW/(g mol^{-1})**	**Structure**	**Compound (Abbreviation)**	**[CAS] Molecular formula MW/(g mol^{-1})**	**Structure**
Diclofenac sodium (DF)	[15307-79-6] $C_{14}H_{10}NO_2Cl_2Na$ 318.13	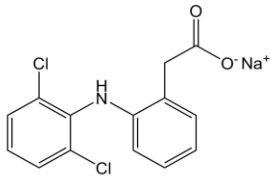	Diclofenac-2,5-iminoquinone (DF-IQ)	[1254576-93-6] $C_{14}H_9NO_3Cl_2$ 310.13	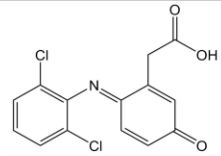
			5-Hydroxydiclofenac (OH-DF)	[69002-84-2] $C_{14}H_{11}NO_3Cl_2$ 312.15	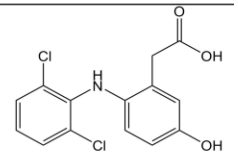
Fluoxetine (FLX)	[54910-89-3] $C_{17}H_{18}F_3NO$ 309.33	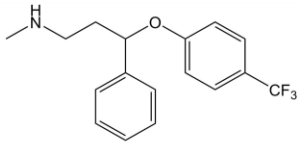	Trifluoroacetic acid (TFA)	[76-05-1] $C_2HF_3O_2$ 114.02	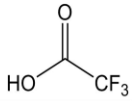

3.9.3 Analysis

Ultra High Performance Liquid Chromatography-Mass Spectrometry (UHPLC-MS) for CBZ, DF and FLX was performed with a Thermo Scientific Dionex UltiMate 3000 system coupled to a Bruker Daltonics maXis HD electrospray ionization quadrupole time-of-flight (ESI-QTOF) mass spectrometer operated in positive-ion mode, equipped with an Acquity UPLC BEH C18-Column (1.7 µm, 130 Å, 2.1 mm × 50 mm). The mobile phase consisted of water with 0.1% formic acid (A), and methanol with 0.1% formic acid (B). The flow rate was 0.4 mL min^{-1}, the injection volume was 20 µL and the column compartment temperature was set to 40°C. Gradient elution was carried out with 1% mobile phase B until 2 min, followed by a linear gradient to 100% B at 5 min, keeping 100% B up until 8 min, thereafter returned to 1% B until 12 min total run time. For MS, the capillary voltage was set to 4500 V, nebulizing gas at 4 bar, drying gas at 12 L min^{-1} at 220°C. The TOF scan range was from 75 to 1000 mass-to-charge ratio (m/z). For effective transmission of ions, the ion energy was set to 6.0 eV with the collision energy for TOF MS acquisition at 7.0 eV. The MS instrument was calibrated using a range of sodium formate clusters introduced by switching valve injection during the first minute of each chromatographic run. The compounds were detected as $[M + H]^+$ ions. Data processing was performed using the Data Analysis software version 4.3 (Bruker Daltonik GmbH, Bremen, Germany).

Samples were spiked with internal standard (final concentration of 100 ng mL^{-1}) and adjusted with methanol to 80/20 (v/v) water/methanol composition, as soon as possible after their collection but no longer than 40 min. Fluoxetine-d_5 (1 mg mL^{-1} in methanol) was used as an internal standard for the analysis of FLX, and CBZ-$^{13}C_6$ (100 µg mL^{-1} in methanol) was used as an internal standard for the analysis of carbamazepine and diclofenac. The spiked samples were filtered with PTFE filters (0.2 µm pore size) and frozen at −20°C until analysis. Quantitative analysis was performed using the Quant Analysis software version 4.3 (Bruker Daltonik GmbH, Bremen, Germany).

Transformation products of CBZ and DF were identified based on literature data, mass accuracy (less than 10 ppm mass error in all cases), and consistent retention time. MS/MS analysis in MRM (multiple reaction monitoring) mode was performed

to further support the identification of CBZ and DF transformation products. The collision energy used was 15 eV to 30 eV. Observed fragmentation patterns are provided in SI, Section 3.9.8. Semi-quantitative analysis of the transformation products was performed using the same internal standard that was used for the parent compounds.

Direct injection was used for the analysis of TFA, ACE and its ozonation product OP168. DMS and NDMA samples were pre-concentrated with solid phase extraction (SPE) prior the analysis. For DMS a sample volume of 50 mL was adjusted to pH 5 for SPE. After, extraction cartridges were dried under nitrogen and DMS was eluted with a mixture of dichloromethane and methanol (4:1 v/v). The eluate was blown down using nitrogen and reconstituted in 1 mL of a water/methanol mixture (8:2 v/v). For NDMA analysis, samples were pre-concentrated as described in (1).

TFA analysis was performed using ion exchange liquid chromatography-electrospray tandem mass spectrometry (LC-ESI-MS/MS) according to a recently developed method (2). Briefly, chromatographic separation was achieved in an Agilent 1200 LC system (Waldbronn, Germany) with a Dionex IonPac AS17-C column equipped with a Dionex IonPac AG17-C precolumn. The eluents were ultra-pure water containing 50 mmol L^{-1} ammonium bicarbonate and methanol.

ACE and OP168 were retained using a DIONEX Ion Pac AG 20 (2 mm x 50 mm). Eluents were ultra-pure water + 10% acetonitrile (A) and ultra-pure water + 10% acetonitrile with 50 mmol L^{-1} ammonium bicarbonate (B). The gradient program started at 10% (B), was increased within 5 min to 100% and held for 5 min. Starting conditions were re-established with a ramp of 1 min. Equilibration time of the column was 5 min and the flow rate was 0.25 mL min^{-1}. Detection was achieved with an API 5500 Q-Trap triple quadrupole mass spectrometer (Applied Biosystems/MDS Sciex Instruments, Concord, ON, Canada) with an electrospray interface operated in negative ionization.

DMS was measured with a similar instrumentation. A Luna C18 column (250 mm x 2 mm, 5 µm) from Phenomenex (Aschaffenburg, Germany) was used for retention. Eluents were ultra-pure water (A) and methanol (B) both with 2 mmol L^{-1} ammonium acetate. The gradient program started with 10% (B), held for 7 min and

then increased within 1 min to 100%, then held for 7 min and decreased to the starting conditions within 1 min. The flow rate was 0.2 mL min^{-1}.

The analysis of NDMA was performed after solid-phase extraction (SPE) with NDMA-d_6 as internal standard (1). GC analysis for NDMA was carried out with a series 6890 gas chromatograph connected to a MSD 5973 inert mass spectrometer (both Agilent, Waldbronn, Germany) in positive chemical ionization. A ZB-WAXplus column (30 m x 0.25 mm from Phenomenex) was used for the separation of the analytes (flow rate 0.8 mL min^{-1}). The temperature program started at 40°C and was held for 3 min, ramped 10°C/min to 150°C (held for 2 min), and ramped 10°C/min to 250°C and held for another 2 min.

Quantitative analytical method performance data for ACE, CBZ, DF, DMS, FLX, NDMA and ACE OP168 are provided in Table 3.9.3. No quantitative analytical method performance data are available for BQM, BaQD, DF-IQ and OH-DF due to the unavailability of analytical standards of these compounds.

Table 3.9.3. Analytical method performance data for trace organic contaminants analysed with LC-MS.

Compound	Linearity		Intra-day performance[a]		LOD[b]/ (ng mL^{-1})
	Range/ (ng mL^{-1})	R^2	Precision/ %	Accuracy/ %	
ACE	0.01 – 6	0.999	1.4	96	0.01
CBZ	5 – 500	0.995	3.9	83	5
DF	5 – 500	0.994	2.9	121	1
DMS	0.01 – 1	0.999	0.4	98	0.01
FLX	0.5 – 500	0.996	1.1	82	0.5
NDMA	0.001 – 0.2	0.998	0.3	96	0.001
ACE OP168	5 – 200	0.999	*	*	6

[a]Precision is represented by the relative standard deviation (RSD) of triplicate measurements. Accuracy is represented by the measured concentration over the known added concentration of analyte. [b]LOD: Limit of Detection *Specifically developed non-routine IC-ESI-MS/MS method that has not been statistically evaluated.

3.9.4 Determination of ozone dose and concentration

System 1

Determination of the ozone concentration:

The ozone concentration at the outlet of the bubble column was determined according to DIN 38408. The indigo reagent was placed in a volumetric flask and the ozone solution from the bubble column was collected. This process allows the slowly dripping of water to react immediately with the indigo dye.

Determination of the ozone dose:

The determination of the ozone dose by gas input into the water sample in the bubble column was determined by the indigo method. A stock solution (772 mg L^{-1} tripotassium indigotrisulfonate (MW 616.7 g mol^{-1}) dissolved in ultrapure water with an addition of 1 mL concentrated phosphoric acid) was used in accordance with DIN 38408. The DIN standard states that the purity of the indigo dye is typically around 80%. Taking this information into account, the stock solution contains a dye concentration of 1 mmol L^{-1}. This value is then also in accordance with the calculation formula specified in DIN.

This stock solution was diluted with ultrapure water 1 + 9 and pumped through the bubble column as a water sample (0.1 mmol L^{-1}, 77.2 mg L^{-1}). Bleaching the dye by the reaction with ozone is a stoichiometric reaction. Since one part ozone reacts with one part dye, 0.1 mmol L^{-1} ozone (= 4.8 mg L^{-1}) can be captured via this solution. The degree of bleaching can be determined by the decrease in absorbance by photometry. The maximum absorbance of the blue dye is 600 nm. Parallel to a laboratory spectrophotometer, a self-built flow photometer based on light emitting diodes was successfully used. The emission wavelength of 595 nm requires a slightly lower absorbance, but nevertheless a linear calibration results in the working range (Figure 3.9.2).

A flow-through cuvette with a thickness of 3 mm was used for the test to determine the current-dependent ozone input (Figure 3.9.3). The 1:10 diluted indigo stock solution has an expected value of approx. 650 mAU (i.e. no ozone entry into the bubble column). After applying current to the ozone-micro-cell, ozone gas is introduced into the bubble column and the dye is partially destroyed. It takes about

1 hour to reach a state of equilibrium. The reasons for this are the complete replacement of the volume in the bubble column and the warming up time of the ozone-micro-cell.

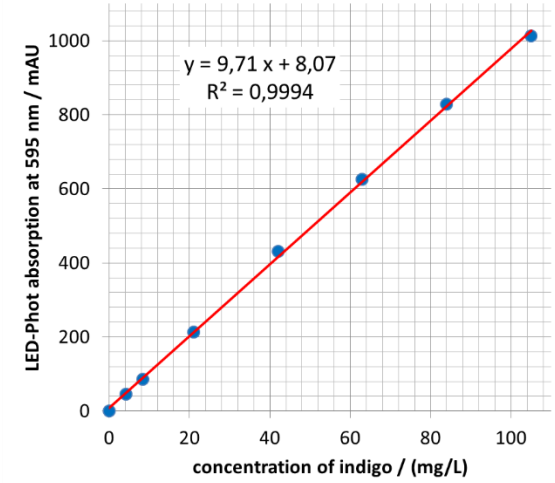

Figure 3.9.2. Calibration and test of linearity of the home-built online LED-photometer with indigo standards (optical path length = 10 mm).

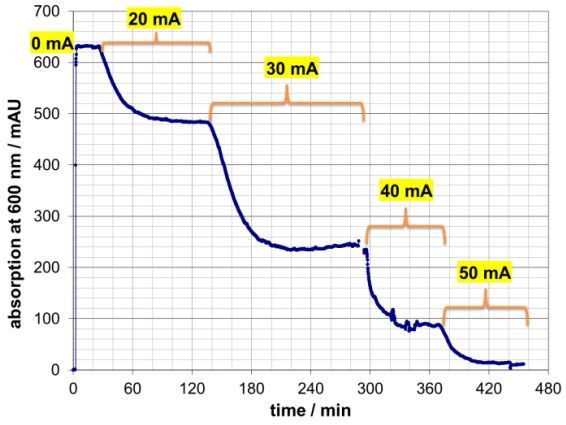

Figure 3.9.3. Determination of ozone input depending on the cell current determined online via the reduction rates of the indigo dye (flow rate = 6 mL min^{-1}, optical path length = 3 mm).

Using the flow rate and relative dye bleaching values, the temporal or volumetric input of ozone can be calculated. In the first step, the relative decrease in absorbance in percent is calculated from the photometric measurements.

$$DB = \left(1 - \frac{A_{(Ix)}}{A_{(I0)}}\right) \times 100 \qquad (3.9.1)$$

DB: Dye-Bleaching in %

$A_{(IX)}$: Absorbance at I = x mA

$A_{(I0)}$: Absorbance at I = 0 mA

The time-dependent ozone input (OzIn) can then be calculated. This value also gives an impression of the production rate of the ozone micro-cell.

$$\mathrm{OzIn} = 0.0048 \times \mathrm{FR} \times \mathrm{DB} \qquad (3.9.2)$$

OzIn: Ozone-Intake in mg min^{-1}

0.0048: Conversion factor in mg mL^{-1}

FR: Flow rate in mL min^{-1}

DB: Dye bleaching in %

The following equation can be used to determine the ozone dose (OzDo).

$$\mathrm{OzDo} = \left(1 - \frac{A_{(Ix)}}{A_{(I0)}}\right) \times 4.8 \qquad (3.9.3)$$

OzDo: Ozone dose in mg L^{-1}

4.8: Ozone in mg L^{-1} (corresponds to the max. turnover of 0.1 mmol L^{-1})

Table 3.9.4 contains a comparison of the percentage of dye destruction determined by LED flow photometer and laboratory photometer. The measured values show that both devices provide equivalent data.

Table 3.9.4. Comparison of the reduction rates depending on the cell current measured by two photometer methods (online and offline).

Cell current/mA	Indigo reduction measured online by LED-Phot/%	Indigo reduction measured offline by EVO300/%
0	0.0	0.0
20	23.2	25.6
30	61.4	62.8
40	86.3	86.5
50	98.3	98.1

If the current in the ozone-micro-cell is kept constant, but the flow rate varies, the same amount of ozone is added to different volumes of indigo solution per time unit. If the flow rate is finally deducted from the measured values, the same production rate should be found for all settings. In a flow range from 2 mL min^{-1} to 10 mL min^{-1} this is also largely the case (Figure 3.9.4A).

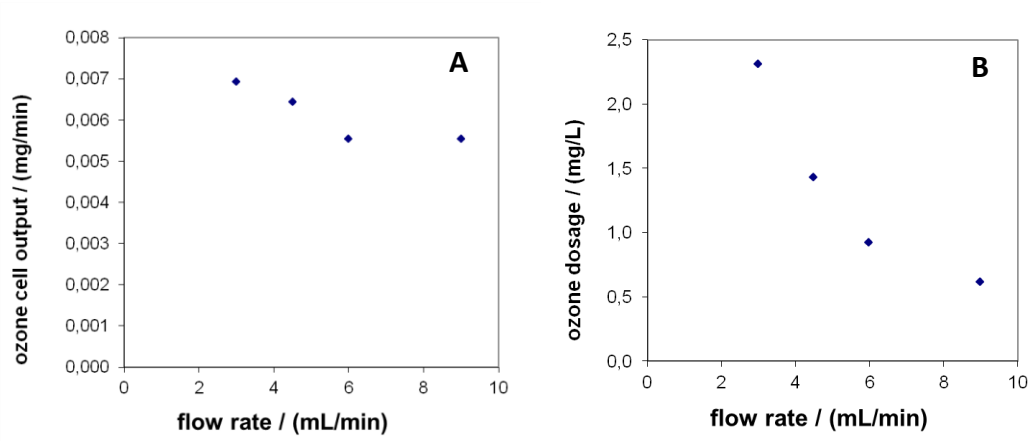

Figure 3.9.4. A) Absolute ozone intake into indigo solution at different flow rates (current = 20 mA). B) Ozone dosage into indigo solution at different flow rates (current = 20 mA).

The same values can also be used to calculate the flux-dependent ozone dose (Figure 3.9.4B).

System 2

The dissolved ozone concentration in the ozonation column was measured in deionized water with the indigo method (3). A standard indigo solution was prepared by dissolving 1° mmol L^{-1} potassium indigotrisulfonate in deionized water acidified with 20°mM phosphoric acid. In 10 mL volumetric flasks, 1 mL of phosphate buffer of pH°=°2, 100°µL of the indigo standard solution and 1°mL to 5°mL of water sampled directly from the ozonation column were added and the flask was filled with deionized water to the mark. All the reagents were added in quick succession with vigorous stirring. The samples were retrieved from the ozonation column after an equilibration time of approximately 1 hour for each value of the electrical current. The absorbance was measured at 600 nm with an Agilent UV/VIS Cary 100 spectrophotometer.

3.9.5 Synthetic wastewater

Table 3.9.5. Properties of the synthetic wastewater prepared with tap water or DI water.

	Concentration/(mg L^{-1})
peptone	16
meat extract	11
urea	3
anhydrous dipotassium hydrogen phosphate (K_2HPO_4)	2.8
sodium chloride (NaCl)	0.7
calcium chloride dihydrate ($CaCl_2.2H_2O$)	0.4
magnesium sulphate heptahydrate ($Mg_2SO_4.7H_2O$)	0.2
TOC (freshly prepared)[a,b]	13 ± 1[d]
TOC (after 1 day of storage)	4 ± 1
TOC (after 2 days of storage)	3 ± 1
TN (tap water)[a,c]	10 ± 1
TN (DI water)	5 ± 1
	Value
pH (tap water)[e]	7.4 ± 0.2

[a] The concentration of total organic carbon (TOC) as non-purgeable organic carbon and total nitrogen (TN) was determined using a TOC analyzer (TOC-5000A, Shimadzu).
[b] The TOC content was similar in tap water and in DI water. Storage was at room temperature, in the influent tank.
[c] There was little change of the TN content during 2 days of storage at room temperature. Ammonia, nitrite and nitrate were not measured, but it can be assumed that ammonification and nitrification took place, while N-species remained in the aqueous phase.
[d] The ± errors are the standard deviation of samples taken on different days (n = 3 to 5).
[e] In DI water, some of the buffering capacity was lost but pH was close to 8.

3.9.6 Tracer tests

System 1

For tracer tests, the drinking water pumped through the system was fortified with 0.5 mg L^{-1} fluorescein. The flow rate was 6 mL min^{-1}. At regular intervals, 0.5 mL samples were taken from each of the different sampling points. These were mixed with 0.5 mL ammonia buffer. The fluorescein content was determined using a flow-through fluorimeter (821-FP, Jasco, Japan; ex = 491 nm, em = 512 nm). Since the tracer substance fluorescein reacts with ozone, the breakthrough curves would suffer

disturbances. Thus, ozonation was switched off during the experiment and a comparable turbulence in the bubble column was achieved by the introduction of nitrogen.

The advantage of manual sampling is that all sampling points can be sampled simultaneously. Alternatively, the flow-through fluorimeter can also be connected to the flow system. An additional peristaltic pump actively pumps a certain proportion of the water through the fluorimeter. Figure 3.9.5 gives an impression of this online measurement. With this procedure, only one sampling point can be sampled per run. A residence time of approx. 6 hours results over the entire system.

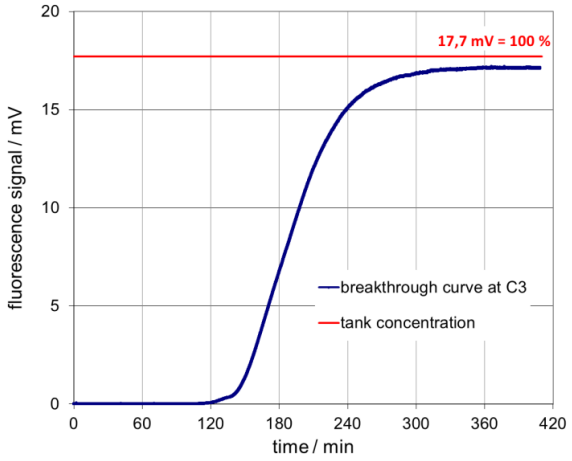

Figure 3.9.5. Breakthrough of fluorescein (500 µg L^{-1} in tap water) through the complete System 1 (flow rate = 6 mL min^{-1}) measured by online fluorescence detection at sample point C3 (ex = 491 nm, em = 512 nm, sample rate = 1 Hz).

System 2

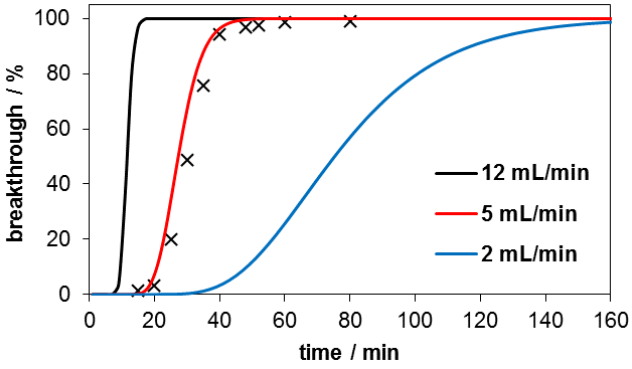

Figure 3.9.6. Tracer breakthrough in the outlet of a single column for three flow rates modeled with CXTFIT. Crosses represent experimental data upon which the modeling was based (fluorescein breakthrough curve).

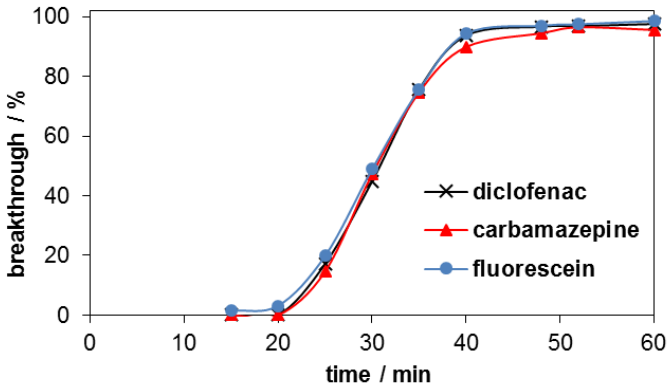

Figure 3.9.7. Breakthrough curve of diclofenac, carbamazepine and fluorescein through a single sand column (not inoculated). Flow rate was 5 mL min^{-1}. The compounds were spiked in tap water (initial concentration of diclofenac and carbamazepine approx. 1 µmol L^{-1}).

3.9.7 Formation of ozonation products in System 2

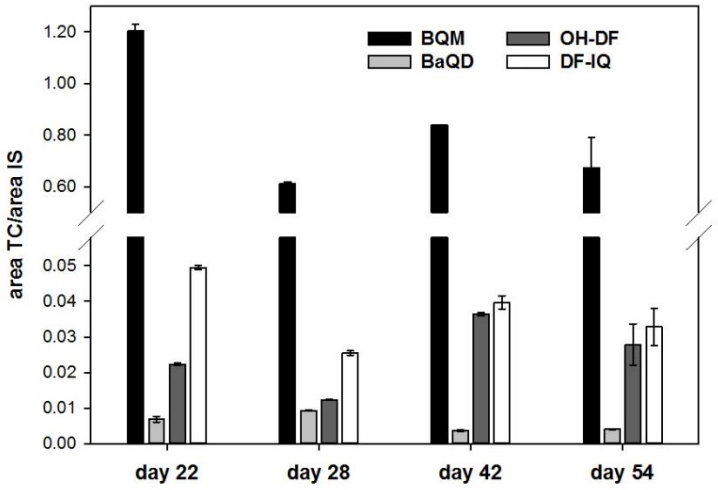

Figure 3.9.8. Formation of carbamazepine and diclofenac transformation products during ozonation on four different days. The samples were taken after the ozonation column. The ratio of the area of the target compound over the area of the internal standard is shown. Ozone dose was 1 mg L^{-1} to 2 mg L^{-1} and ozonation contact time was 10 minutes. Error bars refer to the standard deviation of duplicate samples. The internal standard was carbamazepine-$^{13}C_6$ (100 ng mL^{-1}).

3.9.8 MS/MS data for ozonation products in System 2

Table 3.9.6. MS/MS data for the studied ozonation products of carbamazepine and diclofenac.

Compound	MS/MS fragments (observed)	Comments	References
BQM	195.0674	two-bond cleavage of the hetero-ring	(4, 5)
	223.0869	loss of HCN	
	208.0766	loss of HNCO	
	180.0812	acridine	
BaQD	265.0617	loss of H_2O	(5, 6)
	222.0559	loss of HNCO and CO_2	
	196.0763	loss of HNCO and H_2O	
DF-IQ	291.9935	loss of OH	(7)
	263.9982	loss of CO_2H	
	229.0280	loss of CO_2H and Cl	
OH-DF	294.0100	loss of OH	(7)
	266.0143	loss of CO_2H	
	231.0456	loss of CO_2H and Cl	

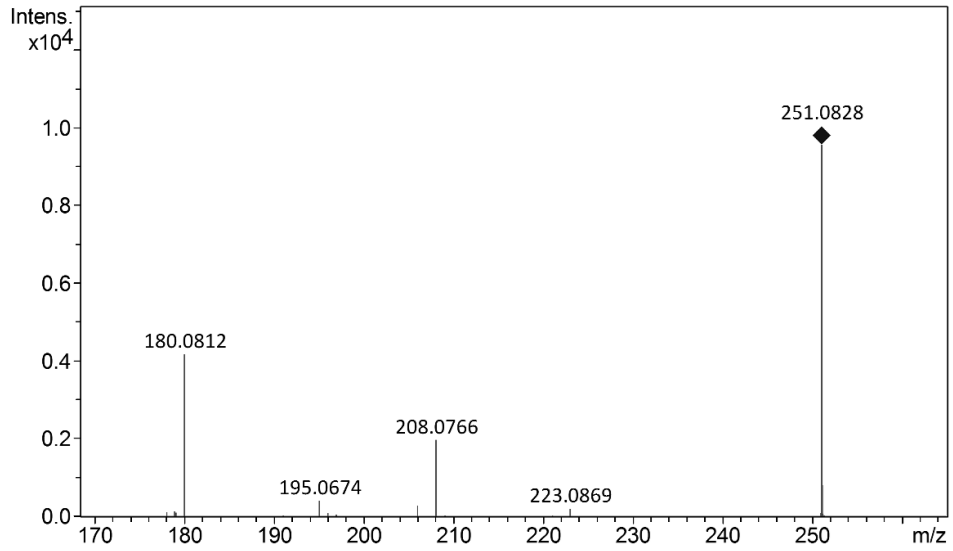

Figure 3.9.9. MS/MS MRM spectrum of BQM in a sample taken after C2 (CE = 30 eV).

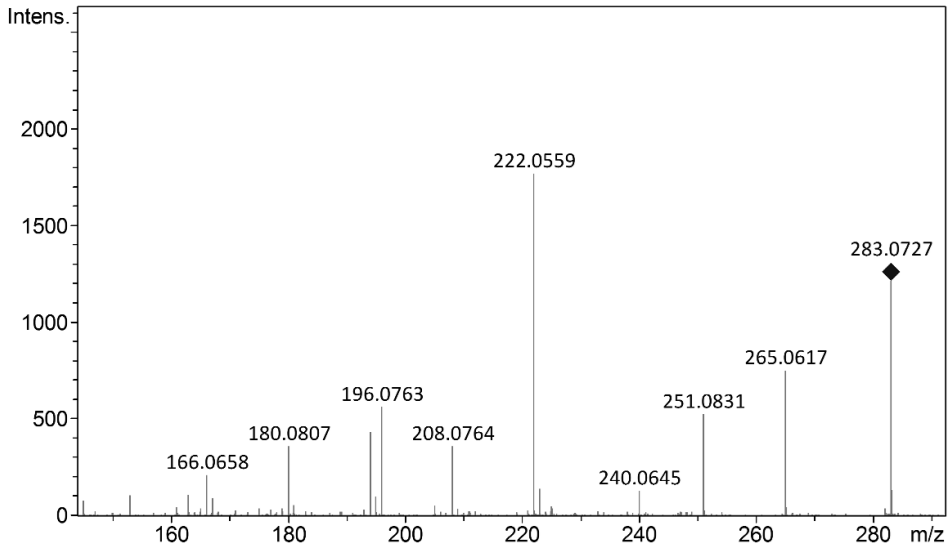

Figure 3.9.10. MS/MS MRM spectrum of BaQD in a sample taken after C2 (CE = 30 eV).

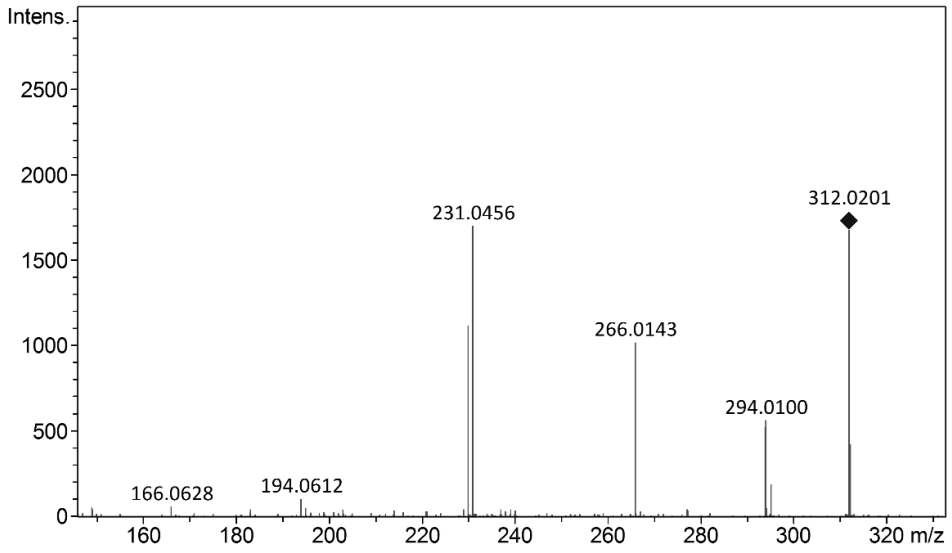

Figure 3.9.11. MS/MS MRM spectrum of OH-DF in a sample taken after C2 (CE = 30 eV).

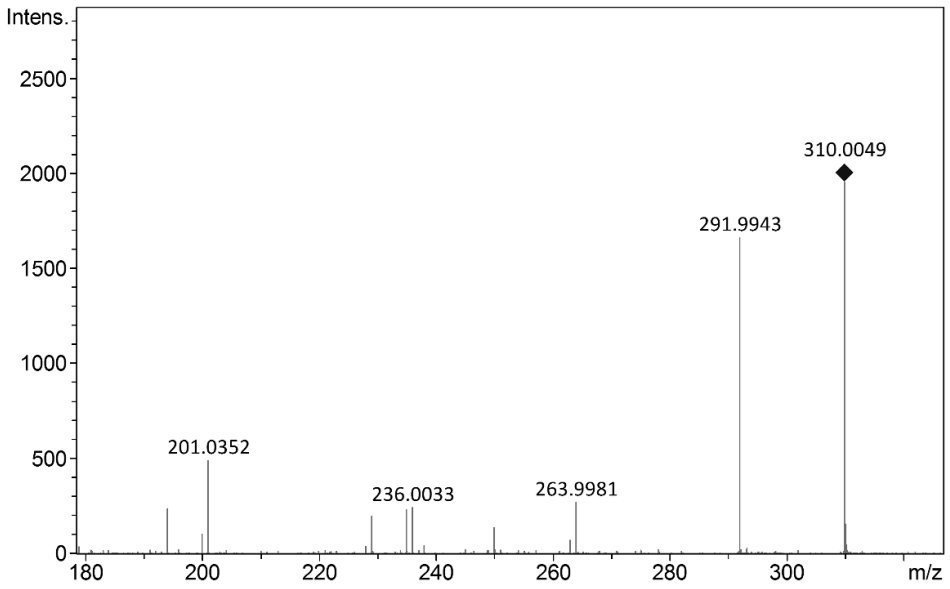

Figure 3.9.12. MS/MS MRM spectrum of DF-IQ in a sample taken after C1 (CE = 30 eV).

3.9.9 References

1. Lee C, Schmidt C, Yoon J, von Gunten U. Oxidation of *N*-Nitrosodimethylamine (NDMA) Precursors with Ozone and Chlorine Dioxide: Kinetics and Effect on NDMA Formation Potential. Environmental Science & Technology. 2007;41(6):2056-63.
2. Scheurer M, Nodler K, Freeling F, Janda J, Happel O, Riegel M, Muller U, Storck FR, Fleig M, Lange FT, Brunsch A, Brauch HJ. Small, mobile, persistent: Trifluoroacetate in the water cycle - Overlooked sources, pathways, and consequences for drinking water supply. Water Res. 2017;126:460-71.
3. Bader H, Hoigné J. Determination of ozone in water by the indigo method. Water Research. 1981;15(4):449-56.
4. McDowell DC, Huber MM, Wagner M, von Gunten U, Ternes TA. Ozonation of Carbamazepine in Drinking Water: Identification and Kinetic Study of Major Oxidation Products. Environmental Science & Technology. 2005;39(20):8014-22.
5. Hübner U, Seiwert B, Reemtsma T, Jekel M. Ozonation products of carbamazepine and their removal from secondary effluents by soil aquifer treatment – Indications from column experiments. Water Research. 2014;49:34-43.
6. Kaiser E, Prasse C, Wagner M, Broder K, Ternes TA. Transformation of oxcarbazepine and human metabolites of carbamazepine and oxcarbazepine in wastewater treatment and sand filters. Environ Sci Technol. 2014;48(17):10208-16.
7. Kosjek T, Zigon D, Kralj B, Heath E. The use of quadrupole-time-of-flight mass spectrometer for the elucidation of diclofenac biotransformation products in wastewater. J Chromatogr A. 2008;1215(1-2):57-63.

Chapter 4: Ozone mass transfer and reactions in bubble-less ozonation using membrane contactors

This work is presented as a conventional thesis chapter.

Parts of this work have been published as a peer-reviewed research paper in October 2018 (DOI: https://doi.org/10.3390/w10101416):

Zoumpouli GA, Baker R, Taylor CM, Chippendale MJ, Smithers C, Ho SSX, Mattia D, Chew YMJ, Wenk J. A Single Tube Contactor for Testing Membrane Ozonation. Water. 2018;10(10):1416.

Further content will be included in a manuscript that is currently being prepared for submission:

Kämmler J, Zoumpouli GA, Chew YMJ, Wenk J, Ernst M. Natural organic matter (NOM) colour removal and bromate formation by membrane ozonation of groundwater. Manuscript in preparation.

Contributions: The work presented was performed by the author of this thesis under the supervision of Dr Jannis Wenk and the co-supervision of Prof John Chew and Prof Barbara Kasprzyk-Hordern, with contributions from co-authors and collaborators as detailed below.

Robert Baker built a prototype single tube membrane contactor and conducted some of the initial experiments. Undergraduate researchers Matthew Chippendale and Chloë Smithers assisted with experiments. Dr Kathryn Proctor performed the LC-MS analysis of trace organic contaminants. The experiments on bromate formation during membrane ozonation were performed in collaboration with Jakob Kämmler and Prof Mathias Ernst from the Hamburg University of Technology.

4.1 Summary

The use of membrane contactors for the bubble-less transfer of ozone into water and wastewater offers several advantages over conventional ozonation reactors. These advantages include a large and well-defined interfacial surface area and improved control over the ozone dosage. The aim of this study was to characterise the ozone mass transfer in a single tube membrane contactor and a hollow fibre membrane module. In addition, the ozone-induced oxidation of natural organic matter and trace organic contaminants and the formation of bromate as a by-product were investigated. Non-porous PDMS membranes of three different sizes were tested for the single tube setup, while the hollow fibre module consisted of 490 porous PTFE fibres. The ozone concentrations transferred into pure water ranged from below 1 to 25 mg O_3 L^{-1} with varying water flow rates and feed gas ozone concentrations. High dissolved ozone concentrations were achieved with low water flow rates, due to longer water residence times. Using the hollow fibre module to transfer a specific ozone dose of approximately 0.5 g O_3/g C, a removal of at least 90% was observed for 19 out of 31 trace organic contaminants that were detected in wastewater effluent. The membrane-assisted ozonation of bromide-containing groundwater indicated that the non-uniform distribution of ozone inside the membranes can contribute to the formation of elevated bromate concentrations exceeding the regulatory limit of 10 µg bromate L^{-1}. Overall, the single tube setup allowed a better fundamental understanding of membrane ozonation, while the larger membrane module shed light on issues that are relevant for practical applications. Based on the results, recommendations were made for the optimisation of membrane ozonation processes, including module design and operational range.

4.2 Introduction

In ozonation plants for water and wastewater treatment, ozone is transferred from the gas into the liquid phase using bubble diffusers or side-stream injection (1) (see also Chapter 1, Section 1.3). Bubble-less ozonation using membrane contactors has emerged as an alternative technology with the potential to address issues associated with the traditional ozone delivery methods. These issues include short-circuiting and stagnant zones within the reactor (2), the formation of foam in waters with high

surfactants content (3), the difficulty in controlling the interfacial surface area of bubbles (4), and the loss of ozone in the off-gas, where it needs to be converted back to oxygen for disposal or reuse (5, 6).

Membranes are mainly used in water and wastewater treatment for desalination, water purification and polishing of treated wastewater using the pressure-driven processes of membrane filtration and reverse osmosis (7). Membrane ozonation is a gas-liquid contacting process that is based on keeping the ozone gas and the water being treated separated by an ozone-permeable membrane that allows for bubble-less transfer of ozone (8). Membrane contactors offer several advantages, including a large and well-defined interfacial surface area and more straightforward scale-up compared to multi-chamber reactors (9). Membrane fouling, a common disadvantage of membrane processes, is less relevant for membrane ozonation reactors due to the concentration-driven rather than pressure-driven mass transfer (9). Finally, membrane ozonation may allow easier and more economical recycling of the off-gas, due to the lower uptake of moisture by the gas which remains separated from the water (10).

Membranes for bubble-less ozonation can be porous or non-porous (dense). The species transport through non-porous membranes is described by the solution-diffusion mechanism, according to which molecules adsorb onto the membrane surface, diffuse through the membrane, and desorb on the other side (11, 12). Non-porous membranes can separate molecules of similar size based on their different solubility, but the flux through them is generally three to five orders of magnitude lower than through porous membranes (13).

The transport of ozone in a non-porous membrane contactor is demonstrated schematically in Figure 4.2.1. The mass transfer is governed by the gas and liquid films (boundary layers), the two solubility laws, and the diffusivity of ozone in the membrane material (14). Further details on mass transfer theory for membrane ozonation are provided in Section 4.4. Here, specific characteristics of the ozone concentration profile during the bubble-less ozone transfer by membrane contactors should be pointed out. Firstly, the ozone concentration in the liquid phase is not uniform, but decreases with increasing distance from the membrane wall (14). Secondly, the ozone dosage is distributed over the length of the membrane, so that low ozone concentrations are continuously injected along the water flow path (15).

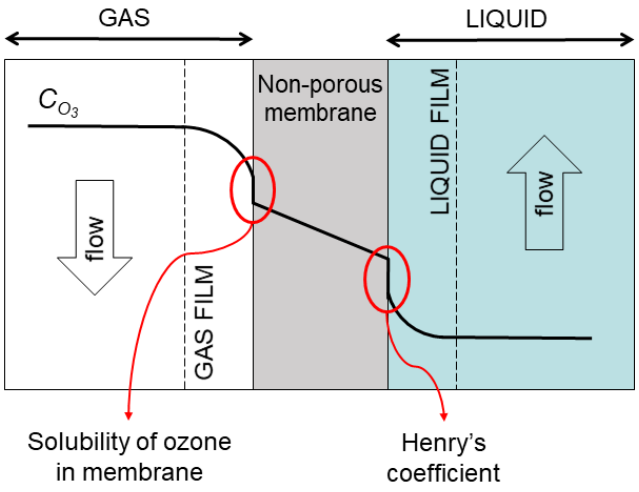

Figure 4.2.1. Schematic of the concentration profile of ozone as it is transferred from a gaseous phase, across a non-porous membrane, into a liquid phase. Adapted from (14).

In porous membranes used for gas-liquid contacting, the operational mode depends on the pressure difference between the two phases, as demonstrated in Figure 4.2.2. The liquid pressure has to be higher than the gas pressure to minimise bubble formation (16). The critical entry pressure (or breakthrough pressure) is the pressure at which the liquid penetrates inside the membrane pores, and depends on the surface tension of the liquid, the contact angle, and the size and shape of the membrane pores (17, 18). Since the diffusivity of ozone in water is four orders of magnitude lower than in the gas phase (14), it is advantageous for the membrane pores in ozone contactors to be flooded with gas to decrease the mass transfer resistance. Therefore, hydrophobic membranes are preferred for ozone transfer (19, 20). In non-wetted micro-porous membranes, both continuum diffusion and Knudsen diffusion determine the ozone diffusivity inside the membrane (21). Knudsen diffusion occurs when the mean free path of the diffusing molecules becomes larger than the pore size (22).

Overall, a similar ozone concentration profile as shown in Figure 4.2.1 can be expected in micro-porous membrane contactors. The main difference is that the solubility of ozone in the porous membrane material can be assumed to have a negligible effect (23).

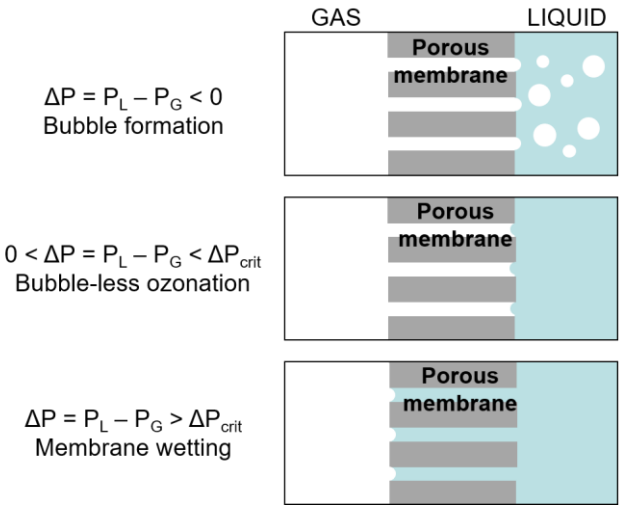

Figure 4.2.2. Operational modes of gas-liquid contacting for ozone transfer using a hydrophobic micro-porous membrane at different liquid and gas pressures. P_L: liquid pressure, P_G: gas pressure, ΔP_{crit}: critical pressure difference.

Experimental studies on bubble-less ozonation using different membrane materials and configurations are presented in Table 4.2.1. Among the commonly employed membrane configurations, hollow fibre modules have the largest specific surface area of around 2,000 to 5,000 $m^2\ m^{-3}$ (24). For the same ozone transfer into a water stream, a hollow fibre setup can be two orders of magnitude smaller than a conventional bubble diffuser (25). In hollow fibre modules the packing density and the fibre length are key parameters affecting pressure drop, flow profiles and flux distribution (26, 27).

Both ceramic and polymeric membranes have been used for ozone transfer (Table 4.2.1). In addition to the membrane's porosity and hydrophobicity which affect mass transfer, the membrane stability during long-term ozone exposure is crucial for practical applications (28). Ceramic membranes consist of different inorganic oxides and are characterised by high thermal, chemical and mechanical stability (29). Although ceramic membranes are ozone-resistant, their inherent hydrophilicity means that surface modification is required to obtain the hydrophobic behaviour that is beneficial for ozone mass transfer (20). In addition, maximising the specific surface area and minimising the associated membrane module size is limited by the difficulty of producing ceramic membranes with low internal diameters (30).

Table 4.2.1. Membrane materials and configurations used for bubble-less ozonation.

	Membrane material		Membrane configuration	References
Inorganic/ceramic	zirconia (hydrophobized)	ZrO_2	single tubular	(31)
	Shirasu porous glass (hydrophilic and hydrophobized)	SiO_2, Al_2O_3, etc.	tubular membranes in parallel	(19)
	alumina (hydrophilic and hydrophobized)	Al_2O_3	single tubular	(31-33)
Polymeric	non-porous PDMS	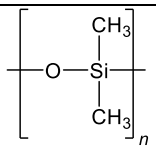	hollow fibre module	(8, 34)
	non-porous PTFE	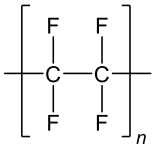	flat sheet	(25)
	porous PTFE		flat sheet hollow fibre module	(25) (15, 23)
	porous PVDF	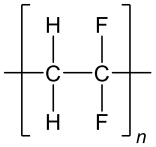	flat sheet hollow fibre module	(25) (23, 35)

Polymeric membranes are generally cheaper than ceramic membranes, but also have a shorter lifespan (36). Their main advantages for ozone transfer are their inherent hydrophobicity and the well-established production of hollow fibres with diameters of a few μm (37). Polypropylene, polyethersulfone and other polymeric materials used for hollow fibre membranes are attacked by ozone, which results in structural changes and deterioration of mechanical properties (28). Polymers not readily reactive with ozone include polytetrafluoroethylene (PTFE), polydimethylsiloxane (PDMS) and polyvinylidene fluoride (PVDF), which are therefore the preferred materials for membrane ozonation (37).

The membrane ozonation studies summarised in Table 4.2.1 investigated theoretical and practical aspects of ozone mass transfer, including the effect of membrane properties, module design and operational parameters on the transferred ozone concentrations. Important operational parameters include the water flow rate, the ozone concentration in the feed gas and the gas pressure (38, 39). Mathematical models have also been developed to describe the phenomena occurring in membrane

ozonation (14, 30, 39). Mass transfer studies were mostly performed in pure water or with model pollutants. In addition, membrane ozonation has been applied to study the oxidation of natural organic matter (NOM), which is a much more complex system (15, 32).

NOM is a heterogeneous mixture of both low-molecular-weight species and macromolecules, such as proteins and polysaccharides, comprising various functional groups (40). A major source of NOM is the biological decay of plant tissue (41). The composition of NOM can be studied using a wide range of analytical techniques encompassing spectroscopy, chromatography, mass spectrometry and their combinations (42). NOM reacts with ozone during water treatment and can therefore increase the required ozone dose and cause the formation of by-products (43, 44).

Chromophoric NOM containing unsaturated and conjugated structures absorbs ultraviolet and visible (UV-Vis) light. Certain structures thereof, mainly humic acids and proteins, also emit light as fluorophores (41). Spectroscopic techniques that measure optical parameters, such as UV-Vis absorbance and fluorescence, have been used to investigate the ozone degradation of NOM (45-47). In particular, UV absorbance at 254 nm (UV_{254}) is a widely applied indicator of aromaticity that correlates well with the ozone reactivity of organic matter (48, 49). Excitation-emission matrices (EEMs) are three-dimensional matrices (excitation, emission and fluorescence intensity) that can provide information on the oxidative removal of different fluorescent NOM fractions (50). For example, EEMs have been used to compare the effects of conventional ozonation and membrane ozonation on NOM composition (32).

In some drinking water sources, the presence of NOM imparts colour to the water, affecting its aesthetic quality (51). The colour of water can be represented by the visible absorbance at 436 nm (VIS_{436}) (52). Ozonation treatment can achieve the removal of colour because colour-absorbing NOM moieties are highly conjugated electron-rich systems that react readily with ozone (53, 54). Membrane ozonation has been applied for colour reduction in NOM-containing water, with the decolourisation rate constant depending on the water flow rate (55).

Despite the existing literature summarised above, there are still considerable knowledge gaps in the membrane ozonation field. In contrast to conventional ozonation (see Chapters 2 and 3), very few studies have investigated the membrane ozonation of trace organic contaminants (TrOCs). The available studies used specific compounds at artificially elevated concentrations (15, 33). Therefore, the abatement of a wide range of compounds at levels intrinsically occurring in environmental samples has not yet been analysed in membrane ozonation systems.

Another aspect of membrane ozonation that has been so far insufficiently addressed is the formation of bromate as a hazardous by-product in bromide-containing waters (see also Chapter 1, Section 1.4). All ozonation processes need to be optimized to achieve treatment goals whilst mitigating by-product formation. For example, improved NOM degradation is usually accompanied by increased bromate concentrations, although the reactor design and operational conditions can impact this trade-off (56). A technology that has shown potential in this regard is the membrane peroxone process, which is membrane ozonation combined with hydrogen peroxide addition to increase the formation of OH radicals (15). In this case, the gradual dosage of ozone along the membrane contactor may decrease the formed bromate concentrations compared to systems with fewer ozone dosing points (15).

The aim of this study was to examine the use of different membrane ozonation systems for the treatment of water and wastewater, elucidating both the ozone mass transfer and specific applications. Initially, a single tube membrane contactor equipped with non-porous PDMS membranes was developed to allow for the study of fundamental mass transfer phenomena and comparison between experimental and theoretical findings. In the next step of the study, a much larger membrane module containing 490 hollow fibres made of porous PTFE was used to represent more realistically how membrane ozonation can be applied in practice. In addition to experiments with pure water, complex water matrices were used to study the ozone-induced degradation of dissolved organic matter, the abatement of trace organic contaminants and the formation of bromate.

The objectives that were pursued in this study were:

- Elucidate the bubble-less ozone mass transfer into pure water, including comparison with computational findings

- Examine the ozonation of model pollutants and natural organic matter
- Investigate the abatement of trace organic contaminants at their inherent concentrations in wastewater effluent
- Analyse the formation of bromate in bromide-containing groundwater
- Compare the single-tube and the multi-tube membrane contactor and make recommendations for the design and operation of membrane modules for ozonation

4.3 Materials and Methods

4.3.1 Chemicals and water samples

All chemicals and analytical consumables were purchased from commercial sources, such as Sigma Aldrich and Fisher Scientific. Ultrapure water (resistivity >18 MΩ cm^{-1}) and deionised water were produced with a Milli-Q (Merck, Darmstadt, Germany) or an ELGA (Veolia, Paris, France) water purification system.

Experiments were performed with pure (deionised) water or with one of the following: a) 10 μM *para*-chlorobenzoic acid (*p*CBA) in 10 mM phosphate buffer at pH 7, as an ozone-resistant model compound, b) humic acid sodium salt (Sigma Aldrich, CAS number 68131-04-4) at various concentrations (total organic carbon, TOC of 1.3 to 13.7 mg L^{-1}) in 10 mM phosphate buffer at pH 7, to study the ozonation of dissolved organic matter, c) river water, d) secondary treated wastewater effluent and e) treated groundwater, to study the ozonation of real water matrices. All the environmental samples were grab samples. Their properties along with sampling dates and locations are shown in Table 4.3.1. The river water and the wastewater effluent were filtered with glass microfiber filters of grade GF/F (nominal particle retention: 0.7 μm, Whatman) to avoid particle clogging of membranes.

Table 4.3.1. Water samples used as feed water in experiments (n/a: not measured).

	Groundwater	**River water**	**Wastewater effluent**	
Sampling date	February 2020	March 2018	March 2018	December 2019
Sampling location	Waterworks in N Germany (finished water)[a]	River Avon in SW England	Wastewater treatment plant in SW England (final effluent)[b]	
pH	8.0	7.2	7.9	8.1
TOC (mg L^{-1})	5.7	7.2	10.2	11.7
Bromide (μg L^{-1})	82	n/a	n/a	n/a
Alkalinity (mg $CaCO_3$ L^{-1})	80	240	180	n/a
UV absorbance at 254 nm (m^{-1})	15.3	19.8	14.0	17.7
VIS absorbance at 436 nm (m^{-1})	0.48	n/a	n/a	n/a

[a] aeration, flocculation and softening, two-stage sand filtration and degassing
[b] primary and secondary (biological) treatment

4.3.2 Experimental setups

PDMS single tube contactor

The experimental setup developed for this study is shown schematically in Figure 4.3.1. The specifications of the membrane contactor are presented in Table 4.3.2. A glass column (length 20 cm, outer diameter 22 mm, inner diameter 18 mm) with four ports was used as a single tube membrane contactor, with gas in the shell side and liquid inside the tube. A single PDMS membrane tube (Silastic®, Cole-Parmer, St. Neots, UK) was fixed at the central axis of the column and held in place by silicone seals. Perfluoroalkoxy alkane (PFA) tubing (outer diameter of 1/4" or 1/8'') was used for connections both in the gas line and in the liquid line. The influent water was pumped using a diaphragm pump (FMM 20 KPDC-P, KNF, Sursee, Switzerland). The water flow was from bottom to top, in counter-flow with the gas. A three-port valve was installed near the water outlet of the contactor as a sampling port.

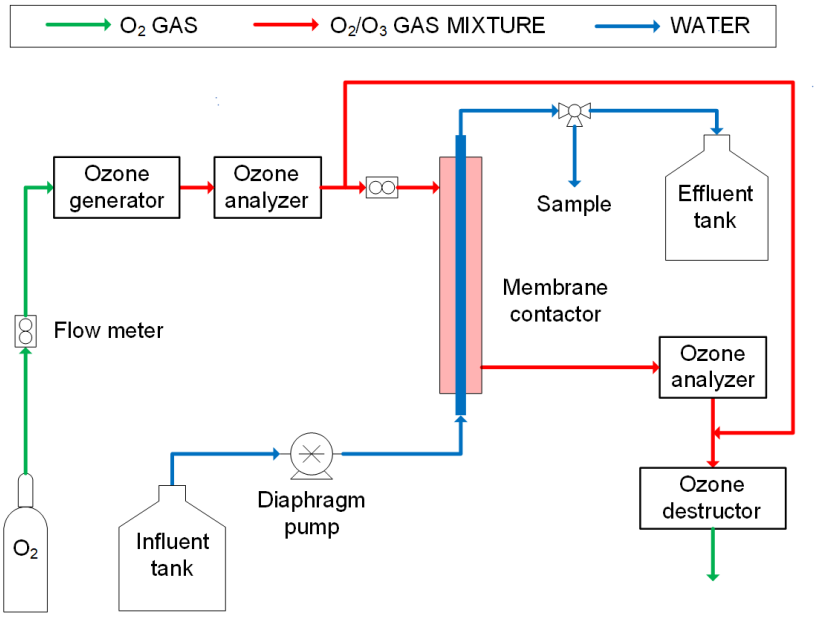

Figure 4.3.1. Schematic of the experimental setup for single PDMS membrane ozonation (Configuration 2).

Two different configurations were used for the gas line:

Configuration 1 (initial configuration): The flow rate of oxygen (99.5 % purity, BOC, Guildford, UK) was controlled with a rotameter (FLDO3306ST, Omega Engineering, Manchester, UK). Oxygen was supplied to the ozone generator (BMT 803N, BMT Messtechnik, Berlin, Germany). The outlet of the ozone generator was connected to an ozone analyser (BMT 964, BMT Messtechnik). The reactor gas outlet was connected to a heated catalyst (CAT-RS, BMT Messtechnik) that converted off-gas ozone back to oxygen. An additional line connecting the reactor directly with the oxygen supply was included to purge the system with oxygen when needed.

Configuration 2 (upgraded configuration): Analogous to Configuration 1, the flow rate of oxygen was controlled with a rotameter (GY-68560-52, Cole-Parmer, St. Neots, UK) and supplied to the ozone generator whose outlet was connected to an ozone analyser. To simultaneously achieve low ozone concentrations and low gas flow rates entering the reactor, a flow split was used that by-passed a portion of the gas directly into the waste stream. Accurate split-flow control was achieved via a second rotameter (FLDO3306ST, Omega Engineering, Manchester, UK). The gas outlet of the membrane contactor was connected to a second identical ozone analyser prior to the heated catalyst.

Table 4.3.2. Specifications of the two membrane contactors.

Membrane contactor	Hollow fibre module	Single tube contactor		
Membrane material	porous PTFE	non-porous PDMS		
Fibre outer diameter (mm)	1.9	2.1	3.2	6.4
Fibre inner diameter (mm)	1.5	1.0	1.6	3.2
Fibre wall thickness (mm)	0.2	0.6	0.8	1.6
Fibre length (cm)	46	20	20	20
Number of fibres	490	1	1	1
Lumen volume (mL)	400	0.2	0.4	1.6
Shell volume, minus the lumen (mL)	1000	50	50	50
Membrane surface area (m^2)*	1.1	0.0006	0.0010	0.0020
Membrane specific surface area (m^2 m^{-3})*	2670	4000	2500	1250

*Based on the inner diameter

PTFE hollow fibre module

A custom-made PTFE hollow fibre module, at half the size of commercial modules, was provided by Markel Corp (Plymouth Meeting, PA, USA). The experimental setup is shown schematically in Figure 4.3.2. The specifications of the module are presented in Table 4.3.2. The module was installed vertically using a metal frame. The module was operated with gas in the shell side and liquid in the lumen. Gas was distributed within the module through a perforated tube located at the central axis of the module (Figure 4.3.3). The module contained a single central baffle, in 'transverse-flow' design (57). The membrane material consisting of porous PTFE had a maximum pore size of 0.82 μm. The membrane porosity was assumed to be equal to 0.4. PFA tubing (outer diameter of 1/4" and 1/8'') was used for connections both in the gas line and in the liquid line.

The influent water was pumped using a peristaltic pump (503U, Watson-Marlow, Cornwall, UK). The liquid flow was from bottom to top, while the gas flow was either co-current or counter-current. A needle valve placed after the liquid outlet of the membrane module was used to adjust the liquid side pressure. A pressure sensor (PXM319-3.5GI, Omega Engineering, Manchester, UK) was installed between the liquid outlet of the module and the needle valve.

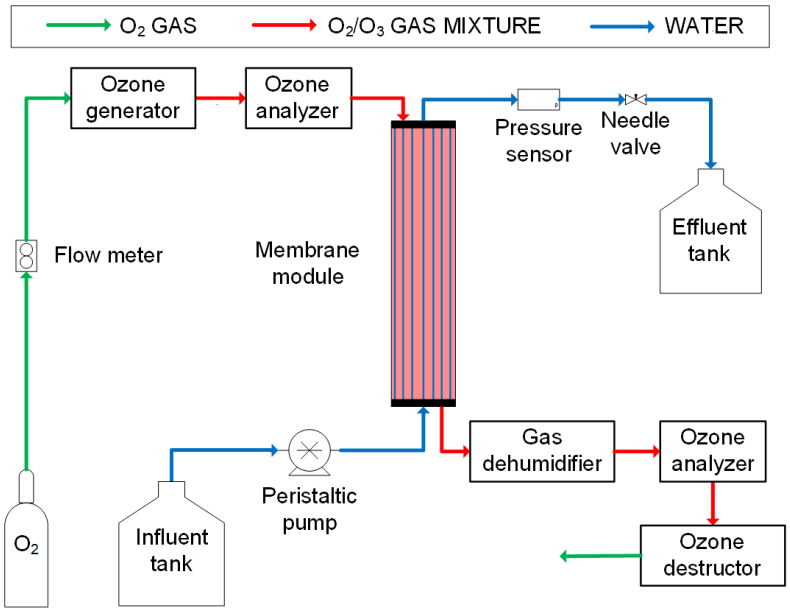

Figure 4.3.2. Schematic of the experimental setup for PTFE membrane ozonation.

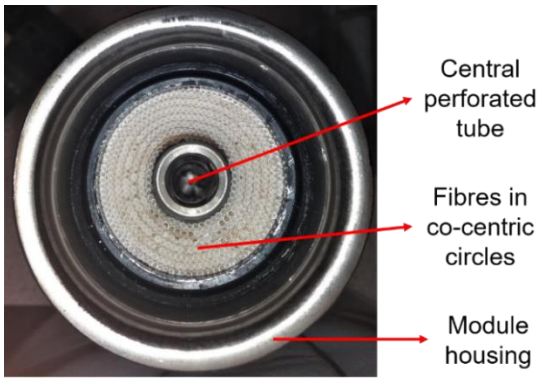

Figure 4.3.3. Top view of the hollow fibre module, with the end cap removed.

The flow rate of oxygen (99.5 % purity, BOC, Guildford, UK) was controlled with a rotameter (GY-68560-52, Cole-Parmer, St. Neots, UK). Oxygen was supplied to the ozone generator (BMT 803N, BMT Messtechnik, Berlin, Germany). The outlet of the ozone generator was connected to an ozone analyser (BMT 964, BMT Messtechnik). The oxygen/ozone mixture was then directed into the membrane module. The module gas outlet was connected to a gas dehumidifier (DT 100, BMT Messtechnik), a second identical ozone analyser and a heated catalyst (CAT-RS, BMT Messtechnik) to convert ozone back to oxygen.

4.3.3 Experimental procedure

The experiments were performed at room temperature, which varied between 15°C and 20°C.

In experiments with the single tube contactor, the PDMS membrane was replaced after a few hours of use. The pressure exiting the oxygen cylinder was set to 0.9 bar. Gas pressure measurements were provided by the ozone analysers. Since the gas line was open to the atmosphere (at the outlet of the ozone destructor), the gas pressure was slightly above atmospheric (less than 1.1 bar) in configuration 1, and higher (1.2 to 1.4 bar) in configuration 2. The gas flow rate through the contactor was set to 100 mL min^{-1} (gas residence time of 30 s). Experiments with different ozone concentrations in the feed gas were performed (25 to 200 mg L^{-1}). The water flow rate was varied between 0.5 and 17 mL min^{-1} and measured at the beginning of each experiment using deionized water and a balance. No control or measurement of the water pressure was performed due to the use of a non-porous membrane. The system was left to equilibrate for at least 10 minutes under given conditions before samples were taken.

In experiments with the hollow fibre module, the pressure exiting the oxygen cylinder was set to 0.9 bar. Gas pressure measurements were provided by the ozone analysers. Since the gas line was open to the atmosphere (at the outlet of the ozone destructor), the gas pressure was slightly above atmospheric (less than 1.1 bar). An oxygen flow rate of 1 L min^{-1} was used (gas residence time in the contactor of less than 1 min). Experiments with different ozone gas concentrations were performed (15 to 90 mg L^{-1}). The water flow rate was varied between 40 and 1000 mL min^{-1} and measured gravimetrically or volumetrically. At low water flow rates, the pressure of the liquid side was increased to 1.1 bar by partially closing the needle valve, to avoid bubble formation. At higher water flow rates (>500 mL min^{-1}) the needle valve was completely open, as the pump provided enough pressure to prevent gas bubbles (up to 1.4 bar). The absence of bubbles was verified by visual observation of the liquid outlet, since the PFA tubing used was translucent. The system was left to equilibrate for at least twice the liquid residence time in the module before samples were taken.

4.3.4 Analytical methods

The residual ozone was not quenched in samples taken for the analysis of optical parameters, trace organic contaminants, bromate and total organic carbon, described below. An appropriate time period ranging from one hour to overnight was allowed before analysis to ensure that the residual ozone had been naturally depleted. The samples were stored at room temperature in the dark until analysis.

Dissolved ozone concentration

The concentration of dissolved ozone in water was measured with the indigo method (58). An indigo stock solution was prepared by dissolving 1 mM potassium indigotrisulfonate in deionized water acidified with 20 mM phosphoric acid. A defined volume of ozonated water sample was added to a mixture of phosphate buffer for pH 2, indigo stock solution and non-ozonated water. Absorbance measurements at 600 nm were performed with a UV-1601 spectrophotometer (Shimadzu, Milton Keynes, UK) or a Cary 100 spectrophotometer (Agilent, Stockport, UK) using 1 cm quartz glass cuvettes. The reduction in colour of the mixture is proportional to the ozone concentration added.

UV-Vis and fluorescence spectroscopy

Spectrophotometric analysis of samples was performed either with a Cary 100 spectrophotometer (Agilent, Stockport, UK) using 1 cm quartz glass cuvettes, or with a Hach Lange DR 5000 spectrophotometer (Hach, Loveland, USA) using 5 cm quartz glass cuvettes. Groundwater samples that were not filtered before the experiments, were filtered prior to analysis using 0.45 µm polypropylene syringe filters (VWR International, Radnor, USA). Absorbance scans or absorbance measurements at specific wavelengths were performed. UV absorbance at 254 nm (UV_{254}) was chosen to study the degradation of NOM. Specific UV absorbance (SUVA) was calculated by diving the UV_{254} by the TOC concentration. Visible absorbance at 436 nm (VIS_{436}) was chosen to represent colour (52).

Excitation-emission matrices (EEMs) were obtained with a Cary Eclipse fluorescence spectrophotometer (Agilent, Stockport, UK) using a 1 cm quartz glass cuvette. Excitation wavelengths were varied from 225 to 450 nm in 5 nm increments and emission wavelengths from 250 to 580 nm in 1 nm increments. The data was

processed according to established methods (59, 60). Rayleigh and Raman scatter peaks were eliminated using an algorithm implemented with MATLAB R2018b. The inner filter effects were corrected using absorbance values (measured separately at the same scan rate of 600 nm min^{-1}). The fluorescence intensity was converted from arbitrary units to Raman units (RU) using the Raman peak of deionised water. Total fluorescence was calculated as the sum of the regionally integrated fluorescence intensity of five operationally defined regions of the EEM with specified boundaries of excitation and emission wavelengths (see Appendix, Table 4.8.2).

Trace organic contaminants

The samples of wastewater effluent before and after ozonation were analysed with a method that can detect 90 compounds by liquid chromatography-tandem mass spectrometry (LC-MS) using a Waters Acquity UPLC system (Waters, Manchester, UK) coupled to a Xevo Triple Quadrupole Mass Spectrometer (Waters, Manchester, UK) equipped with an electrospray ionisation source. The determination of acidic and basic compounds was performed in negative and positive ionisation mode, respectively. Prior to LC-MS analysis, solid phase extraction was performed using Oasis HLB cartridges (Waters, Manchester, UK) to concentrate the samples by a factor of 100. A detailed description of the analytical protocol, including method performance, can be found elsewhere (61). Triplicate samples were analysed for the initial wastewater effluent and duplicate samples after each ozonation experiment. The analytical protocol was started on the same day as the experiments.

A sample of the initial wastewater effluent and an ozonated sample were subsequently also analysed using a Dionex UltiMate 3000 UHPLC system (Thermo Fisher Scientific, UK) connected to a maXis HD QToF mass spectrometer (Bruker, Coventry, UK) with a previously established method (62). The collection of full-scan spectra allowed for the potential detection of unknown or suspect compounds not included in a pre-defined target list. Data processing was performed using the Data Analysis software version 4.3 (Bruker Daltonik GmbH, Bremen, Germany). Suspect screening was performed based on the mass of molecular ions ($[M+H]^+$ or $[M–H]^–$) within a mass accuracy of ± 0.005. Only peaks with absolute intensity higher than 2000 were considered. Peaks that were also present in a MilliQ water blank sample were excluded.

Other parameters

The concentration of total organic carbon (TOC) was determined using a TOC-5000A analyser (Shimadzu, Milton Keynes, UK). TOC was measured as non-purgeable organic carbon. The pH was measured with a FE20 pH meter (Mettler Toledo, Leicester, UK). Alkalinity was determined by titration with 0.1 N hydrochloric acid according to ISO standard 9963-1:1994 (63).

Bromate concentrations were measured at the Hamburg University of Technology according to ISO 11206:2011 by ion chromatography with post-column reaction and UV detection of triiodide (64). A Metrohm IC with an ASupp16 column (Metrohm AG, Herisau, Switzerland) was used. Bromide was measured by ion chromatography with conductivity detection using the same Metrohm IC with an ASupp5 column (Metrohm AG, Herisau, Switzerland).

4.4. Theory and Calculations

The overall mass transfer coefficient of ozone (K_L) in membrane ozonation can be described as a series of resistance terms: resistance of the gas film, the membrane and the liquid film (14). This is demonstrated in equation 4.4.1.

$$\frac{1}{d_{m,ln} K_L} = \frac{1}{d_{m,ln} k_m} + \frac{S}{d_{m,o} k_G} + \frac{1}{H\, d_{m,in} k_L} \qquad (4.4.1)$$

Where k_m, k_G and k_L are the mass transfer coefficients of ozone within the membrane, the gas and the liquid, respectively, $d_{m,o}$ is the outer membrane diameter, $d_{m,in}$ the inner membrane diameter, $d_{m,ln}$ the logarithmic mean membrane diameter, H the solubility (Henry's law constant) of ozone in water and S the solubility of ozone in the membrane material. For the PTFE hollow fibres, S was considered equal to 1 (namely solubility in the porous membranes was ignored).

The mass transfer coefficient of ozone within the non-porous PDMS membrane can be calculated from (65):

$$k_m = \frac{P}{\delta} \times RT \qquad (4.4.2)$$

Where P is the permeability of ozone through PDMS, $\delta = (d_{m,o}-d_{m,in})/2$ the membrane thickness, T the absolute temperature and R the universal gas constant.

The following equations apply for the porous PTFE membrane, assuming that the pores are completely flooded with gas (23):

$$k_m = \frac{D_{m,O_3}\varepsilon}{\delta\tau} \qquad (4.4.3)$$

$$\tau = \frac{(2-\varepsilon)^2}{\varepsilon} \qquad \frac{1}{D_{m,O_3}} = \frac{1}{D_{g,O_3}} + \frac{1}{D_K} \qquad D_K = \frac{2r_p}{3}\sqrt{\frac{8RT}{\pi M_{O_3}}} \qquad (4.4.4)$$

Where ε is the membrane porosity, τ the membrane tortuosity, $D_{m,O3}$ the effective diffusion coefficient of ozone in the membrane, $D_{g,O3}$ the continuum gas diffusion coefficient, D_K the Knudsen diffusion coefficient, M_{O3} the molecular weight of ozone and r_p the membrane pore radius.

The gas-side and the liquid-side mass transfer coefficients of ozone can be calculated from the Sherwood number (Sh), which can be estimated from the Reynolds number (Re) and the Schmidt number (Sc) using a mass transfer correlation. Re and Sc for the liquid and the gas phase were calculated as follows:

$$Re = \frac{ud\rho}{\mu} \qquad Sc = \frac{\nu}{D_{O_3}} \qquad (4.4.5)$$

Where u is the flow velocity, ρ the density, μ the viscosity, $\nu = \mu/\rho$ the kinematic viscosity and D_{O3} the diffusivity of ozone in each phase ($D_{L,O3}$ or $D_{G,O3}$). The diameter used is the inner diameter of the membrane ($d_{m,in}$) for the liquid and the hydraulic diameter of the shell ($d_{s,h}$) for the gas. The $d_{s,h}$ of the hollow fibre module was calculated as follows (66):

$$d_{s,h} = \frac{d_{s,in}^2 - d_{t,o}^2 - n d_{m,o}^2}{n d_{m,o}} \qquad (4.4.6)$$

Where $d_{s,in}$ is the inner diameter of the shell, $d_{t,o}$ the outer diameter of the central tube and n the number of fibres.

For the liquid in the lumen of the single tube contactor and the hollow fibre module, the Leveque correlation was used, which predicts tube-side mass transfer coefficients when the Graetz number is large (9). The Graetz number is the product of Re, Sc and the ratio of diameter over length of the tube (L).

$$Sh = \frac{k_L d_{m,in}}{D_{L,O_3}} = 1.62 \left(Re\, Sc\, \frac{d_{m,in}}{L} \right)^{1/3} \qquad (4.4.7)$$

For the gas in the shell of the single tube contactor and the hollow fibre module a generalized correlation applicable to both commercial and custom-made modules was used (66):

$$Sh = \frac{k_G d_{s,h}}{D_{G,O_3}} = 0.055\, Re^{0.72} Sc^{0.33} \qquad (4.4.8)$$

After calculating k_m, k_L and k_G, K_L can be determined from equation 4.4.1. In addition, K_L can be calculated from experimental data (14):

$$K_L = \frac{u_L\, H}{\alpha\, L} \ln \left(\frac{SC_g}{SC_g - \frac{C_{L,out}}{H}} \right) \qquad (4.4.9)$$

Where α is the surface area of the membrane per unit volume of liquid (specific surface area), C_g the ozone concentration in the gas phase (assumed to be constant and equal to the feed gas concentration) and $C_{L,out}$ the ozone concentration in the effluent of the reactor.

The physical properties of ozone used in the calculations above are shown in Table 4.4.1.

Table 4.4.1. Physical properties of ozone used for mass transfer calculations.

Property	**Value**	**Reference**
Solubility in PDMS (S)	0.881	(67)
Solubility in water (H)	0.30 at 20°C, 0.35 at 15°C	(68)
Permeability in PDMS (P)	10^{-12} mol m^{-1} s^{-1} Pa^{-1}	(69)
Diffusivity in water ($D_{L,O3}$)	1.55×10^{-9} m^2 s^{-1}	(70)
Diffusivity in oxygen ($D_{G,O3}$)	1.65×10^{-5} m^2 s^{-1}	(71)

The presence of chemical reactions in the liquid phase promotes the ozone transfer through the membrane, by increasing the concentration gradient (72, 73). The Hatta number (Ha) is defined as the ratio of the rate of ozone consumed in the liquid film to the rate of mass transfer across the liquid film. If it is assumed that the ozone decay due to reaction with dissolved organic matter is a single first-order irreversible reaction (74), the Hatta number can be calculated from the k_L and the first-order rate constant for ozone decay (k_{O3}) (75).

$$Ha = \frac{\sqrt{k_{O_3} D_{L,O_3}}}{k_L} \qquad (4.4.10)$$

Three kinetic regimes can be distinguished based on the value of the Hatta number: slow, intermediate and fast. In the slow regime, the reaction takes place in the liquid bulk and the mass transfer is not enhanced (Ha<0.3). In the intermediate regime, the reaction occurs both in the liquid film and in the bulk and the mass transfer is accelerated (0.3<Ha<3). In the fast regime (Ha>3), the reaction occurs only within the liquid film leading to a high enhancement of mass transfer (76).

4.5 Results and discussion

4.5.1 Transfer of ozone into pure water using a single tube membrane contactor

The PDMS single tube contactor was used to study the parameters affecting the transfer of ozone into pure (deionised) water. Based on the literature and on mass transfer theory, two of the main operational parameters in membrane ozonation are the water flow rate (liquid side velocity and liquid residence time) and the ozone concentration in the feed gas (38, 39). The single tube contactor also allowed for the study of the membrane size. For the commercially available PDMS membranes, the thickness and inner diameter changed simultaneously (see Table 4.3.1). The effect of the water flow rate, the feed gas ozone concentration and the membrane size on the bubble-less ozonation of pure water is demonstrated in Figure 4.5.1.

The feed gas ozone concentration had a small or moderate influence on the dissolved ozone concentration. Doubling the gas concentration increased the dissolved concentration by less than 50%, and mainly at the lowest water flow rates. This is due to the high gas concentrations used in these experiments, which meant that the available amount of ozone entering the system was not the factor limiting mass transfer.

The transferred ozone concentration increased with decreasing water velocity and with increasing water residence time. All flow rates used were in the laminar flow regime (Re<300), while the residence time varied from <1 s to 100 s. The bubble-less transfer of ozone into water is liquid-phase controlled, i.e. the main resistance for ozone transfer is in the liquid film (25, 35). Higher flow rates are beneficial for mass

transfer because they decrease the thickness of the liquid film (39). Despite this, a long residence time (low flow rate) was more important to achieve high ozone concentrations in this setup. In practice, sufficiently long residence times could be maintained during water treatment by operating multiple membranes in parallel.

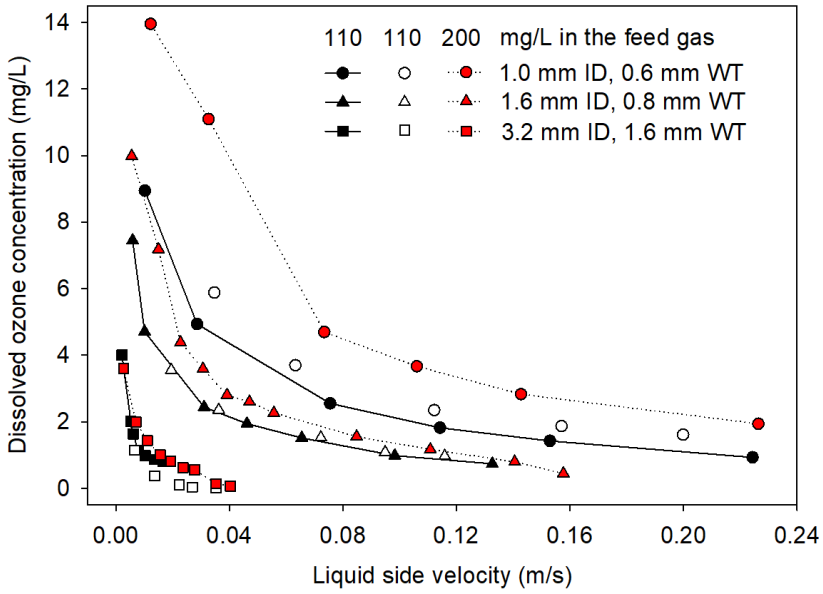

Figure 4.5.1. Dissolved ozone concentration in the outlet of the PDMS single tube contactor vs. the liquid side velocity, with three different membrane sizes (ID: inner diameter, WT: wall thickness) and two feed gas ozone concentrations (110 and 200 mg L^{-1}). The feed water was pure (deionised) water.

It is expected that an increase in the wall thickness of a non-porous membrane increases the resistance to mass transfer (see equation 4.4.2). Indeed, the ozone concentration was lower in the outlet of the thickest tube (3.2 mm inner diameter, 1.6 mm wall thickness), even though the residence time was longer for a given water velocity. The effect of membrane thickness is generally minor for porous membranes (25, 77), with the exception of hydrophilic membranes with wetted pores (19). The wall thickness affects not only the ozone mass transfer through non-porous membranes, but also their mechanical properties (78), which should be taken into account when designing a membrane contactor.

Since the membranes used were non-porous, control of the pressure difference between the gas and the liquid phase was not implemented for this setup. The formation of small bubbles was observed in the liquid phase in some of the experiments, mainly at high liquid flow rates. This may be due to non-uniform initial

wetting of the internal membrane surface, which created patches with lower resistance to ozone transfer. Bubbles usually disappeared during the equilibration period.

The experiments were repeated with different membranes (pieces cut from one length of tubing). The results showed good repeatability (see Figure 4.5.1 where two repeats are shown for the feed gas ozone concentration of 110 mg L^{-1}). The experimental uncertainty was calculated as approximately ±0.2 mg L^{-1}.

The effect of the three parameters discussed above on membrane ozonation using a PDMS single tube contactor has been previously described by Computational Fluid Dynamics (CFD) simulations (14). The experimental results of this study were compared to CFD results obtained using the same conditions, and close agreement between the two was found (Appendix, Section 4.8.1). Therefore, fundamental convection-diffusion theory can be used to predict the ozone transfer in a single tube contactor in the absence of chemical reactions.

4.5.2 Transfer of ozone into pure water using a hollow fibre module

Single membrane contactors are not realistic from a practical viewpoint but can serve as a simplified system to understand more complex membrane module construction and operation. A module comprising 490 porous PTFE fibres was used as a more realistic representation of the flow conditions and potential operational challenges that are present in a large-scale ozonation system.

Experiments with pure water showed a linear relationship between the dissolved ozone concentration in the water outlet of the module and the ozone concentration of the feed gas (Figure 4.5.2). The slope of the trend line decreased at higher water flow rates, due to shorter residence times in the contactor. When the residence time was increased to more than 2 minutes (liquid velocity less than 0.002 m s^{-1}), the dissolved ozone concentration did not increase further, having reached a maximum value that was around 10% lower than the Henry's coefficient of ozone (0.35 at 15°C (68)).

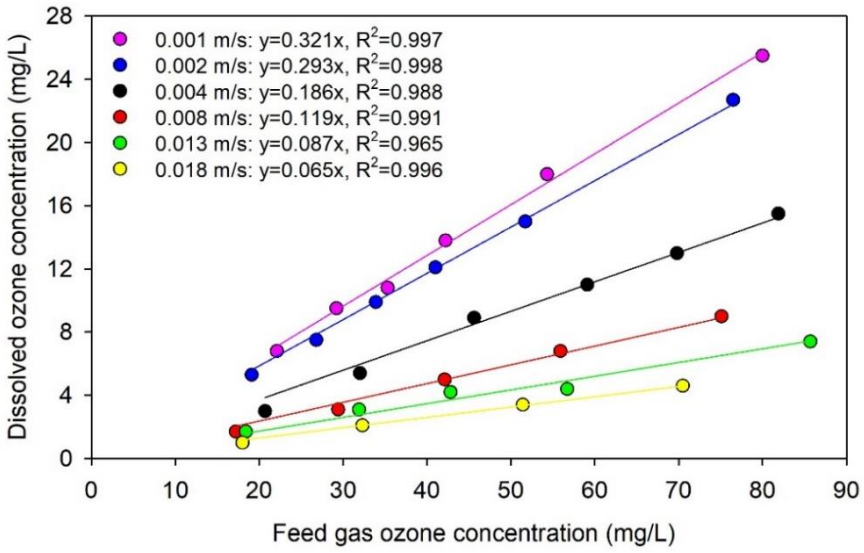

Figure 4.5.2. Dissolved ozone concentration in the outlet of the hollow fibre module versus feed gas ozone concentration at different liquid side velocities, with linear trend lines and their equations and R^2 coefficients. The feed water was pure (deionised) water.

It is crucial to establish a range of operational pressures for micro-porous membrane ozonation, to minimise both bubble formation and membrane pore wetting (38). All the experiments shown in Figure 4.5.2 were performed at the same liquid pressure of 1.10 bar, except for those at the highest flow rate (950 mL min^{-1}) where the minimum pressure delivered by the pump was 1.23 bar. The range of transmembrane pressures was therefore approximately 0.05 to 0.20 bar, which is similar to the values reported for membrane ozonation with flat sheet PTFE membranes (25), and with tubular ceramic membranes (30). The critical pressure for a water-air system at the surface of micro-porous PTFE fibres is approximately 0.8 bar (18), which is much higher than the transmembrane pressure used in the experiments.

As mentioned previously, convection-diffusion theory can offer valid estimations of the ozone transfer in a single tubular membrane. However, there are additional factors affecting mass transfer in larger membrane modules, due to their more complex structure and shell-side flow patterns (9, 57). Despite the 'transverse-flow' design of the module used in this study, it is possible that some of the gas passes through the module without contacting the membranes (gas by-pass), while inner membranes positioned close to the central distribution tube likely receive more ozone than the outer membranes (see Figure 4.3.3). The experiments cannot provide information on the spatial distribution of ozone inside the module. Initial results

(Appendix, Section 4.8.2) indicated that CFD simulations can be a valuable tool to optimise the design of hollow fibre modules for membrane ozonation, though this was not further pursued in this study.

4.5.3 Mass transfer coefficients of ozone in membrane ozonation

The mass transfer coefficients of ozone for the membrane ozonation of pure water were calculated both theoretically and from experimental data, as described in Section 4.4. The theoretical membrane, liquid-side and gas-side mass transfer coefficients for the four setups used in the experiments are shown in Table 4.5.1. It is sometimes assumed that the total mass transfer resistance in membrane ozonation is approximately equal to the liquid-side resistance (55). Nevertheless, previous studies have pointed out that the membrane resistance (14), and the gas-side resistance (39), can have a significant contribution.

Table 4.5.1. Theoretical membrane, gas-side and liquid-side mass transfer coefficients of ozone for the four membrane setups, at a liquid flow velocity of 0.01 m s^{-1}.

	PDMS 1.0 mm ID	**PDMS 1.6 mm ID**	**PDMS 3.2 mm ID**	**PTFE**
k_m (m s^{-1})	4.4×10^{-6}	3.0×10^{-6}	1.5×10^{-6}	4.4×10^{-3}
k_G (m s^{-1})	2.2×10^{-4}	2.3×10^{-4}	2.7×10^{-4}	5.4×10^{-4}
k_L (m s^{-1})	8.0×10^{-6}	6.8×10^{-6}	5.4×10^{-6}	4.9×10^{-6}

The membrane resistance was negligible for the porous PTFE membranes. In contrast, it constituted 30 to 46% of the total resistance for the non-porous PDMS membranes, which agrees with the experimentally observed effect of the membrane thickness for the PDMS contactor. The gas film resistance was very low and contributed less than 1% to the total resistance in all setups. However, the calculation of k_G was based on a general empirical mass transfer correlation that may not be accurate for all module designs (66). The liquid film resistance was of the same order of magnitude as the membrane resistance for the PDMS contactor, while it was practically equal to the total resistance for the PTFE hollow fibre module.

Figure 4.5.3 shows a comparison between the experimental and theoretical overall mass transfer coefficients of ozone (K_L) for the two membrane contactors. The

theoretical K_L does not depend on the feed gas ozone concentration, so an average of different feed gas ozone concentrations is shown for the experimental K_L. The experimental K_L of the PTFE module was comparable to the values of the PDMS contactor. It should be noted that similar K_L values may correspond to very different dissolved ozone concentrations. Therefore, both the K_L and the transferred ozone concentration should be taken into account when optimising the operation of a membrane contactor for ozonation (39).

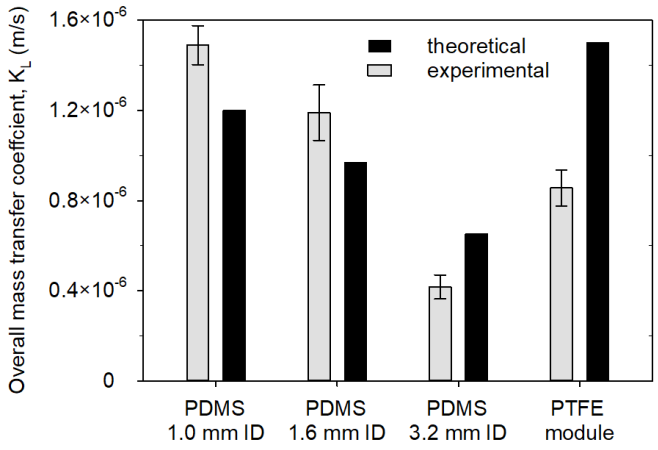

Figure 4.5.3. Overall mass transfer coefficients of ozone (K_L) for the two membrane contactors at a liquid side velocity of 0.01 m s^{-1}. Error bars indicate the range of feed gas concentrations applied in the experiments (two for PDMS, five for PTFE).

For the single tube contactor, the theoretical prediction of K_L was generally in good agreement with the experimental values, with an average relative difference of 31% across all membrane sizes and liquid side velocities. The theoretical K_L underwent a smaller decrease with increasing membrane size than the experimental K_L, indicating that some effects of the membrane size are not captured by the theoretical approach. This could include effects on experimental measurements, for example lower ozone concentrations were measured with larger membrane size.

An average relative difference of 36% was observed for the hollow fibre module, with higher theoretical than experimental values. This discrepancy can be attributed to an underestimation of the gas and liquid film resistances by the theoretical approach, for example due to non-ideal flow conditions within the module shell, such as gas by-pass, that may not be captured by the mass transfer correlation used for the gas (66). In addition, experimental errors (e.g. ozone losses) may have led to an underestimation of the experimental K_L (37).

4.5.4 Ozone reactions in a single tube membrane contactor

In addition to studying ozone mass transfer in pure water, the effect of operational parameters on the membrane ozonation of organic compounds needs to be assessed. *p*CBA was chosen as an ozone-resistant model contaminant since it has been extensively used as a probe compound to assess OH radical-induced oxidation processes in ozonation (79). The enhancement of ozone mass transfer can be assumed to be negligible in experiments with *p*CBA in pure buffered water due to the low concentration used (10 μM) and the very low ozone reactivity of *p*CBA. In addition, experiments were performed with complex water matrices of humic acids, river water and wastewater effluent. In this case, the mass transfer enhancement may have been substantial, however it was not the focus of this set of experiments.

Figure 4.5.4.A shows the degradation of *p*CBA in pure water with different membrane sizes and varying residence time in the reactor. The *p*CBA removal increased with lower membrane thickness and with longer contact times, due to higher transferred ozone concentrations leading to increased OH radical formation. As a result, the thickest membrane tube achieved only partial removal of *p*CBA even with the longest residence time of 30 s. For the middle-sized membrane, the removal of *p*CBA in a humic acid solution, in river water and in wastewater effluent is also shown. The complex water matrices significantly lowered the removal efficiency of *p*CBA compared to pure water, due to matrix components acting as OH radical and ozone scavengers (80). The lowest removal was observed in wastewater effluent, which had the highest TOC content among the tested waters.

The degradation of ozone-resistant compounds such as *p*CBA can be improved by addition of hydrogen peroxide to the water prior to passage through the membrane contactor (membrane peroxone process) (15). However, adding hydrogen peroxide only made a marginal difference in the single tube membrane contactor, and was therefore not investigated further. An ozone to hydrogen peroxide ratio of 2:1 was chosen as it is generally considered optimal to maximise the formation of OH radicals (81). The limited effect of hydrogen peroxide addition may have been due to the non-uniform concentration of ozone inside the membrane (see Figure 4.2.1), which influenced the local ozone to hydrogen peroxide ratio (33). Moreover, the ratio

was calculated without taking into account the potential enhancement of ozone mass transfer due to reaction with hydrogen peroxide and matrix components (37).

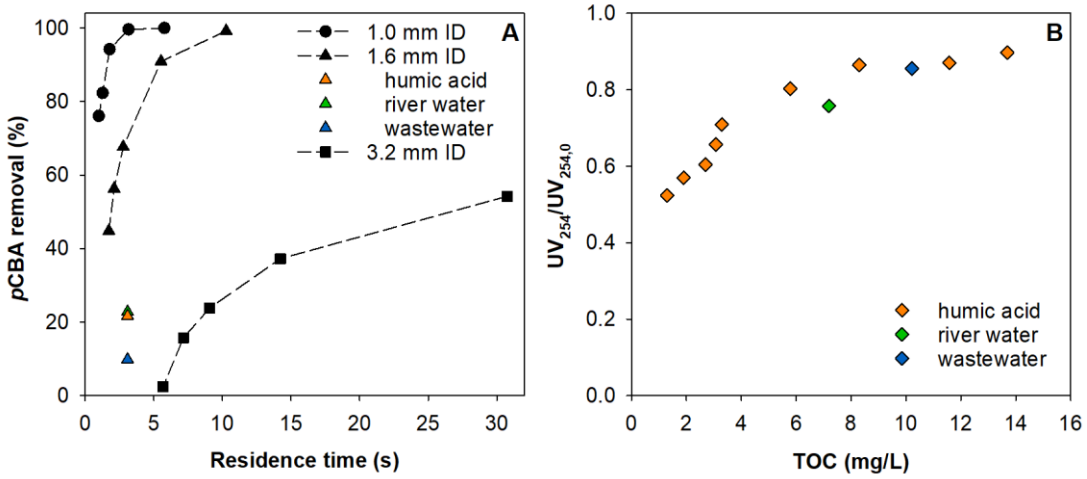

Figure 4.5.4. A. Removal of *p*CBA in different water matrices with three membrane sizes and a feed gas ozone concentration of 110 mg L^{-1}. Black symbols represent pure buffered water, and coloured symbols represent a humic acid solution (TOC 8.3 mg L^{-1}), river water (TOC 7.2 mg L^{-1}) and wastewater effluent (TOC 10.2 mg L^{-1}). B. Relative change in UV_{254} absorbance for river water, wastewater effluent and humic acid solutions of different TOC, 1.6 mm ID membrane, 4 s residence time, 110 mg L^{-1} feed gas ozone concentration.

In addition to the removal of a model contaminant, the degradation of the dissolved organic matter in different water matrices (river water, wastewater effluent and humic acid solutions) was studied by measuring UV_{254} absorbance. Figure 4.5.4.B shows relative changes in UV_{254} versus the feed water TOC, at a set water velocity and feed gas ozone concentration. Since all other parameters were fixed, an increase in TOC signifies a decrease in specific ozone dose (g O_3/g C). The ozone concentration measured in pure water under the same conditions (1.9 mg O_3 L^{-1}) gives an indication of the minimum transferred ozone doses (0.1 to 1.5 g O_3/g C) if the mass transfer enhancement is low.

The UV_{254} removal decreased strongly with increasing TOC up to around 4 mg C L^{-1} and plateaued after that. Two distinct phases have been previously observed for the UV_{254} removal versus the specific ozone dose and are attributed to organic matter moieties with different ozonation kinetics (i.e. fast-reacting moieties are depleted at low ozone doses while slowly-reacting moieties at higher ozone doses) (82). The results for river water and wastewater effluent, which correspond to one TOC concentration each, were in line with those for humic acid, for which a range of

different TOC concentrations was tested. Differences in alkalinity (see Table 4.3.1) and the origin of the sample can affect the ozone reactivity of organic matter (80), however these effects appeared to be minor in this case.

Overall, the data from membrane ozonation of *p*CBA and dissolved organic matter demonstrate the versality of the single tube setup for experimental investigations requiring a range of ozonation conditions. The dissolved ozone concentration can be easily controlled by varying water flow rate and membrane size, leading to the desired extent of target contaminant removal or change in water quality parameters. It is, however, important to assess whether this straightforward adjustment of treatment conditions can be extended to larger-scale membrane ozonation systems.

4.5.5 Membrane ozonation of trace organic contaminants and dissolved organic matter using a hollow fibre module

The hollow fibre module was used to assess the abatement of TrOCs that were present in a secondary treated wastewater sample at very low, intrinsically occurring concentrations. In addition, the ozonation of the dissolved organic matter was evaluated using spectrophotometric analysis. A constant water flow rate was applied, leading to a residence time in the reactor of 4 min, while the feed gas ozone concentration was varied to achieve three different ozone doses. The transferred specific ozone doses can be estimated from pure water measurements (assuming negligible enhancement of mass transfer) as 0.5, 0.9 and 1.3 g O_3/g C. Table 4.5.2 shows the change in some water quality parameters with varying feed gas ozone concentration.

As expected, little mineralisation (TOC removal) was achieved under the employed conditions. The removal of UV_{254} absorbance ranged from 49% to 59% (see also Appendix, Figure 4.8.5). Therefore, more than doubling the feed gas ozone concentration led to a small improvement of UV_{254} reduction. This indicates that the highly reactive fraction of organic matter was already oxidised at the lowest ozone dose, while the additional ozone transferred at the other two ozone doses partly oxidised the less reactive fraction (83).

Table 4.5.2. Main parameters of the wastewater effluent before and after ozonation with three ozone doses.

	Wastewater effluent	Low ozone	Medium ozone	High ozone
Feed gas ozone concentration (mg L^{-1})	-	22	35	53
Residual dissolved ozone concentration (mg L^{-1})	-	2.2	4.9	7.6
pH	8.1	8.0	8.0	7.8
TOC (mg L^{-1})	11.7	12.1	11.5	10.5
UV_{254} (cm^{-1})	0.177	0.090	0.080	0.073
SUVA (L mg^{-1} m^{-1})	1.51	0.75	0.70	0.69
Total Fluorescence (RU nm^2)	322400	18900	7600	2100

The lowest ozone concentration applied was enough to achieve a 94% removal of total fluorescence (TF) (Table 4.5.2). Higher ozone doses had a minor additional effect on the remaining fluorescence. TF generally undergoes greater decrease than UV_{254} at a given ozone dose (84, 85). This can be explained by differences in reactivity and/or in reaction mechanisms. Oxidised dissolved organic matter maintains some residual UV absorbance because of the formation of UV-absorbing reaction products that do not, however, fluoresce (47). In addition, it has been suggested that electronic interactions (e.g. charge transfer) between oxidised molecules result in an 'inert fraction' of dissolved organic matter which absorbs UV light even after treatment with high ozone doses (84, 86).

In addition to TF, which is a bulk parameter, more detailed information can be obtained by examining the different peaks in the EEM (Appendix, Figure 4.8.6 and Table 4.8.2). The major fluorescent components of dissolved organic matter are humic material containing aromatic carbonyl moieties, and protein fractions with structures related to tryptophan and tyrosine (87-89). Five previously proposed regions defined by specific excitation and emission wavelengths were present in the EEM of the initial wastewater sample (Appendix, Figure 4.8.6A): tyrosine-like aromatic protein, tryptophan-like aromatic protein, fulvic acid-like matter, soluble microbial by-product-like matter and humic acid-like matter (59, 90). Protein peaks are usually sewage-derived, while humic and fulvic acids originate from natural organic matter, such as plant material (91).

The protein peaks were removed first by membrane ozonation, while fulvic acids and humic acids were more ozone-resistant (Appendix, Figure 4.8.6B, C, D). This is in accordance with previous ozonation studies (50, 92, 93), and could be an indication of differences in concentration, molecular size and ozone-reactive sites for the different compound types (94). Aromatic amino acids are the main sites for ozone attack in protein structures (95). The ozone reactivity of humic acids depends on their chemical structure, which varies depending on hydrologic, seasonal and many other factors (48).

Out of the 90 TrOCs included in the employed LC-MS method, 12 were quantified in the wastewater effluent. 8 of those could also be quantified in one or more of the ozonated samples, while 4 were below the limit of quantification after ozonation. 17 further TrOCs were detected in the wastewater effluent but could not be quantified due to analytical issues, such as quality controls not meeting the required criteria or concentrations exceeding the linear range of the calibration curve. The results for these compounds are provided semi-quantitatively. 11 of the semi-quantitative compounds were also detected in one or more of the ozonated samples. The concentration of the 29 TrOCs before and after ozonation is shown in the Appendix, Table 4.8.3, while ozonation removal percentages are presented in Figure 4.5.5.

The compound with the highest quantified concentration in the wastewater effluent sample was acetaminophen (1.5 μg L^{-1}), while other compounds detected with high signals that could not be accurately quantified were benzophenone-4, metformin, 1,7-dimethylxanthine and carbamazepine-10,11-epoxide. The results are generally in line with other studies that analysed wastewater effluent sampled in the same region (SW England) (61, 96).

The abatement of TrOCs at their original low concentrations in wastewater effluent has been well studied with conventional ozonation systems, including pilot-scale and large-scale plants (97-100). However, there is no information available for membrane ozonation systems. In this study, a removal higher than 90% was observed for 21 of the detected compounds. In addition, this removal was in most cases already achieved with the lowest ozone dose. This agrees with the results of the spectrophotometric analysis. It has been reported that a UV_{254} reduction higher than 50% and a TF reduction higher than 90% is required to achieve an elimination of at least 90% for

TrOCs with high and moderate ozone reactivity (101). Cotinine and metformin were the compounds that demonstrated the effect of the ozone dose most clearly, since they both have a low ozone reactivity (see Chapter 2, Table 2.4.1 for more information on the ozone reactivity of the analysed TrOCs). In many cases the effect of varying the ozone dose could not be observed due to the TrOC concentrations being close to or below the method quantification limit.

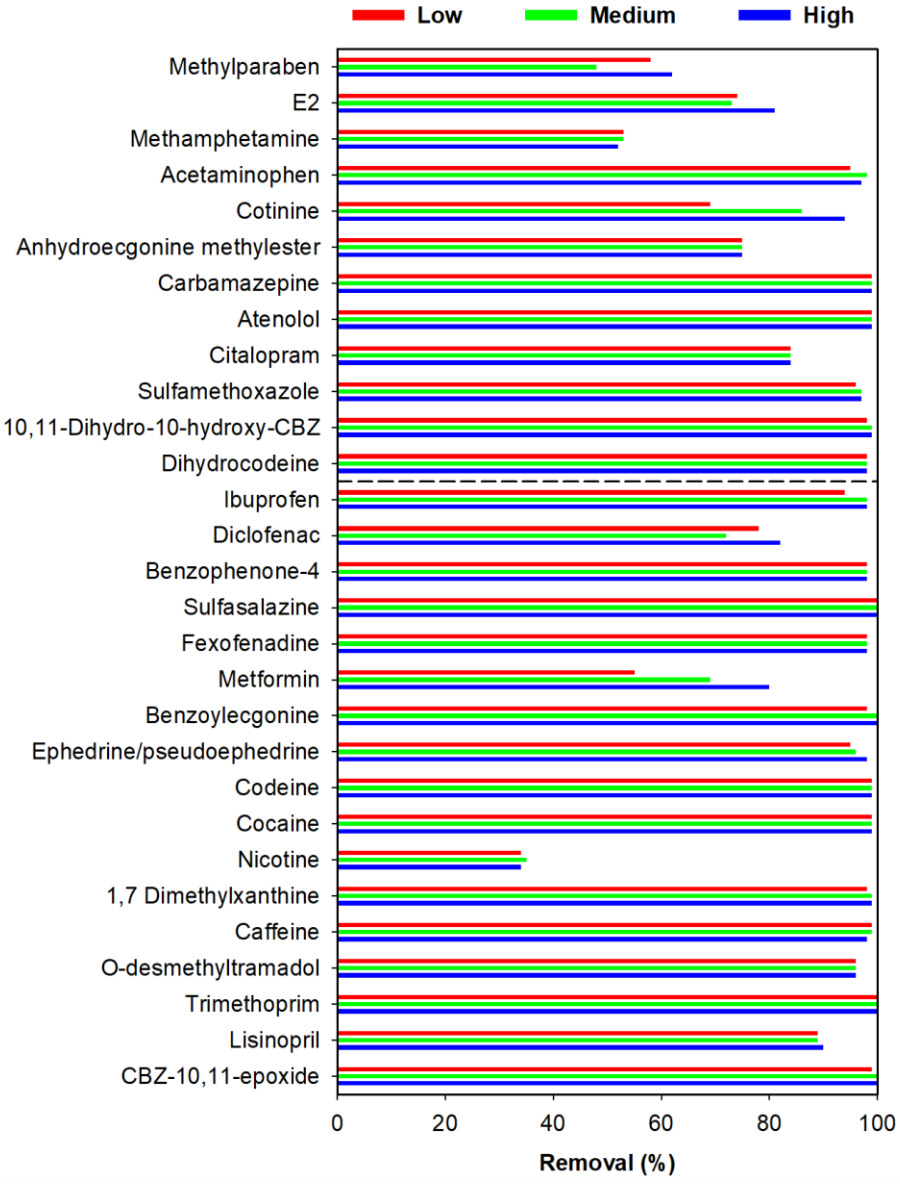

Figure 4.5.5. Removal percentage of TrOCs with three ozone doses (low, medium and high, see Table 4.5.1). TrOCs that were analysed quantitatively are shown above the dashed line and semi-quantitatively below the dashed line. Concentrations below the method quantification limit were considered equal to the method quantification limit in order to calculate the removal percentage.

When comparing these results with those presented in Chapter 2, different removal percentages were observed for several compounds, despite the use of similar specific ozone doses. An important difference between the two datasets is that experiments in Chapter 2 were performed with elevated concentrations of TrOCs (approximately 100 μg L^{-1} each). In this work, TrOCs were only present at trace concentrations (most of them below 1 μg L^{-1}), therefore the wastewater effluent matrix was dominated by the bulk organic matter. Even when the ozone dose is normalised to the TOC content, the varying reactivity of the aqueous matrix can lead to different extents of TrOC attenuation (102). In addition, the data of Chapter 2 were obtained by performing batch experiments with injection of ozone stock solution under stirring. The different ozone concentration profile in those experiments (uniform ozone distribution after a single injection) compared to membrane ozonation (areas of increased ozone concentration and continuous injection) may have also affected the observed abatement of TrOCs. As a next step, it would be of particular interest to compare the abatement of TrOCs in membrane ozonation and in conventional ozonation (e.g. a bubble reactor) under equivalent conditions.

The removal efficiencies of the parent compounds in membrane ozonation should be accompanied by information on reaction mechanisms and product formation. High resolution mass spectrometry with subsequent suspect screening was employed to observe the formation of ozonation products. A list of 176 TrOC ozonation products was compiled based on the available literature (Appendix, Table 4.8.4). A sample of the initial wastewater effluent and a sample ozonated with the lowest ozone dose were analysed and screened. In positive mode, 64 out of 174 suspect masses were detected in the initial wastewater effluent prior to ozonation, with 30 of them disappearing after ozonation. This could indicate that these masses did not correspond to ozonation products or that the compounds reported as ozonation products had already been formed in the wastewater effluent from different processes such as microbial degradation of TrOCs. 17 suspect masses were only present after ozonation, but with very low intensities, including masses corresponding to ozonation products of fexofenadine, metformin and trimethoprim. Similarly, in negative mode, 98 out of 174 suspect masses were detected in the initial wastewater effluent prior to ozonation, with 43 of them disappearing after ozonation, while 14 masses were only present after ozonation.

Non-target and suspect screening of TrOCs and their transformation products has attracted increasing attention in recent years, leading to the development of sophisticated methods and workflows (103-106). Non-target screening refers to the detection of unknown compounds without prior information, while suspect screening relies on available compound-specific information, such as molecular formula and structure, but does not require reference standards (107). Even if the mass of a suspect compound is detected in samples, additional confirmatory steps need to be applied to reduce or eliminated false positive findings (107). Further work is thus required to improve and validate the methodology used in this study. Next steps should include the implementation of automated routines to filter the primary mass search results (e.g. taking into account the isotope pattern and the predicted retention time) and interpretation of fragmentation patterns generated by tandem mass spectrometry to support structure assignment. In addition, the initial results presented here are only based on the analysis of two samples. The development of an automated routine would allow for processing of a larger volume of data which could provide valuable insights into the formation of transformation products in membrane ozonation.

Overall, this study demonstrated that high removals of TrOCs in wastewater effluent can be achieved with a hollow fibre module resembling commercial systems operating with a feed gas ozone concentration of 22 mg L^{-1} or higher and a liquid residence time of 4 min. Reaction mechanisms and product formation need to be further elucidated according to the initial findings of this study.

4.5.6 Bromate formation in membrane ozonation treatment of groundwater

A bromide-containing groundwater was used to assess the formation of bromate along with the removal of colour during membrane ozonation with the PDMS single tube contactor and the PTFE hollow fibre module. The groundwater used had a high TOC concentration (5.7 mg L^{-1}) and a high colour (VIS_{436} = 0.48 m^{-1}). Figure 4.5.6 shows the four parameters measured at the water outlet of the two ozone contactors: residual ozone concentration, UV_{254} and VIS_{436} absorbance, and bromate concentration. Gas-liquid co-current flow instead of counter-current flow was tested for one water flow rate with the hollow fibre module but had minor effects on the measured parameters.

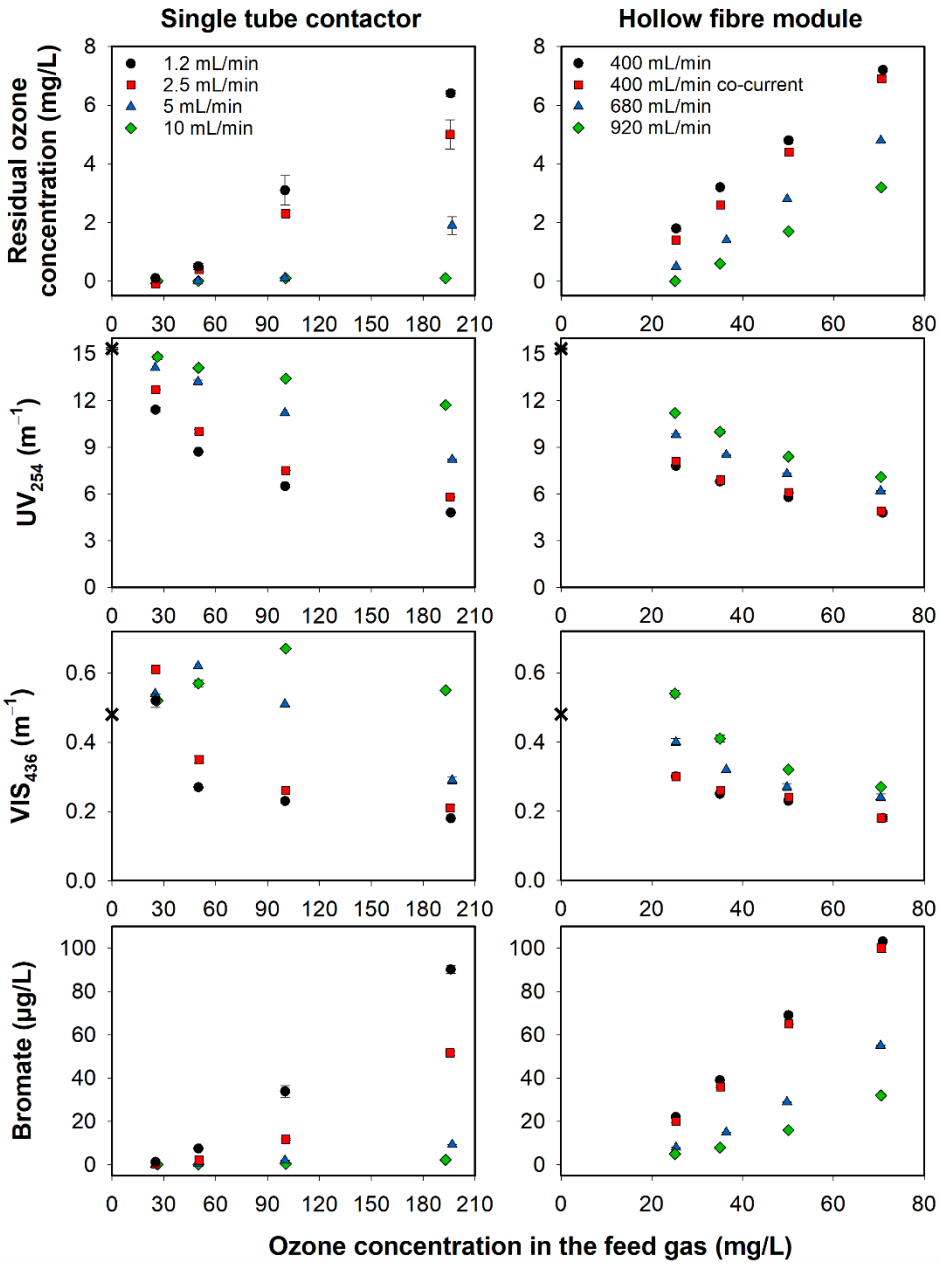

Figure 4.5.6. Change of residual ozone concentration, UV absorbance at 254 nm, VIS absorbance at 436 nm and bromate concentration in ozonated groundwater versus the ozone concentration in the feed gas for the single tube contactor and the hollow fibre module. Starting values of UV_{254} and VIS_{436} are marked as X.

As in experiments with pure water (Section 4.5.2), a linear relationship between the dissolved (residual) ozone concentration and the feed gas ozone concentration was observed with the hollow fibre module. Using groundwater instead of pure water did not significantly alter the slopes of the trendlines. However, in experiments with pure water the y-intercept of the trendlines was close to zero (see Figure 4.5.2). The negative y-intercept obtained from the groundwater data (–2 to –1 mg L^{-1}) roughly represents the amount of ozone immediately reacting with the water matrix during the

residence time in the reactor (26 to 60 s). The amount of ozone consumed within 20 s after ozone addition is termed instantaneous ozone demand (108).

Lower residual ozone concentrations were generally measured for the single tube contactor compared to the larger membrane module at the same or even at higher feed gas ozone concentrations. This can be partly attributed to the different membrane material and surface area, but also to shorter residence times in the single tube contactor (2 to 20 s). Due to the different water flow rates used in the two systems, there may have also been higher ozone degradation between the single tube contactor outlet and the sampling point.

In agreement with previous observations (85), UV_{254} decreased with increasing dissolved ozone concentrations and ozonation times, which were achieved with higher feed gas ozone concentrations and/or lower water flow rates. The maximum UV_{254} removal achieved by both membrane contactors was 69%, but it occurred under different conditions (higher feed gas ozone concentration and shorter residence time for the single tube contactor).

The visible colour (VIS_{436}) followed a similar trend as UV_{254} absorbance for the hollow fibre module, although in this case the decrease levelled off at high ozone concentrations. At the lowest feed gas ozone concentration of 25 mg L^{-1} and the highest water flow rate of 920 mL min^{-1}, VIS_{436} increased compared to the initial value of the feed water. This phenomenon was more obvious for the single tube contactor, where more data at low ozone concentrations were collected. At the highest flow rate of 10 mL min^{-1}, VIS_{436} increased by 42%. Colour is expected to decrease with increasing ozone dose, as colour-inducing moieties of NOM are further oxidised (55, 109). The unexpected behaviour of this groundwater may be due to the oxidation of iron/NOM complexes by small amounts of ozone (110, 111). Further investigation was beyond the scope of this study.

Figure 4.5.7A shows the relative UV_{254} absorbance versus the relative VIS_{436} absorbance of the ozonated water for all experiments. In general, NOM chromophores absorbing at longer wavelengths tend to be preferentially oxidised because they comprise highly conjugated electron-rich systems that are readily reactive with ozone (53, 54). In contrast, UV_{254} absorbance underwent a stronger relative decrease than VIS_{436} absorbance in almost all membrane ozonation experiments. The single

tube contactor achieved slightly higher VIS_{436} removals for similar UV_{254} removal compared to the hollow fibre module, which suggests that the two contactor types may favour the ozonation of different fractions of organic matter.

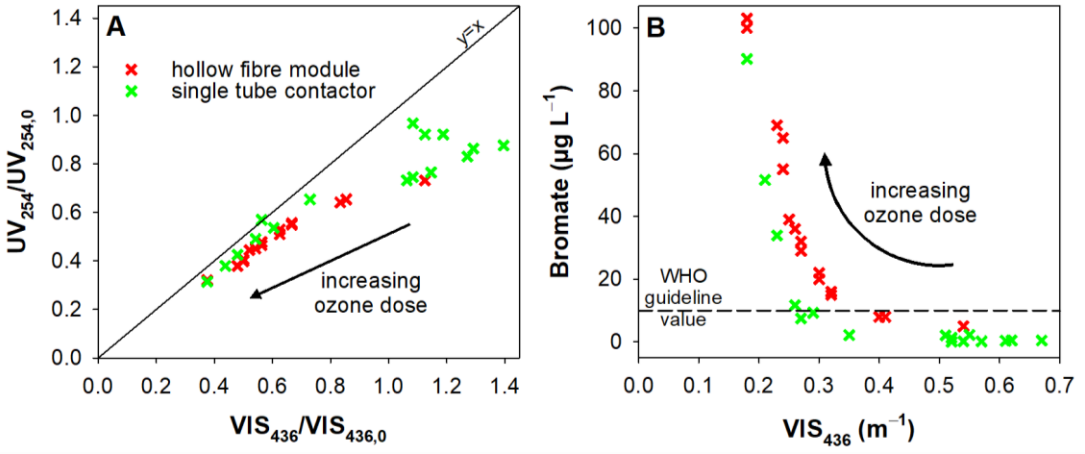

Figure 4.5.7. A. Relative UV absorbance at 254 nm versus relative VIS absorbance at 436 nm, and B. Bromate concentration formed versus VIS absorbance at 436 nm, for all experiments with the single tube contactor and the hollow fibre module.

The Hatta number (Ha) provides a comparison of the rate of ozone consumption and the rate of ozone mass transfer in the liquid film (see Section 4.4). The values calculated for the two membrane contactors (Appendix, Table 4.8.1) were in the intermediate regime (0.3<Ha<3), indicating that reactions occurred both in the liquid film and in the bulk. This means that ozone is not immediately consumed by reactions after it is transferred into the water (also confirmed by the presence of high ozone residuals in the outlet of each contactor), allowing thus the oxidation of compounds with slower reaction kinetics.

Bromate molar yields (i.e. the bromate molar concentration over the initial bromide molar concentration) ranged from 0.1% to 61% for the single tube contactor and from 3% to 78% for the hollow fibre module, consistent with previous studies (56). Due to lower dissolved ozone concentrations in the single tube contactor, the bromate concentrations formed were in many cases below the WHO limit for drinking water of 10 µg L^{-1}. However, the bromate concentration increased strongly at water flow rates of 1.2 and 2.5 mL min^{-1} and feed gas ozone concentrations of 100 and 200 mg L^{-1} (Figure 4.5.6). In the hollow fibre module, the bromate concentration exceeded the limit of 10 µg L^{-1} under most conditions. Comparison of these results

with the bromate formation in batch ozonation experiments is ongoing work conducted at the Hamburg University of Technology by the collaborators in this study.

Colour reduction and bromate formation during groundwater ozonation treatment can be considered trade-off parameters. Figure 4.5.7B shows the bromate concentration formed versus the VIS_{436} of the treated water. Two distinct areas can be identified in the data: a) increase or moderate decrease in colour with low bromate formation (around 10 μg L^{-1}), and b) little further decrease in colour with significantly enhanced bromate formation. As mentioned previously, the increase in colour might be specific for the groundwater used. Therefore, area (a) would be preferred over area (b) due to the regulation of bromate levels. It has been reported that there is a threshold in UV_{254} removal above which significant bromate formation occurs in ozonation of wastewater effluent and surface water (82, 85). In this study, considering the bromate limit of 10 μg L^{-1}, the threshold for UV_{254} removal was found to be approximately 50% for the single tube contactor and 45% for the hollow fibre module. The corresponding thresholds for colour removal were 46% for the single tube contactor and 33% for the hollow fibre module. The presence of these thresholds is attributed to the rapid consumption of ozone by fast-reacting organic moieties at low ozone doses, limiting its availability for reaction with bromide (85). In agreement with this, low ozone doses lead to higher Hatta numbers (Appendix, Section 4.8.3). Therefore, operational conditions associated with higher Hatta numbers are considered optimal for selective membrane ozonation that favours the reaction of NOM over bromide.

The single tube contactor led to lower bromate concentrations than the hollow fibre module for the same decrease in colour, which is in line with the UV_{254} versus VIS_{436} data. These observations can be attributed to the uneven ozone distribution in the bundle of hollow fibres, which entails higher ozone concentrations in the fibres located closer to the central axis of the module (see Appendix, Figure 4.8.3 for visualisation). This variation is in addition to the non-uniform ozone concentration inside each fibre (higher concentration closer to the membrane wall), a phenomenon also present in the single tube contactor (14). The Reynolds numbers in the single PDMS membrane (Re = 18 to 145) were higher than in the hollow fibres (Re = 13 to 30), suggesting a reduced radial variation of ozone concentration in the single membrane due to enhanced mixing. A distribution of ozone exposures can also arise

in conventional ozonation reactors as a result of complex, suboptimal hydraulics, and compromise the trade-off between bromate formation and disinfection or oxidation efficiency (112, 113). These findings have important implications for the applicability of membrane ozonation and the design of membrane ozone contactors (see next Section 4.5.7).

4.5.7 Remarks on process feasibility

Bubble-less ozonation using membrane contactors has not yet been implemented at a large scale for water or wastewater treatment. It is therefore necessary to reflect on the applicability of this technology based on existing laboratory experience.

The selection of membrane material is crucial and will affect capital and operational costs due to replacement of membranes after use for certain time periods. In addition, gradual degradation of the membrane material may affect the quality of the treated water. This was observed in some experiments with PDMS membranes, where the TOC of the water increased after membrane ozonation (Appendix, Figure 4.8.4). This increase could be an indication of membrane degradation through oxidative attack of PDMS by OH radicals and ozone (28, 114). The stability of PDMS membranes is influenced by several factors, such as the feed gas ozone concentration, the water matrix and the presence of UV light (8, 114). A stability experiment with continuous operation over several days was not attempted in this study due to safety concerns using the existing ozonation setup. However, the potential leaching of different membrane materials during prolonged ozone exposure should be evaluated. There was no indication of membrane degradation in experiments with the PTFE hollow fibre module, in accordance with the known ozone stability of PTFE (23).

An important attribute of conventional ozonation reactors is the ozone concentration profile. This holds true also for membrane contactors used for bubble-less ozonation. Our results suggest that the presence of high localised ozone concentrations in some fibres and/or within a single fibre (see Appendix, Figure 4.8.3) may have significant implications for the oxidation of organic compounds and the formation of bromate. In the hollow fibre module that we used, the variation of ozone concentration across different fibres was caused by the delivery of ozone gas through a central tube combined with the close proximity of the fibres. The design of multi-tube modules

should therefore ensure good mixing of the gas in the shell side. This can be achieved with improved transverse-flow modules, for example containing multiple baffles, helically wound fibres, or an optimised fibre bundle layout (9, 26, 57).

Moreover, a key property of membranes for bubble-less ozonation is their inner diameter. In addition to determining the specific surface area, the diameter affects the radial ozone distribution within the membrane. At a set water flow rate, a lower diameter leads to a higher Reynolds number and thus, to a more homogeneous ozone concentration profile. The downsides of small diameters are the possibility of clogging, especially if the feed water contains particles, and the higher pressure drop across the membrane contactor. At a set fibre diameter, mixing of the liquid phase inside the fibres can be enhanced by using higher water flow rates. However, this is accompanied by reduced water residence times in the contactor and, thus, lower transferred concentrations of ozone. Another approach to improve mixing inside the fibres while maintaining low flow rates is to use helical rather than linear fibres, where secondary flows (Dean vortices) can arise (39).

The main operational parameters that require optimisation in membrane ozonation are the water flow rate, the feed gas ozone concentration and the pressure of the gas and liquid phases (especially in the case of porous membranes). These parameters affect the transferred ozone dose, which in turn determines the attainment of the desired treatment goals, as well as the trade-off with the formation of by-products. For example, conditions leading to high Hatta numbers (e.g. low feed gas ozone concentrations) are needed to enhance the selectivity of membrane ozonation towards NOM degradation rather than reaction with bromide leading to bromate formation.

A further issue that needs to be considered is the transfer efficiency of ozone, namely the percentage of feed gas ozone that is transferred into the water. In conventional ozonation systems, the transfer efficiency depends on the design characteristics of the ozone contactor, the operational conditions (e.g. gas flow rate and ozone dose), and the properties of the water being treated (115). Design values for the transfer efficiency of bubble diffusers and side-stream injection systems are typically 95% (116). In the lab-scale membrane ozonation experiments, the transfer efficiency of ozone was very low, around 10% for the hollow fibre module and even lower for the single tube contactor. This was mainly due to the high ratio of gas flow rate over

water flow rate, which was dictated by the much larger shell volume compared to the lumen volume and by considerations about the water and gas residence times in the contactor.

In lab experiments, a low transfer efficiency of ozone is often desirable, as it ensures an almost constant ozone concentration in the shell. In this way, the dissolved ozone concentration is not limited by gradual ozone depletion across the length of the contactor. However, a high concentration of ozone in the off-gas means that a large amount of the generated ozone is wasted. If the ozone transfer efficiency is not significantly increased compared to lab-scale values, large-scale membrane ozonation would only be economically viable with implementation of off-gas recycling. An alternative strategy suggested by recent research is to apply dead-end filtration, namely to operate the membrane contactor without a gas outflow (117).

Finally, a techno-economic assessment of membrane ozonation is required. It is stipulated that while the introduction of membrane contactors would increase the capital cost of ozonation processes, this could be offset by a decrease of the operational cost (118). More information is required to assess whether membrane ozonation can compete commercially with the already established ozonation methods.

4.6 Conclusions

Although research on bubble-less ozonation using membrane contactors has been conducted for more than 20 years, there are still substantial knowledge gaps in this field. Proof of concept has been achieved for a few membrane materials and configurations but there is a lack of information on elimination of trace organic contaminants, by-product formation and large-scale applications.

This study aimed to address those knowledge gaps by developing two experimental setups that can be used for a wide range of membrane ozonation investigations. A simple, model system consisting of a single membrane allowed us to gain a better understanding of the membrane ozonation process, focusing on the effect of operational parameters on ozone transfer and on the oxidation of a model pollutant and of dissolved organic matter in different aqueous matrices. In addition, we compared the experimental findings with results of a previously developed CFD

model and found that this system can be well described by theoretical predictions. Further work utilised a larger and more complex hollow fibre module consisting of multiple membranes which allowed us to assess the challenges posed by real applications at industrial scale, such as the uneven distribution of ozone inside the membrane contactor. We also used this module to conduct one of the first membrane ozonation studies on the abatement of trace organic contaminants at their inherent concentrations in wastewater effluent and identified next steps that need to be undertaken in this research area. Finally, we compared the performance of both systems in the treatment of bromide-containing groundwater, focusing on bromate formation and the associated implications for the design and operation of membrane ozonation.

Overall, the aims and objectives pursued by this study were attained. However, future work is needed to further develop this technology and assess whether it is competitive with established ozonation processes based on bubble diffusers or gas injectors. Firstly, the membrane contactor design is crucial for process efficiency and water quality and should be optimised through a combination of experimental and computational investigations. For example, a CFD model should be developed, validated through comparison with experimental results, and used to study parameters that are difficult or costly to vary in the lab (e.g. diameter, length and position of fibres). Furthermore, a comprehensive comparison between membrane ozonation and conventional ozonation in terms of trace organic contaminant abatement, by-product formation, energy consumption and cost needs to be performed, initially at lab scale and subsequently at pilot or large scale. Based on the results, specific applications should be identified where the adoption of membrane ozonation may be of particular benefit.

4.7 References

1. Rakness KL. Ozone Side-Stream Design Options and Operating Considerations. Ozone: Science & Engineering. 2007;29(4):231-44.
2. Schulz CR, Bellamy WD. The Role of Mixing in Ozone Dissolution Systems. Ozone: Science & Engineering. 2000;22(4):329-50.
3. Janknecht P, Wilderer PA, Picard C, Larbot A, Sarrazin J. Bubble-free Ozone Contacting with Ceramic Membranes for Wet Oxidative Treatment. Chemical Engineering & Technology. 2000;23(8):674-7.
4. Zhou H, Smith DW. Ozone mass transfer in water and wastewater treatment: experimental observations using a 2D laser particle dynamics analyzer. Water Research. 2000;34(3):909-21.
5. Zhou H, Smith DW. Ozonation Dynamics and Its Implication for Off-Gas Ozone Control in Treating Pulp Mill Wastewaters. Ozone: Science & Engineering. 2000;22(1):31-51.
6. Oneby MA, Bromley CO, Borchardt JH, Harrison DS. Ozone Treatment of Secondary Effluent at U.S. Municipal Wastewater Treatment Plants. Ozone: Science & Engineering. 2010;32(1):43-55.
7. Crittenden JC, Trussell RR, Hand DW, Howe KJ, Tchobanoglous G. Membrane Filtration. In: Crittenden JC, Trussell RR, Hand DW, Howe KJ, Tchobanoglous G, editors. MWH's Water Treatment: Principles and Design, Third Edition: Wiley; 2012. p. 819-902.
8. Shanbhag PV, Guha AK, Sirkar KK. Membrane-Based Ozonation of Organic Compounds. Industrial & Engineering Chemistry Research. 1998;37(11):4388-98.
9. Gabelman A, Hwang S-T. Hollow fiber membrane contactors. Journal of Membrane Science. 1999;159(1):61-106.
10. Janknecht P, Wilderer PA, Picard C, Larbot A. Ozone–water contacting by ceramic membranes. Sep Purif Technol. 2001;25(1):341-6.
11. Ismail AF, Khulbe KC, Matsuura T. Fundamentals of Gas Permeation Through Membranes. In: Ismail AF, Khulbe KC, Matsuura T, editors. Gas Separation Membranes: Polymeric and Inorganic. Cham: Springer International Publishing; 2015. p. 11-35.
12. Mulder M. Transport in Membranes. In: Mulder M, editor. Basic Principles of Membrane Technology. Dordrecht: Springer Netherlands; 1991. p. 145-97.

13. Ismail AF, Khulbe KC, Matsuura T. Gas Separation Membrane Materials and Structures. In: Ismail AF, Khulbe KC, Matsuura T, editors. Gas Separation Membranes: Polymeric and Inorganic. Cham: Springer International Publishing; 2015. p. 37-192.

14. Berry M, Taylor C, King W, Chew Y, Wenk J. Modelling of Ozone Mass-Transfer through Non-Porous Membranes for Water Treatment. Water. 2017;9(7):452.

15. Merle T, Pronk W, von Gunten U. MEMBRO$_3$X, a Novel Combination of a Membrane Contactor with Advanced Oxidation (O_3/H_2O_2) for Simultaneous Micropollutant Abatement and Bromate Minimization. Environmental Science & Technology Letters. 2017;4(5):180-5.

16. Sirkar KK. Other New Membrane Processes. In: Ho WSW, Sirkar KK, editors. Membrane Handbook. Boston, MA: Springer US; 1992. p. 885-912.

17. Mosadegh-Sedghi S, Rodrigue D, Brisson J, Iliuta MC. Wetting phenomenon in membrane contactors – Causes and prevention. Journal of Membrane Science. 2014;452:332-53.

18. Kim B-S, Harriott P. Critical entry pressure for liquids in hydrophobic membranes. Journal of Colloid and Interface Science. 1987;115(1):1-8.

19. Kukuzaki M, Fujimoto K, Kai S, Ohe K, Oshima T, Baba Y. Ozone mass transfer in an ozone–water contacting process with Shirasu porous glass (SPG) membranes—A comparative study of hydrophilic and hydrophobic membranes. Sep Purif Technol. 2010;72(3):347-56.

20. Stylianou SK, Sklari SD, Zamboulis D, Zaspalis VT, Zouboulis AI. Development of bubble-less ozonation and membrane filtration process for the treatment of contaminated water. Journal of Membrane Science. 2015;492:40-7.

21. Kreulen H, Smolders CA, Versteeg GF, Van Swaaij WPM. Determination of mass transfer rates in wetted and non-wetted microporous membranes. Chemical Engineering Science. 1993;48(11):2093-102.

22. Bitter JGA. Transport Mechanisms in Membrane Separation Processes. Boston, MA: Boston, MA : Springer US : Imprint: Springer; 1991.

23. Bamperng S, Suwannachart T, Atchariyawut S, Jiraratananon R. Ozonation of dye wastewater by membrane contactor using PVDF and PTFE membranes. Sep Purif Technol. 2010;72(2):186-93.

24. Ismail AF, Khulbe KC, Matsuura T. Membrane Modules and Process Design. In: Ismail AF, Khulbe KC, Matsuura T, editors. Gas Separation Membranes: Polymeric and Inorganic. Cham: Springer International Publishing; 2015. p. 221-40.
25. Pines DS, Min K-N, Ergas SJ, Reckhow DA. Investigation of an Ozone Membrane Contactor System. Ozone: Science & Engineering. 2005;27(3):209-17.
26. Ma C, Liu Y, Li F, Shen C, Huang M, Wang Z, Cao C, Zhou Q, Sheng Y, Sand W. CFD simulations of fiber-fiber interaction in a hollow fiber membrane bundle: Fiber distance and position matters. Sep Purif Technol. 2019;209:707-13.
27. Lim KB, Wang PC, An H, Yu SCM. Computational Studies for the Design Parameters of Hollow Fibre Membrane Modules. Journal of Membrane Science. 2017;529:263-73.
28. Santos FRAd, Borges CP, Fonseca FVd. Polymeric Materials for Membrane Contactor Devices Applied to Water Treatment by Ozonation. Materials Research. 2015;18(5):1015-22.
29. He Z, Lyu Z, Gu Q, Zhang L, Wang J. Ceramic-based membranes for water and wastewater treatment. Colloids and Surfaces A: Physicochemical and Engineering Aspects. 2019;578:123513.
30. Stylianou SK, Kostoglou M, Zouboulis AI. Ozone Mass Transfer Studies in a Hydrophobized Ceramic Membrane Contactor: Experiments and Analysis. Industrial & Engineering Chemistry Research. 2016;55(28):7587-97.
31. Janknecht P, Picard C, Larbot A, Wilderer PA. Membrane Ozonation in Wastewater Treatment. Acta Hydroch Hydrob. 2004;32(1):33-9.
32. Stylianou SK, Katsoyiannis IA, Ernst M, Zouboulis AI. Impact of O_3 or O_3/H_2O_2 treatment via a membrane contacting system on the composition and characteristics of the natural organic matter of surface waters. Environ Sci Pollut Res Int. 2018;25(13):12246-55.
33. Stylianou SK, Katsoyiannis IA, Mitrakas M, Zouboulis AI. Application of a ceramic membrane contacting process for ozone and peroxone treatment of micropollutant contaminated surface water. J Hazard Mater. 2018;358:129-35.
34. Shanbhag PV, Guha AK, Sirkar KK. Single-phase membrane ozonation of hazardous organic compounds in aqueous streams. Journal of Hazardous Materials. 1995;41(1):95-104.

35. Atchariyawut S, Phattaranawik J, Leiknes T, Jiraratananon R. Application of ozonation membrane contacting system for dye wastewater treatment. Sep Purif Technol. 2009;66(1):153-8.
36. Guerra K, Pellegrino J. Development of a Techno-Economic Model to Compare Ceramic and Polymeric Membranes. Sep Sci Technol. 2013;48(1):51-65.
37. Bein E, Zucker I, Drewes JE, Hübner U. Ozone membrane contactors for water and wastewater treatment: A critical review on materials selection, mass transfer and process design. Chemical Engineering Journal. 2020:127393.
38. Schmitt A, Mendret J, Roustan M, Brosillon S. Ozonation using hollow fiber contactor technology and its perspectives for micropollutants removal in water: A review. Sci Total Environ. 2020;729:138664.
39. Sabelfeld M, Geißen S-U. Effect of helical structure on ozone mass transfer in a hollow fiber membrane contactor. Journal of Membrane Science. 2019;574:222-34.
40. Leenheer JA, Croué J-P. Peer Reviewed: Characterizing Aquatic Dissolved Organic Matter. Environmental Science & Technology. 2003;37(1):18A-26A.
41. Nebbioso A, Piccolo A. Molecular characterization of dissolved organic matter (DOM): a critical review. Analytical and Bioanalytical Chemistry. 2013;405(1):109-24.
42. Matilainen A, Gjessing ET, Lahtinen T, Hed L, Bhatnagar A, Sillanpää M. An overview of the methods used in the characterisation of natural organic matter (NOM) in relation to drinking water treatment. Chemosphere. 2011;83(11):1431-42.
43. Katsoyiannis IA, Canonica S, von Gunten U. Efficiency and energy requirements for the transformation of organic micropollutants by ozone, O_3/H_2O_2 and UV/H_2O_2. Water Research. 2011;45(13):3811-22.
44. Papageorgiou A, Stylianou SK, Kaffes P, Zouboulis AI, Voutsa D. Effects of ozonation pretreatment on natural organic matter and wastewater derived organic matter - Possible implications on the formation of ozonation by-products. Chemosphere. 2017;170:33-40.
45. Świetlik J, Sikorska E. Application of fluorescence spectroscopy in the studies of natural organic matter fractions reactivity with chlorine dioxide and ozone. Water Research. 2004;38(17):3791-9.
46. Leresche F, McKay G, Kurtz T, von Gunten U, Canonica S, Rosario-Ortiz FL. Effects of Ozone on the Photochemical and Photophysical Properties of Dissolved Organic Matter. Environ Sci Technol. 2019;53(10):5622-32.

47. Önnby L, Salhi E, McKay G, Rosario-Ortiz FL, von Gunten U. Ozone and chlorine reactions with dissolved organic matter - Assessment of oxidant-reactive moieties by optical measurements and the electron donating capacities. Water Research. 2018;144:64-75.

48. Westerhoff P, Aiken G, Amy G, Debroux J. Relationships between the structure of natural organic matter and its reactivity towards molecular ozone and hydroxyl radicals. Water Research. 1999;33(10):2265-76.

49. Weishaar JL, Aiken GR, Bergamaschi BA, Fram MS, Fujii R, Mopper K. Evaluation of Specific Ultraviolet Absorbance as an Indicator of the Chemical Composition and Reactivity of Dissolved Organic Carbon. Environmental Science & Technology. 2003;37(20):4702-8.

50. Liu T, Chen Z-l, Yu W-z, You S-j. Characterization of organic membrane foulants in a submerged membrane bioreactor with pre-ozonation using three-dimensional excitation–emission matrix fluorescence spectroscopy. Water Research. 2011;45(5):2111-21.

51. Crittenden JC, Trussell RR, Hand DW, Howe KJ, Tchobanoglous G. Physical and Chemical Quality of Water. In: Crittenden JC, Trussell RR, Hand DW, Howe KJ, Tchobanoglous G, editors. MWH's Water Treatment: Principles and Design, Third Edition: Wiley; 2012. p. 17-71.

52. Frimmel FH, Abbt-Braun G. Basic characterization of reference NOM from Central Europe — Similarities and differences. Environment International. 1999;25(2):191-207.

53. Wenk J, Aeschbacher M, Salhi E, Canonica S, von Gunten U, Sander M. Chemical Oxidation of Dissolved Organic Matter by Chlorine Dioxide, Chlorine, And Ozone: Effects on Its Optical and Antioxidant Properties. Environmental Science & Technology. 2013;47(19):11147-56.

54. Nöthe T, Fahlenkamp H, Sonntag Cv. Ozonation of Wastewater: Rate of Ozone Consumption and Hydroxyl Radical Yield. Environmental Science & Technology. 2009;43(15):5990-5.

55. Leiknes T, Phattaranawik J, Boller M, von Gunten U, Pronk W. Ozone transfer and design concepts for NOM decolourization in tubular membrane contactor. Chemical Engineering Journal. 2005;111(1):53-61.

56. Yang J, Dong Z, Jiang C, Wang C, Liu H. An overview of bromate formation in chemical oxidation processes: Occurrence, mechanism, influencing factors, risk assessment, and control strategies. Chemosphere. 2019;237:124521.
57. Sengupta A, Peterson PA, Miller BD, Schneider J, Fulk CW. Large-scale application of membrane contactors for gas transfer from or to ultrapure water. Sep Purif Technol. 1998;14(1):189-200.
58. Bader H, Hoigné J. Determination of ozone in water by the indigo method. Water Research. 1981;15(4):449-56.
59. Park M, Snyder SA. Sample handling and data processing for fluorescent excitation-emission matrix (EEM) of dissolved organic matter (DOM). Chemosphere. 2018;193:530-7.
60. Zepp RG, Sheldon WM, Moran MA. Dissolved organic fluorophores in southeastern US coastal waters: correction method for eliminating Rayleigh and Raman scattering peaks in excitation–emission matrices. Mar Chem. 2004;89(1):15-36.
61. Petrie B, Youdan J, Barden R, Kasprzyk-Hordern B. Multi-residue analysis of 90 emerging contaminants in liquid and solid environmental matrices by ultra-high-performance liquid chromatography tandem mass spectrometry. J Chromatogr A. 2016;1431:64-78.
62. Lopardo L, Rydevik A, Kasprzyk-Hordern B. A new analytical framework for multi-residue analysis of chemically diverse endocrine disruptors in complex environmental matrices utilising ultra-performance liquid chromatography coupled with high-resolution tandem quadrupole time-of-flight mass spectrometry. Anal Bioanal Chem. 2019;411(3):689-704.
63. International Organization for Standardization. ISO 9963-1:1994 Water quality — Determination of alkalinity — Part 1: Determination of total and composite alkalinity. 1994.
64. International Organization for Standardization. ISO 11206:2011 Water quality — Determination of dissolved bromate — Method using ion chromatography (IC) and post column reaction (PCR). 2011.
65. Al-saffar HB, Ozturk B, Hughes R. A Comparison of Porous and Non-Porous Gas-Liquid Membrane Contactors for Gas Separation. Chem Eng Res Des. 1997;75(7):685-92.

66. Shen S, Kentish SE, Stevens GW. Shell-Side Mass-Transfer Performance in Hollow-Fiber Membrane Contactors. Solvent Extr Ion Exch. 2010;28(6):817-44.
67. Dingemans M, Dewulf J, Van Hecke W, Van Langenhove H. Determination of ozone solubility in polymeric materials. Chemical Engineering Journal. 2008;138(1-3):172-8.
68. Gottschalk C, Libra JA, Saupe A. Ozonation of water and waste water: A practical guide to understanding ozone and its applications: John Wiley & Sons; 2009.
69. Shanbhag PV, Sirkar KK. Ozone and oxygen permeation behavior of silicone capillary membranes employed in membrane ozonators. J Appl Polym Sci. 1998;69(7):1263-73.
70. Johnson PN, Davis RA. Diffusivity of Ozone in Water. Journal of Chemical & Engineering Data. 1996;41(6):1485-7.
71. Massman WJ. A review of the molecular diffusivities of H_2O, CO_2, CH_4, CO, O_3, SO_2, NH_3, N_2O, NO, and NO_2 in air, O_2 and N_2 near STP. Atmos Environ. 1998;32(6):1111-27.
72. Phattaranawik J, Leiknes T, Pronk W. Mass transfer studies in flat-sheet membrane contactor with ozonation. Journal of Membrane Science. 2005;247(1-2):153-67.
73. Jansen RHS, de Rijk JW, Zwijnenburg A, Mulder MHV, Wessling M. Hollow fiber membrane contactors—A means to study the reaction kinetics of humic substance ozonation. Journal of Membrane Science. 2005;257(1-2):48-59.
74. Gardoni D, Vailati A, Canziani R. Decay of Ozone in Water: A Review. Ozone: Science & Engineering. 2012;34(4):233-42.
75. Beltrán FJ. Theoretical Aspects Of The Kinetics Of Competitive Ozone Reactions In Water. Ozone: Science & Engineering. 1995;17(2):163-81.
76. Benbelkacem H, Mathé S, Debellefontaine H. Taking mass transfer limitation into account during ozonation of pollutants reacting fairly quickly. Water Science and Technology. 2004;49(4):25-30.
77. Zhang Y, Li K, Wang J, Hou D, Liu H. Ozone mass transfer behaviors on physical and chemical absorption for hollow fiber membrane contactors. Water Sci Technol. 2017;76(5-6):1360-9.
78. Liu M, Sun J, Sun Y, Bock C, Chen Q. Thickness-dependent mechanical properties of polydimethylsiloxane membranes. Journal of Micromechanics and Microengineering. 2009;19(3):035028.

79. Elovitz MS, von Gunten U. Hydroxyl Radical/Ozone Ratios During Ozonation Processes. I. The R_{ct} Concept. Ozone: Science & Engineering. 1999;21(3):239-60.

80. Elovitz MS, von Gunten U, Kaiser H-P. Hydroxyl Radical/Ozone Ratios During Ozonation Processes. II. The Effect of Temperature, pH, Alkalinity, and DOM Properties. Ozone: Science & Engineering. 2000;22(2):123-50.

81. Hübner U, Zucker I, Jekel M. Options and limitations of hydrogen peroxide addition to enhance radical formation during ozonation of secondary effluents. Journal of Water Reuse and Desalination. 2014;5(1):8-16.

82. Chon K, Salhi E, von Gunten U. Combination of UV absorbance and electron donating capacity to assess degradation of micropollutants and formation of bromate during ozonation of wastewater effluents. Water Research. 2015;81:388-97.

83. Nanaboina V, Korshin GV. Evolution of Absorbance Spectra of Ozonated Wastewater and Its Relationship with the Degradation of Trace-Level Organic Species. Environmental Science & Technology. 2010;44(16):6130-7.

84. Park M, Anumol T, Daniels KD, Wu S, Ziska AD, Snyder SA. Predicting trace organic compound attenuation by ozone oxidation: Development of indicator and surrogate models. Water Res. 2017;119:21-32.

85. Li W-T, Cao M-J, Young T, Ruffino B, Dodd M, Li A-M, Korshin G. Application of UV absorbance and fluorescence indicators to assess the formation of biodegradable dissolved organic carbon and bromate during ozonation. Water Research. 2017;111:154-62.

86. Sharpless CM, Blough NV. The importance of charge-transfer interactions in determining chromophoric dissolved organic matter (CDOM) optical and photochemical properties. Environmental Science: Processes & Impacts. 2014;16(4):654-71.

87. Stedmon CA, Markager S, Bro R. Tracing dissolved organic matter in aquatic environments using a new approach to fluorescence spectroscopy. Mar Chem. 2003;82(3):239-54.

88. Cory RM, McKnight DM. Fluorescence Spectroscopy Reveals Ubiquitous Presence of Oxidized and Reduced Quinones in Dissolved Organic Matter. Environmental Science & Technology. 2005;39(21):8142-9.

89. Del Vecchio R, Schendorf TM, Blough NV. Contribution of Quinones and Ketones/Aldehydes to the Optical Properties of Humic Substances (HS) and

Chromophoric Dissolved Organic Matter (CDOM). Environmental Science & Technology. 2017;51(23):13624-32.

90. Chen W, Westerhoff P, Leenheer JA, Booksh K. Fluorescence Excitation−Emission Matrix Regional Integration to Quantify Spectra for Dissolved Organic Matter. Environmental Science & Technology. 2003;37(24):5701-10.

91. Henderson RK, Baker A, Murphy KR, Hambly A, Stuetz RM, Khan SJ. Fluorescence as a potential monitoring tool for recycled water systems: a review. Water Res. 2009;43(4):863-81.

92. Spiliotopoulou A, Martin R, Pedersen L-F, Andersen HR. Use of fluorescence spectroscopy to control ozone dosage in recirculating aquaculture systems. Water Research. 2017;111:357-65.

93. Tang K, Ooi G, Spiliotopoulou A, Kaarsholm K, Sundmark K, Florian B, Kragelund C, Bester K, Andersen H. Removal of Pharmaceuticals, Toxicity and Natural Fluorescence by Ozonation in Biologically Pre-Treated Municipal Wastewater, in Comparison to Subsequent Polishing Biofilm Reactors. Water. 2020;12(4).

94. Park M, Anumol T, Simon J, Zraick F, Snyder SA. Pre-ozonation for high recovery of nanofiltration (NF) membrane system: Membrane fouling reduction and trace organic compound attenuation. Journal of Membrane Science. 2017;523:255-63.

95. Cataldo F. On the action of ozone on proteins. Polym Degrad Stab. 2003;82(1):105-14.

96. Proctor K, Petrie B, Barden R, Arnot T, Kasprzyk-Hordern B. Multi-residue ultra-performance liquid chromatography coupled with tandem mass spectrometry method for comprehensive multi-class anthropogenic compounds of emerging concern analysis in a catchment-based exposure-driven study. Analytical and Bioanalytical Chemistry. 2019;411(27):7061-86.

97. Hollender J, Zimmermann SG, Koepke S, Krauss M, McArdell CS, Ort C, Singer H, von Gunten U, Siegrist H. Elimination of organic micropollutants in a municipal wastewater treatment plant upgraded with a full-scale post-ozonation followed by sand filtration. Environmental Science and Technology. 2009;43(20):7862-9.

98. Knopp G, Prasse C, Ternes TA, Cornel P. Elimination of micropollutants and transformation products from a wastewater treatment plant effluent through pilot scale

ozonation followed by various activated carbon and biological filters. Water Research. 2016;100:580-92.

99. El-taliawy H, Ekblad M, Nilsson F, Hagman M, Paxeus N, Jönsson K, Cimbritz M, la Cour Jansen J, Bester K. Ozonation efficiency in removing organic micro pollutants from wastewater with respect to hydraulic loading rates and different wastewaters. Chemical Engineering Journal. 2017;325:310-21.

100. Bourgin M, Beck B, Boehler M, Borowska E, Fleiner J, Salhi E, Teichler R, von Gunten U, Siegrist H, McArdell CS. Evaluation of a full-scale wastewater treatment plant upgraded with ozonation and biological post-treatments: Abatement of micropollutants, formation of transformation products and oxidation by-products. Water Research. 2018;129:486-98.

101. Gerrity D, Gamage S, Jones D, Korshin GV, Lee Y, Pisarenko A, Trenholm RA, von Gunten U, Wert EC, Snyder SA. Development of surrogate correlation models to predict trace organic contaminant oxidation and microbial inactivation during ozonation. Water Research. 2012;46(19):6257-72.

102. Wert EC, Rosario-Ortiz FL, Snyder SA. Effect of ozone exposure on the oxidation of trace organic contaminants in wastewater. Water Research. 2009;43(4):1005-14.

103. Schymanski EL, Singer HP, Longrée P, Loos M, Ruff M, Stravs MA, Ripollés Vidal C, Hollender J. Strategies to Characterize Polar Organic Contamination in Wastewater: Exploring the Capability of High Resolution Mass Spectrometry. Environmental Science & Technology. 2014;48(3):1811-8.

104. Deeb AA, Stephan S, Schmitz OJ, Schmidt TC. Suspect screening of micropollutants and their transformation products in advanced wastewater treatment. Sci Total Environ. 2017;601-602:1247-53.

105. Schollée JE, Bourgin M, von Gunten U, McArdell CS, Hollender J. Non-target screening to trace ozonation transformation products in a wastewater treatment train including different post-treatments. Water Research. 2018;142:267-78.

106. Itzel F, Baetz N, Hohrenk LL, Gehrmann L, Antakyali D, Schmidt TC, Tuerk J. Evaluation of a biological post-treatment after full-scale ozonation at a municipal wastewater treatment plant. Water Research. 2020;170:115316.

107. Krauss M, Singer H, Hollender J. LC–high resolution MS in environmental analysis: from target screening to the identification of unknowns. Analytical and Bioanalytical Chemistry. 2010;397(3):943-51.

108. Buffle M-O, Schumacher J, Salhi E, Jekel M, von Gunten U. Measurement of the initial phase of ozone decomposition in water and wastewater by means of a continuous quench-flow system: Application to disinfection and pharmaceutical oxidation. Water Research. 2006;40(9):1884-94.

109. Rittmann BE, Stilwell D, Garside JC, Amy GL, Spangenberg C, Kalinsky A, Akiyoshi E. Treatment of a colored groundwater by ozone-biofiltration: pilot studies and modeling interpretation. Water Research. 2002;36(13):3387-97.

110. Reckhow DA, Knocke WR, Kearney MJ, Parks CA. Oxidation Of Iron And Manganese By Ozone. Ozone: Science & Engineering. 1991;13(6):675-95.

111. Barazesh JM, Prasse C, Wenk J, Berg S, Remucal CK, Sedlak DL. Trace Element Removal in Distributed Drinking Water Treatment Systems by Cathodic H_2O_2 Production and UV Photolysis. Environmental Science & Technology. 2018;52(1):195-204.

112. Wols BA, Hofman JAMH, Uijttewaal WSJ, Rietveld LC, van Dijk JC. Evaluation of different disinfection calculation methods using CFD. Environmental Modelling & Software. 2010;25(4):573-82.

113. Yang J, Li J, Zhu J, Dong Z, Luo F, Wang Y, Liu H, Jiang C, Yuan H. A novel design for an ozone contact reactor and its performance on hydrodynamics, disinfection, bromate formation and oxidation. Chemical Engineering Journal. 2017;328:207-14.

114. Ouyang M, Yuan C, Muisener RJ, Boulares A, Koberstein JT. Conversion of Some Siloxane Polymers to Silicon Oxide by UV/Ozone Photochemical Processes. Chem Mater. 2000;12(6):1591-6.

115. Rakness KL, Renner RC, Hegg BA, Hill AG. Practical Design Model for Calculating Bubble Diffuser Contactor Ozone Transfer Efficiency. Ozone: Science & Engineering. 1988;10(2):173-214.

116. Rakness KL, Hunter G, Lew J, Mundy B, Wert EC. Design Considerations for Cost-Effective Ozone Mass Transfer in Sidestream Systems. Ozone: Science & Engineering. 2018;40(3):159-72.

117. Kaprara E, Kostoglou M, Koutsiantzi C, Psaltou S, Zouboulis AI, Mitrakas M. Enhancement of ozonation efficiency employing dead-end hollow fiber membranes. Environmental Science: Water Research & Technology. 2020;6(9):2619-27.

118. Psaltou S, Zouboulis A. Catalytic Ozonation and Membrane Contactors—A Review Concerning Fouling Occurrence and Pollutant Removal. Water. 2020;12(11):2964.

4.8 Appendix

4.8.1 Comparison with CFD simulations for the PDMS single tube contactor

Computational fluid dynamics (CFD) simulations for the single tube contactor were conducted with COMSOL Multiphysics V5.3 by Prof John Chew and his group, using a similar methodology to the one described in (1). The main difference from that methodology was that the liquid phase was inside the tube and the gas phase was in the shell side of the reactor, as in the experimental setup. The geometry and operational parameters applied were the same as those used in the experiments. Figure 4.8.1 demonstrates the CFD results for the dissolved ozone concentration in pure water along with the corresponding experimental results.

CFD generally over-predicted the ozone concentration, but this translated into an average absolute deviation of less than 0.5 mg L^{-1}, which is comparable to the experimental error. Possible reasons for this difference include inaccuracies in model parameters taken from the literature (e.g. ozone diffusivities and solubilities) and non-ideal flow conditions in the experiments.

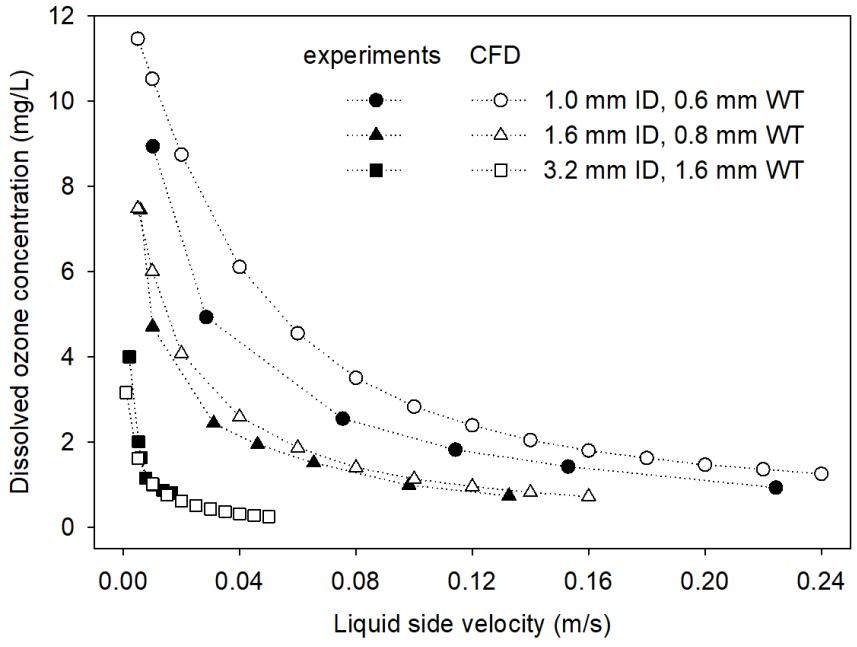

Figure 4.8.1. Experimentally measured and modelled dissolved ozone concentration at the outlet of the PDMS single tube contactor vs. the liquid side velocity, with three different membrane sizes (ID: inner diameter, WT: wall thickness) at feed gas ozone concentration of 110 mg L^{-1}.

4.8.2 Development of CFD simulations for the PTFE hollow fibre module

CFD simulations for the hollow fibre module were conducted using ANSYS Fluent V19.1 with a similar approach to that previously applied for the single tube contactor (1). ANSYS solves the fundamental conservation equations of momentum and mass. The module was assumed to be isothermal, so the energy conservation equation was ignored. A steady-state condition was assumed.

The dimensions of the modelled domains were based on the dimensions of the membrane module. The module is axisymmetric, so a 30° wedge was modelled to reduce computational cost (Figure 4.8.2). 40.5 fibres were placed in 9 rows (concentric arcs) in this wedge, corresponding to a total of 486 fibres in the entire module (versus 490 fibres in the experimental membrane module).

Triangular mesh was applied to the top surface and was 'swept' down the axial length of each domain. Scaling was applied in the z-direction since the module length was much greater than the fibre diameter and thickness. A scaling factor of 10 was selected for the module length, ozone diffusivity in the z-direction, and the gas and liquid inlet velocities. The residual for successive iterations for all variables (convergence criteria) was set to 10^{-4}.

The membrane was modelled as a solid (non-porous) domain, so no bulk flow was calculated within the membrane domain. It was assumed that the fluids are ideal, flow is laminar, and the density and viscosity are constant within the liquid and gas phases. The effect of gravity was ignored. The concentration of ozone was included in the model as a 'user-defined scalar'. Custom boundary conditions and concentration sources or sinks due to reactions were implemented with user-defined functions written in C. The water-gas interface was located at the membrane-water boundary (i.e. the membrane pores were assumed to be flooded with gas). At this interface, the ozone concentration in the water was related to the ozone concentration in the gas by the dimensionless Henry's coefficient, H. Any concentration change at the gas-membrane boundary due to the solubility of ozone in the membrane material was considered to be minor and was therefore ignored.

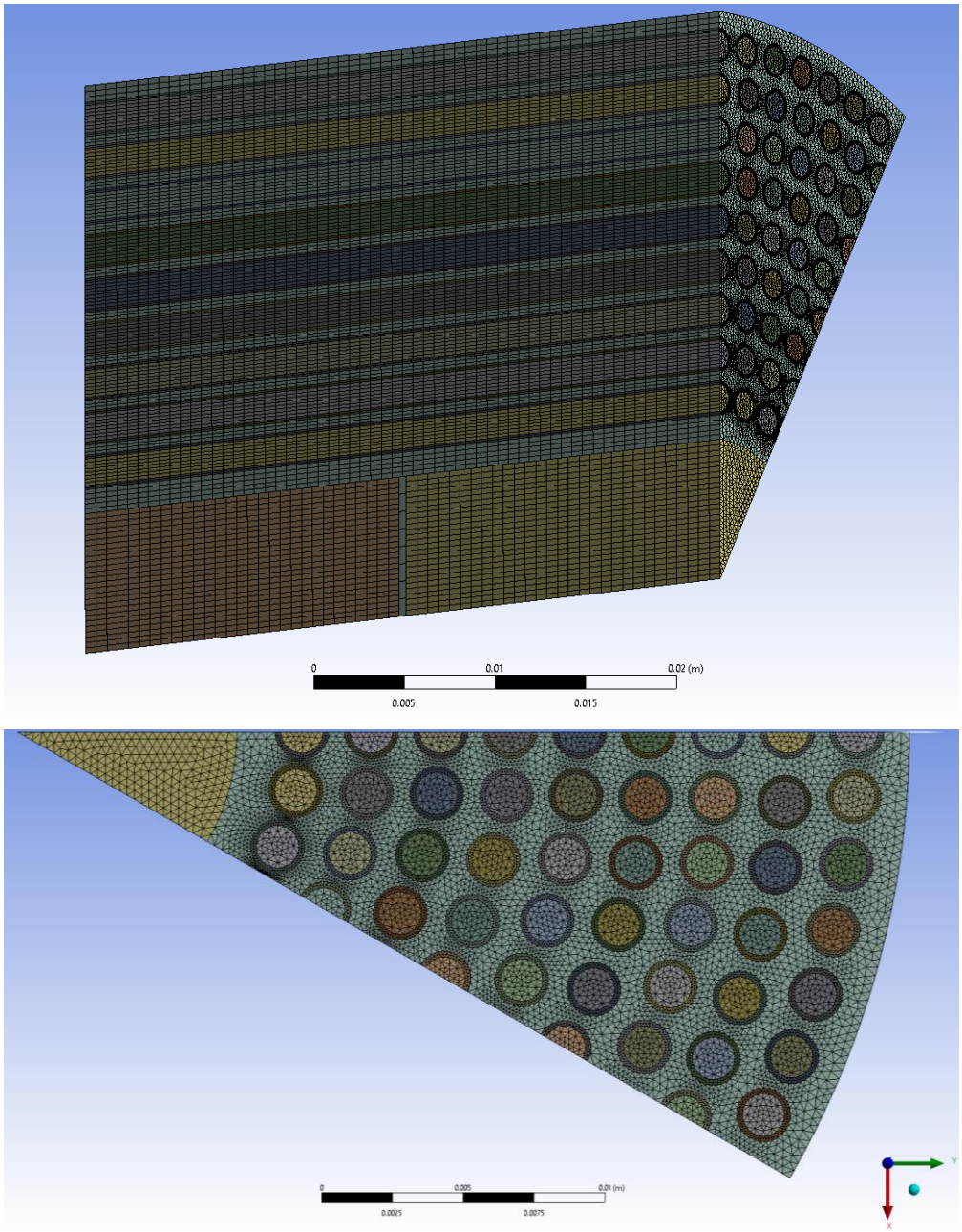

Figure 4.8.2. Modelled geometry of the hollow fibre module with the mesh shown.

Figure 4.8.3 shows the distribution of ozone inside the lumen at three locations along the module. Since the model has not been validated, these results should be treated as qualitative. It can be seen that, at least under certain conditions, there is significant spatial variation of the dissolved ozone concentration within the module. This variation exists both inside each fibre where the ozone concentration is higher near the membrane wall and decreases towards the fibre centre, and across the different fibres where the ozone concentration is higher in those located close to the central distribution tube and decreases towards the outer wall of the shell.

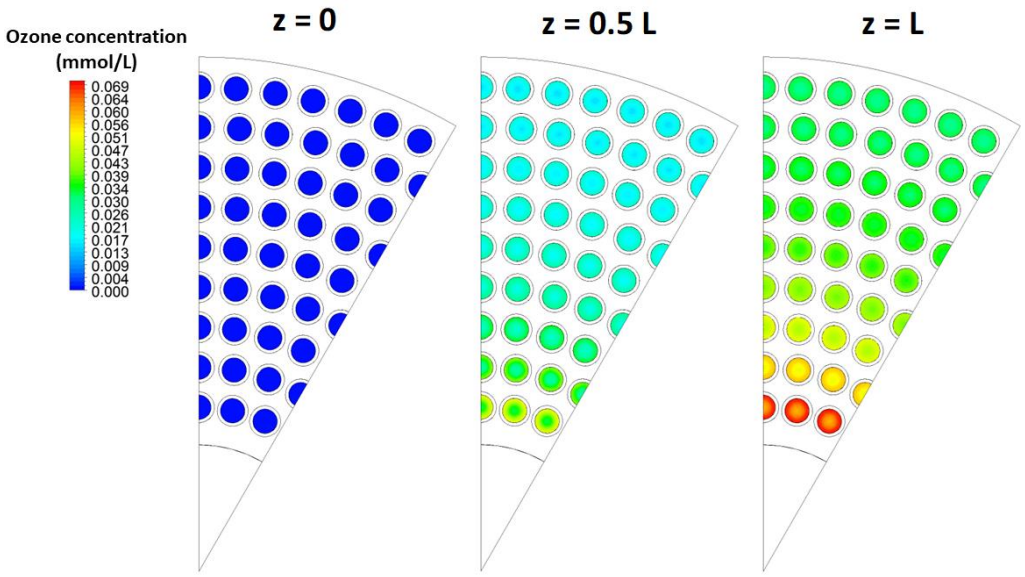

Figure 4.8.3. Distribution of ozone inside the lumen at the liquid inlet (z=0), half way through the reactor length (z=0.5 L), and at the liquid outlet of the membrane module (z=L=46 cm) at water velocity of 0.001 m s^{-1} and inlet ozone gas concentration of 24 mg L^{-1}.

4.8.3 Ozone mass transfer in groundwater

The first-order ozone decay rate constant (k_{O3}) in groundwater was measured at different ozone doses by Jakob Kämmler in the Hamburg University of Technology. The k_{O3} in the membrane ozonation experiments was extrapolated from the measured values. The Hatta number was then calculated for each membrane contactor and for the different conditions used according to equation 4.4.10. At a set water flow rate, an increase in feed gas ozone concentration leads to an increase in the transferred ozone dose, which decreases the k_{O3} and therefore also decreases the Hatta number.

Table 4.8.1. Hatta numbers for the membrane ozonation treatment of groundwater with two membrane contactors. The range of values shown for each water flow rate corresponds to the range of applied feed gas ozone concentrations.

Membrane contactor	Water flow rate (mL min^{-1})	Hatta number
Single tube contactor	1.2	0.3-1.6
	2.5	0.3-1.6
	5	0.5-1.7
	10	0.8-1.5
Hollow fibre module	400	0.5-1.1
	680	0.5-1.5
	920	0.7-1.7

4.8.4 TOC increase in PDMS membrane ozonation

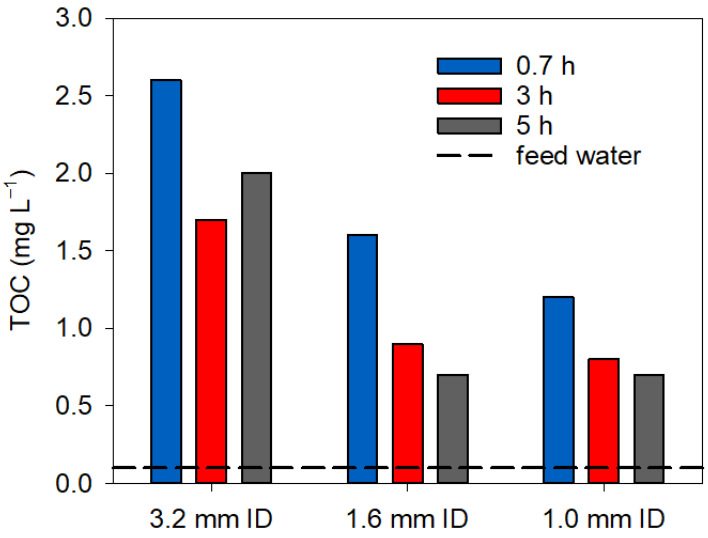

Figure 4.8.4. TOC concentration of deionised water before and after PDMS membrane ozonation during a 5-hour experiment. Three reactors were operated in parallel with membranes of different size. Feed gas ozone concentration 165 mg L^{-1}, total water flow rate 11 mL min^{-1}.

4.8.5 Spectrophotometric characterisation of wastewater effluent before and after membrane ozonation

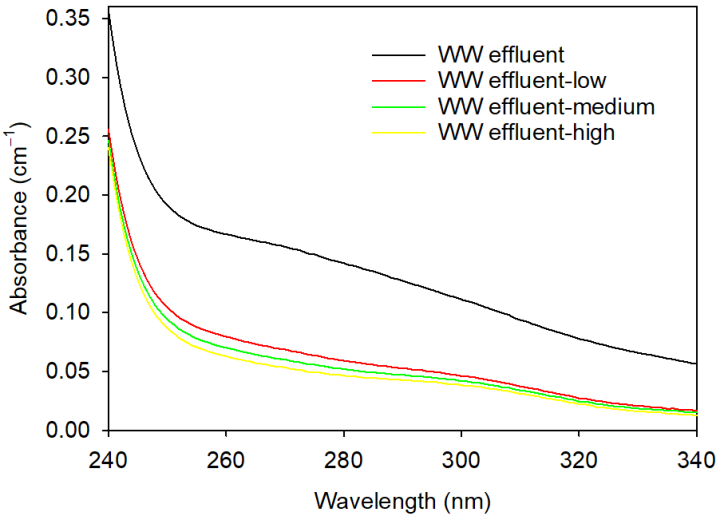

Figure 4.8.5. Extract from the UV scans of wastewater (WW) effluent before and after membrane ozonation with three different ozone doses (see Table 4.5.2).

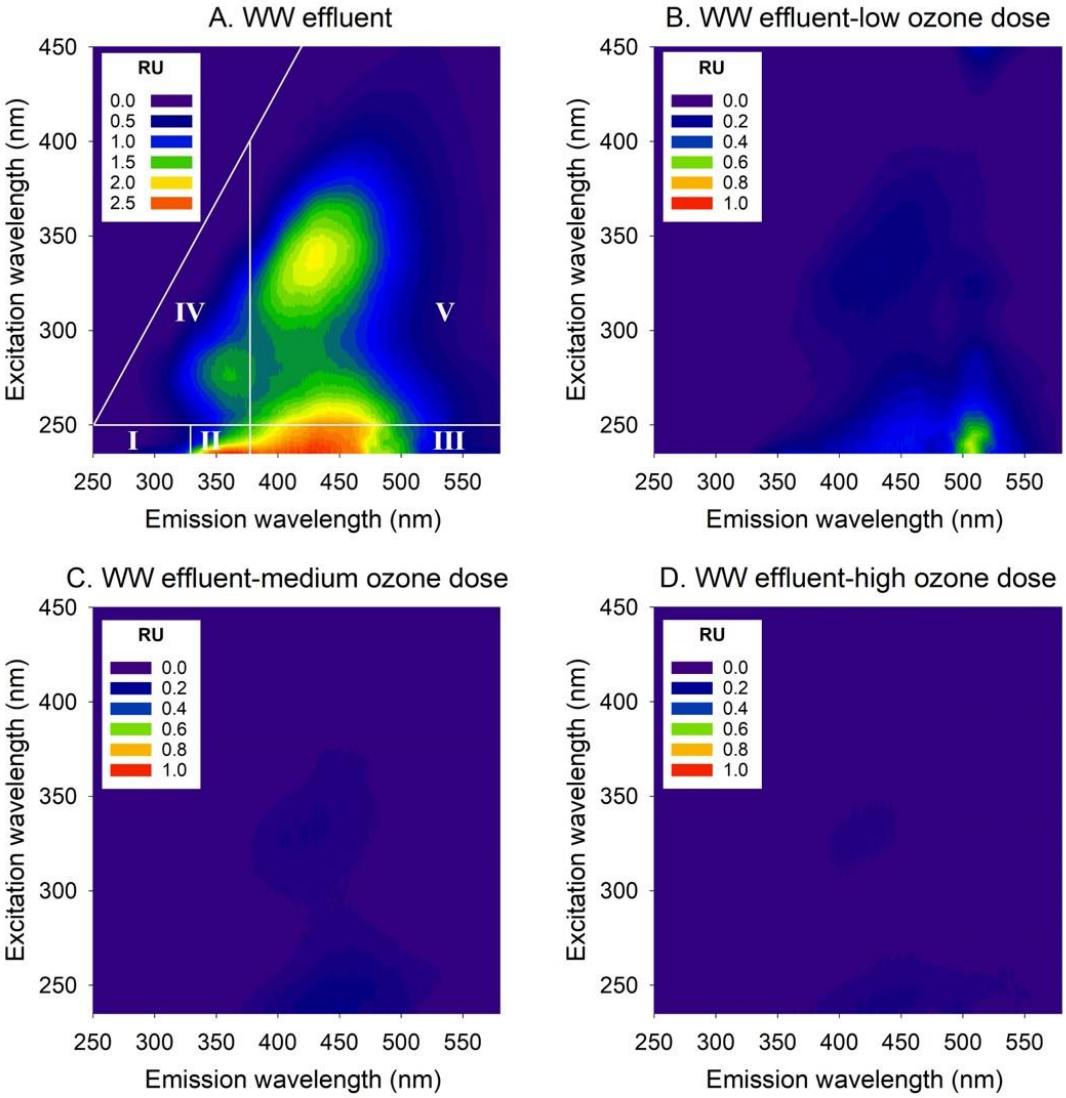

Figure 4.8.6. Excitation-emission matrix (EEM) of wastewater effluent before and after membrane ozonation with three different ozone doses (see Table 4.5.2). The five marked regions are: I tyrosine-like aromatic protein, II tryptophan-like aromatic protein, III fulvic acid-like matter, IV soluble microbial by-product-like matter, V humic acid-like matter. Note, a different scale has been used for ozonated samples.

Table 4.8.2. Wavelength boundaries used for integration and integrated fluorescence of the five marked regions shown in Figure 4.8.6.

EEM region	Excitation wavelength (nm)	Emission wavelength (nm)	Regional integrated fluorescence intensity (RU nm^2)			
			WW effluent	Low ozone	Medium ozone	High ozone
I	225-250	250-330	39070	1440	3500	0
II	225-250	330-380	120230	3400	610	420
III	225-250	380-550	98780	9450	2100	1060
IV	250-400	280-380	26670	1040	340	160
V	250-400	380-550	37660	3600	1010	450

4.8.6 Concentrations of TrOCs in wastewater effluent

Table 4.8.3. Concentration of trace organic contaminants in wastewater effluent before and after membrane ozonation treatment with three ozone doses (see Table 4.5.2). The average of duplicate or triplicate samples is shown. MQL: method quantification limit.

Compound	Concentration (ng/L)			
	Low ozone	Medium ozone	High ozone	WW effluent
Quantitative data				
Methylparaben	16	21	15	39
E2	8	8	6	31
Methamphetamine	4	4	5	9
Acetaminophen	81	30	41	1511
Cotinine	114	53	23	365
Anhydroecgonine methylester	<MQL	<MQL	<MQL	40
Carbamazepine (CBZ)	<MQL	<MQL	<MQL	171
Atenolol	3	3	3	225
Citalopram	<MQL	<MQL	<MQL	90
Sulfamethoxazole	30	26	26	766
10,11-Dihydro-10-hydroxy-CBZ	16	<MQL	<MQL	995
Dihydrocodeine	<MQL	<MQL	<MQL	90
Semi-quantitative data				
Ibuprofen	53	19	18	852
Diclofenac	209	265	172	959
Benzophenone-4	<MQL	<MQL	<MQL	8937
Sulfasalazine	<MQL	<MQL	<MQL	192
Fexofenadine	<MQL	<MQL	<MQL	603
Metformin	11144	7632	4919	24955
Benzoylecgonine	10	<MQL	<MQL	613
Ephedrine/pseudoephedrine	20	14	8	396
Codeine	3	3	3	575
Cocaine	<MQL	<MQL	<MQL	114
Nicotine	36	35	35	54
1,7 Dimethylxanthine	139	49	46	6000
Caffeine	45	20	51	3312
O-desmethyltramadol	<MQL	<MQL	<MQL	744
Trimethoprim	<MQL	<MQL	<MQL	1012
Lisinopril	60	61	58	554
CBZ-10,11-epoxide	179	9	3	14422

4.8.7 Ozonation products of TrOCs

A list of ozonation products of 44 TrOCs according to the literature is shown in Table 4.8.4. Structures of the products are not shown, but have been suggested for most of them, albeit with varying levels of confidence. Some metabolites have been grouped together with their parent compound due to structural similarity (i.e. the same ozonation products may be expected from parent compound and metabolite). For other metabolites possible ozonation products were inferred from the information available for the parent compound (e.g. when metabolite and parent compound differ by one methyl group). The list is not exhaustive, as certain minor ozonation products reported in the referenced studies have not been included.

Table 4.8.4. Ozonation products of trace organic contaminants reported in the literature or suggested based on structurally similar compounds.

Parent compounds	Ozonation products	Molecular formula of ozonation products	Analytical methods and comments	References
Acetaminophen	Product I	$C_6H_6O_2$	LC-UV and/or LC-MS (positive and negative mode)	(2)
	Product II	$C_8H_9NO_3$		
	Product III	$C_8H_9NO_5$		
Atenolol	AT-237	$C_{13}H_{19}NO_3$	LC-MS (positive mode)	(3)
	AT-272	$C_{12}H_{20}N_2O_5$		
	AT-280	$C_{14}H_{20}N_2O_4$		
	AT-298	$C_{14}H_{22}N_2O_5$		
Benzophenone-2	P1	$C_7H_6O_4$	LC-MS (negative mode)	(4)
	P4	$C_2H_2O_4$		
	P8	$C_4H_4O_4$		
	P10	$C_4H_6O_6$		
	P11	$C_3H_4O_5$		
	P12	$C_{13}H_8O_6$		
Benzophenone-3	m/z 125	$C_7H_8O_2$	LC-MS (positive and negative mode)	(5, 6)
	m/z 245	$C_{14}H_{12}O_4$		
	m/z 247	$C_{13}H_{10}O_5$		
	m/z 259	$C_{14}H_{12}O_5$		
	m/z 217	$C_{12}H_{10}O_4$		
	m/z 233	$C_{12}H_{10}O_5$		
	m/z 239	$C_{10}H_8O_7$		

Parent compounds	Ozonation products	Molecular formula of ozonation products	Analytical methods and comments	References
Benzophenone-4	P1	$C_{14}H_{12}O_7S$	LC-MS (negative mode)	(7)
	P2	$C_{14}H_{12}O_8S$		
	P3	$C_{14}H_{12}O_9S$		
	P4	$C_{14}H_{12}O_{10}S$		
	P6	$C_7H_8O_8S$		
	P7	$C_5H_6O_7S$		
Bezafibrate	A	$C_{10}H_{10}ClNO_3$	LC-MS (positive and negative mode)	(8)
	B	$C_{17}H_{18}ClNO_6$		
	C	$C_{19}H_{20}ClNO_6$		
	D, E	$C_{19}H_{20}ClNO_7$		
Bisphenol A	B1	$C_{15}H_{16}O_5$	LC-UV and/or LC-MS (negative mode)	(9)
	B2	$C_6H_4O_2$		
	B3	$C_9H_{12}O_2$		
	B4	$C_{15}H_{14}O_3$		
	B5	$C_{15}H_{16}O_3$		
Caffeine	P1	$C_8H_{10}N_4O_5$	LC-MS (positive mode) for caffeine. Suggested products for 1,7-dimethylxanthine.	(10)
	P2	$C_8H_{12}N_4O_4$		
	P3	$C_7H_{10}N_4O_3$		
	P4	$C_5H_8N_2O_3$		
	P5	$C_6H_9N_3O_4$		
	P6	$C_8H_{10}N_4O_4$		
1,7-Dimethylxanthine	P1'	$C_7H_8N_4O_5$		
	P2'	$C_7H_{10}N_4O_4$		
	P3'	$C_6H_8N_4O_3$		
	P4'	$C_4H_6N_2O_3$		
	P5'	$C_5H_7N_3O_4$		
	P6'	$C_7H_8N_4O_4$		

Parent compounds	Ozonation products	Molecular formula of ozonation products	Analytical methods and comments	References
Carbamazepine	BQM	$C_{15}H_{10}N_2O_2$	LC-MS (positive mode)	(11, 12)
Carbamazepine-10,11-epoxide	BaQD	$C_{15}H_{10}N_2O_4$		
10,11-Dihydro-10-hydroxycarbamazepine	BQD	$C_{15}H_{10}N_2O_3$		
	XIII	$C_{14}H_9NO$		
	X	$C_{14}H_9NO_2$		
	XI	$C_{13}H_9NO$		
	II	$C_{15}H_{14}N_2O_3$		
Citalopram	DCIT	$C_{19}H_{19}N_2OF$	LC-MS (positive mode) for citalopram. Suggested products for desmethylcitalopram.	(13)
	CIT-NO	$C_{20}H_{21}N_2O_2F$		
	TP-339	$C_{20}H_{19}N_2O_2F$		
	TP-323	$C_{20}H_{22}N_2O_2$		
Desmethylcitalopram	DCIT-hydroxylamine	$C_{19}H_{19}N_2O_2F$		
	TP-325	$C_{19}H_{17}N_2O_2F$		
	TP-309	$C_{19}H_{20}N_2O_2$		
Clarithromycin	Clarithromycin-*N*-oxide	$C_{38}H_{69}NO_{14}$	LC-MS (positive mode)	(14)
	Demethylated Clarithromycin	$C_{37}H_{67}NO_{13}$		
Cocaine	OTP-305	$C_{16}H_{19}O_5N$	LC-MS (positive mode) for cocaine and benzoylecgonine. Suggested product for cocaethylene.	(15, 16)
Benzoylecgonine	OTP-319	$C_{17}H_{21}O_5N$		
	OTP-321	$C_{16}H_{19}O_6N$		
Cocaethylene	OTP-333	$C_{18}H_{23}O_5N$		
Diclofenac	5-hydroxydiclofenac	$C_{14}H_{11}Cl_2NO_3$	LC-MS (positive and negative mode)	(17, 18)
	2,6- dichloroaniline	$C_6H_5Cl_2N$		
	diclofenac-2,5- iminoquinone	$C_{14}H_9Cl_2NO_3$		
	D10	C_6H_6NOCl		
	D13	C_7H_7N		

Parent compounds	Ozonation products	Molecular formula of ozonation products	Analytical methods and comments	References
E2	DEO, 2-hydroxyestradiol	C18H24O3	GC-MS and LC-MS (negative mode)	(19-21)
	m/z 277	C16H22O4		
	m/z 285	C18H22O3		
	m/z 319	C18H24O5		
	testosterone	C19H28O2		
Fexofenadine	FXF-TP1	$C_{32}H_{39}O_5N$	LC-MS (positive mode)	(22)
	FXF-TP2	$C_{18}H_{21}ON$		
	FXF-TP3	$C_{14}H_{21}O_3N$		
	FXF-TP4	$C_{32}H_{37}O_5N$		
	FXF-TP5/6	$C_{18}H_{21}O_2N$		
	FXF-TP7	$C_{14}H_{21}O_4N$		
Fluoxetine	TP 325	$C_{17}H_{18}F_3NO_2$	LC-MS (positive mode)	(23)
	TP 357	$C_{17}H_{18}F_3NO_4$		
	TP 165	$C_{10}H_{15}NO$		
	TP 163	$C_{10}H_{13}NO$		
	TP 259	$C_{12}H_{12}F_3NO_2$		
	TP 237	$C_9H_{10}F_3NO_3$		
Norfluoxetine	TP 311	$C_{16}H_{16}F_3NO_2$		
	TP 343	$C_{16}H_{16}F_3NO_4$		
	TP 151	$C_9H_{13}NO$		
	TP 149	$C_9H_{11}NO$		
	TP 233	$C_{10}H_{10}F_3NO_2$		
Ibuprofen	oxo-ibuprofen	$C_{13}H_{16}O_3$	LC-MS (negative mode)	(24)
	4-isobutylacetophenone	$C_{12}H_{16}O$		
	4-acetylbenzoic acid	$C_9H_9O_3$		
	4-ethylbenzaldehyde	$C_9H_{11}O$		

Parent compounds	Ozonation products	Molecular formula of ozonation products	Analytical methods and comments	References
Ketoprofen	m/z 211	$C_{15}H_{14}O$	LC-UV and LC-MS (positive mode)	(25)
	m/z 227	$C_{15}H_{14}O_2$		
	m/z 243	$C_{15}H_{14}O_3$		
	m/z 225	$C_{15}H_{12}O_2$		
MDMA	OTP-213	$C_{10}H_{15}O_4N$	LC-MS (positive mode)	(15)
	OTP-229	$C_{10}H_{15}O_5N$		
Metformin	methylbiguanide	$C_3H_9N_5$	LC-MS (positive mode)	(26)
	4,2,1-AIMT	$C_4H_7N_5$		
Methylparaben	Hydroxy-methylparaben	$C_8H_8O_4$	GC-MS	(27)
	Dihydroxy-methylparaben	$C_8H_8O_5$		
	Trihydroxy-methylparaben	$C_8H_8O_6$		
Metoprolol	M3/299	$C_{15}H_{25}NO_5$	LC-UV and LC-MS (positive mode)	(28)
	M3/241	$C_{12}H_{19}NO_4$		
	M3/273	$C_{13}H_{23}NO_5$		
	M8/283	$C_{14}H_{21}NO_5$		
	M8/253	$C_{14}H_{23}NO_3$		
	M8/239	$C_{12}H_{17}NO_4$		
	M8/225	$C_{12}H_{19}NO_3$		
Naproxen	m/z 185	$C_{13}H_{14}O$	LC-MS (negative mode)	(29)
	m/z 170	$C_{12}H_{12}O$		
	m/z 216	$C_{13}H_{14}O_3$		

Parent compounds	Ozonation products	Molecular formula of ozonation products	Analytical methods and comments	References
Nicotine	Nicotine *N*-oxide	$C_{10}H_{14}N_2O$	LC-MS (positive mode). TP1', TP5' and TP7' are suggested products.	(30, 31)
	P8	$C_{10}H_{12}N_2$		
	P4	$C_9H_{10}N_2$		
	P13	$C_9H_{10}N_2O_3$		
	TP1'	$C_9H_{12}N_2$		
	TP5'	$C_{10}H_{14}N_2O_2$		
	TP7'	$C_6H_{11}NO_2$		
Cotinine	Cotinine *N*-oxide, TP6	$C_{10}H_{12}N_2O_2$		
	TP1	$C_9H_{10}N_2O$		
	TP2	$C_6H_5NO_2$		
	TP3	$C_5H_7NO_2$		
	TP4	$C_5H_9NO_2$		
	TP5	$C_{10}H_{12}N_2O_3$		
	TP7	$C_6H_9NO_3$		
Propranolol	OP-291	$C_{16}H_{21}NO_4$	LC-UV and LC-MS (positive mode)	(32)
	OP-307	$C_{16}H_{21}NO_5$		
	OP-281	$C_{14}H_{19}NO_5$		
	OP-265	$C_{14}H_{19}NO_4$		
Ranitidine	TP-330	$C_{13}H_{22}N_4O_4S$	LC-MS (positive mode)	(33)
	TP-299	$C_{13}H_{21}N_3O_3S$		
	TP-304	$C_{12}H_{20}N_2O_5S$		
	TP-315	$C_{13}H_{21}N_3O_4S$		
	TP-331	$C_{13}H_{21}N_3O_5S$		
	TP-333	$C_{13}H_{23}N_3O_5S$		
	TP-283	$C_{13}H_{21}N_3O_2S$		
	TP-214	$C_{10}H_{18}N_2OS$		

Parent compounds	Ozonation products	Molecular formula of ozonation products	Analytical methods and comments	References
Sulfamethoxazole	TP-99	$C_4H_6N_2O$	LC-MS (positive mode)	(34)
	TP-284	$C_{10}H_9N_3O_5S$		
	TP-270	$C_{10}H_{11}N_3O_4S$		
	TP-288	$C_{10}H_{13}N_3O_5S$		
Sulfasalazine	m/z 282	$C_{11}H_{11}N_3O_4S$	LC-MS (positive mode)	(35)
	m/z 323	$C_{13}H_{10}N_2O_6S$		
	m/z 338	$C_{13}H_{11}N_3O_6S$		
	m/z 205	$C_6H_8N_2O_4S$		
	m/z 191	$C_5H_6N_2O_4S$		
Tamoxifen	TP 270	$C_{17}H_{19}NO_2$	LC-MS (positive mode)	(36, 37)
	TP 286	$C_{17}H_{19}NO_3$		
	TP 388, TAM-*N*-oxide	$C_{26}H_{29}NO_2$		
	TP 404	$C_{26}H_{29}NO_3$		
	TP 214	$C_{11}H_{19}NO_3$		
	TP 224	$C_8H_{17}NO_6$		
Tramadol *O*-desmethyltramadol *N*-desmethyltramadol	*N*-desmethyltramadol	$C_{15}H_{23}NO_2$	GC-MS and LC-MS (positive and negative mode). *N*-oxide-desmethyl is a suggested product for *O*-, *N*-desmethyltramadol.	(38)
	N-oxide	$C_{16}H_{25}NO_3$		
	N-bisdesmethyl	$C_{14}H_{21}NO_2$		
	N-oxide-desmethyl	$C_{15}H_{23}NO_3$		
Triclosan	2,4-Dichlorophenol	$C_6H_4Cl_2O$	GC-MS and LC-MS (negative mode)	(39)
	4-Chloro-catechol/resorcinol	$C_6H_5ClO_2$		
	Mono-hydroxy-triclosan	$C_{12}H_7Cl_3O_3$		
	Di-hydroxy-triclosan	$C_{12}H_7Cl_3O_4$		

Parent compounds	Ozonation products	Molecular formula of ozonation products	Analytical methods and comments	References
Trimethoprim	OP294	$C_{13}H_{18}N_4O_4$	LC-MS (positive mode)	(40)
	OP322	$C_{14}H_{18}N_4O_5$		
	OP324	$C_{14}H_{20}N_4O_5$		
	OP339	$C_{14}H_{18}N_4O_6$		
Venlafaxine	*N*-oxide	$C_{17}H_{27}NO_3$	LC-MS (positive mode). Bisdesmethyl is a suggested product for desvenlafaxine.	(41, 42)
	N-desmethyl	$C_{16}H_{25}NO_2$		
Desvenlafaxine	*N*-oxide-desmethyl	$C_{16}H_{25}NO_3$		
	Bisdesmethyl	$C_{15}H_{23}NO_2$		

4.8.7 References

1. Berry M, Taylor C, King W, Chew Y, Wenk J. Modelling of Ozone Mass-Transfer through Non-Porous Membranes for Water Treatment. Water. 2017;9(7):452.

2. Hamdi El Najjar N, Touffet A, Deborde M, Journel R, Karpel Vel Leitner N. Kinetics of paracetamol oxidation by ozone and hydroxyl radicals, formation of transformation products and toxicity. Sep Purif Technol. 2014;136:137-43.

3. Tay KS, Rahman NA, Abas MRB. Characterization of atenolol transformation products in ozonation by using rapid resolution high-performance liquid chromatography/quadrupole-time-of-flight mass spectrometry. Microchem J. 2011;99(2):312-26.

4. Wang S, Wang X, Chen J, Qu R, Wang Z. Removal of the UV Filter Benzophenone-2 in Aqueous Solution by Ozonation: Kinetics, Intermediates, Pathways and Toxicity. Ozone: Science & Engineering. 2018;40(2):122-32.

5. Hopkins ZR, Snowberger S, Blaney L. Ozonation of the oxybenzone, octinoxate, and octocrylene UV-filters: Reaction kinetics, absorbance characteristics, and transformation products. Journal of Hazardous Materials. 2017;338:23-32.

6. Guo Y, Lin Q, Xu B, Qi F. Degradation of benzophenone-3 by the ozonation in aqueous solution: kinetics, intermediates and toxicity. Environmental Science and Pollution Research. 2016;23(8):7962-74.

7. Liu H, Sun P, He Q, Feng M, Liu H, Yang S, Wang L, Wang Z. Ozonation of the UV filter benzophenone-4 in aquatic environments: Intermediates and pathways. Chemosphere. 2016;149:76-83.

8. Dantas RF, Canterino M, Marotta R, Sans C, Esplugas S, Andreozzi R. Bezafibrate removal by means of ozonation: Primary intermediates, kinetics, and toxicity assessment. Water Research. 2007;41(12):2525-32.

9. Deborde M, Rabouan S, Mazellier P, Duguet J-P, Legube B. Oxidation of bisphenol A by ozone in aqueous solution. Water Research. 2008;42(16):4299-308.

10. Rosal R, Rodríguez A, Perdigón-Melón JA, Petre A, García-Calvo E, Gómez MJ, Agüera A, Fernández-Alba AR. Degradation of caffeine and identification of the transformation products generated by ozonation. Chemosphere. 2009;74(6):825-31.

11. Hübner U, Seiwert B, Reemtsma T, Jekel M. Ozonation products of carbamazepine and their removal from secondary effluents by soil aquifer treatment – Indications from column experiments. Water Research. 2014;49:34-43.

12. Brezina E, Prasse C, Meyer J, Muckter H, Ternes TA. Investigation and risk evaluation of the occurrence of carbamazepine, oxcarbazepine, their human metabolites and transformation products in the urban water cycle. Environ Pollut. 2017;225:261-9.

13. Horsing M, Kosjek T, Andersen HR, Heath E, Ledin A. Fate of citalopram during water treatment with O_3, ClO_2, UV and Fenton oxidation. Chemosphere. 2012;89(2):129-35.

14. Lange F, Cornelissen S, Kubac D, Sein MM, von Sonntag J, Hannich CB, Golloch A, Heipieper HJ, Möder M, von Sonntag C. Degradation of macrolide antibiotics by ozone: A mechanistic case study with clarithromycin. Chemosphere. 2006;65(1):17-23.

15. Rodayan A, Segura PA, Yargeau V. Ozonation of wastewater: Removal and transformation products of drugs of abuse. Science of The Total Environment. 2014;487:763-70.

16. Russo D, Spasiano D, Vaccaro M, Cochran KH, Richardson SD, Andreozzi R, Li Puma G, Reis NM, Marotta R. Investigation on the removal of the major cocaine metabolite (benzoylecgonine) in water matrices by UV_{254}/H_2O_2 process by using a flow microcapillary film array photoreactor as an efficient experimental tool. Water Research. 2016;89:375-83.

17. Sein MM, Zedda M, Tuerk J, Schmidt TC, Golloch A, Sonntag Cv. Oxidation of Diclofenac with Ozone in Aqueous Solution. Environmental Science & Technology. 2008;42(17):6656-62.

18. Coelho AD, Sans C, Aguera A, Gomez MJ, Esplugas S, Dezotti M. Effects of ozone pre-treatment on diclofenac: intermediates, biodegradability and toxicity assessment. Sci Total Environ. 2009;407(11):3572-8.

19. Bila D, Montalvão AF, Azevedo DdA, Dezotti M. Estrogenic activity removal of 17β-estradiol by ozonation and identification of by-products. Chemosphere. 2007;69(5):736-46.

20. Pereira RdO, de Alda ML, Joglar J, Daniel LA, Barceló D. Identification of new ozonation disinfection byproducts of 17β-estradiol and estrone in water. Chemosphere. 2011;84(11):1535-41.

21. Irmak S, Erbatur O, Akgerman A. Degradation of 17β-estradiol and bisphenol A in aqueous medium by using ozone and ozone/UV techniques. Journal of Hazardous Materials. 2005;126(1):54-62.

22. Borowska E, Bourgin M, Hollender J, Kienle C, McArdell CS, von Gunten U. Oxidation of cetirizine, fexofenadine and hydrochlorothiazide during ozonation: Kinetics and formation of transformation products. Water Research. 2016;94:350-62.

23. Zhao Y, Yu G, Chen S, Zhang S, Wang B, Huang J, Deng S, Wang Y. Ozonation of antidepressant fluoxetine and its metabolite product norfluoxetine: Kinetics, intermediates and toxicity. Chemical Engineering Journal. 2017;316:951-63.

24. Yargeau V, Danylo F. Removal and transformation products of ibuprofen obtained during ozone- and ultrasound-based oxidative treatment. Water Science and Technology. 2015;72(3):491-500.

25. Illés E, Szabó E, Takács E, Wojnárovits L, Dombi A, Gajda-Schrantz K. Ketoprofen removal by O_3 and O_3/UV processes: Kinetics, transformation products and ecotoxicity. Science of The Total Environment. 2014;472:178-84.

26. Quintão FJO, Freitas JRL, de Fátima Machado C, Aquino SF, de Queiroz Silva S, de Cássia Franco Afonso RJ. Characterization of metformin by-products under photolysis, photocatalysis, ozonation and chlorination by high-performance liquid chromatography coupled to high-resolution mass spectrometry. Rapid Commun Mass Spectrom. 2016;30(21):2360-8.

27. Tay KS, Rahman NA, Abas MRB. Ozonation of parabens in aqueous solution: Kinetics and mechanism of degradation. Chemosphere. 2010;81(11):1446-53.

28. Benner J, Ternes TA. Ozonation of Metoprolol: Elucidation of Oxidation Pathways and Major Oxidation Products. Environmental Science & Technology. 2009;43(14):5472-80.

29. Patel S, Majumder SK, Das P, Ghosh P. Ozone microbubble-aided intensification of degradation of naproxen in a plant prototype. Journal of Environmental Chemical Engineering. 2019;7(3):103102.

30. Krupež J, Kovačević VV, Jović M, Roglić GM, Natić MM, Kuraica MM, Obradović BM, Dojčinović BP. Degradation of nicotine in water solutions using a water falling film DBD plasma reactor: direct and indirect treatment. J Phys D: Appl Phys. 2018;51(17):174003.

31. Rivas FJ, Solís RR, Beltrán FJ, Gimeno O. Sunlight driven photolytic ozonation as an advanced oxidation process in the oxidation of bezafibrate, cotinine and iopamidol. Water Research. 2019;151:226-42.
32. Benner J, Ternes TA. Ozonation of Propranolol: Formation of Oxidation Products. Environmental Science & Technology. 2009;43(13):5086-93.
33. Christophoridis C, Nika MC, Aalizadeh R, Thomaidis NS. Ozonation of ranitidine: Effect of experimental parameters and identification of transformation products. Sci Total Environ. 2016;557-558:170-82.
34. Gómez-Ramos MdM, Mezcua M, Agüera A, Fernández-Alba AR, Gonzalo S, Rodríguez A, Rosal R. Chemical and toxicological evolution of the antibiotic sulfamethoxazole under ozone treatment in water solution. Journal of Hazardous Materials. 2011;192(1):18-25.
35. Pelalak R, Alizadeh R, Ghareshabani E, Heidari Z. Degradation of sulfonamide antibiotics using ozone-based advanced oxidation process: Experimental, modeling, transformation mechanism and DFT study. Science of The Total Environment. 2020;734:139446.
36. Knoop O, Hohrenk LL, Lutze HV, Schmidt TC. Ozonation of Tamoxifen and Toremifene: Reaction Kinetics and Transformation Products. Environmental Science & Technology. 2018;52(21):12583-91.
37. Ferrando-Climent L, Gonzalez-Olmos R, Anfruns A, Aymerich I, Corominas L, Barceló D, Rodriguez-Mozaz S. Elimination study of the chemotherapy drug tamoxifen by different advanced oxidation processes: Transformation products and toxicity assessment. Chemosphere. 2017;168:284-92.
38. Zimmermann SG, Schmukat A, Schulz M, Benner J, Gunten Uv, Ternes TA. Kinetic and Mechanistic Investigations of the Oxidation of Tramadol by Ferrate and Ozone. Environmental Science & Technology. 2012;46(2):876-84.
39. Chen X, Richard J, Liu Y, Dopp E, Tuerk J, Bester K. Ozonation products of triclosan in advanced wastewater treatment. Water Research. 2012;46(7):2247-56.
40. Kuang J, Huang J, Wang B, Cao Q, Deng S, Yu G. Ozonation of trimethoprim in aqueous solution: Identification of reaction products and their toxicity. Water Research. 2013;47(8):2863-72.
41. Zucker I, Mamane H, Riani A, Gozlan I, Avisar D. Formation and degradation of N-oxide venlafaxine during ozonation and biological post-treatment. Sci Total Environ. 2018;619-620:578-86.

42. Lajeunesse A, Blais M, Barbeau B, Sauvé S, Gagnon C. Ozone oxidation of antidepressants in wastewater –Treatment evaluation and characterization of new by-products by LC-QToFMS. Chemistry Central Journal. 2013;7(1):15.

Chapter 5: Aqueous ozonation of furans: Kinetics and transformation mechanisms leading to the formation of α,β-unsaturated dicarbonyl compounds

This chapter is presented in publication format and has been submitted for review to Water Research (Elsevier).

Context: The following study began with my internship at Johns Hopkins University and continued as a collaboration between the two labs after my return to Bath. We chose to study the aqueous ozonation of furans, since a review of the relevant literature revealed that very little information on this topic is available, in contrast to other functional groups of organic contaminants, such as benzene rings. The formation of toxic α,β-unsaturated dicarbonyls had been previously reported for the metabolism of furans and for the aqueous oxidation of phenols. We therefore targeted this class of compounds as potential ozonation products with a recently developed analytical approach based on their reaction with amino acids. Kinetics and formation of other ozonation products were also elucidated for furans with different substituents.

Contributions: The work presented was performed by the author of this thesis under the supervision of Dr Carsten Prasse (Johns Hopkins University) and Dr Jannis Wenk, with contributions from manuscript co-author Zhuoyue Zhang who performed supporting experiments, analysis and data interpretation.

First authorship of the manuscript is shared between the author of this thesis and Zhuoyue Zhang.

Aqueous Ozonation of Furans: Kinetics and Transformation Mechanisms Leading to the Formation of α,β-Unsaturated Dicarbonyl Compounds

Garyfalia A. Zoumpouli[a,b,c,d], Zhuoyue Zhang[d], Jannis Wenk[b,c], Carsten Prasse[d,*]

[a] Centre for Doctoral Training, Centre for Sustainable Chemical Technologies, University of Bath, Bath BA2 7AY, UK.

[b] Department of Chemical Engineering, University of Bath, Bath BA2 7AY, UK.

[c] Water Innovation and Research Centre (WIRC), University of Bath, Bath BA2 7AY, UK.

[d] Department of Environmental Health and Engineering, Johns Hopkins University, Baltimore, MD 21218, USA.

*Corresponding author

5.1 Abstract

Despite the widespread occurrence of furan moieties in synthetic and natural compounds, their fate in aqueous ozonation has not been investigated in detail. Reaction rate constants of seven commonly used furans with ozone were measured and ranged from $k_{O3} = 8.5 \times 10^4$ to 3.2×10^6 M^{-1} s^{-1}, depending on the type and position of furan ring substituents. Transformation product analysis of the reaction of furans with ozone focusing on the formation of toxic organic electrophiles using a novel amino acid reactivity assay revealed the formation of α,β-unsaturated dicarbonyl compounds, 2-butene-1,4-dial (BDA) and its substituted analogues (BDA-Rs). Their formation can be attributed to ozone attack at the reactive α-C position leading to furan ring opening. The molar yields of α,β-unsaturated dicarbonyl compounds varied with the applied ozone concentration reaching maximum values of 7% for 2-furoic acid. The identified α,β-unsaturated dicarbonyls are well-known toxicophores that are also formed by enzymatic oxidation of furans in the human body. In addition to providing data on kinetics, transformation product analysis and proposed reaction mechanisms for the ozonation of furans, this study raises concern about the presence of α,β-unsaturated dicarbonyl compounds in water treatment and the resulting effects on human and environmental health.

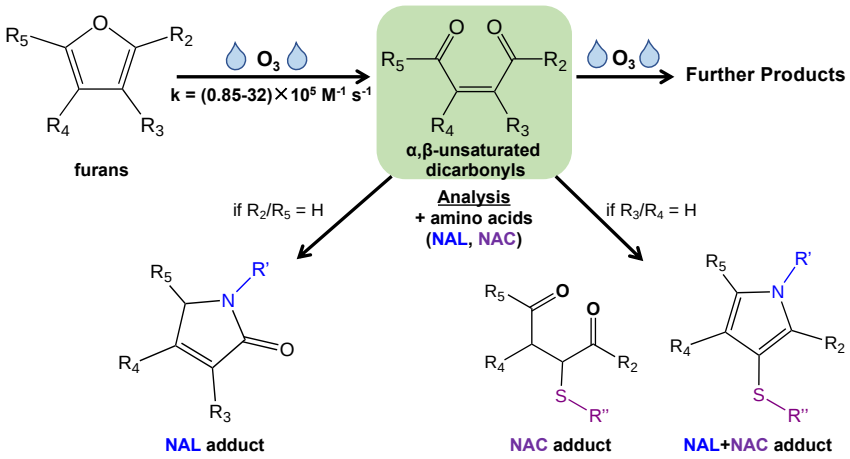

5.2 Introduction

Furans are heterocyclic aromatics comprising a five-membered ring of four carbons and one oxygen atom. The use of furan derivatives for the production of biomass-derived fuels, polymers and other chemicals has dramatically increased over the last decades (1-4). Furfural, a commodity chemical and precursor of many other furans, has a global production capacity of 280 kTon per year, with 65% used to produce furfuryl alcohol (5). In addition to their industrial applications, furans are common moieties in a variety of naturally occurring compounds including terpenes and fatty acids, and can be formed abiotically from the oxidation of natural organic matter (6-8). The extensive use of furan-containing chemicals and their natural occurrence make them likely contaminants in wastewater and drinking water resources as evidenced by the detection of furan-containing compounds, particularly pharmaceuticals, in wastewater effluent and surface water (9-11).

Ozonation is increasingly used for the elimination of trace organic contaminants in wastewater treatment, wastewater reuse and drinking water production (12). Ozone is a selective oxidant that primarily reacts with electron-rich moieties such as double bonds (13, 14). Transformation products of the ozonation of organic compounds include carbonyls formed by cleavage of olefinic bonds or benzene rings, *N*-oxides and hydroxylamines by oxidation of amines, and sulfoxides by oxidation of thioethers (15, 16). The identification of ozone transformation products with (eco)toxicological implications is of importance (17). For example, the main ozonation product of carboxy-acyclovir inhibits the growth of green algae, an effect not observed for the parent compond (18). Similarly, embryotoxicity in a zebrafish

assay was observed for the ozonation products of carbamazepine while no effects were observed for carbamazepine itself (19).

Despite extensive research on the reaction of ozone with several classes of organic compounds including olefins, phenols and nitrogen-containing compounds (20), studies focussing on the transformation of furans during aqueous ozonation are limited. The dimethylfuran moiety present in the antacid drug ranitidine has been shown to contribute to the high reactivity of this compound with ozone (21). However, no transformation products that are specific for the reaction of ozone with the furan moiety were reported (22, 23). For the diuretic drug furosemide, two ozonation products were identified indicating the potential relevance of cleavage and/or opening of the furan ring by ozone (24).

Studies investigating the reaction of furans with ozone in organic solvents or organic solvent/water mixtures suggest the potential involvement of different reaction mechanisms (25-28). Jibben et al. (26) identified glyoxal (a C_2 dicarbonyl) as the sole ozone transformation product of furan and attributed its formation to the reaction of ozone with the two carbon-carbon double bonds (α-β bonds) of the furan ring, leading to a C_2 dicarbonyl containing both β-C atoms, and/or to β,β-addition of ozone, leading to two C_2 dicarbonyls that contain one α- and one β-C atom of the furan ring (see Table 5.4.1 for nomenclature). In contrast, Bailey et al. (25, 28) observed the formation of α,β-unsaturated dicarbonyl compounds containing all four carbons of the furan ring in experiments with diarylfurans such as 2,5-diphenylfuran. The results of Bailey et al. indicate the relevance of two distinct reaction pathways: (i) ozonolysis of a carbon-carbon double bond (α-β bond), and (ii) electrophilic ozone attack at the reactive α-C position in either a bidentate or monodentate manner, followed by ring cleavage to form a C_4 dicarbonyl (29). These C_4 dicarbonyls then form lower-molecular weight transformation products through further reaction with ozone (29).

Given the absence of kinetic and mechanistic information on the ozonation of furans in aqueous solutions, the aim of this study was to determine the ozonation kinetics of various commonly used furans and elucidate the formation of ozonation products in water. The specific focus was on the formation of α,β-unsaturated dicarbonyl transformation products which have been recently identified as novel, highly toxic by-products formed during the oxidation of phenols with various oxidants including

hydroxyl radicals and chlorine (30, 31). In addition, α,β-unsaturated dicarbonyls are also formed during the enzymatic oxidation of furans in the human body (catalyzed by cytochrome P450) and are responsible for their toxicity (32-34). The studied furans included two high usage pharmaceuticals (furosemide, ranitidine) that can be frequently found in the effluent of wastewater treatment plants (9), and seven high production volume industrial chemicals (furfuryl alcohol, 2-furoic acid, 2,5-dimethylfuran, 2-methyl-3-furoic acid, 3-(2-furyl)propanoic acid, 3,4-bis(hydroxymethyl)furan, furan-2,5-dicarboxylic acid) (2, 3). Transformation product formation was followed using liquid chromatography-high resolution mass spectrometry. In addition, an amino acid reactivity assay was used to specifically assess the formation of α,β-unsaturated dicarbonyls (30, 35).

5.3 Materials and Methods

5.3.1 Chemicals

Furfuryl alcohol (FFA, CAS no.: 98-00-0), 3,4-bis(hydroxymethyl)furan (BHF, CAS no.: 14496-24-3), 2,5-dihydro-2,5-dimethoxyfuran (CAS no.: 332-77-4), 2,5-dimethylfuran (DMF, CAS no.: 625-86-5) in liquid form and 2-furoic acid (FA, CAS no.: 98-00-0), 2-methyl-3-furoic acid (MFA, CAS no.: 98-00-0), 3-(2-furyl)propanoic acid (FPA, CAS no.: 935-13-7), furan-2,5-dicarboxylic acid (FDCA, CAS no.: 3238-40-2), furosemide (FRS, CAS no.: 54-31-9), ranitidine (RAN, CAS no.: 66357-59-3) in powder form were purchased from Sigma-Aldrich or Fisher Scientific in high purity (≥97%). *N*-α-acetyl-lysine (NAL) was from Sigma Aldrich (>98% purity). *N*-α-acetyl-cysteine (NAC) was from Fisher Scientific (>98% purity). Solvents for analysis, salts for preparation of buffers and *tert*-butanol were from Fisher Scientific. All experimental and analytical solutions, including stock solutions, were prepared in ultrapure water (resistivity >18 MΩ cm^{-1}) produced with a Milli-Q (Merck) or ELGA (Veolia) water purification system.

5.3.2 Ozonation experiments

Competition kinetics experiments were performed to determine the second order rate constants for the reaction of furans with ozone in pure water buffered at pH 7 (10 mM

phosphate buffer, 10 mM *tert*-butanol). RAN was used as the reference compound, due to its known reaction rate constant with ozone (21), and since initial tests had shown that most of the target furans had an ozone reactivity within approximately one order of magnitude of RAN. For compounds that reacted with ozone with much lower reaction rate constants than RAN, FA was used as the reference compound, after determining its rate constant using RAN. Further details on competition kinetics experiments and calculations are provided in the SI, Section 5.8.1.

Batch ozonation experiments to study the formation of transformation products of furans were performed in 20-mL amber glass vials. The reaction solutions (10 mL) contained 15 μM of the target compound and 10 mM phosphate buffer (pH 7), diluted with ultrapure water. After sampling the initial solution, a volume of concentrated ozone stock solution (see SI, Section 5.8.1) was added to achieve concentrations of 4 to 65 μM ozone (0.3 to 4.3 μM O_3/μM target compound). The samples were left uncapped at room temperature for approximately 2 hours to achieve residual ozone depletion. To assess the influence of OH radical scavenging, a subset of experiments (Figures 5.8.2 and 5.8.3 in the SI) was also performed with addition of 10 mM *tert*-butanol ($k_{OH,\ tert\text{-butanol}} = 6 \times 10^8\ M^{-1}\ s^{-1}$) (36).

Detection of α,β-unsaturated dicarbonyl compounds was accomplished using an amino acid reactivity assay (30, 31, 35). The reaction of NAL with α,β-unsaturated dicarbonyls leads to the formation of NAL adducts which can be detected using liquid chromatography-mass spectrometry (see Section 5.3.3) (30). To this end, a small volume of a NAL stock solution was added to the samples (final concentration 150 μM, equivalent to 10 times the initial concentration of the parent compound) followed by incubation at room temperature for 24 hours. Selected experiments were repeated with higher concentration of the target compound (up to 100 μM) to facilitate the identification of α,β-unsaturated dicarbonyl transformation products. Additionally, for selected samples an equimolar mixture of NAL and NAC stock solutions was used instead of the NAL stock solution, to enable the detection of dicarbonyls that do not form adducts with NAL alone but do form NAC or NAL+NAC adducts (30). All samples were analyzed within 48 hours.

5.3.3 Analytical approaches

Spectrophotometric measurements were conducted in 1 cm quartz glass cuvettes (Hellma) using a Cary 100 UV-VIS spectrophotometer (Agilent Technologies), or in glass tubes using a DR/2000 Spectrophotometer (Hach).

Analysis of furans was performed using high-performance liquid chromatography with UV detection (HPLC-UV). An overview of isocratic elution conditions, retention times and detection wavelengths is provided in Table 5.8.1 of the SI. For batch ozonation a Vanquish HPLC system with a DAD detector (Thermo Scientific) and an Acclaim RSLC 120 C18 column (5 μm, 120 Å, 4.6 × 100 mm) was used. For competition kinetics a Dionex UltiMate 3000 system with a DAD detector (Thermo Scientific) and an Acclaim RSLC 120 C18 column (3 μm, 120 Å, 3 × 75 mm) was used.

The formation of ozonation products and NAL, NAC or NAL+NAC adducts was determined via liquid chromatography-high resolution mass spectrometry (LC-HRMS) using an UltiMate 3000 UHPLC system coupled to a Q Exactive HF Orbitrap MS (both Thermo Scientific). For chromatographic separation, a Phenomenex Synergi Hydro-RP column (4 μm, 80 Å, 1 × 150 mm) was used. External mass calibration was performed every 5 days using a calibration mixture similar to procedures described previously (37). More information on LC-HRMS analysis is provided in the SI, Section 5.8.2.

2-butene-1,4-dial (BDA), the α,β-unsaturated dicarbonyl identified in this work, was quantified with standard addition calibration curves, similar to a method described previously (30). Stock solutions of BDA (1 mM) were prepared through hydrolysis of 2,5-dihydro-2,5-dimethoxyfuran in ultrapure water at room temperature for at least 24 hours. For each experiment, standard addition was applied on one of the samples and the slope of the curve was used for the other samples of that experiment. The limit of detection of BDA in ultrapure water buffered at pH 7 was 1 nM and the limit of quantification was 10 nM. Ozonation yields of BDA were calculated by dividing the molar concentration of BDA with the molar concentration of the parent compound that reacted (difference between initial and final concentrations). Yields of other BDA analogues (BDA-Rs) without a standard available were estimated using BDA as reference standard.

5.4 Results and discussion

5.4.1 Kinetics of the reaction of substituted furans with ozone

Table 5.4.1 shows the second order rate constants for the reaction of nine furans with ozone (k_{O3}) in water at pH 7, including two values that were available in the literature. The competition kinetics plots for seven of the furans are provided in SI, Figure 5.8.1. Initial tests indicated that the studied furans have a high ozone reactivity, which was expected based on the aromaticity of the furan ring. Competition kinetics experiments showed that the k_{O3} of FPA, MFA, FRS, FFA and BHF varies only by a factor of 2 [(1.7±0.2 to 3.2±0.2) × 10^6 M^{-1} s^{-1}], while reaction rates for FA and FDCA were lower [(5.9±0.5) × 10^5 and (8.5±0.7) × 10^4 M^{-1} s^{-1}, respectively]. The ozone reactivity of most tested furans is comparable to that of phenols and anilines at pH 7 (38).

The results indicate that both the type of substituents (e.g. electron-withdrawing versus electron-donating) and their position (e.g. located at an α-carbon versus at a β-carbon) impact the reaction kinetics. Electron-donating substituents such as hydroxyl and methyl groups increase the electron density of the furan ring and are therefore expected to enhance its ozone reactivity, while electron-withdrawing groups such as carboxyl groups have the opposite impact, similar to effects observed for phenols (38). The three acids FPA, MFA and FA have pK_a values ranging from 3 to 4.4 (39), hence they are all dissociated at pH 7. The carboxylate group exerts a weaker electro-withdrawing effect compared to the carboxyl (40), as is also evidenced by the similar ozone reactivity of FA and FFA, which has an electron-donating hydroxymethyl substituent. MFA had a higher rate constant than FA, due to the presence of an additional alkyl group and/or the presence of a carboxylate substituent at a β- rather than an α-carbon. In FPA the carboxylate group is separated from the furan ring by two additional carbons (C_2H_4 group) compared to FA, leading to a 5-fold increase of the rate constant. Comparison of the kinetics of FDCA and FA indicates that the presence of an additional carboxylate group (2,5-substitution of FDCA versus 2-substitution of FA) lowers the ozone reactivity by approximately one order of magnitude. The relatively low rate constant of DMF with ozone that has been reported in the literature (Table 5.4.1) further indicates slower reaction kinetics for furans containing substituents at both α-carbons (2,5-substitution). In contrast,

BHF (3,4-substitution) had the same rate constant as FFA (2-substitution), indicating that substituents located at β-carbons have a lower impact on the reaction rates. Further experiments with a more diverse group of furan compounds are necessary to develop Quantitative Structure-Activity Relationships (QSARs) for substituted furans in oxidative water treatment processes similar to those that have been developed for other compound classes such as phenols and amines (38, 41).

Table 5.4.1. Second order rate constants for the reactions of furans with ozone in buffered water at pH 7. The ± error of each rate constant was calculated through error propagation from the 95% confidence interval of the slope of the linear fit and the error of the rate constant of the reference compound.

Compound	**Structure**	**k_{O3} (M^{-1} s^{-1}) at pH 7**	**Reference**
Substituted furan	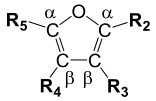		
Ranitidine (RAN)	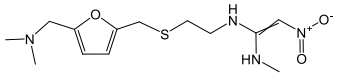	2.1×10^6	(21)
2,5-Dimethylfuran (DMF)	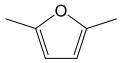	2.2×10^5	(21)
3-(2-Furyl)propanoic acid (FPA)	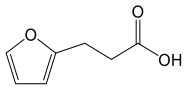	$(3.2 \pm 0.2) \times 10^6$	this study
2-Methyl-3-furoic acid (MFA)	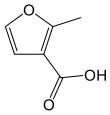	$(2.7 \pm 0.1) \times 10^6$	this study
Furosemide (FRS)	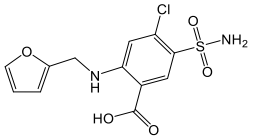	$(2.2 \pm 0.1) \times 10^6$	this study
Furfuryl alcohol (FFA)	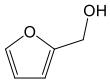	$(1.7 \pm 0.2) \times 10^6$	this study
3,4-Bis(hydroxymethyl)furan (BHF)		$(1.7 \pm 0.1) \times 10^6$	this study
2-Furoic acid (FA)	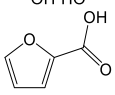	$(5.9 \pm 0.5) \times 10^5$	this study
Furan-2,5-dicarboxylic acid (FDCA)	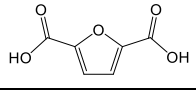	$(8.5 \pm 0.7) \times 10^4$	this study

RAN contains multiple sites contributing to its high ozone reactivity: the furan ring, a tertiary amine, a thioether and an acetamidine, which is the most reactive moiety (21). Similarly, the high rate constant of FRS can be attributed to both a furan ring and an aniline moiety. Based on QSAR calculations, the k_{O3} of FRS has been reported as 6.8×10^4 M^{-1} s^{-1} which was the sum of the contributions of the secondary

amine (pK_a = 3.8, k_{O3} = 6.2 × 10^4 M^{-1} s^{-1}) and the benzene ring (partly deactivated, k_{O3} = 6.5 × 10^3 M^{-1} s^{-1}) (42). This predicted k_{O3} of FRS is similar to the experimentally determined reactivity of compounds with a p-sulfonylaniline moiety (43). The QSAR model, however, did not consider the reactivity of the furan ring, which explains why the k_{O3} determined experimentally for FRS in this study (k_{O3} = 2.2 × 10^6 M^{-1} s^{-1}) is significantly higher than the value predicted by QSAR (42).

5.4.2 Transformation of furans by ozone in water

In addition to determining the ozonation kinetics of furans, the formation of transformation products was investigated. Of particular interest was the formation of α,β-unsaturated dicarbonyl compounds due to their potential toxicity and their recent identification in oxidative water treatment processes (30, 31). Ozonation products were detected either directly with LC-HRMS, or after derivatization with either NAL or a mixture of NAL and NAC (so called reactivity-directed analysis (RDA) assays) (35). OH radicals were not scavenged in these experiments in order to represent real ozonation conditions where both ozone and OH radicals are present.

Transformation of furan-containing pharmaceuticals. For FRS, seven ozonation products were detected (SI, Table 5.8.3 and Figure 5.8.11). The LC-HRMS results indicate that the benzene ring including the chlorine, sulfonamide and carboxyl moieties remained unmodified in all ozonation products. As such, oxidation of FRS can be exclusively attributed to the reaction of ozone with the furfurylamine group, with FRS-278 being the only detected compound that has been previously reported for the reaction with ozone (24). Based on the obtained results, the reaction of ozone with the α-carbon of the furan moiety is indicated to result in the opening of the furan ring (see Section 5.4.3 for more details), leading to the formation of an α,β-unsaturated dicarbonyl transformation product (FRS-347) which has been observed previously in oxidation of FRS in microsomes (44). Formation of FRS-328, which has been identified in the oxidation of FRS by dimethyldioxirane, can most likely be attributed to the intramolecular reaction between the ketoenal group and the amine moiety of FRS-347 (45). FRS-328 is also formed as a product of anodic and electro-Fenton oxidation of FRS (46, 47), and has been identified as a human metabolite of FRS with evidence that it is a physio-pathologically relevant neurodegeneration

inducer (48). LC-HRMS results obtained for FRS-265 indicate the presence of an additional methyl group compared to saluamine, an FRS hydrolysis product (47, 49). The formation of FRS-265 can be explained by cleavage of the substituent on the α-carbon after furan ring opening. The formation of the other transformation products can be explained by transformation of the furan and secondary amine moieties, leading to the formation of carbonyls (FRS-308, FRS-363) and hydroxylamines (FRS-266, FRS-308, FRS-363).

The chemical structures of the observed ozonation products suggest the relevance of two reaction pathways involving the opening of the furan ring (Figure 5.4.1). The NAL assay was used to assess whether α,β-unsaturated dicarbonyls (other than FRS-347) are formed from the transformation of FRS. BDA was detected as a BDA-NAL adduct, indicating the relevance of α,β-unsaturated dicarbonyl formation from the ozone oxidation of furan rings, even though yields were low (<0.1%). BDA and its substituted analogues have been identified as rat liver microsomal metabolites of furan and furan containing compounds (33, 34). The ozone dose-dependent formation of BDA and other FRS ozonation products is shown in SI, Figure 5.8.12.

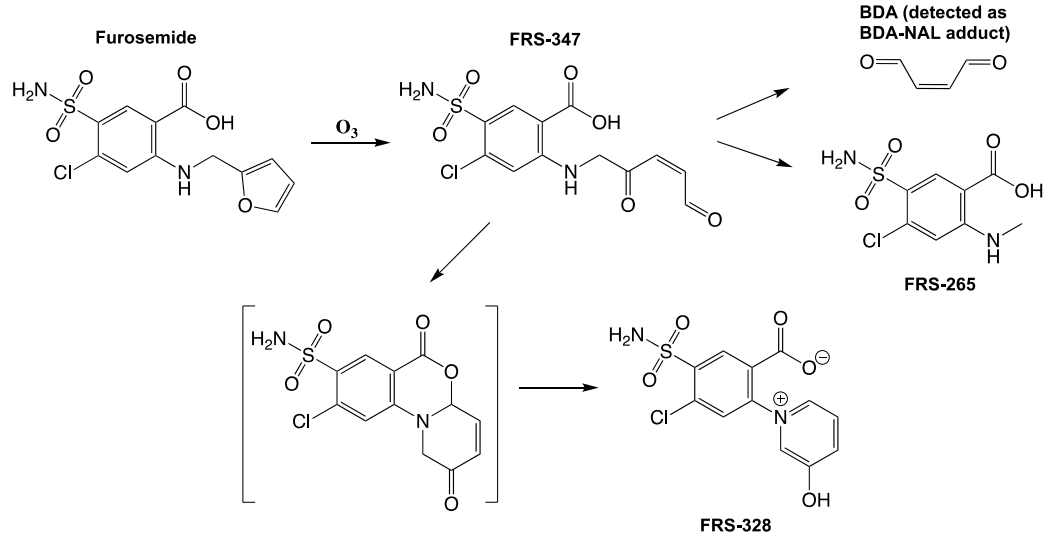

Figure 5.4.1. Proposed pathways of the ozonation of the furan ring of furosemide (FRS).

For RAN, twelve ozonation products were detected with two of them being formed by reaction of ozone with the furan ring (SI, Figures 5.8.13, 5.8.14, 5.8.15 and Table 5.8.4). Similar to results obtained by Christophoridis et al. (22), the LC-HRMS data indicate potential oxidation at different positions of the molecule. However, in

contrast to Christophoridis et al. who observed only one ozonation product containing an additional oxygen atom ($C_{13}H_{22}N_4O_4S$) and identified it as RAN-*S* oxide (22), two distinct peaks were detected in the present study. Based on the MS^2 fragment information of both peaks (Figure 5.8.14a and 5.8.14b), the first peak (retention time: 3.7 min) can most likely be attributed to RAN-*S* oxide and the second peak (retention time: 8.9 min) to RAN-*N* oxide. The formation of both *N*- and *S*-oxides is further supported by the detection of RAN-*S*&*N* oxide ($C_{13}H_{22}N_4O_5S$), which is also indicated by the MS^2 results for this compound (Figure 5.8.14c). The formation of other products also reveals the oxidation of the tertiary amine group (Figure 5.8.14e and 5.8.14h). Transformation products formed during the electrochemical oxidation of RAN have been shown to be more toxic than the parent compound (50), emphasizing the need to elucidate the properties of and the risk posed by the ozonation products of RAN.

Although all the RAN sub-structures react with ozone with high rates (21), the obtained results primarily demonstrated the formation of ozonation products in which the furan ring remains unmodified. The detection of RAN-252 and RAN-236 also indicated the oxidation of the furan moiety, leading to cleavage of parts of the molecule (Figure 5.8.14i and 5.8.14j). However, it is possible that more ozonation products resulting from oxidation of the furan ring were formed but could not be detected by LC-HRMS analysis. No α,β-unsaturated dicarbonyl products were detected directly or after derivatization by NAL or a NAL+NAC mixture, therefore dicarbonyls are either not formed from RAN or are degraded further.

Ozonation products of substituted furans. Based on the results of the furan-containing pharmaceuticals, the formation of α,β-unsaturated dicarbonyls (BDA and BDA-Rs) from simpler substituted furans was investigated to determine how different substituents impact the formation of these toxic by-products. The results for seven tested compounds are summarised in Table 5.4.2 and details are provided in the SI (Table 5.8.2 and Figures 5.8.4-5.8.10). Concentrations of BDA were determined using a reference standard. Due to the absence of reference standards, the yields of BDA-Rs were determined by comparing their peak areas with those obtained for BDA.

Table 5.4.2. Maximum yield of α,β-unsaturated dicarbonyls in the aqueous ozonation of substituted furans, based on the detection of NAL, NAC and NAL+NAC adducts.

Compound	Substituents				Dicarbonyl formed	Max. yield (%)
	R_2	R_3	R_4	R_5		
DMF	$-CH_3$	-H	-H	$-CH_3$	BDA(R_2)(R_5)	Not quantified
FPA	$-C_2H_4COOH$	-H	-H	-H	BDA BDA-R_2	<0.1 2.7
MFA	$-CH_3$	-COOH	-H	-H	BDA(R_2)(R_3)	5.6
FFA	$-CH_2OH$	-H	-H	-H	BDA BDA-R_2	2.4 0.5
BHF	-H	$-CH_2OH$	$-CH_2OH$	-H	BDA(R_3)(R_4)	<0.1
FA	-COOH	-H	-H	-H	BDA	6.7
FDCA	-COOH	-H	-H	-COOH	-	-

The yields of BDA and BDA analogues were strongly dependent on the substituents present in different furans. Ozonation of FFA led to the formation of BDA at a maximum molar yield of 2.4 % (Figure 5.4.2). This is comparable to the BDA yields formed from UV/H_2O_2 oxidation of phenol in water (30). Traces of BDA were also detected in the reaction solutions before the addition of ozone. This indicates the potential formation of BDA via hydrolysis of FFA, which aligns with previous reports on the acid-catalyzed hydrolysis of furans (51). Besides BDA, a second C_4-dicarbonyl compound containing an additional hydroxymethyl group (NAL adduct $C_{13}H_{21}O_5N_2$, m/z 285.1444) was identified in experiments with FFA (BDA-R in Figure 5.4.2). The maximum relative yield of this compound was approximately 0.5%. The MS^2 spectrum of this adduct (SI, Figure 5.8.5) contained characteristic masses (m/z 84.0813 and 126.0914) previously observed for NAL adducts of other dicarbonyls (30). Ozonation of BHF did not lead to BDA formation, despite the structural similarity of BHF and FFA. However, the formation of a NAL adduct with m/z 315.1548 was detected in trace amounts, which can be attributed to the formation of a dialdehyde containing two hydroxymethyl substituents (SI, Figure 5.8.6).

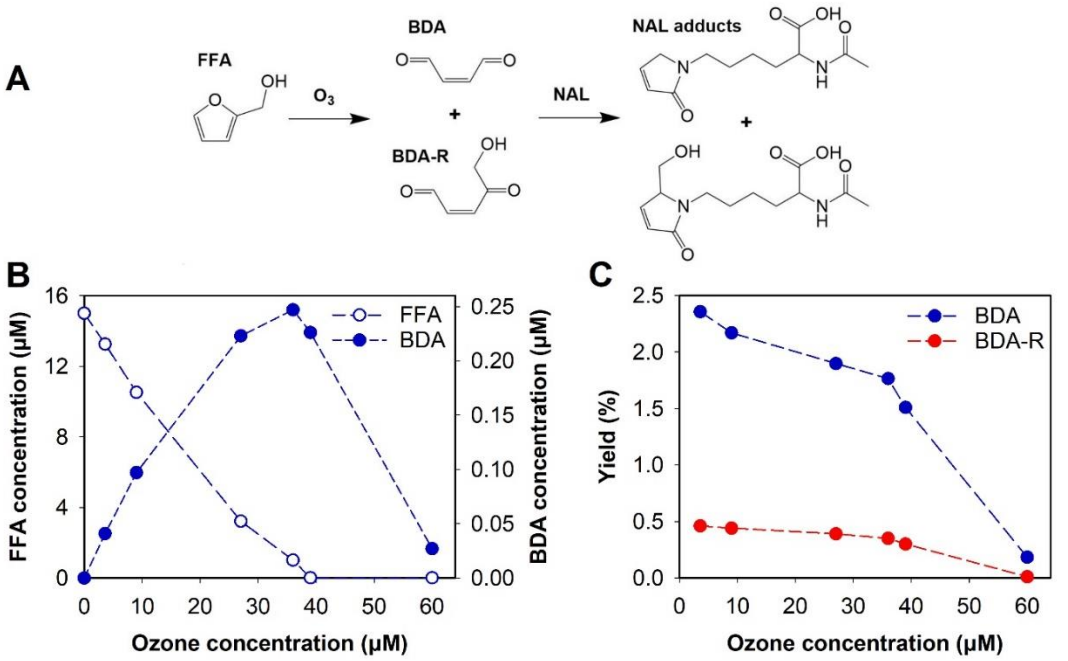

Figure 5.4.2. A. Chemical structures of furfuryl alcohol (FFA) and its dicarbonyl ozonation products based on the formation of NAL adducts. B. Concentration of FFA and 2-butene-1,4-dial (BDA) versus the ozone concentration. C. Molar yield of BDA and hydroxymethyl-BDA (BDA-R) determined by standard addition using a BDA reference standard. Conditions: FFA initial concentration 15 µM, in 10 mM phosphate buffer at pH 7.

BDA was also identified as an ozonation product of FA, at higher molar yields of approximately 7%. No other NAL adducts were detected in FA experiments. For MFA, a BDA analogue with a carboxyl and a methyl group attached was detected (Figures 5.4.3 and 5.8.8), while the ozonation of FPA led to formation of both BDA and a dicarbonyl with a propanoic acid group attached (Figures 5.4.3 and 5.8.7). The BDA molar yield was less than 0.1% in the case of FPA, while the propanoic acid-substituted BDA analogue appeared to be a more important ozonation product with a maximum yield of 2.7%. No NAL or NAC adducts were detected in ozonation of FDCA, in agreement with the results observed for RAN, indicating that the presence of two carboxyl substituents impacts both the reaction kinetics and the ozonation pathway.

The absence of a dimethylated BDA analogue in experiments with DMF can most likely be explained by the inability of this compound to react with NAL in the same way as the other dicarbonyl compounds detected, due to the presence of methyl substituents at both α-carbons. To verify this, additional experiments in the presence of both NAL and NAC were performed and revealed the formation of both NAC and

NAL+NAC adducts (SI, Figures 5.8.9 and 5.8.10). In contrast to NAL which primarily reacts with α,β-unsaturated dicarbonyl compounds via Schiff base formation (i.e. reaction at the carbonyl carbon), reactions of thiols can be attributed to Michael addition (i.e. reaction at the double bond adjacent to the carbonyl group) (52). The formed thiol adducts can then react in a second step with NAL yielding pyrrole products (SI, Figure 5.8.16).

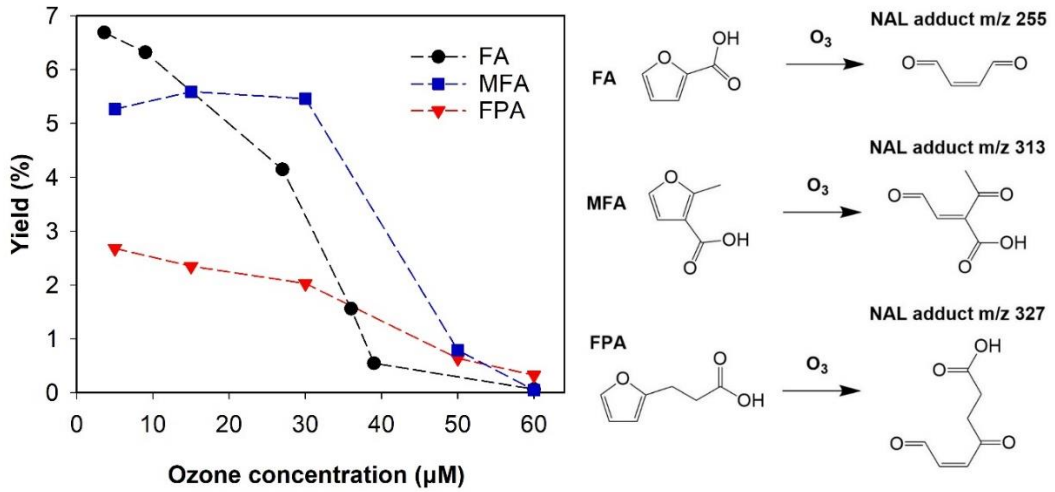

Figure 5.4.3. Molar yields of three α,β-unsaturated dicarbonyls formed in experiments with furan-containing acids at different ozone concentrations. Conditions: furan acid initial concentration 15 µM, in 10 mM phosphate buffer at pH 7. Yields were determined by standard addition using a 2-butene-1,4-dial (BDA) reference standard for all three compounds. For MFA, the ionization fragment m/z 269 was used for calculation of yields due to higher intensity.

The obtained results demonstrate the relevance of toxic α,β-unsaturated dicarbonyl compounds as ozonation products of furans. The yields are generally low (<7%), thus indicating the simultaneous formation of other ozonation products. In addition, the results show that BDA and BDA analogues can be transformed further by ozone (SI, Figure 5.8.3). In the gas phase, BDA reacts with ozone with a rate constant of 1.6×10^{-18} cm^3 $molecule^{-1}$ s^{-1} (53). Based on gas-phase ozonation studies of BDA and other related compounds, the products formed from the further oxidation of BDA include formaldehyde, glyoxal and methylglyoxal (53, 54). These were not analysed in this study, but are the subject of ongoing investigations.

5.4.3 Mechanism for the reaction of furans with ozone leading to α,β-unsaturated dicarbonyls

Even though no information is available about the transformation of furans by ozone in water, previous studies performed in organic solvents have suggested the potential contribution of different reaction mechanisms leading to opening of the furan ring (25, 26, 28). Our detection of C_4 dicarbonyls (BDA analogues) confirms the importance of electrophilic ozone attack at the reactive α-C positions of the furan ring, via reaction of ozone with either one or both α-carbons (Figure 5.4.4) (29). The yields of BDA and substituted BDA analogues, however, suggest ozonolysis of furans via reaction with the α-β double bonds as dominant reaction pathway and/or further reactions of the C_4 dicarbonyls with ozone.

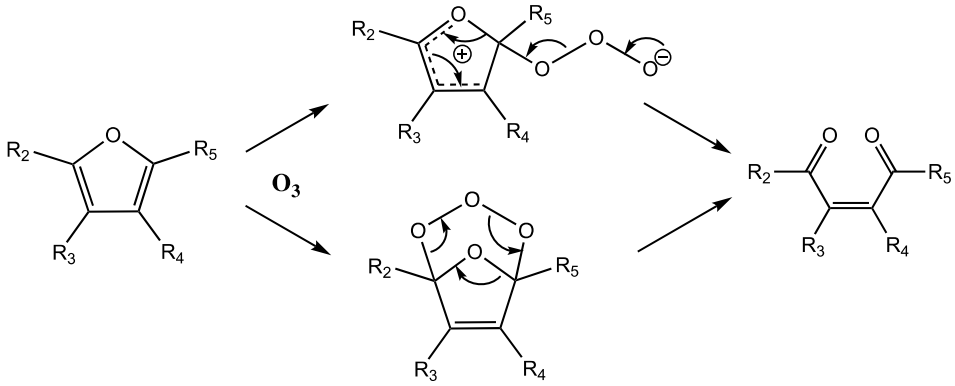

Figure 5.4.4. Postulated mechanism for the reaction of furans with ozone leading to formation of 2-butene-1,4-dial (BDA) and its analogues (BDA-R).

Similar to reaction kinetics, the obtained results further indicate that the yield and type of the formed α-β-unsaturated dicarbonyls strongly depend on the substituents of the parent compound and their position on the furan ring. Two of the tested compounds, MFA and BHF, have substituents on the β-carbon of the furan ring (labelled as R_3 and R_4 in Tables 5.4.1 and 5.4.2). Both the carboxyl group of MFA and the hydroxymethyl groups of BHF were retained on the formed dicarbonyl compounds after ring opening (Table 5.4.2). The results of furans containing substituents on the α-carbon (labelled as R_2 and R_5 in Tables 5.4.1 and 5.4.2) are less consistent. For the ozonation of 2,5-diarylfurans in organic solvents, dicarbonyls containing aryl substituents on both carbonyl carbons have been reported (27, 28). As demonstrated in this study, a similar mechanism is also relevant under aqueous conditions for MFA, FPA and DMF, all of which formed dicarbonyls with their α-C

substituents still attached (Table 5.4.2). This indicates that the reaction of ozone with furans containing alkyl substituents on the α-carbon also results in the formation of BDA analogues with the substituents retained. In contrast, results obtained for furans containing either hydroxymethyl or carboxylic acid substituents at one of the α-carbons, indicate the relevance of reactions leading to the cleavage of the substituent and the formation of BDA. This is particularly true for FA for which only the formation of BDA but not BDA-R was observed. The differences in yield of BDA versus BDA-R for FA, FFA and FPA reveal the significant influence of these α-C substituents on the mechanism of BDA formation. However, based on current evidence, it is unclear whether the substituent on the α-carbon is removed before, after or simultaneously with the opening of the furan ring.

Differences in the degradation of FFA and BDA in experiments performed in the presence and absence of *tert*-butanol as a OH radical scavenger (SI, Figure 5.8.3) were minor. However, the presence of *tert*-butanol appeared to have some effect on the formed concentration of BDA and BDA-R (SI, Figure 5.8.2). The increased formation in the absence of *tert*-butanol indicates that BDA analogues can be formed both from reactions with ozone and with OH radicals.

5.5 Conclusions

The selected organic compounds containing furan rings have a high ozone reactivity and are therefore expected to be efficiently eliminated in water and wastewater ozonation treatment. Further research is required to elucidate the effect of deactivating substituents, such as halogens, on the ozonation rate constant of furans.

In complex water matrices containing various furan-bearing compounds, ozonation is likely to result in the formation of a mixture of α,β-unsaturated dicarbonyls. Depending on the applied ozone dose, the dicarbonyls may decompose into smaller aldehydes and carboxylic acids. Future studies will focus on the detection of these further transformation products in real water treatment systems. In addition, it needs to be assessed whether α,β-unsaturated dicarbonyls can be removed during post-treatment steps, for example activated carbon and biofiltration.

The formation of α,β-unsaturated dicarbonyls such as BDA and its analogues, though only representing a small portion of transformation products from ozonation of furans, is a possible health concern due to their reported toxicity. Furans play an increasing role as 'green chemicals' and are also formed by natural processes in the aquatic environment. The obtained results highlight the necessity to investigate the fate of these compounds in water treatment systems to assess the potential exposures to toxic by-products.

5.6 Acknowledgements

ZZ and GAZ contributed equally to this study. GAZ was supported by a University of Bath (UoB) research scholarship and an EPSRC funded Integrated PhD studentship in Sustainable Chemical Technologies: EP/L016354/1. Additional funding for the research visit of GAZ at Johns Hopkins University was provided by the UoB Doctoral College Placement Support Fund. We further thank Nadezda Ojeda for technical assistance with the ozonation experiments.

5.7 References

1. Keay BA, Dibble PW. 2.08 - Furans and their Benzo Derivatives: Applications. In: Katritzky AR, Rees CW, Scriven EFV, editors. Comprehensive Heterocyclic Chemistry II. Oxford: Pergamon; 1996. p. 395-436.

2. Eldeeb M, Akih-Kumgeh B. Recent Trends in the Production, Combustion and Modeling of Furan-Based Fuels. Energies. 2018;11(3):512.

3. Gandini A, Lacerda TM, Carvalho AJF, Trovatti E. Progress of Polymers from Renewable Resources: Furans, Vegetable Oils, and Polysaccharides. Chem Rev. 2016;116(3):1637-69.

4. Tong X, Ma Y, Li Y. Biomass into chemicals: Conversion of sugars to furan derivatives by catalytic processes. Applied Catalysis A: General. 2010;385(1):1-13.

5. Mariscal R, Maireles-Torres P, Ojeda M, Sádaba I, López Granados M. Furfural: a renewable and versatile platform molecule for the synthesis of chemicals and fuels. Energy & Environmental Science. 2016;9(4):1144-89.

6. Huber SG, Wunderlich S, Schöler HF, Williams J. Natural Abiotic Formation of Furans in Soil. Environmental Science & Technology. 2010;44(15):5799-804.

7. Wang B, Wang L, Li Y, Liu Y. Heterocyclic terpenes: linear furano- and pyrroloterpenoids. RSC Advances. 2014;4(24):12216-34.

8. Hannemann K, Puchta V, Simon E, Ziegler H, Ziegler G, Spiteller G. The common occurrence of furan fatty acids in plants. Lipids. 1989;24(4):296-8.

9. Kostich MS, Batt AL, Lazorchak JM. Concentrations of prioritized pharmaceuticals in effluents from 50 large wastewater treatment plants in the US and implications for risk estimation. Environ Pollut. 2014;184:354-9.

10. Jelic A, Gros M, Ginebreda A, Cespedes-Sánchez R, Ventura F, Petrovic M, Barcelo D. Occurrence, partition and removal of pharmaceuticals in sewage water and sludge during wastewater treatment. Water Research. 2011;45(3):1165-76.

11. Kasprzyk-Hordern B, Dinsdale RM, Guwy AJ. The occurrence of pharmaceuticals, personal care products, endocrine disruptors and illicit drugs in surface water in South Wales, UK. Water Research. 2008;42(13):3498-518.

12. Gottschalk C, Libra JA, Saupe A. Ozonation of water and waste water: A practical guide to understanding ozone and its applications: John Wiley & Sons; 2009.

13. von Gunten U. Ozonation of drinking water: Part I. Oxidation kinetics and product formation. Water Research. 2003;37(7):1443-67.

14. von Sonntag C, von Gunten U. Chemistry of ozone in water and wastewater treatment: IWA publishing; 2012.

15. Hübner U, von Gunten U, Jekel M. Evaluation of the persistence of transformation products from ozonation of trace organic compounds – A critical review. Water Research. 2015;68:150-70.

16. Lee Y, von Gunten U. Advances in predicting organic contaminant abatement during ozonation of municipal wastewater effluent: reaction kinetics, transformation products, and changes of biological effects. Environmental Science: Water Research & Technology. 2016;2(3):421-42.

17. von Gunten U. Oxidation Processes in Water Treatment: Are We on Track? Environ Sci Technol. 2018;52(9):5062-75.

18. Schlüter-Vorberg L, Prasse C, Ternes TA, Mückter H, Coors A. Toxification by Transformation in Conventional and Advanced Wastewater Treatment: The Antiviral Drug Acyclovir. Environmental Science & Technology Letters. 2015;2(12):342-6.

19. Pohl J, Golovko O, Carlsson G, Eriksson J, Glynn A, Orn S, Weiss J. Carbamazepine Ozonation Byproducts: Toxicity in Zebrafish (Danio rerio) Embryos and Chemical Stability. Environ Sci Technol. 2020;54(5):2913-21.

20. Zoumpouli GA, Siqueira Souza F, Petrie B, Féris LA, Kasprzyk-Hordern B, Wenk J. Simultaneous ozonation of 90 organic micropollutants including illicit drugs and their metabolites in different water matrices. Environmental Science: Water Research & Technology. 2020;6(9):2465-78.

21. Jeon D, Kim J, Shin J, Hidayat ZR, Na S, Lee Y. Transformation of ranitidine during water chlorination and ozonation: Moiety-specific reaction kinetics and elimination efficiency of NDMA formation potential. Journal of Hazardous Materials. 2016;318:802-9.

22. Christophoridis C, Nika MC, Aalizadeh R, Thomaidis NS. Ozonation of ranitidine: Effect of experimental parameters and identification of transformation products. Sci Total Environ. 2016;557-558:170-82.

23. Zou R, Liao X, Zhao L, Yuan B. Reduction of *N*-nitrosodimethylamine formation from ranitidine by ozonation preceding chloramination: influencing factors and mechanisms. Environ Sci Pollut Res Int. 2018;25(14):13489-98.

24. Aalizadeh R, Nika MC, Thomaidis NS. Development and application of retention time prediction models in the suspect and non-target screening of emerging contaminants. J Hazard Mater. 2019;363:277-85.

25. Bailey PS, Colomb HO. 1,4-Addition of ozone to furans and pyrroles. J Am Chem Soc. 1957;79(15):4238-.

26. Jibben BP, Wibaut JP. The ozonisation and the ozonolysis of furan and of some methylated furans in connection with the reactivities of the bonds in the ringsystem. Recl Trav Chim Pays-Bas. 1960;79(4):342-60.

27. White HM, Colomb HO, Bailey PS. Ozonation of 2,5-Diphenylfuran1. The Journal of Organic Chemistry. 1965;30(2):481-6.

28. Bailey PS, White HM, Colomb HO. Ozonation of Diarylfurans. The Journal of Organic Chemistry. 1965;30(2):487-91.

29. Bailey PS. Chapter VI - Ozonation of Aromatic Compounds: Heterocyclics. In: Bailey PS, editor. Ozonation in Organic Chemistry: Academic Press; 1982. p. 111-54.

30. Prasse C, Ford B, Nomura DK, Sedlak DL. Unexpected transformation of dissolved phenols to toxic dicarbonyls by hydroxyl radicals and UV light. Proc Natl Acad Sci U S A. 2018;115(10):2311-6.

31. Prasse C, von Gunten U, Sedlak DL. Chlorination of Phenols Revisited: Unexpected Formation of α,β-Unsaturated C_4-Dicarbonyl Ring Cleavage Products. Environmental Science & Technology. 2020;54(2):826-34.

32. Ravindranath V, Burka LT, Boyd MR. Reactive metabolites from the bioactivation of toxic methylfurans. Science. 1984;224(4651):884.

33. Chen L-J, Hecht SS, Peterson LA. Identification of *cis*-2-Butene-1,4-dial as a Microsomal Metabolite of Furan. Chem Res Toxicol. 1995;8(7):903-6.

34. Peterson LA. Reactive metabolites in the biotransformation of molecules containing a furan ring. Chem Res Toxicol. 2013;26(1):6-25.

35. Prasse C. Reactivity-directed analysis – a novel approach for the identification of toxic organic electrophiles in drinking water. Environmental Science: Processes & Impacts. 2021.

36. Buxton GV, Greenstock CL, Helman WP, Ross AB. Critical Review of rate constants for reactions of hydrated electrons, hydrogen atoms and hydroxyl radicals (·OH/·O− in Aqueous Solution. J Phys Chem Ref Data. 1988;17(2):513-886.

37. Prasse C, Wagner M, Schulz R, Ternes TA. Biotransformation of the antiviral drugs acyclovir and penciclovir in activated sludge treatment. Environ Sci Technol. 2011;45(7):2761-9.

38. Lee Y, von Gunten U. Quantitative structure–activity relationships (QSARs) for the transformation of organic micropollutants during oxidative water treatment. Water Research. 2012;46(19):6177-95.

39. Arena G, Cali R, Maccarone E, Passerini A. Thermodynamics of protonation of some five-membered heteroaryl-carboxylates, -alkanoates and -trans-propenoates. Journal of the Chemical Society, Perkin Transactions 2. 1993(10):1941-5.

40. Hansch C, Leo A, Taft RW. A survey of Hammett substituent constants and resonance and field parameters. Chem Rev. 1991;91(2):165-95.

41. Lee M, Zimmermann-Steffens SG, Arey JS, Fenner K, von Gunten U. Development of Prediction Models for the Reactivity of Organic Compounds with Ozone in Aqueous Solution by Quantum Chemical Calculations: The Role of Delocalized and Localized Molecular Orbitals. Environmental Science & Technology. 2015;49(16):9925-35.

42. Lee Y, Kovalova L, McArdell CS, von Gunten U. Prediction of micropollutant elimination during ozonation of a hospital wastewater effluent. Water Research. 2014;64:134-48.

43. Dodd MC, Buffle M-O, von Gunten U. Oxidation of Antibacterial Molecules by Aqueous Ozone: Moiety-Specific Reaction Kinetics and Application to Ozone-Based Wastewater Treatment. Environmental Science & Technology. 2006;40(6):1969-77.

44. Williams DP, Antoine DJ, Butler PJ, Jones R, Randle L, Payne A, Howard M, Gardner I, Blagg J, Park BK. The Metabolism and Toxicity of Furosemide in the Wistar Rat and CD-1 Mouse: a Chemical and Biochemical Definition of the Toxicophore. J Pharmacol Exp Ther. 2007;322(3):1208-20.

45. Chen L-J, Burka LT. Chemical and Enzymatic Oxidation of Furosemide: Formation of Pyridinium Salts. Chem Res Toxicol. 2007;20(12):1741-4.

46. Laurencé C, Rivard M, Lachaise I, Bensemhoun J, Martens T. Preparative access to transformation products (TPs) of furosemide: a versatile application of anodic oxidation. Tetrahedron. 2011;67(49):9518-21.

47. Laurence C, Rivard M, Martens T, Morin C, Buisson D, Bourcier S, Sablier M, Oturan MA. Anticipating the fate and impact of organic environmental contaminants: a new approach applied to the pharmaceutical furosemide. Chemosphere. 2014;113:193-9.

48. Laurence C, Zeghbib N, Rivard M, Lehri-Boufala S, Lachaise I, Barau C, Le Corvoisier P, Martens T, Garrigue-Antar L, Morin C. A new human pyridinium metabolite of furosemide, inhibitor of mitochondrial complex I, is a candidate inducer of neurodegeneration. Biochem Pharmacol. 2019;160:14-23.

49. Cruz JE, Maness DD, Yakatan GJ. Kinetics and mechanism of hydrolysis of furosemide. Int J Pharm. 1979;2(5):275-81.

50. Olvera-Vargas H, Oturan N, Brillas E, Buisson D, Esposito G, Oturan MA. Electrochemical advanced oxidation for cold incineration of the pharmaceutical ranitidine: Mineralization pathway and toxicity evolution. Chemosphere. 2014;117:644-51.

51. Stamhuis EJ, Drenth W, van den Berg H. Mechanism of reactions of furans I: A kinetic study of the acid-catalyzed hydrolysis of furan and 2,5-dimethylfuran. Recl Trav Chim Pays-Bas. 1964;83(2):167-76.

52. LoPachin RM, Gavin T. Molecular Mechanisms of Aldehyde Toxicity: A Chemical Perspective. Chem Res Toxicol. 2014;27(7):1081-91.

53. Liu X, Jeffries HE, Sexton KG. Atmospheric Photochemical Degradation of 1,4-Unsaturated Dicarbonyls. Environmental Science & Technology. 1999;33(23):4212-20.

54. Tuazon EC, Atkinson R, Carter WPL. Atmospheric chemistry of *cis*- and *trans*-3-hexene-2,5-dione. Environmental Science & Technology. 1985;19(3):265-9.

5.8 Supplementary information

5.8.1 Ozonation experiments

The competition kinetics experiments were performed in 20-mL amber glass vials. The reaction solutions (10 or 15 mL) contained 7 μM of the target compound (TC), 7 μM of the reference compound (RC, RAN or FA), 10 mM phosphate buffer (pH 7) and 10 mM *tert*-butanol in ultrapure water. Ozone stock solution was added to achieve concentrations of 1 to 13 μM ozone (0.1 to 0.9 μM O_3/μM target plus reference compound). Samples were magnetically stirred during the addition of the ozone stock solution and then left overnight at room temperature until complete ozone depletion. Residual concentrations of the target and reference compounds were measured within 24 hours. The second order rate constant for the reaction of the target compound with ozone ($k_{O3,TC}$) was calculated from the plot of the natural logarithm of the relative concentration of target compound versus the natural logarithm of the relative concentration of reference compound (see Figure 5.8.1), according to equation 5.8.1 (1).

$$\ln\left(\frac{[TC]}{[TC]_0}\right) = \frac{k_{O_3,TC}}{k_{O_3,RC}} \ln\left(\frac{[RC]}{[RC]_0}\right) \qquad (5.8.1)$$

The ± error of each rate constant was calculated through error propagation from the 95% confidence interval of the slope of the linear fit and the estimated error of $k_{O3,\,RAN}$ ($\pm\ 0.1 \times 10^6\ M^{-1}\ s^{-1}$) (2), or the calculated error of $k_{O3,\,FA}$.

To prepare the concentrated ozone stock solution for either batch ozonation experiments or competition kinetics, two different systems were used. One was a 500-mL glass reactor that was equipped with a gas diffuser and a water jacket, with the temperature of the recirculating water in the jacket set to 2°C. The other was a 1-L glass bottle placed in an ice bath. Both systems were fed with oxygen containing 50 to 100 mg L^{-1} ozone, produced with either a BMT 803N ozone generator (Messtechnik GmbH) or an IOCS integrated ozone system (Pacific Ozone). The dissolved ozone concentration of the ozone stock solution (20 to 30 mg L^{-1}) was measured spectrophotometrically both before and after its addition into the reaction solutions, either directly at 258 nm (molar absorptivity of ozone ε=2900 $M^{-1}\ cm^{-1}$) or with the indigo method (3).

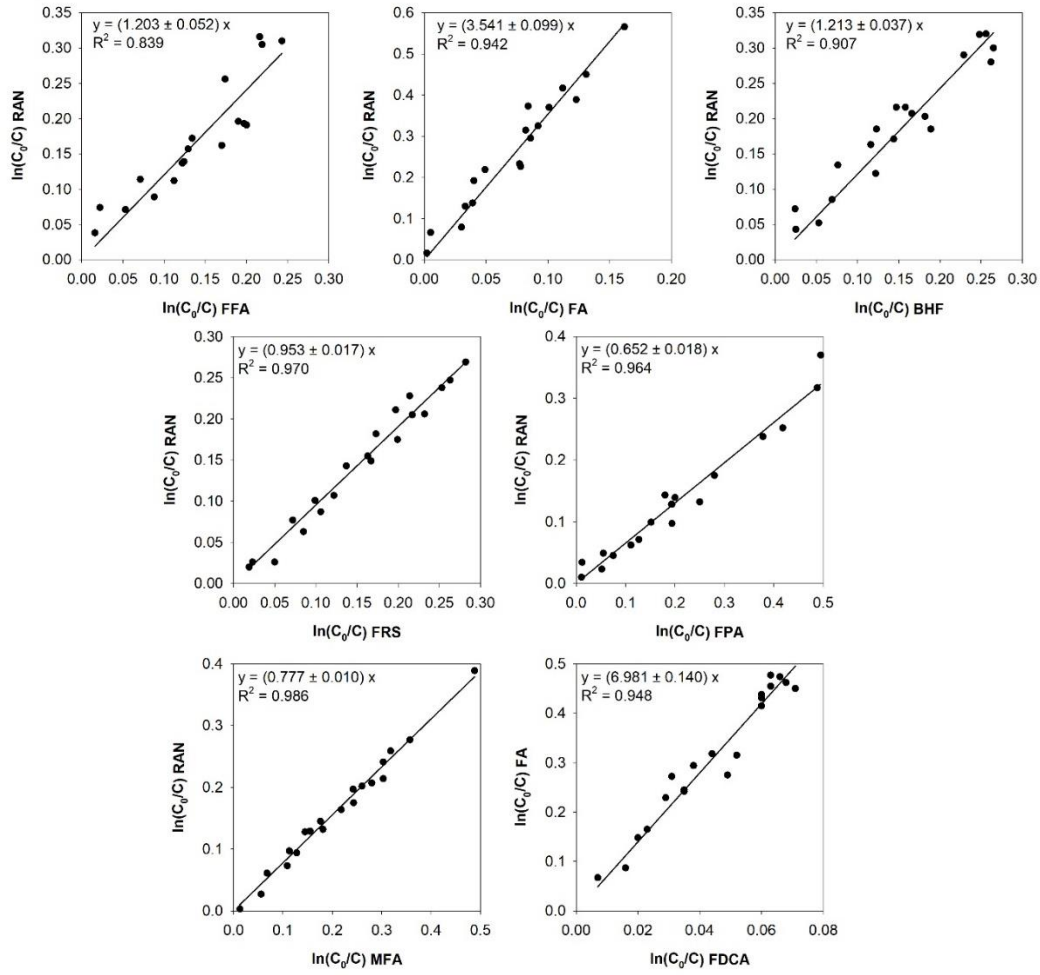

Figure 5.8.1. Plot of the natural logarithm of the relative concentration of the reference compound (RAN or FA) versus the natural logarithm of the relative concentration of the target compound (FFA, FA, FRS, FPA, MFA, BHF, FDCA). Linear fit equations are shown including the standard error of the slope.

5.8.2 Liquid chromatography-high resolution mass spectrometry

For chromatographic separation the gradient program was at 75 μL min^{-1} with ultrapure water containing 0.1 % formic acid (A) and methanol (B). The percentage of A was: 0-3 min, 100%; 3-12 min, linear decrease from 100% to 5%; 12-14 min, 5%; 14.1 min, 100%, total run time 20 min. The injection volume was 10 μL.

The Electrospray ionization (ESI) source parameters were set as follows. Sheath gas flow rate: 20 arbitrary units (AU); aux gas flow rate: 10 AU; spray voltage: 3.8 kV for positive mode and 2.5 kV for negative mode; capillary temperature: 250°C; S-lens RF level: 60; aux gas heater temperature: 100°C. Data-dependent acquisition

was used to conduct MS^2 experiments. Full scan (50-700 m/z, resolution > 120000) was performed followed by data-dependent MS^2 for the 5 most intense ions with resolution > 60000. Collision induced dissociation (CID) with stepped normalized collision energy of 10%, 30% and 50% was used for fragmentation with an isolation window of 1.0 m/z.

Table 5.8.1. HPLC-UV parameters for the detection of furans in competition kinetics experiments. Flow rate 0.5 mL min^{-1}, A: ultrapure water with 0.1 % v/v formic or phosphoric acid, B: acetonitrile.

Compound	A/B (%/%)	Retention time (min)	Detection wavelength (nm)
Furfuryl alcohol (FFA)	90/10	2.9	216
2-Furoic acid (FA)	90/10	3.3	252
2-Methyl-3-furoic acid (MFA)	70/30	2.6	245
3-(2-Furyl)propanoic acid (FPA)	70/30	2.9	220
Furosemide (FRS)	60/40	3.0	228
Ranitidine (RAN)	90/10	2.2	320
Nitrofurantoin (NFT)	70/30	2.1	366
Furan-2,5-dicarboxylic acid (FDCA)	90/10	2.5	265
3,4-Bis(hydroxymethyl)furan (BHF)	90/10	1.8	215

Table 5.8.2. NAL, NAC and NAL+NAC adducts detected in this study with LC-HRMS.

Parent compound	Amino acid added	Adduct m/z (observed)	m/z error (ppm)	Adduct formula $[M+H]^+$	Dicarbonyl formula
FFA, FA, FPA, FRS	NAL	255.1338	-0.39	$C_{12}H_{19}O_4N_2$	$C_4H_4O_2$
FFA	NAL	285.1444	-0.35	$C_{13}H_{21}O_5N_2$	$C_5H_6O_3$
FPA	NAL	327.1549	-0.61	$C_{15}H_{23}O_6N_2$	$C_7H_8O_4$
MFA	NAL	313.1391	-0.96	$C_{14}H_{21}O_6N_2$	$C_6H_6O_4$
BHF	NAL	315.1548	-0.95	$C_{14}H_{23}O_6N_2$	$C_6H_8O_4$
DMF	NAC	276.0899	-0.36	$C_{11}H_{18}O_5NS$	$C_6H_8O_2$
DMF	NAL+NAC	428.1852	0.48	$C_{19}H_{30}O_6N_3S$	$C_6H_8O_2$

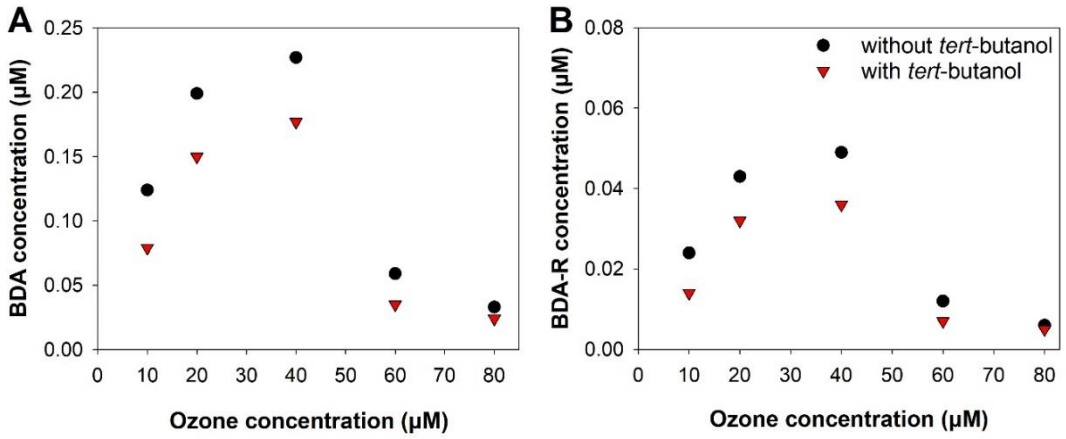

Figure 5.8.2. Effect of *tert*-butanol addition on the formation of A) BDA and B) BDA-R (hydroxymethyl-BDA) during the ozonation of FFA. FFA initial concentration 15 μM, *tert*-butanol concentration 10 mM, in 10 mM phosphate buffer at pH 7.

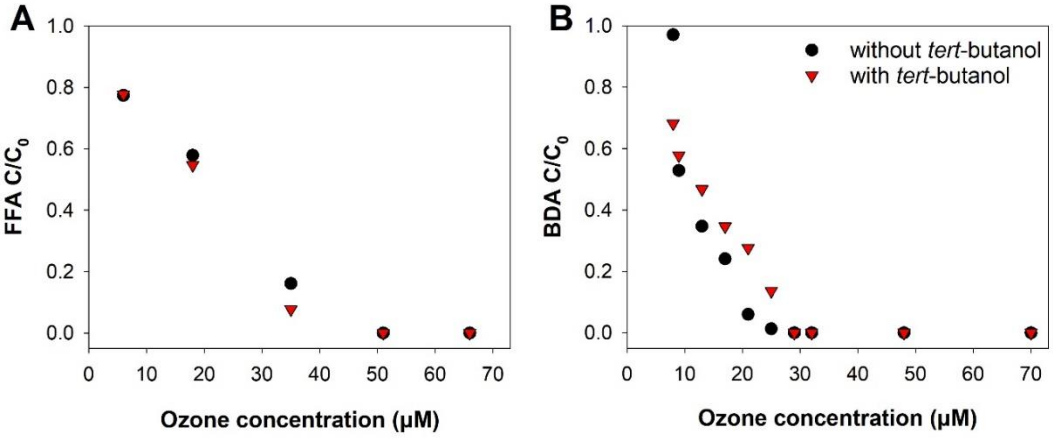

Figure 5.8.3. Degradation of A) FFA and B) BDA at different ozone concentrations, with or without addition of 10 mM *tert*-butanol, in 10 mM phosphate buffer at pH 7.

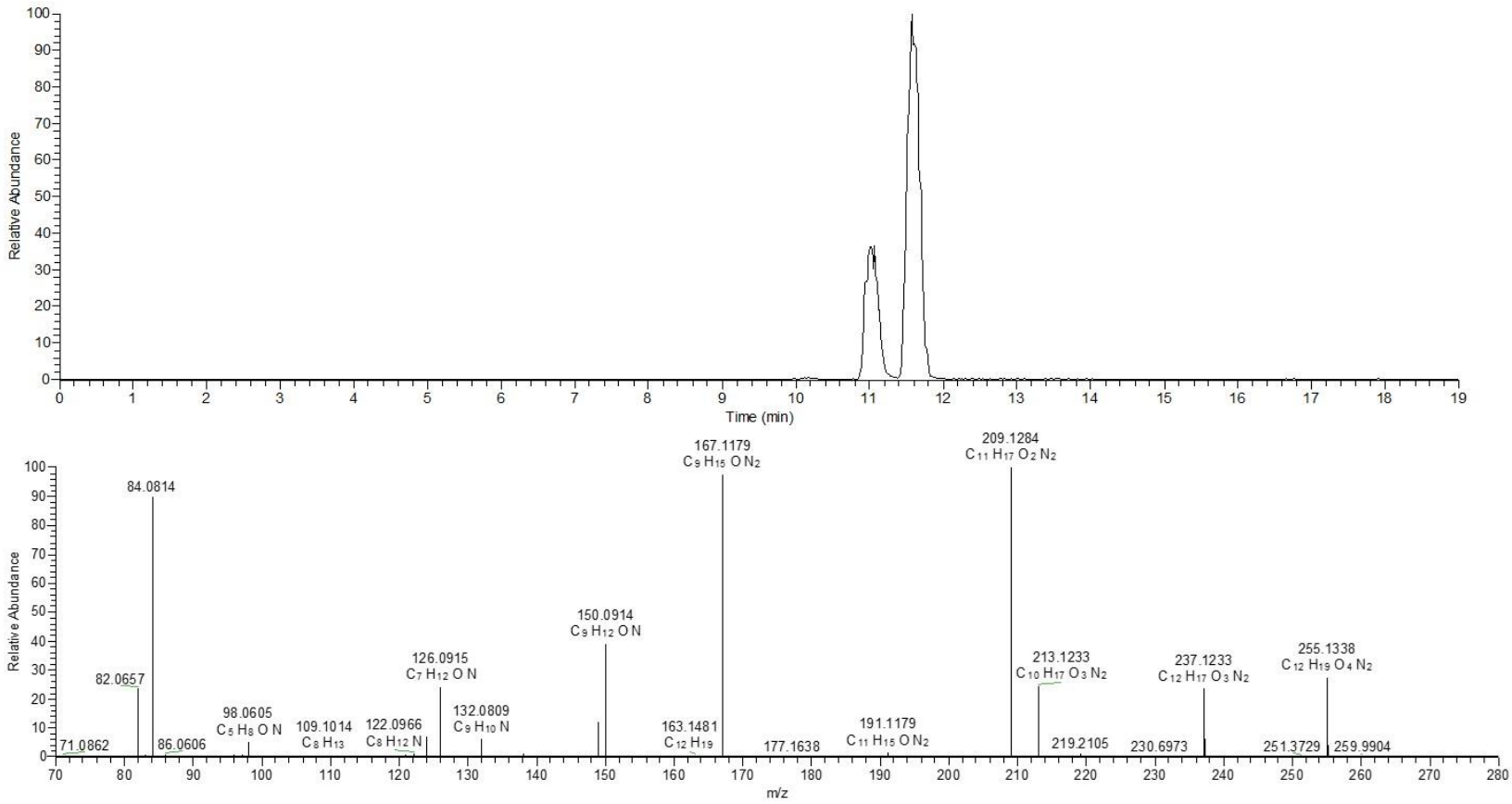

Figure 5.8.4. Base peak chromatogram and MS^2 spectrum of m/z 255 (NAL adduct of BDA) identified in ozonation experiments with furfuryl alcohol (15 μM initial concentration).

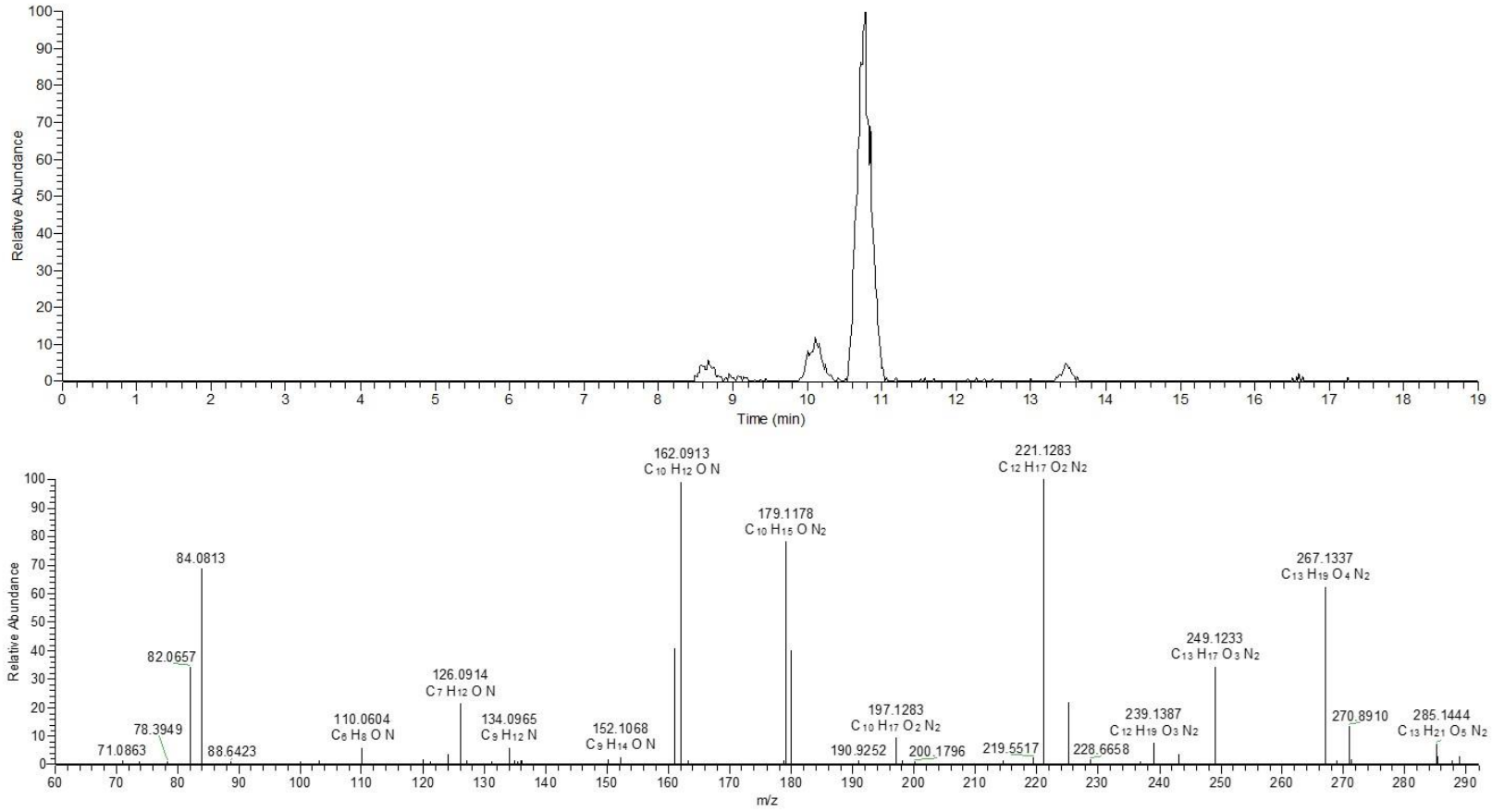

Figure 5.8.5. Base peak chromatogram and MS^2 spectrum of m/z 285 identified in ozonation experiments with furfuryl alcohol (15 μM initial concentration).

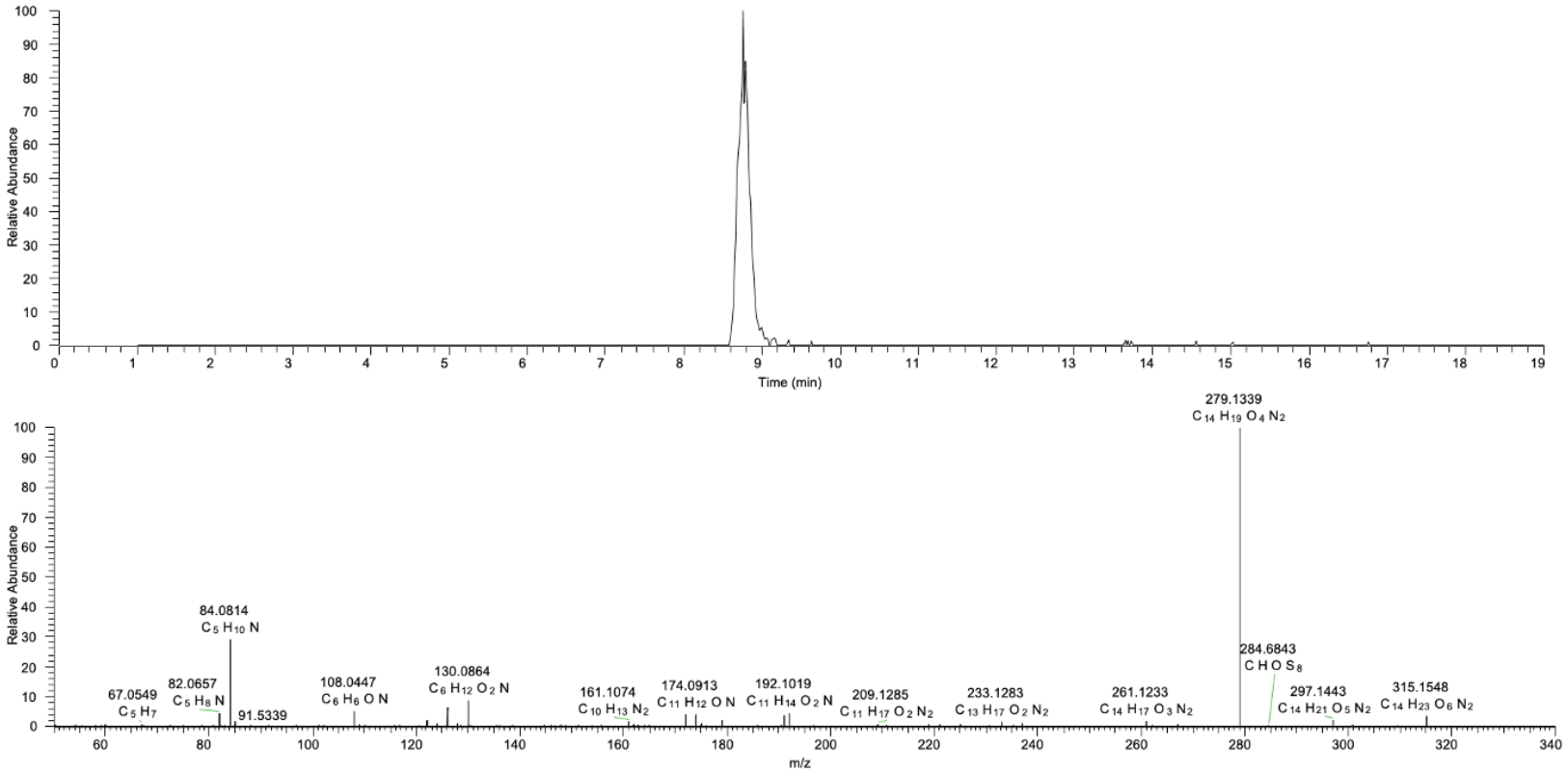

Figure 5.8.6. Base peak chromatogram and MS^2 spectrum of m/z 315 identified in ozonation experiments with 3,4-bis(hydroxymethyl)furan (100 μM initial concentration).

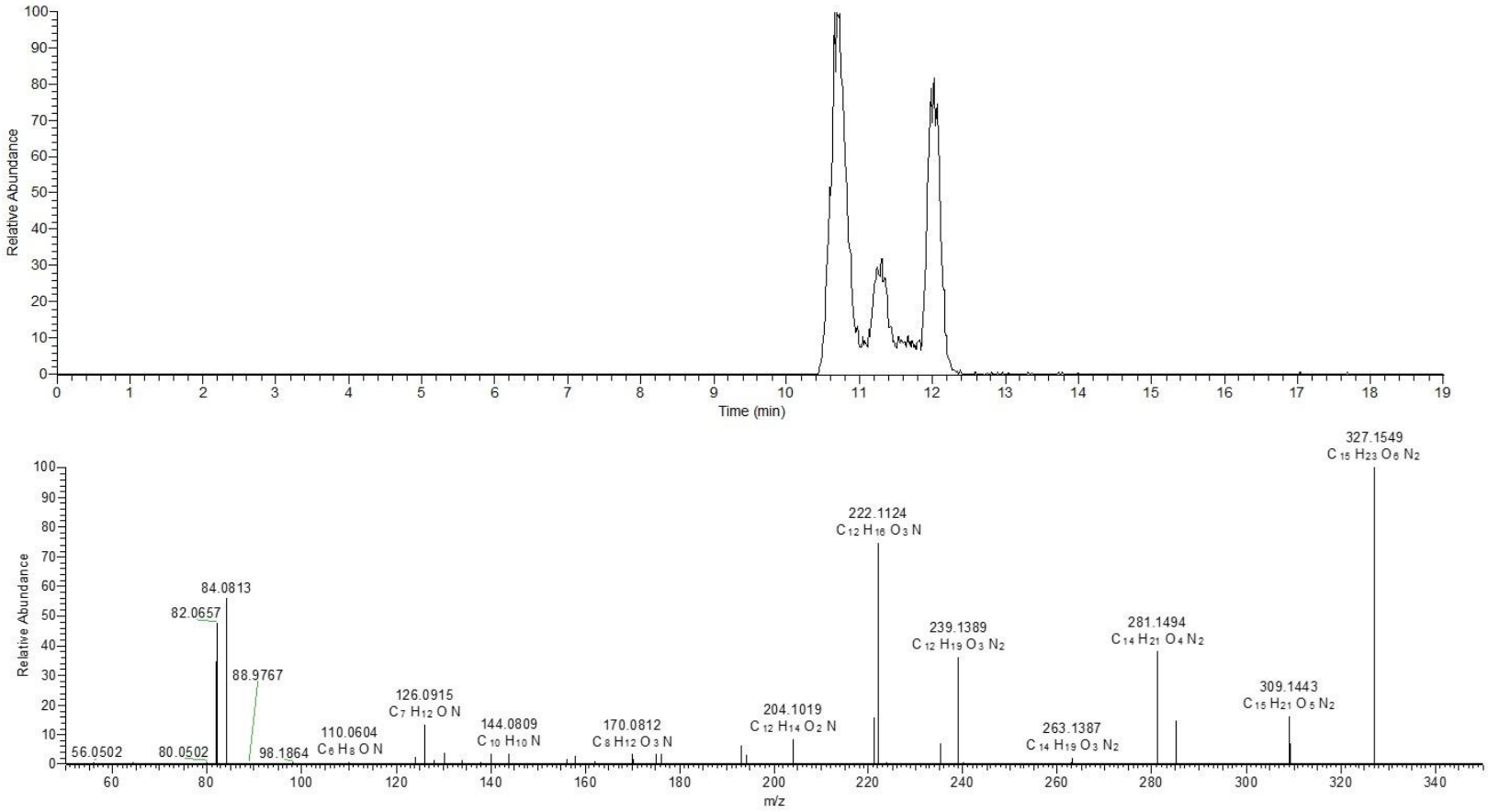

Figure 5.8.7. Base peak chromatogram and MS^2 spectrum of m/z 327 identified in ozonation experiments with 3-(2-furyl)propanoic acid (15 μM initial concentration).

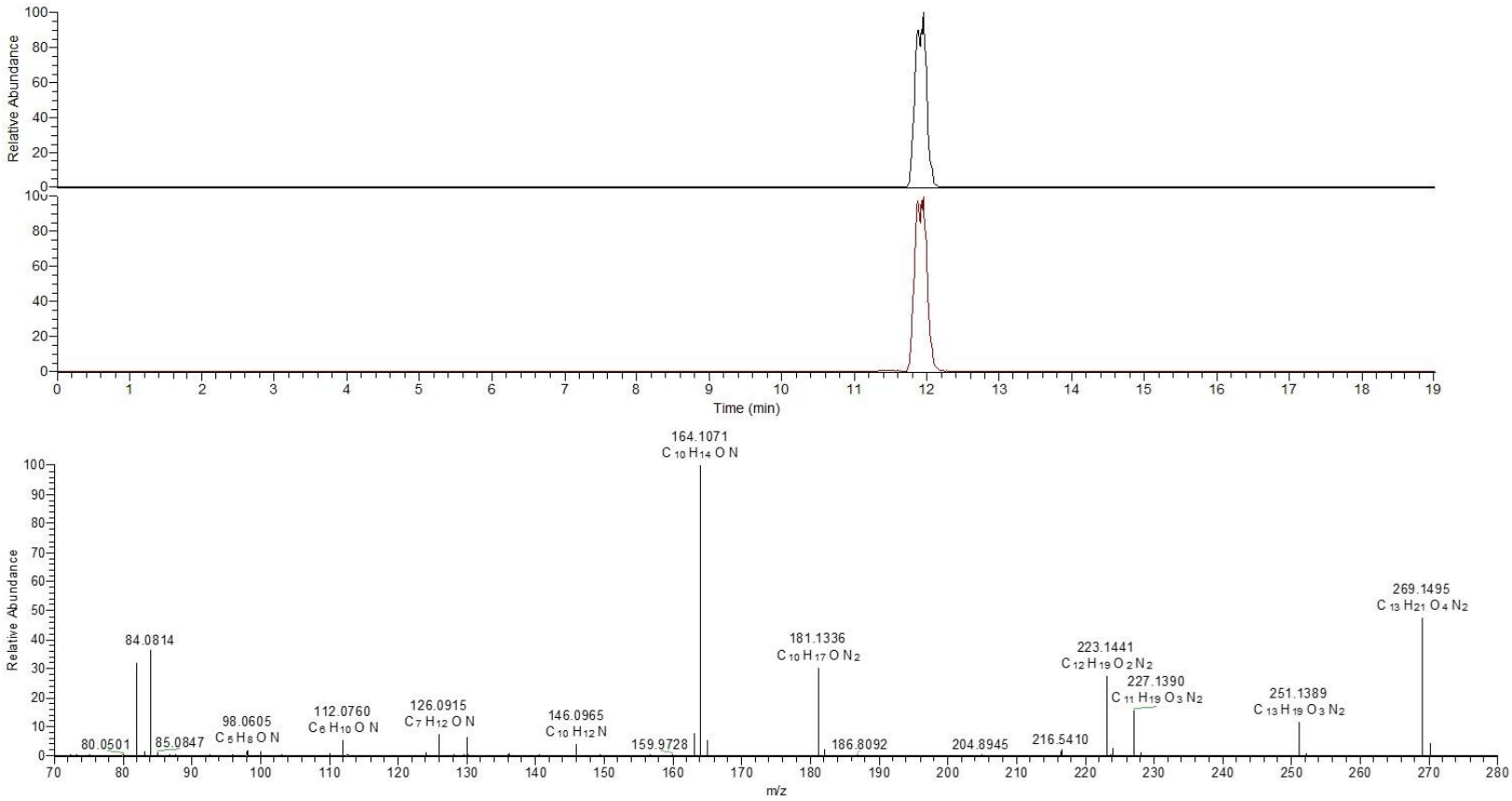

Figure 5.8.8. Base peak chromatogram of m/z 313 (top), base peak chromatogram and MS^2 spectrum of m/z 269 (m/z 313 after loss of CO_2) identified in ozonation experiments with 2-methyl-3-furoic acid (15 μM initial concentration).

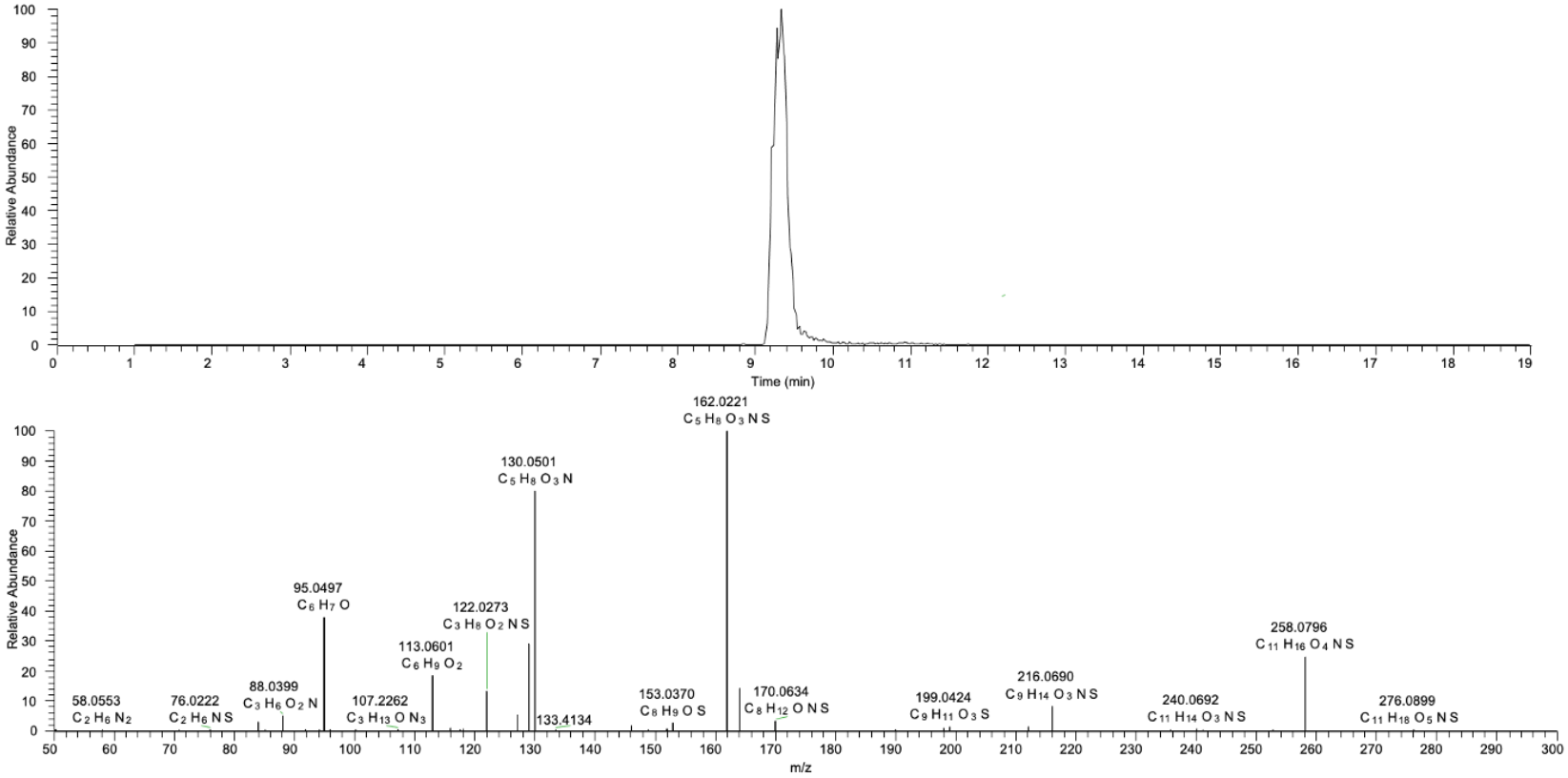

Figure 5.8.9. Base peak chromatogram and MS^2 spectrum of m/z 276 identified in ozonation experiments with 2,5-dimethylfuran (100 μM initial concentration).

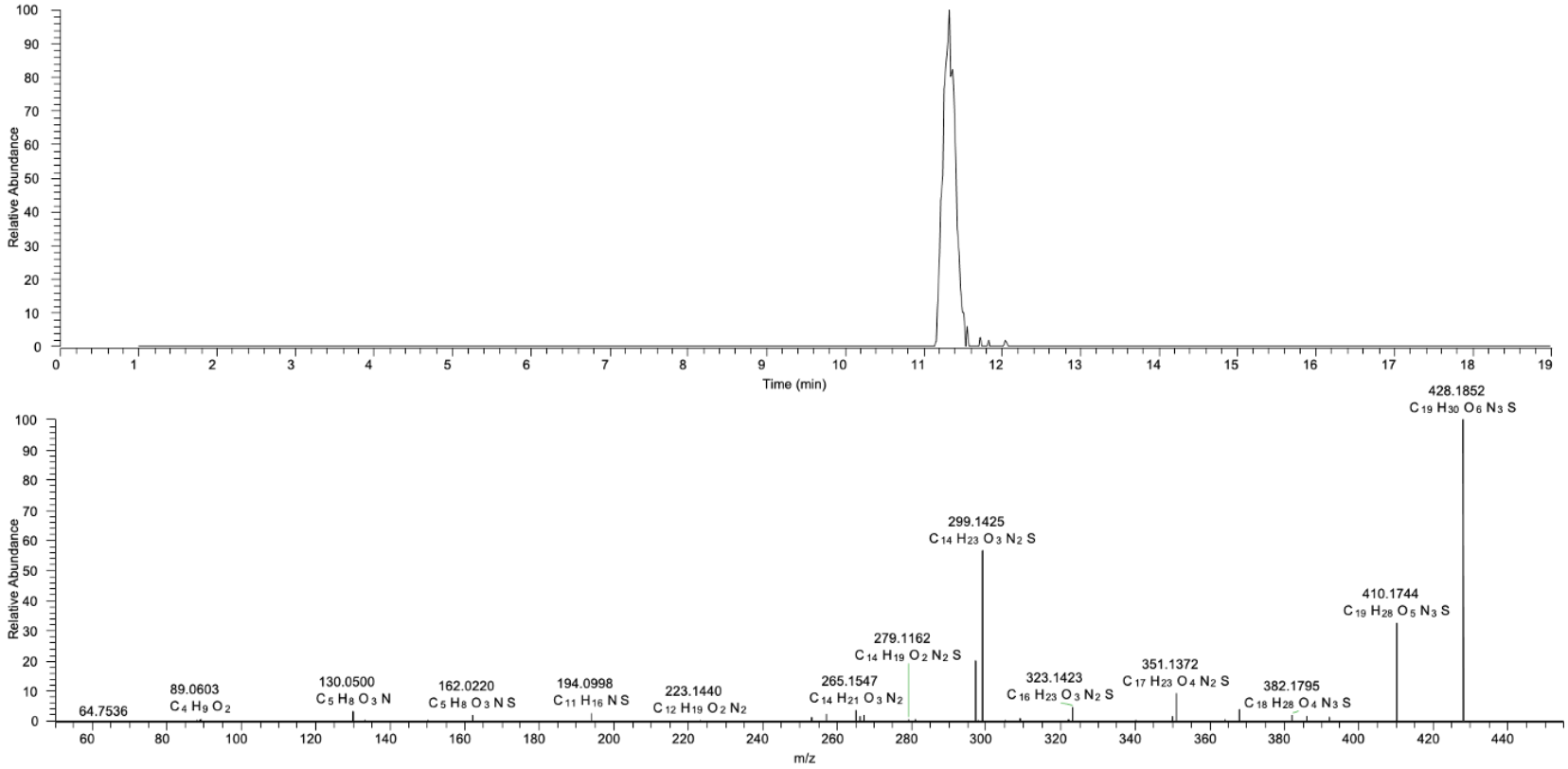

Figure 5.8.10. Base peak chromatogram and MS^2 spectrum of m/z 428 identified in ozonation experiments with 2,5-dimethylfuran (100 μM initial concentration).

Table 5.8.3. Furosemide ozonation products detected with LC-HRMS, including MS^2 fragmentation information. Suggested structures are supported by comparison with literature (4, 5), and/or based on MS^2 spectra (Figure 5.8.11).

Compound	Retention time (min)	m/z (observed)	m/z error (ppm)	Formula $[M+H]^+$	Suggested structure
FRS	14.1	331.0143 250.9885 232.9780 185.9951	2.1 1.1 0.9 0.8	$C_{12}H_{12}O_5N_2ClS$ $C_7H_8O_4N_2ClS$ $C_7H_6O_3N_2ClS$ $C_7H_5O_3NCl$	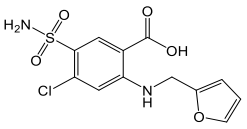
FRS-265	11.1	265.0042 250.9886 232.9782 185.9952	0.9 0.7 0.1 0.3	$C_8H_{10}O_4N_2ClS$ $C_7H_8O_4N_2ClS$ $C_7H_6O_3N_2ClS$ $C_7H_5O_3NCl$	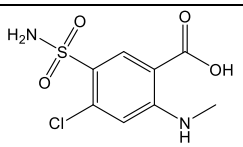
FRS-328	8.0	328.9989 310.9880 281.0082 266.0211 249.0184	1.4 2.5 1.3 1.4 1.3	$C_{12}H_{10}O_5N_2ClS$ $C_{12}H_8O_4N_2ClS$ $C_{12}H_8O_5NCl$ $C_{12}H_9O_4NCl$ $C_{12}H_8O_3NCl$	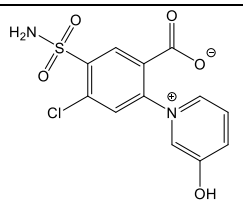
FRS-308	12.0	308.9939 290.9834 262.9886 244.9781	1.2 1.0 0.7 0.5	$C_9H_{10}O_6N_2ClS$ $C_9H_8O_5N_2ClS$ $C_8H_8O_4N_2ClS$ $C_8H_6O_3N_2ClS$	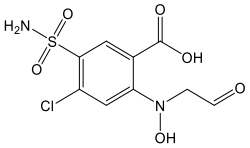
FRS-363 (two peaks)	9.1, 10.0	363.0043 335.0095 316.9990 262.9886	1.4 1.2 1.1 0.7	$C_{12}H_{12}O_7N_2ClS$ $C_{11}H_{12}O_6N_2ClS$ $C_{11}H_{10}O_5N_2ClS$ $C_8H_8O_4N_2ClS$	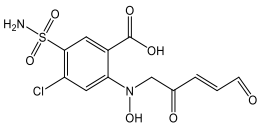
FRS-347	11.8	347.0097 328.9994 262.9885 244.9780	0.6 -0.2 1.1 0.9	$C_{12}H_{12}O_6N_2ClS$ $C_{12}H_{10}O_5N_2ClS$ $C_8H_8O_4N_2ClS$ $C_8H_6O_3N_2ClS$	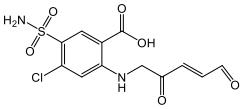
FRS-266	10.6	266.9834 248.9729	1.1 0.9	$C_7H_8O_5N_2ClS$ $C_7H_6O_4N_2ClS$	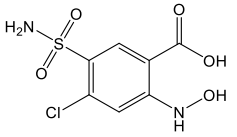
FRS-278	11.8	278.9834	1.1	$C_8H_8O_5N_2ClS$	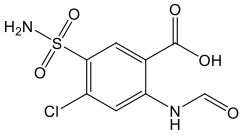

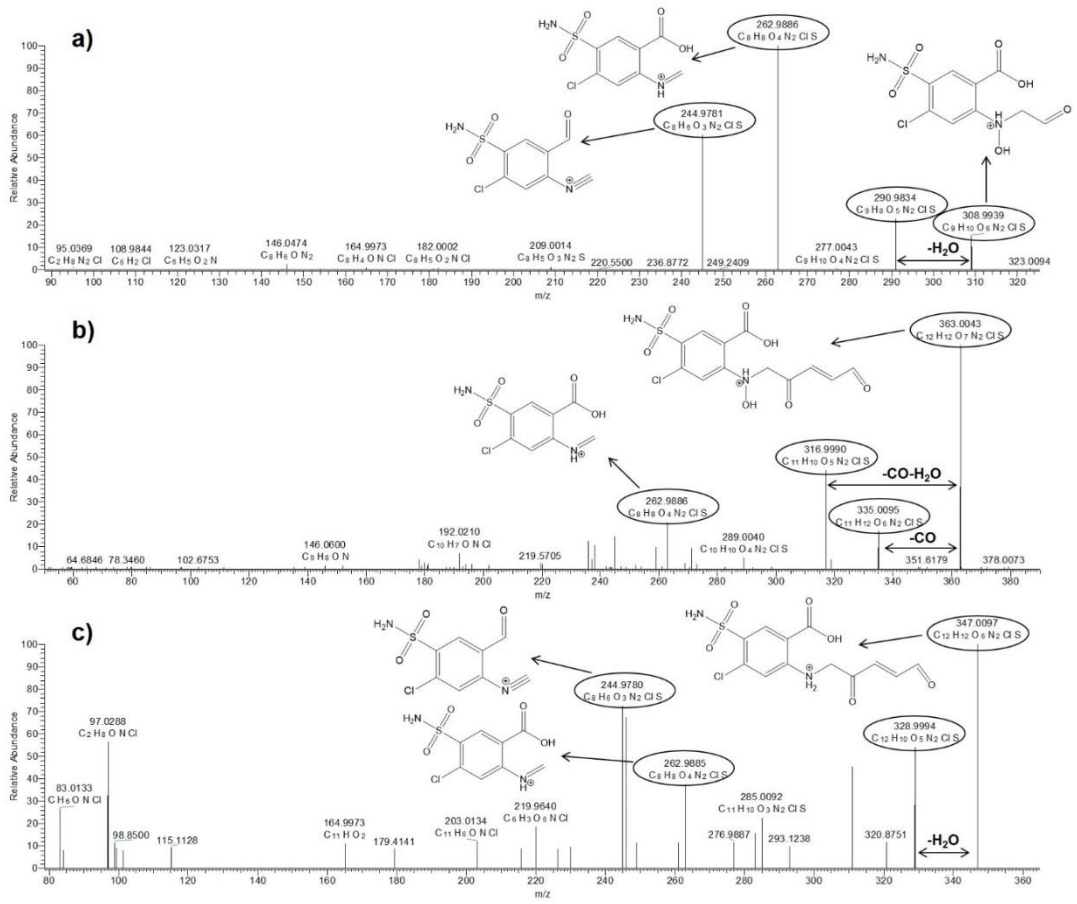

Figure 5.8.11. MS^2 spectra including fragment structures for the newly detected products a) FRS-308, b) FRS-363 and c) FRS-347 identified in ozonation experiments with furosemide (15 μM initial concentration).

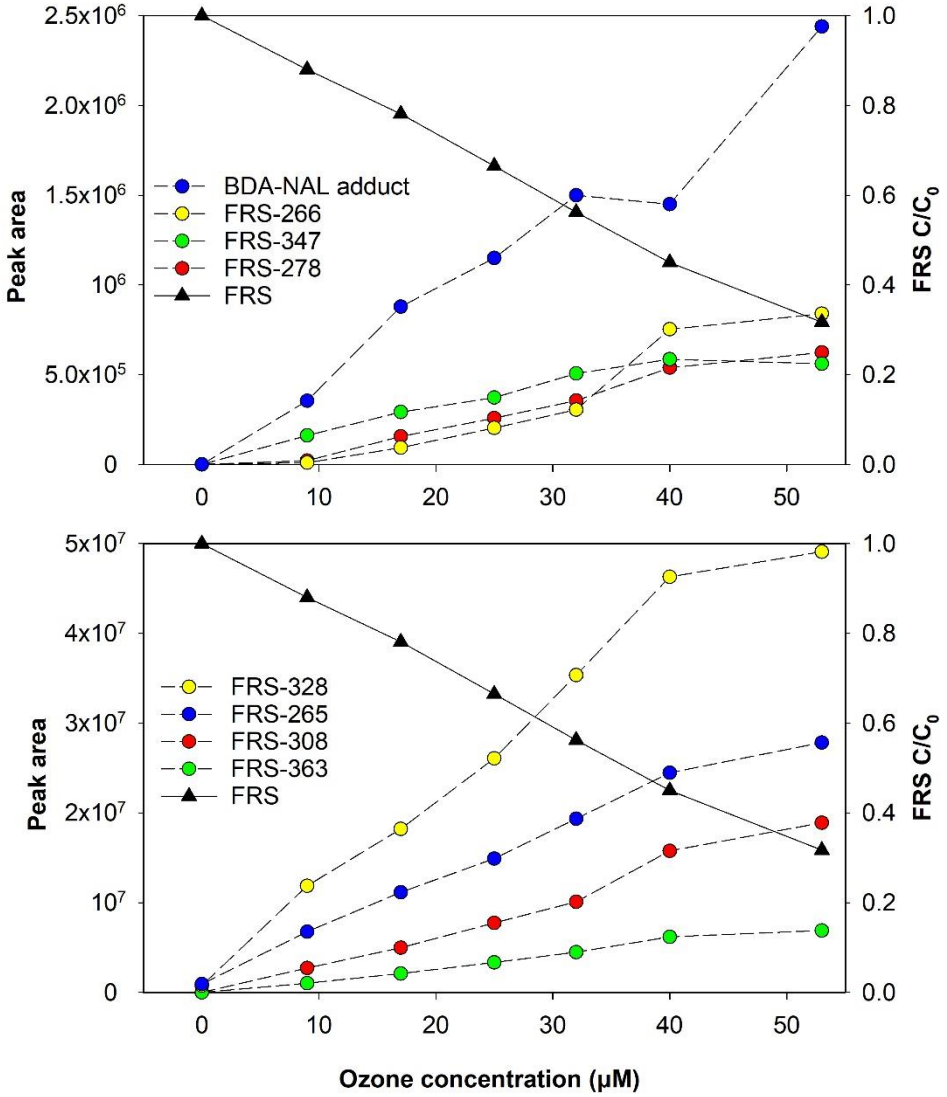

Figure 5.8.12. Peak area of furosemide (FRS) ozonation products and FRS degradation at different ozone concentrations. BDA is shown as the BDA-NAL adduct. For FRS-265 the peak area of the ionisation fragment m/z 250 is shown. Data points are the average of duplicate experiments (error bars have been omitted). Furosemide initial concentration 15 µM.

Table 5.8.4. Ranitidine ozonation products detected with LC-HRMS, including MS^2 fragmentation information. Suggested structures are supported by comparison with literature (6), and/or based on MS^2 spectra (Figure 5.8.14).

Compound	Retention time (min)	m/z (observed)	m/z error (ppm)	Formula $[M+H]^+$	Suggested structure
RAN	8.7	315.1481	-1.5	$C_{13}H_{23}O_3N_4S$	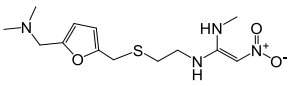
		270.0902	-1.8	$C_{11}H_{16}O_3N_3S$	
		224.0974	-1.6	$C_{11}H_{16}ON_2S$	
		176.0487	-0.8	$C_5H_{10}O_2N_3S$	
		144.0766	-1.2	$C_5H_{10}O_2N_3$	
		124.0757	0.2	$C_7H_{10}ON$	
		117.0481	0.2	$C_4H_9N_2S$	
		98.0842	3.1	$C_5H_{10}N_2$	
		58.0658	11.0	C_3H_8N	
RAN-S oxide	3.7	331.1430	-1.3	$C_{13}H_{23}O_4N_4S$	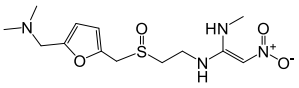
		313.1330	0.4	$C_{13}H_{21}O_3N_4S$	
		286.0851	-1.9	$C_{11}H_{16}O_4N_3S$	
		240.0924	-1.3	$C_{11}H_{16}O_2N_2S$	
		222.0818	-1.4	$C_{11}H_{14}ON_2S$	
		192.0435	-1.5	$C_5H_{10}O_3N_3S$	
		188.0738	-1.1	$C_8H_{14}O_2NS$	
		138.0913	-0.2	$C_8H_{12}ON$	
		110.0967	2.0	$C_7H_{12}N$	
		94.0417	3.5	C_6H_6O	
		82.0656	6.1	C_5H_8N	
		58.0658	11.0	C_3H_8N	
RAN-N oxide	8.9	331.1429	-1.8	$C_{13}H_{23}O_4N_4S$	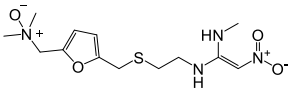
		270.0902	-1.7	$C_{11}H_{16}O_3N_3S$	
		224.0974	-1.7	$C_{11}H_{16}ON_2S$	
		176.0486	-1.0	$C_5H_{10}O_2N_3S$	
		144.0766	-1.2	$C_5H_{10}O_2N_3$	
		130.0559	1.2	$C_5H_{10}N_2S$	
		98.0842	3.2	$C_5H_{10}N_2$	
		88.0220	4.7	C_3H_6NS	
RAN-S&N oxide	4.2	347.1379	-1.7	$C_{13}H_{23}O_5N_4S$	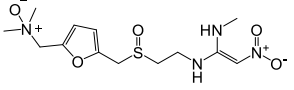
		286.0850	-2.0	$C_{11}H_{16}O_4N_3S$	
		240.0920	-2.7	$C_{11}H_{16}O_2N_2S$	
		193.0513	-1.4	$C_5H_{11}O_3N_3S$	
		192.0434	-1.7	$C_5H_{10}O_3N_3S$	
		146.0506	-1.6	$C_5H_{10}ON_2S$	
		130.0610	-1.1	$C_4H_8O_2N_3$	
		100.0998	2.5	$C_5H_{12}N_2$	
		73.0765	7.0	$C_3H_9N_2$	

RAN-300S	2.0	300.1371	-1.6	$C_{13}H_{22}O_3N_3S$	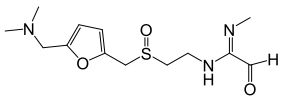
		282.1266	-1.6	$C_{13}H_{20}O_2N_3S$	
		255.0793	-2.0	$C_{11}H_{15}O_3N_2S$	
		237.0687	-2.0	$C_{11}H_{13}O_3N_2S$	
		188.0737	-1.5	$C_8H_{14}O_2NS$	
		138.0913	-0.3	$C_8H_{12}ON$	
		110.0966	1.8	$C_7H_{12}N$	
		94.0416	3.5	C_6H_6O	
		82.0656	6.1	C_5H_8N	
		58.0658	11.0	C_3H_8N	
RAN-300b	6.0	300.1369	-2.5	$C_{13}H_{22}O_3N_3S$	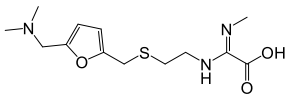
		256.1473	-2.1	$C_{12}H_{22}ON_3S$	
		211.0896	-1.9	$C_{10}H_{15}ON_2S$	
		170.0631	-1.9	$C_8H_{12}ONS$	
		153.0366	-1.9	C_8H_9OS	
		138.0911	-1.4	$C_8H_{12}ON$	
		125.0055	-0.8	C_6H_5OS	
		124.0757	-0.2	$C_7H_{10}ON$	
		117.0481	0.4	$C_4H_9N_2S$	
		85.0764	4.8	$C_4H_9N_2$	
RAN-316S	2.3	316.1320	-1.8	$C_{13}H_{22}O_4N_3S$	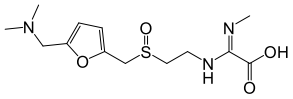
		272.1423	-1.7	$C_{12}H_{22}O_2N_3S$	
		254.1317	-1.8	$C_{12}H_{20}ON_3S$	
		227.0845	-1.7	$C_{10}H_{15}O_2N_2S$	
		209.0741	-0.9	$C_{10}H_{13}ON_2S$	
		188.0738	-1.1	$C_8H_{14}O_2NS$	
		138.0912	-0.7	$C_8H_{12}ON$	
		110.0966	1.7	$C_7H_{12}N$	
		85.0765	5.4	$C_4H_9N_2$	
		58.0658	11.0	C_3H_8N	
RAN-316N	7.2	316.1317	-2.8	$C_{13}H_{22}O_4N_3S$	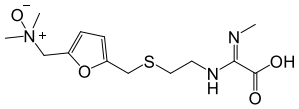
		272.1421	-2.3	$C_{12}H_{22}O_2N_3S$	
		212.0973	-2.2	$C_{10}H_{16}ON_2S$	
		170.0631	-1.7	$C_8H_{12}ONS$	
		153.0365	-2.4	C_8H_9OS	
		118.0559	0.1	$C_4H_{10}N_2S$	
		85.0764	4.7	$C_4H_9N_2$	
RAN-332	4.0	332.1270	-1.4	$C_{13}H_{22}O_5N_3S$	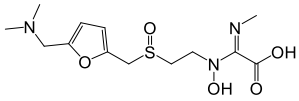
		288.1372	-1.5	$C_{12}H_{22}O_3N_3S$	
		243.0795	-1.3	$C_{10}H_{15}O_3N_2S$	
		227.0847	-0.8	$C_{10}H_{15}O_2N_2S$	
		151.0534	-0.9	$C_4H_{11}O_2N_2S$	
		149.0378	-0.9	$C_4H_9O_2N_2S$	
		138.0912	-0.8	$C_8H_{12}ON$	
		134.0508	-0.5	$C_4H_{10}ON_2S$	
		110.0966	1.4	$C_7H_{12}N$	
		85.0765	5.2	$C_4H_9N_2$	

RAN-305	2.2	305.1159	-2.1	$C_{12}H_{21}O_5N_2S$	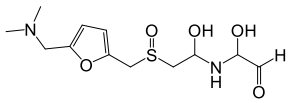
		287.1054	-2.0	$C_{12}H_{19}O_4N_2S$	
		166.0165	-2.0	$C_4H_8O_4NS$	
		138.0912	-1.1	$C_8H_{12}NO$	
		110.0966	1.5	$C_7H_{12}N$	
		94.0417	4.3	C_6H_6O	
RAN-334	2.2	334.1426	-1.4	$C_{13}H_{24}O_5N_3S$	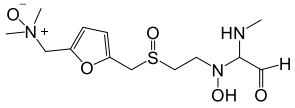
		316.1317	-2.8	$C_{13}H_{22}O_4N_3S$	
		255.0790	-3.0	$C_{11}H_{15}O_3N_2S$	
		180.0558	-1.8	$C_5H_{12}O_3N_2S$	
		177.0326	-1.1	$C_5H_9O_3N_2S$	
		162.0456	-1.2	$C_5H_{10}O_2N_2S$	
		161.0375	-2.4	$C_5H_9O_2N_2S$	
		113.0710	0.1	$C_5H_9ON_2$	
		95.0494	2.4	C_6H_7O	
RAN-236	7.5	236.0697	-1.2	$C_7H_{14}O_4N_3S$	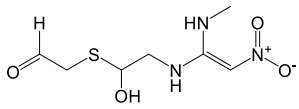
		219.0670	-1.2	$C_7H_{13}O_3N_3S$	
		190.0768	-1.6	$C_7H_{14}O_2N_2S$	
		131.0638	0.0	$C_5H_{11}N_2S$	
		119.0163	1.1	$C_4H_7O_2S$	
		73.0112	8.1	C_3H_5S	
RAN-252	2.4	252.0645	-1.3	$C_7H_{14}O_5N_3S$	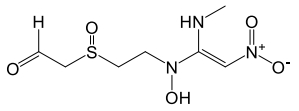
		234.0540	-1.4	$C_7H_{12}O_4N_3S$	
		206.0719	-0.1	$C_7H_{14}O_3N_2S$	
		193.0518	1.2	$C_5H_{11}O_3N_3S$	
		188.0612	-1.0	$C_7H_{12}O_2N_2S$	
		176.0251	0.5	$C_5H_8O_3N_2S$	
		160.0299	-1.1	$C_5H_8O_2N_2S$	
		144.0766	-1.0	$C_5H_{10}O_2N_3S$	
		134.0270	-0.5	$C_4H_8O_2NS$	
		98.0842	3.5	$C_5H_{10}N_2$	

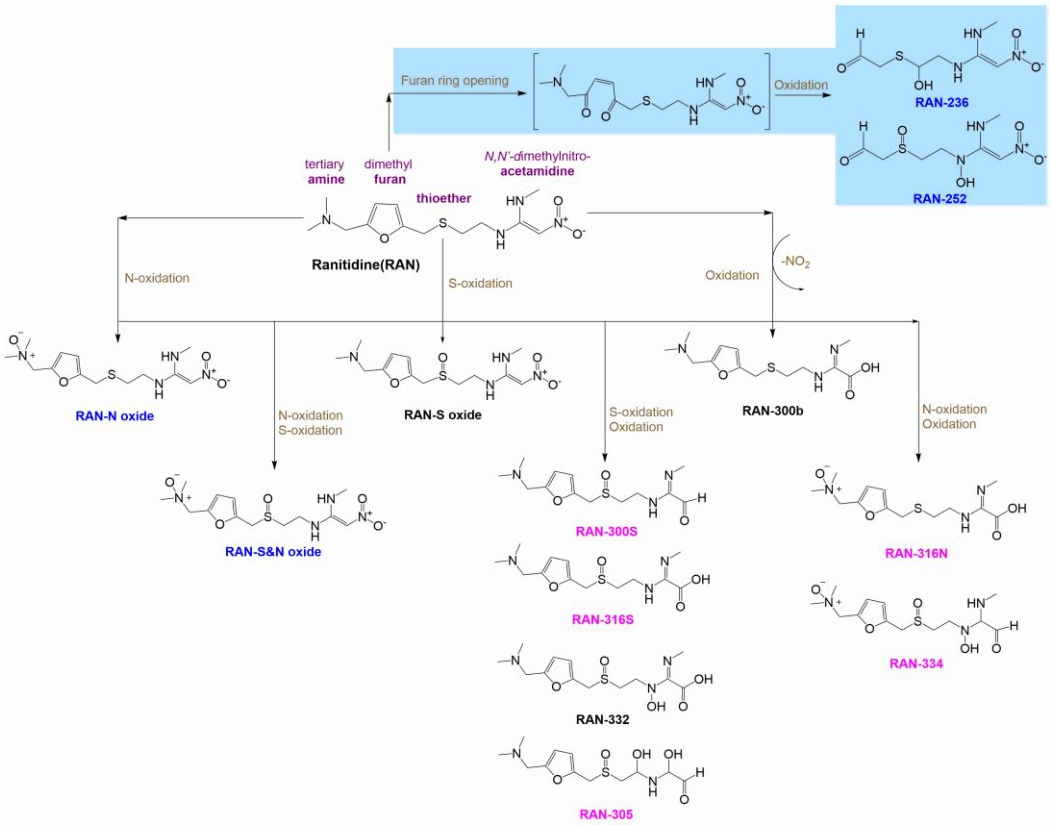

Figure 5.8.13. Proposed reaction pathways for the ozonation of ranitidine. Transformation products are labelled as follows: blue ones are newly detected, black ones are previously reported (6), while pink ones are those having the same molecular ion m/z as previously reported (6), but different suggested structures based on MS^2 fragment information obtained (Figure 5.8.14).

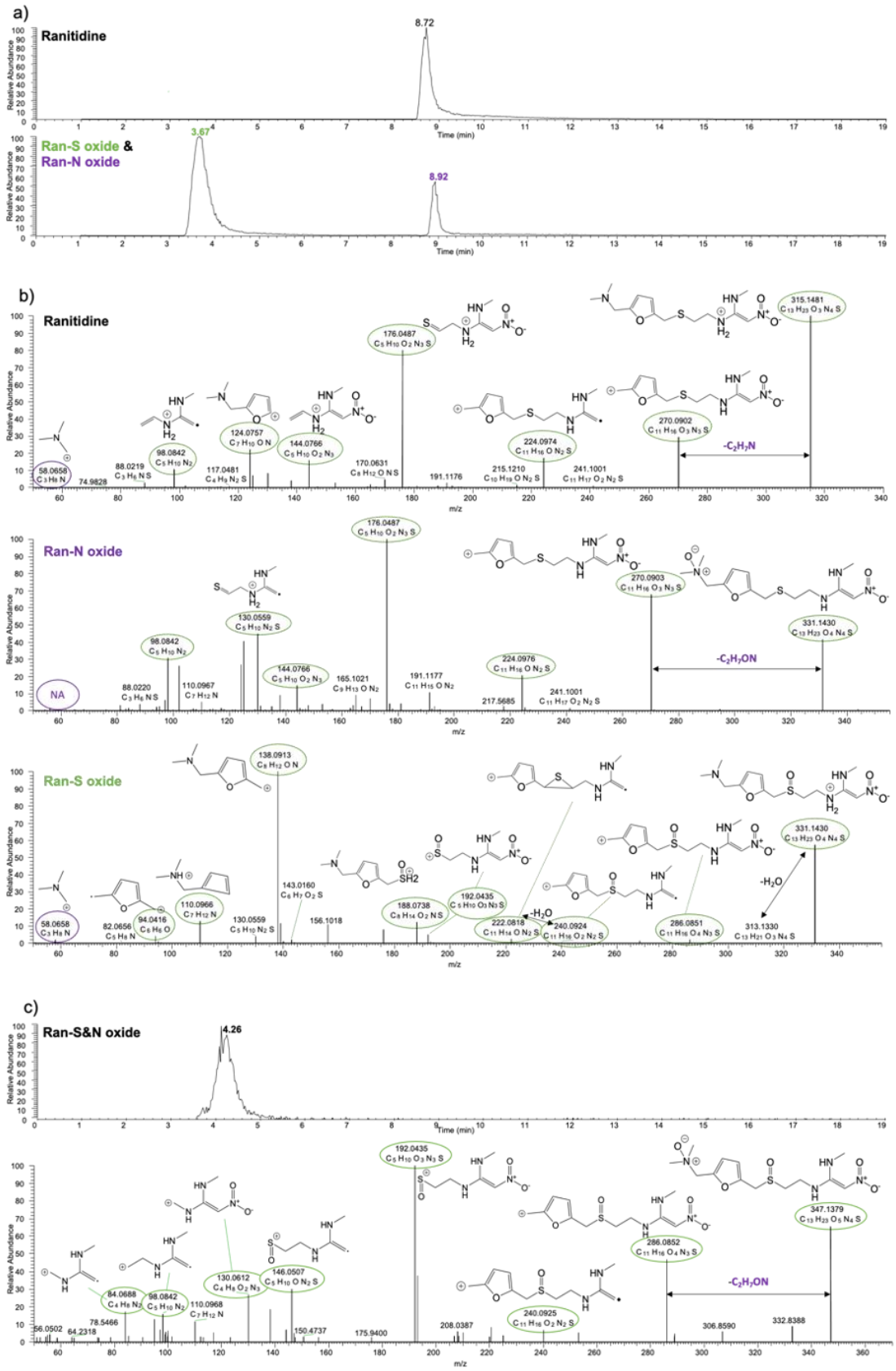
a)
Ranitidine
8.72
Ran-S oxide &
Ran-N oxide
3.67
8.92
Relative Abundance
Time (min)
b)
Ranitidine
176.0487
C5 H10 O2 N3 S
315.1481
C13 H23 O3 N4 S
270.0902
C11 H16 O3 N3 S
-C2H7N
224.0974
C11 H16 O N2 S
144.0766
C5 H10 O2 N3
124.0757
C7 H10 O N
98.0842
C5 H10 N2
58.0658
C3 H8 N
88.0219
C3 H6 N S
74.9828
117.0481
C4 H9 N2 S
170.0631
C6 H12 O N S
191.1176
215.1210
C10 H19 O N2 S
241.1001
C11 H17 O2 N2 S
m/z
Ran-N oxide
176.0487
C5 H10 O2 N3 S
270.0903
C11 H16 O3 N3 S
331.1430
C13 H23 O4 N4 S
-C2H7ON
130.0559
C5 H10 N2 S
98.0842
C5 H10 N2
144.0766
C5 H10 O2 N3
224.0976
C11 H16 O N2 S
NA
88.0220
C3 H6 N S
110.0967
C7 H12 N
165.1021
C9 H13 O N2
191.1177
C11 H15 O N2
217.5685
241.1001
C11 H17 O2 N2 S
m/z
Ran-S oxide
138.0913
C8 H12 O N
331.1430
C13 H23 O4 N4 S
-H2O
143.0160
C6 H7 O2 S
192.0435
C5 H10 O3 N3 S
110.0966
C7 H12 N
188.0738
C8 H14 O2 N S
58.0658
C3 H8 N
94.0416
C6 H6 O
82.0656
C5 H8 N
130.0559
C5 H10 N2 S
156.1018
222.0818
C11 H14 O N2 S
-H2O
240.0924
C11 H16 O2 N2 S
286.0851
C11 H16 O4 N3 S
313.1330
C13 H21 O3 N4 S
m/z
c)
Ran-S&N oxide
4.26
Time (min)
192.0435
C5 H10 O3 N3 S
347.1379
C13 H23 O5 N4 S
286.0852
C11 H16 O4 N3 S
-C2H7ON
130.0612
C4 H8 O2 N3
146.0507
C5 H10 O N2 S
84.0688
C4 H8 N2
98.0842
C5 H10 N2
110.0968
C7 H12 N
240.0925
C11 H16 O2 N2 S
56.0502
64.2318
78.5466
150.4737
175.9400
208.0387
306.8590
332.8388
m/z

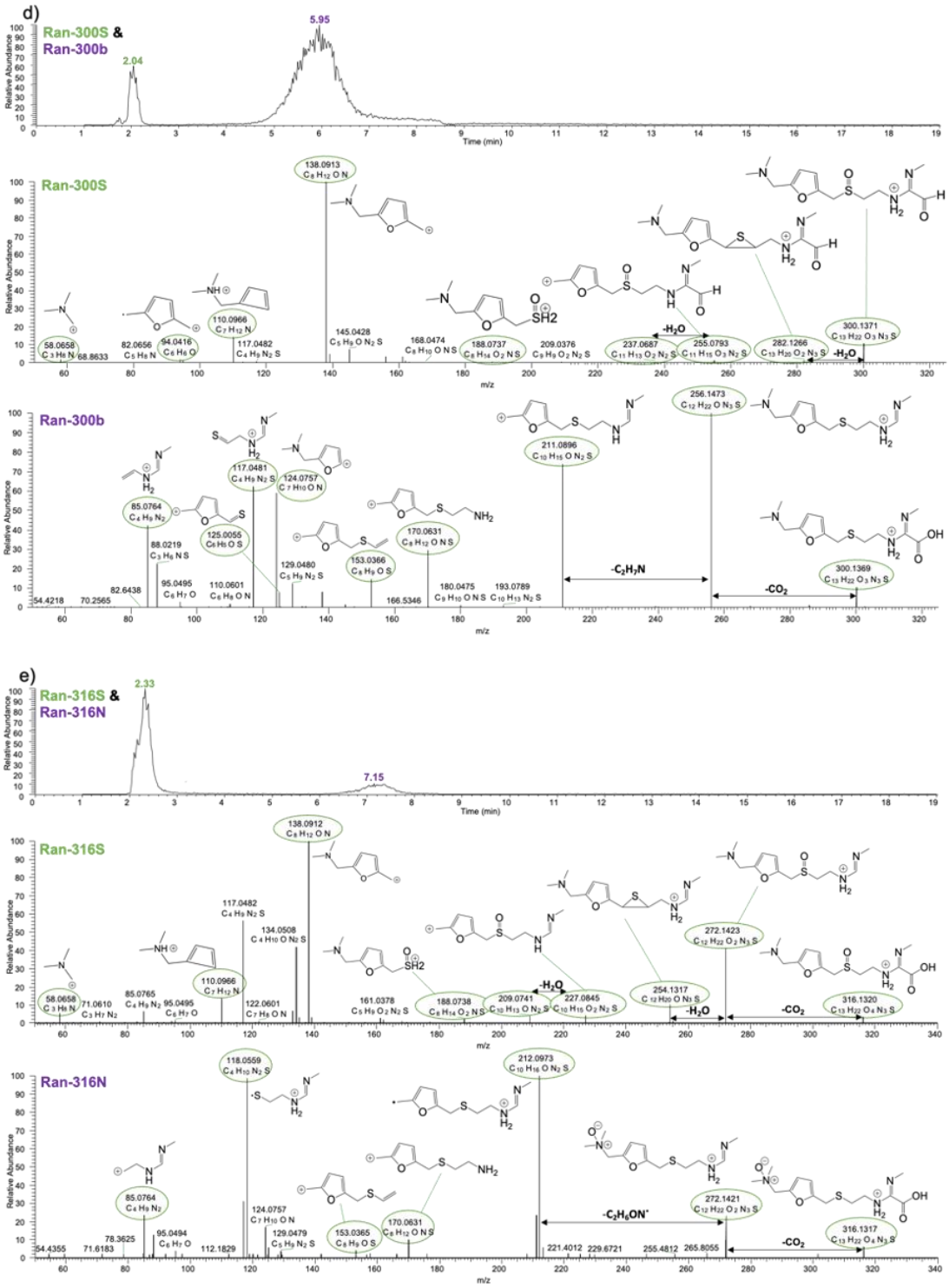
d)
Ran-300S &
Ran-300b
2.04
5.95
Relative Abundance
Time (min)
Ran-300S
138.0913
C8 H12 O N
110.0966
C7 H12 N
58.0658
C3 H8 N
68.8633
82.0656
C5 H8 N
94.0416
C6 H6 O
117.0482
C4 H9 N2 S
145.0428
C5 H9 O N2 S
168.0474
C8 H10 O N S
188.0737
C8 H14 O2 N S
209.0376
C9 H9 O2 N2 S
237.0687
C11 H13 O2 N2 S
255.0793
C11 H15 O3 N2 S
282.1266
C13 H20 O2 N3 S
300.1371
C13 H22 O3 N3 S
-H2O
-H2O
m/z
Ran-300b
117.0481
C4 H9 N2 S
124.0757
C7 H10 O N
85.0764
C4 H9 N2
125.0055
C6 H6 O S
88.0219
C3 H6 N S
129.0480
C5 H9 N2 S
153.0366
C8 H9 O S
170.0631
C8 H12 O N S
211.0896
C10 H15 O N2 S
256.1473
C12 H22 O N3 S
300.1369
C13 H22 O3 N3 S
-C2H7N
-CO2
54.4218
70.2565
82.6438
95.0495
C6 H7 O
110.0601
C6 H8 O N
166.5346
180.0475
C9 H10 O N S
193.0789
C10 H13 N2 S
m/z
e)
Ran-316S &
Ran-316N
2.33
7.15
Relative Abundance
Time (min)
Ran-316S
138.0912
C8 H12 O N
117.0482
C4 H9 N2 S
134.0508
C4 H10 O N2 S
110.0966
C7 H12 N
58.0658
C3 H8 N
71.0610
C3 H7 N2
85.0765
C4 H9 N2
95.0495
C6 H7 O
122.0601
C7 H8 O N
161.0378
C5 H9 O2 N2 S
188.0738
C8 H14 O2 N S
209.0741
C10 H13 O N2 S
227.0845
C10 H15 O2 N2 S
254.1317
C12 H20 O N3 S
272.1423
C12 H22 O2 N3 S
316.1320
C13 H22 O4 N3 S
-H2O
-H2O
-CO2
m/z
Ran-316N
118.0559
C4 H10 N2 S
212.0973
C10 H16 O N2 S
85.0764
C4 H9 N2
124.0757
C7 H10 O N
78.3625
95.0494
C6 H7 O
112.1829
129.0479
C5 H9 N2 S
153.0365
C8 H9 O S
170.0631
C8 H12 O N S
272.1421
C12 H22 O2 N3 S
316.1317
C13 H22 O4 N3 S
-C2H6ON•
-CO2
54.4355
71.6183
221.4012
229.6721
255.4812
265.8055
m/z

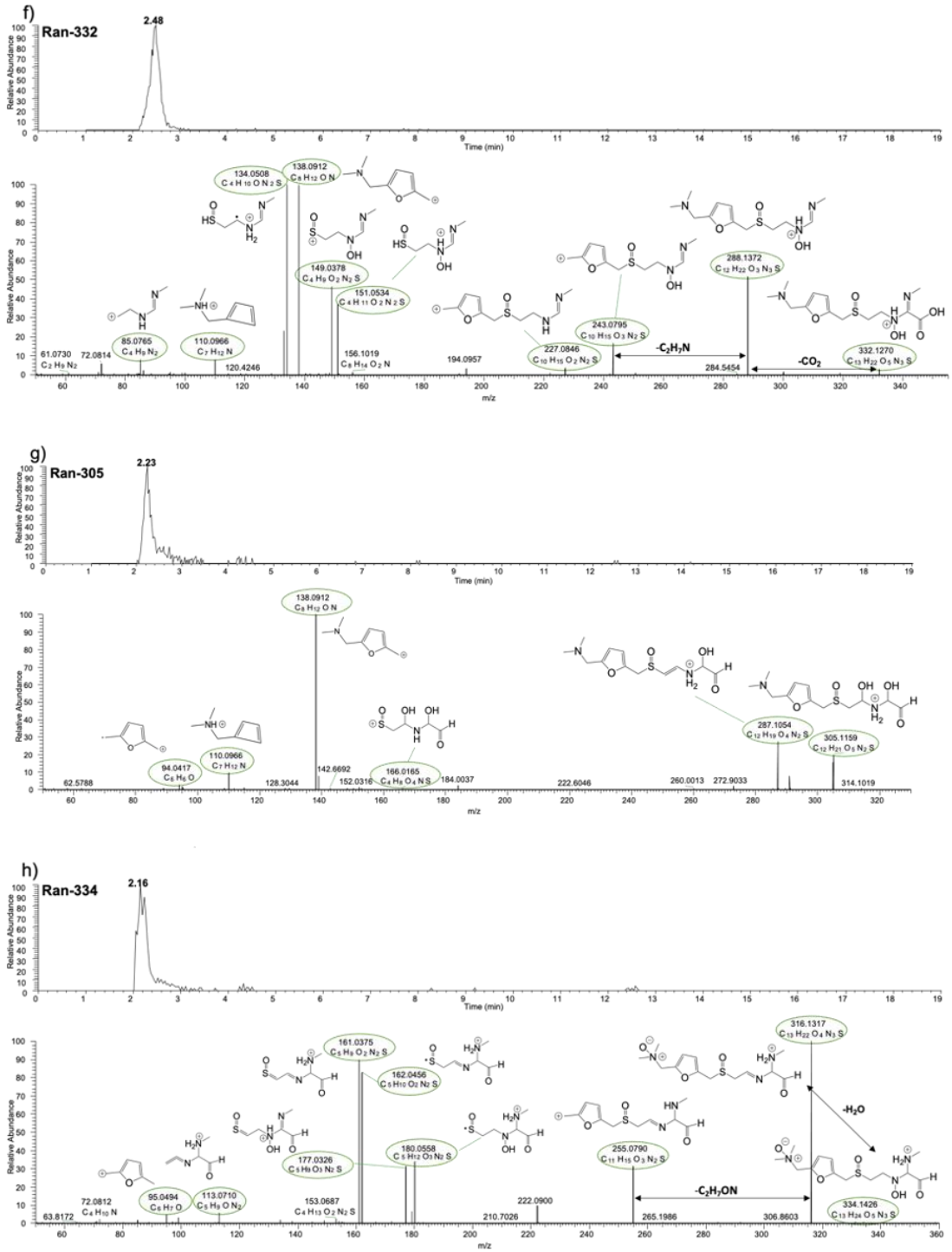
f)
Ran-332
2.48
Relative Abundance
Time (min)
m/z
138.0912
C8 H12 O N
134.0508
C4 H10 O N2 S
149.0378
C4 H9 O2 N2 S
151.0534
C4 H11 O2 N2 S
288.1372
C12 H22 O3 N3 S
243.0795
C10 H15 O3 N2 S
227.0846
C10 H15 O2 N2 S
-C2H7N
-CO2
332.1270
C13 H22 O5 N3 S
85.0765
C4 H9 N2
110.0966
C7 H12 N
61.0730
C2 H9 N2
72.0814
120.4246
156.1019
C8 H14 O2 N
194.0957
284.5454
g)
Ran-305
2.23
138.0912
C8 H12 O N
110.0966
C7 H12 N
94.0417
C6 H6 O
142.6692
166.0165
C4 H8 O4 N S
62.5788
128.3044
152.0316
184.0037
222.6046
260.0013
272.9033
287.1054
C12 H19 O4 N2 S
305.1159
C12 H21 O5 N2 S
314.1019
h)
Ran-334
2.16
316.1317
C13 H22 O4 N3 S
161.0375
C5 H9 O2 N2 S
162.0456
C5 H10 O2 N2 S
177.0326
C5 H9 O3 N2 S
180.0558
C5 H12 O3 N2 S
-H2O
255.0790
C11 H15 O3 N2 S
-C2H7ON
334.1426
C13 H24 O5 N3 S
95.0494
C6 H7 O
113.0710
C5 H9 O N2
72.0812
C4 H10 N
63.8172
153.0687
C4 H13 O2 N2 S
210.7026
222.0900
265.1986
306.8603

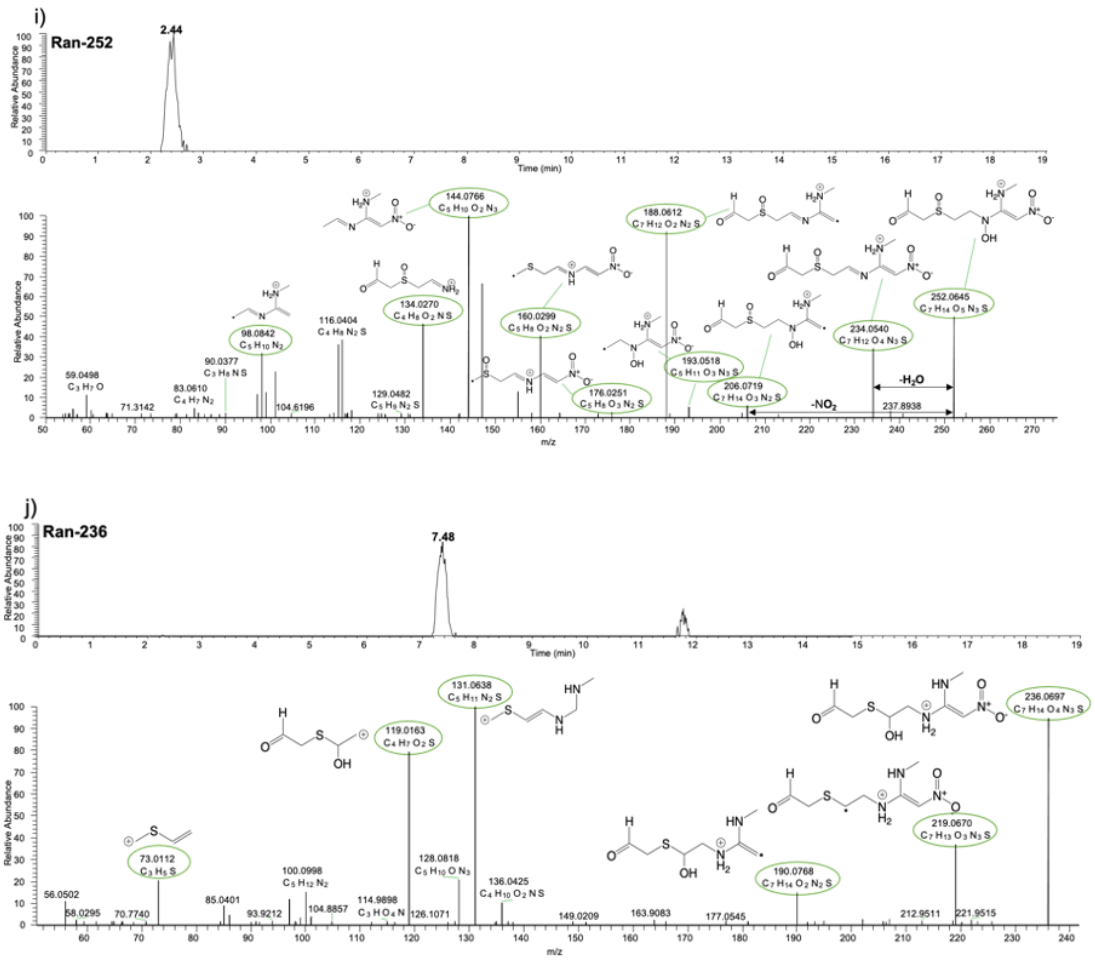

Figure 5.8.14. (a-j) Base peak chromatograms and MS^2 spectra including fragment structures for ranitidine and its transformation products identified in ozonation experiments (ranitidine initial concentration 50 µM).

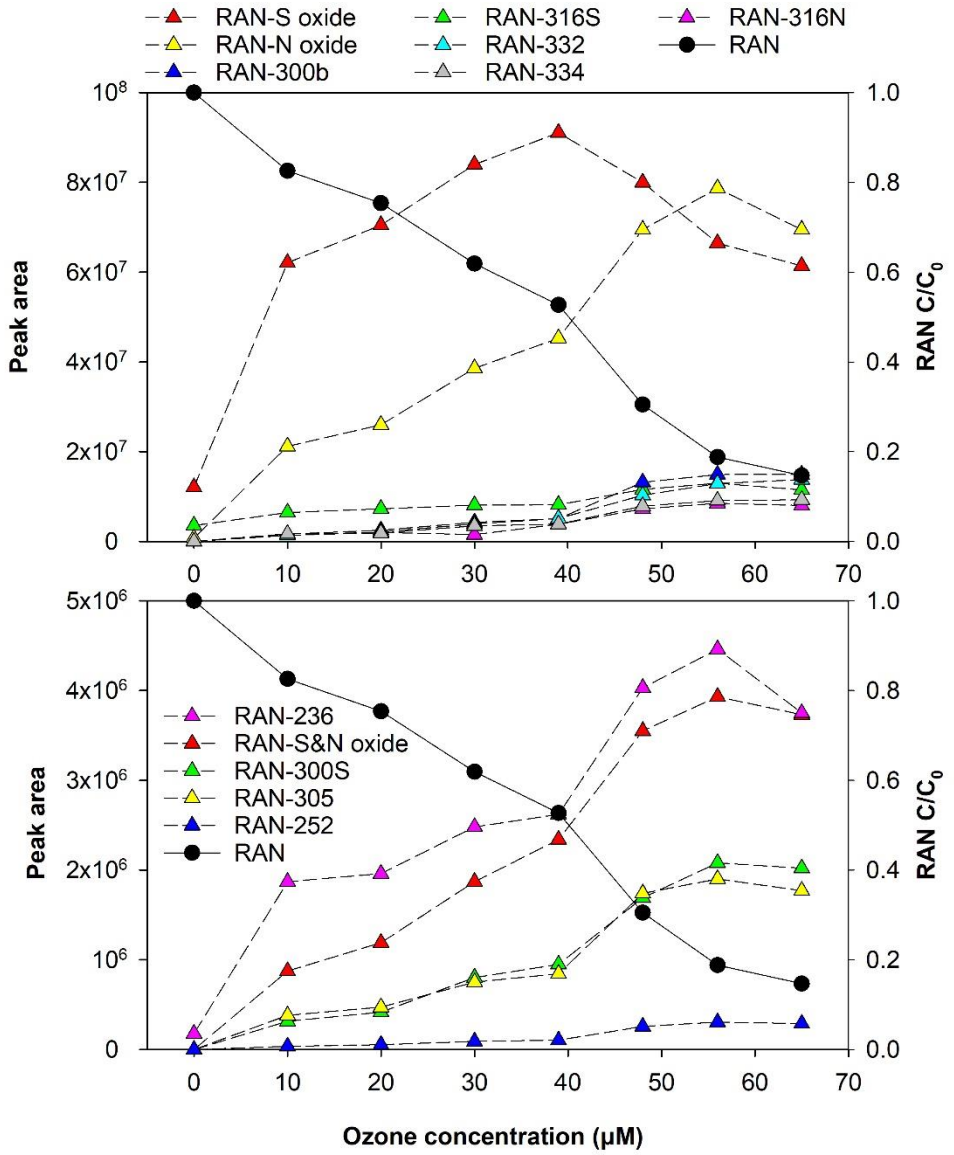

Figure 5.8.15. Peak area of ranitidine (RAN) ozonation products and RAN degradation at different ozone concentrations. Data points are the average of duplicate experiments (error bars have been omitted). Ranitidine initial concentration 15 μM.

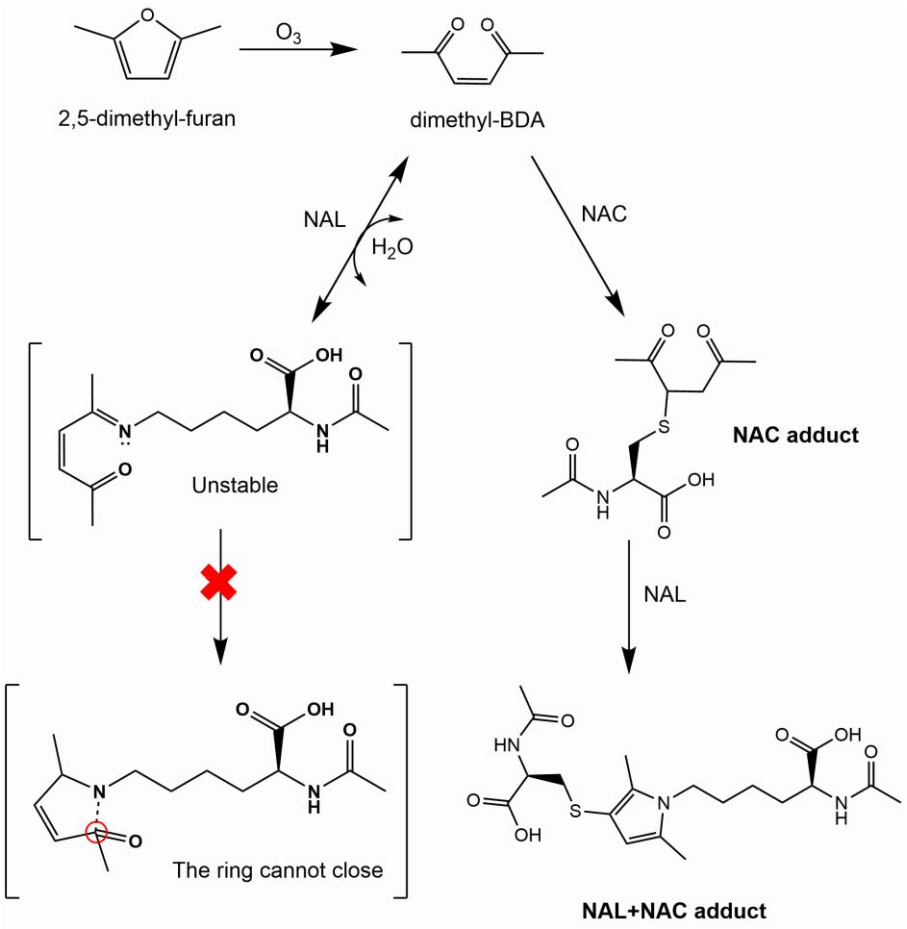

Figure 5.8.16. Reaction of dimethyl-BDA with NAL versus a NAL+NAC mixture, leading to formation of adducts detected with LC-HRMS.

5.8.3 References

1. Huber MM, Canonica S, Park G-Y, von Gunten U. Oxidation of Pharmaceuticals during Ozonation and Advanced Oxidation Processes. Environmental Science & Technology. 2003;37(5):1016-24.

2. Jeon D, Kim J, Shin J, Hidayat ZR, Na S, Lee Y. Transformation of ranitidine during water chlorination and ozonation: Moiety-specific reaction kinetics and elimination efficiency of NDMA formation potential. Journal of Hazardous Materials. 2016;318:802-9.

3. Bader H, Hoigné J. Determination of ozone in water by the indigo method. Water Research. 1981;15(4):449-56.

4. Aalizadeh R, Nika MC, Thomaidis NS. Development and application of retention time prediction models in the suspect and non-target screening of emerging contaminants. J Hazard Mater. 2019;363:277-85.

5. Laurence C, Rivard M, Martens T, Morin C, Buisson D, Bourcier S, Sablier M, Oturan MA. Anticipating the fate and impact of organic environmental contaminants: a new approach applied to the pharmaceutical furosemide. Chemosphere. 2014;113:193-9.

6. Christophoridis C, Nika MC, Aalizadeh R, Thomaidis NS. Ozonation of ranitidine: Effect of experimental parameters and identification of transformation products. Sci Total Environ. 2016;557-558:170-82.

5.9 Additional commentary

Nitrofurantoin (NFT) is an antimicrobial agent that is relevant for the spread of antimicrobial resistance through wastewater (1), in addition to exhibiting high toxicity for different organisms (2). NFT was also included in the study, although it was excluded from the manuscript due to insufficient results. NFT contains a hydantoin ring and a nitro-substituted furan ring, with an imine (carbon-nitrogen double bond) between them. The mutagenicity of nitrofurantoin has been shown to decrease with aqueous ozonation (3). However, the kinetics and reaction pathway of nitrofurantoin ozonation have not yet been elucidated.

The second order rate constant for the reaction of NFT with ozone could not be measured using RAN as the reference compound, indicating that NFT has a much lower ozone reactivity. Competition kinetics using the slower-reacting FA as reference were also unsuccessful. This suggests that the deactivation of the furan ring caused by the electron-withdrawing nitro group led to an estimated ozone rate constant equal to or lower than 10^4 M^{-1} s^{-1}. It would be possible to measure the rate constant using an appropriate non-furanic compound as reference, but this was not attempted in this study.

The hydrolysis of NFT induced by direct photolysis produces nitrofuraldehyde and aminohydantoin through cleavage of the imine bond (4). The formation of nitrofuroic acid was observed during ozonation of NFT, although there was no clear trend with increasing ozone concentration. Other ozonation products were not identified. No NAL adducts demonstrating the formation of α,β-unsaturated dicarbonyls from NFT ozonation were detected, in accordance with results from FA, RAN and DMF. Future work employing different derivatization methods and direct LC-HRMS analysis is therefore needed to elucidate the ozonation pathway of NFT.

References

1. Luczkiewicz A, Jankowska K, Fudala-Ksiazek S, Olanczuk-Neyman K. Antimicrobial resistance of fecal indicators in municipal wastewater treatment plant. Water Res. 2010;44(17):5089-97.

2. Lewkowski J, Rogacz D, Rychter P. Hazardous ecotoxicological impact of two commonly used nitrofuran-derived antibacterial drugs: Furazolidone and nitrofurantoin. Chemosphere. 2019;222:381-90.

3. Burleson GR, Chambers TM. Effect of ozonation on the mutagenicity of carcinogens in aqueous solution. Environmental Mutagenesis. 1982;4(4):469-76.

4. Szabó-Bárdos E, Cafuta A, Hegedűs P, Fónagy O, Kiss G, Babić S, Škorić I, Horváth O. Photolytic and photocatalytic degradation of nitrofurantoin and its photohydrolytic products. Journal of Photochemistry and Photobiology A: Chemistry. 2020;386:112093.

Chapter 6: General conclusions and future work

This chapter draws conclusions from all the research conducted as part of this PhD and presented in this thesis. It also provides recommendations for future work.

6.1 Conclusions

Since ozonation is a widely applied process with numerous large-scale plants around the world, extensive research exists on its different aspects, including mass transfer, process optimisation, reactor design, different applications, reaction mechanisms, and kinetics. However, as the capacity of installed ozone treatment is increasing, and interest in advanced treatment in general is growing, important questions remain unanswered or poorly understood.

The ozone reactivity of trace organic contaminants is often viewed as a well investigated topic, since several compilations of kinetic parameters exist in the literature, along with predictive models (1). However, there is still scarce information on certain classes of environmentally relevant compounds, for example illicit drugs and their metabolites. Even ubiquitously occurring ozone-reactive functional groups such as the furan ring have not been comprehensively studied. We addressed this knowledge gap with three different approaches: a) conducting an extensive literature review for 90 compounds (including several illicit drugs and metabolites) that were selected for their relevance for water and wastewater treatment, b) performing multi-compound ozonation experiments with varying ozone concentration, pH and water matrix to simultaneously assess the ozone reactivity of the 90 compounds, and c) measuring the ozonation rate constant of contaminants and model compounds containing a furan ring. Reactivity studies should continue being performed to cover even a small fraction of the hundreds of trace organic contaminants that are present in the environment. Kinetic data is also necessary for the further development and validation of computational models (such as quantitative structure-activity

relationships, QSARs) that can facilitate the prediction of the ozone reactivity of different compounds.

As with other oxidants, an important issue in ozonation is the formation and the properties of transformation products and by-products. One of the starting points of this PhD was to investigate the fate of the ozonation products of trace organic contaminants in sand filtration post-treatment. Available literature reported that dissolved organic matter becomes more biodegradable during ozonation and can therefore be easily removed with a biofiltration step after ozonation (2, 3). It was not clear, however, whether this extends to trace organic contaminants, which exhibit a wide range of complex molecular structures and unique functional characteristics (4). Using a novel low-cost laboratory setup suitable for long-term continuous tests, we showed that the ozonation products of certain trace organic contaminants are recalcitrant to biodegradation and may be present in the final effluent discharged into the environment. We also demonstrated that the developed laboratory setup produced results that were in good agreement with previous large-scale studies, indicating that our experimental approach can be a valuable tool to enhance the understanding of the fate of trace organic contaminants in ozonation-biofiltration and other advanced treatment schemes.

The identified ozonation products of trace organic contaminants can rarely account for the entire amount of the parent compound that is transformed by ozone. This suggests that some ozonation products remain unknown, especially those that are difficult to analyse with commonly used analytical techniques. In the case of furans, we used an amino acid derivatisation method to detect a class of ozonation products that has recently attracted attention in aqueous oxidation processes: α,β-unsaturated dicarbonyls (5). The employed analytical method also demonstrates the reactivity of the α,β-unsaturated dicarbonyls with biomolecules, and therefore their ecotoxicological relevance. A greater focus needs to be placed on the development and application of diverse analytical techniques that can capture a wider range of transformation processes induced by ozone. A combination of target and non-target mass spectrometry with bioassays appears to be a promising approach.

One way of minimising the formation of hazardous ozonation by-products, such as bromate, is the optimisation of reactor design (6). We investigated an alternative

method of ozone delivery that uses membrane contactors to achieve bubble-less transfer of ozone gas into the aqueous matrix. Based on experiments with two membrane materials and two membrane configurations, we identified key benefits (e.g. easy control of the ozone dosage) and drawbacks (e.g. high localised ozone concentrations) of membrane ozonation. Our study is one of the first to use a realistic downsized commercial membrane module to treat several real water and wastewater matrices. Membrane ozonation may achieve high treatment performance, but only with specific operational conditions and reactor characteristics, for example optimised water residence time and uniform distribution of the ozone gas. Performing a meaningful comparison between membrane ozonation and conventional ozonation is currently challenging due to the lack of data from large-scale membrane ozonation systems.

Overall, this thesis has made important contributions to the research of ozonation products and ozone mass transfer, and their implications for water and wastewater treatment. The investigated topics relate to major issues of modern ozonation treatment, such as the formation of persistent and hazardous by-products and the development of efficient reactors and processes. By developing several laboratory systems, the work presented here will also facilitate future research in this field.

6.2 Future work and impact

Despite advances and discoveries over several decades, the field of ozonation treatment includes several knowledge gaps. These gaps mainly concern the identification and characterisation of the transformation products formed from the organic and inorganic compounds, and the development of risk mitigating solutions when necessary, such as optimisation of both the ozonation process and post-treatment steps. The main barriers to addressing these knowledge gaps are a) limitations of existing analytical techniques, including high cost and need for specialised personnel; b) the ever-increasing number of synthetic chemicals that exist in the already complex and highly variable water or wastewater matrix; c) the lack or limited scope of regulations regarding trace organic contaminants, transformation products and tertiary or advanced treatment. Future work is therefore proposed, both

for the specific topics that were studied in this thesis, and for the wider ozonation field. Finally, the impact that this thesis can have on policy and practice is described.

6.2.1 Future work on the specific topics of this thesis

The COMBI system opens numerous opportunities for research on the ozonation-biofiltration scheme with low requirements of resources, for example comparison of different filtration media and configurations (e.g. pre-ozonation versus post-ozonation). An aspect that was beyond the scope of our study is investigating the microbial community that develops under different pre-ozonation conditions (e.g. using ATP assays for microbial activity or advanced sequencing analysis of microbial community structure) (7). It is also important to examine whether the microbial community characteristics observed in large-scale systems can be replicated by a laboratory setup like the developed COMBI system (8). The COMBI setup could be improved by the addition of redox probes in the filtration columns, to better characterise the established biofiltration conditions.

Future research on membrane ozonation should focus on scaling up the technology, which will provide more data to perform a techno-economic assessment and a comparison with conventional ozonation systems. In addition, pilot-scale systems would facilitate long-term experiments (e.g. to assess membrane stability) that are often not possible in the lab due to safety concerns. Recycling of the off-gas needs to be developed and incorporated in the techno-economic assessment. Modelling and simulations should be used to support the design of membrane modules with improved mass transfer characteristics and to optimise the process parameters (9).

Our study on the aqueous ozonation of furans was the first one on this topic, which means that additional work should follow. In particular, the reaction mechanism should be better elucidated, including the role of OH radicals and the products formed from further oxidation of α,β-unsaturated dicarbonyls. In addition, the kinetics of furans with more types of substituents, such as halogens, should be studied, which could lead to the development of a predictive model for the ozone reactivity of furan-containing contaminants (10). Experiments with real complex water matrices should be performed to analyse the total yield of α,β-unsaturated dicarbonyls from all furans and potentially from other compounds present.

6.2.2 General directions for future research

At a more general level, future work on the ozonation products of trace organic contaminants should put greater emphasis on quantifying the concentrations that are formed under different conditions. Combined with analytical approaches involving high-resolution mass spectrometry for suspect and non-target screening, quantification can help close the mass balance and fully elucidate the ozone transformation pathways. Moreover, the major properties of the ozonation products, such as toxicity and persistence, need to be studied in order to evaluate the effects of the treatment. For example, the application of bioassays can help identify toxic transformation products that should be prioritised in further investigations (11). Synthesis or isolation from laboratory samples of ozonation products to produce standards in cases when they are not commercially available is required for both quantification and measurement of bio-physico-chemical properties (12, 13).

More quantitative data (rather than qualitative trends) are needed to perform a risk assessment of ozonated waters and inform policy and practice related to ozonation treatment. For instance, low yields of highly toxic products were observed for furans (Chapter 5), indicating the need to further evaluate the expected risk to human or environmental health, taking into account the total concentration of precursors that may be present in the water being treated. The risk associated with the formation of potentially hazardous by-products should be assessed within the framework of other risks that increase or decrease during ozonation treatment (e.g. the concentrations of parent compounds are reduced, other water quality parameters are also improved) (14). Different applications such as production of drinking water or polishing of wastewater effluent require separate assessments (15).

As ozonation is increasingly applied for water and wastewater treatment, on-going research should ensure that it is a sustainable technology, namely that it does not compromise water quality through the creation of hazardous by-products, and that it is energy-efficient (16). The cost, energy consumption and carbon footprint of advanced treatment including ozonation needs to be examined in the context of climate change and the efforts towards a net zero water sector undertaken in the UK and other countries. Multi-barrier approaches combining advanced oxidation processes with nature-based solutions, for example constructed wetlands (17), may

achieve high treatment performance and compliance with environmental and water quality standards, whilst minimising the required ozone production.

6.2.3 Impact on policy and ozonation practice

The research results presented here can provide valuable information to regulatory agencies regarding the properties and risks of transformation products and potential mitigating solutions. As policy on trace organic contaminants evolves (18), studies demonstrating that their transformation products can be persistent (Chapter 3) or toxic (Chapter 5) highlight the need to include this aspect in future policy.

Water and wastewater utilities employing ozonation treatment can benefit greatly from the findings of this PhD. When there are specific compounds or groups of compounds that cause concern due to environmental occurrence evidence and/or proposed regulations, information on ozone reactivity (Chapters 2 and 5) should be reviewed to assess whether ozonation is likely to be an appropriate solution. In addition, if the installation of ozonation treatment is considered for a specific waterworks or wastewater treatment plant, a resource-efficient COMBI system (Chapter 3) can be easily set up on-site to provide initial information on process performance with regards to trace organic contaminants, transformation products or other water quality parameters that depend strongly on the water or wastewater matrix. For ozonation plants facing issues with ozone mass transfer, foaming, or control of the ozone dosage, trialling bubble-less ozonation using membrane contactors may be considered (Chapter 4). The membrane ozonation results will also be of interest to manufacturers of membranes and membrane modules.

6.3 References

1. Lee Y, von Gunten U. Advances in predicting organic contaminant abatement during ozonation of municipal wastewater effluent: reaction kinetics, transformation products, and changes of biological effects. Environmental Science: Water Research & Technology. 2016;2(3):421-42.
2. Drewes JE, Jekel M. Behavior of DOC and AOX using advanced treated wastewater for groundwater recharge. Water Research. 1998;32(10):3125-33.

3. Escobar IC, Randall AA. Assimilable organic carbon (AOC) and biodegradable dissolved organic carbon (BDOC): complementary measurements. Water Research. 2001;35(18):4444-54.

4. Hübner U, von Gunten U, Jekel M. Evaluation of the persistence of transformation products from ozonation of trace organic compounds – A critical review. Water Research. 2015;68:150-70.

5. Prasse C, Ford B, Nomura DK, Sedlak DL. Unexpected transformation of dissolved phenols to toxic dicarbonyls by hydroxyl radicals and UV light. Proc Natl Acad Sci U S A. 2018;115(10):2311-6.

6. Yang J, Dong Z, Jiang C, Wang C, Liu H. An overview of bromate formation in chemical oxidation processes: Occurrence, mechanism, influencing factors, risk assessment, and control strategies. Chemosphere. 2019;237:124521.

7. Zhang S, Courtois S, Gitungo S, Raczko RF, Dyksen JE, Li M, Axe L. Microbial community analysis in biologically active filters exhibiting efficient removal of emerging contaminants and impact of operational conditions. Science of The Total Environment. 2018;640-641:1455-64.

8. Onesios-Barry KM, Berry D, Proescher JB, Sivakumar IA, Bouwer EJ. Removal of pharmaceuticals and personal care products during water recycling: microbial community structure and effects of substrate concentration. Applied and environmental microbiology. 2014;80(8):2440-50.

9. Lim KB, Wang PC, An H, Yu SCM. Computational Studies for the Design Parameters of Hollow Fibre Membrane Modules. Journal of Membrane Science. 2017;529:263-73.

10. Lee M, Zimmermann-Steffens SG, Arey JS, Fenner K, von Gunten U. Development of Prediction Models for the Reactivity of Organic Compounds with Ozone in Aqueous Solution by Quantum Chemical Calculations: The Role of Delocalized and Localized Molecular Orbitals. Environmental Science & Technology. 2015;49(16):9925-35.

11. Chibwe L, Titaley IA, Hoh E, Simonich SLM. Integrated Framework for Identifying Toxic Transformation Products in Complex Environmental Mixtures. Environmental Science & Technology Letters. 2017;4(2):32-43.

12. Escher BI, Fenner K. Recent advances in environmental risk assessment of transformation products. Environ Sci Technol. 2011;45(9):3835-47.

13. Buchner E-M, Happel O, Schmidt CK, Scheurer M, Schmutz B, Kramer M, Knauer M, Gartiser S, Hollert H. Approach for analytical characterization and toxicological assessment of ozonation products in drinking water on the example of acesulfame. Water Research. 2019;153:357-68.
14. Stalter D, Magdeburg A, Weil M, Knacker T, Oehlmann J. Toxication or detoxication? In vivo toxicity assessment of ozonation as advanced wastewater treatment with the rainbow trout. Water Res. 2010;44(2):439-48.
15. Muñoz I, Rodríguez A, Rosal R, Fernández-Alba AR. Life Cycle Assessment of urban wastewater reuse with ozonation as tertiary treatment: A focus on toxicity-related impacts. Science of The Total Environment. 2009;407(4):1245-56.
16. Bui XT, Vo TP, Ngo HH, Guo WS, Nguyen TT. Multicriteria assessment of advanced treatment technologies for micropollutants removal at large-scale applications. Sci Total Environ. 2016;563-564:1050-67.
17. Antoniadis A, Takavakoglou V, Zalidis G, Poulios I. Development and evaluation of an alternative method for municipal wastewater treatment using homogeneous photocatalysis and constructed wetlands. Catal Today. 2007;124(3):260-5.
18. Bieber S, Snyder SA, Dagnino S, Rauch-Williams T, Drewes JE. Management strategies for trace organic chemicals in water - A review of international approaches. Chemosphere. 2018;195:410-26.

Appendix: Statements of authorship

This declaration concerns the article entitled:			
Simultaneous ozonation of 90 organic micropollutants including illicit drugs and their metabolites in different water matrices.			
Publication status (tick one) **Draft manuscript** [ ] **Submitted** [ ] **In review** [ ] **Accepted** [ ] **Published** [x]			
Publication details (reference)	Zoumpouli GA, Siqueira Souza F, Petrie B, Féris LA, Kasprzyk-Hordern B, Wenk J. Simultaneous ozonation of 90 organic micropollutants including illicit drugs and their metabolites in different water matrices. Environmental Science: Water Research & Technology. 2020;6(9):2465-78. DOI: https://doi.org/10.1039/D0EW00260G		
Copyright status (tick the appropriate statement) I hold the copyright for this material [x] Copyright is retained by the publisher, but I have been given permission to replicate the material here [ ]			
Candidate's contribution to the paper (provide details, and also indicate as a percentage)	The candidate contributed to… Formulation of ideas: 50% The original project was conceived and planned by co-authors FSS, JW and BKH before the candidate started her PhD research. The candidate contributed further ideas and interpretation of previously obtained results. Design of methodology: 50% The candidate designed the methodology for literature review, data analysis and calculations under the supervision of JW and BKH. Experimental methodology was designed by FSS, JW and BKH. Experimental work: 40% The candidate analysed raw experimental data obtained by FSS and BP. Presentation of data in journal format: 85% The candidate wrote the manuscript and prepared graphs and tables under the supervision of JW and BKH. Input was offered by all co-authors.		
Statement from Candidate	This paper reports on original research I conducted during the period of my Higher Degree by Research candidature.		
Signed		**Date**	26/03/2021

This declaration concerns the article entitled:			
COMBI, continuous ozonation merged with biofiltration to study oxidative and microbial transformation of trace organic contaminants.			
Publication status (tick one) **Draft manuscript** [ ] **Submitted** [ ] **In review** [ ] **Accepted** [ ] **Published** [x]			
Publication details (reference)	Zoumpouli GA, Scheurer M, Brauch H-J, Kasprzyk-Hordern B, Wenk J, Happel O. COMBI, continuous ozonation merged with biofiltration to study oxidative and microbial transformation of trace organic contaminants. Environmental Science: Water Research & Technology. 2019;5(3):552-63. DOI: https://doi.org/10.1039/C8EW00855H		
Copyright status (tick the appropriate statement) I hold the copyright for this material [x] Copyright is retained by the publisher, but I have been given permission to replicate the material here [ ]			
Candidate's contribution to the paper (provide details, and also indicate as a percentage)	The candidate contributed to… Formulation of ideas: 60% The original COMBI setup design was conceived by co-authors MS and OH. The candidate contributed ideas on the design of an additional setup in Bath and on experiments with synthetic wastewater, under the supervision of JW and BKH. Design of methodology: 60% The candidate designed the methodology for experiments and analysis performed in Bath, with feedback from all co-authors. Experimental work: 60% The candidate built and tested the COMBI system in Bath and performed experiments with carbamazepine, diclofenac and fluoxetine and related analysis. Presentation of data in journal format: 85% The candidate wrote the manuscript and prepared graphs and tables under the supervision of JW and BKH. Input was offered by all co-authors.		
Statement from Candidate	This paper reports on original research I conducted during the period of my Higher Degree by Research candidature.		
Signed		**Date**	26/03/2021

This declaration concerns the article entitled:			
Aqueous Ozonation of Furans: Kinetics and Transformation Mechanisms Leading to the Formation of α,β-Unsaturated Dicarbonyl Compounds.			
Publication status (tick one) **Draft manuscript** [ ] **Submitted** [x] **In review** [ ] **Accepted** [ ] **Published** [ ]			
Publication details (reference)	Zoumpouli GA, Zhang Z, Wenk J, Prasse C. Aqueous Ozonation of Furans: Kinetics and Transformation Mechanisms Leading to the Formation of α,β-Unsaturated Dicarbonyl Compounds. Manuscript submitted.		
Copyright status (tick the appropriate statement) I hold the copyright for this material [ ] Copyright is retained by the publisher, but I have been given permission to replicate the material here [x]			
Candidate's contribution to the paper (provide details, and also indicate as a percentage)	The candidate contributed to… Formulation of ideas: 80% The candidate conceived the research ideas and objectives under the supervision of CP and JW. Design of methodology: 85% The candidate designed the experimental and analytical methodology with input from all co-authors. Experimental work: 70% The candidate performed all the kinetic experiments and the initial transformation product experiments with all target compounds. ZZ performed repeats of transformation product experiments and additional experiments using NAL+NAC. Presentation of data in journal format: 75% The candidate wrote the manuscript and prepared graphs and tables under the supervision of CP and JW and with input from ZZ.		
Statement from Candidate	This paper reports on original research I conducted during the period of my Higher Degree by Research candidature.		
Signed		**Date**	26/03/2021